AD_____

Award Number: W81XWH-05-1-0330

TITLE: A Biophysico-computational Perspective of Breast Cancer Pathogenesis and Treatment Response

PRINCIPAL INVESTIGATOR: Valerie M. Weaver Ph.D.

CONTRACTING ORGANIZATION: University of Pennsylvania
Philadelphia, PA 19104

REPORT DATE: March 2007

TYPE OF REPORT: Annual

PREPARED FOR: U.S. Army Medical Research and Materiel Command
Fort Detrick, Maryland 21702-5012

DISTRIBUTION STATEMENT: Approved for Public Release;
Distribution Unlimited

REPORT DOCUMENTATION PAGE

Form Approved
OMB No. 0704-0188

1. REPORT DATE *(DD-MM-YYYY)*	**2. REPORT TYPE**	**3. DATES COVERED** *(From - To)*
01-03-2007	Annual	1 MAR 2006 - 28 FEB 2007

4. TITLE AND SUBTITLE
A Biophysico-computational Perspective of Breast Cancer Pathogenesis and Treatment Response

5a. CONTRACT NUMBER

5b. GRANT NUMBER
W81XWH-05-1-0330

5c. PROGRAM ELEMENT NUMBER

6. AUTHOR(S)
Valerie M. Weaver Ph.D.

E-Mail: vmweaver@mail.med.upenn.edu

5d. PROJECT NUMBER

5e. TASK NUMBER

5f. WORK UNIT NUMBER

7. PERFORMING ORGANIZATION NAME(S) AND ADDRESS(ES)
University of Pennsylvania
Philadelphia, PA 19104

8. PERFORMING ORGANIZATION REPORT NUMBER

9. SPONSORING / MONITORING AGENCY NAME(S) AND ADDRESS(ES)
U.S. Army Medical Research and Materiel Command
Fort Detrick, Maryland 21702-5012

10. SPONSOR/MONITOR'S ACRONYM(S)

11. SPONSOR/MONITOR'S REPORT NUMBER(S)

12. DISTRIBUTION / AVAILABILITY STATEMENT
Approved for Public Release; Distribution Unlimited

13. SUPPLEMENTARY NOTES

14. ABSTRACT Apoptosis resistance regulates breast transformation and treatment responsiveness, yet the mechanism(s) enhancing breast cancer cell survival remain unclear. We showed that malignant transformation is associated with increased matrix deposition, cross-linking and reorganization that correlate with a progressive stiffening of the gland. Organotypic culture experiments, demonstrated that stiffening the extracellular matrix (ECM) destabilizes cell-cell junctions, enhances integrin-dependent adhesions, alters survival, and compromises mammary morphogenesis and the integrity of differentiated mammary tissues. Matrix force also promotes oncogene-mediated invasion and malignant transformation of mammary epithelial cells (MECs) in culture and in vivo, by inducing cell-generated force and RhoGTPase, ERK, PI3 kinase and JNK signaling. Consistently, deterministic modeling predicted that chronically-activated ERK drives cell transformation, and while the model does not incorporate adhesion-dependent force, we did find that pre-malignant MECs with genetically modified integrins have elevated ERK signaling, and are invasion in culture and tumorigenic in vivo. We are now testing whether inhibiting ECM stiffening or changing integrin signaling will either prevent or promote malignant transformation in vivo.

15. SUBJECT TERMS
Extracellular matrix, stiffness, mechanical, force, apoptosis, resistance, Bioengineering, cross-disciplinary, computational, breast tumor treatment

16. SECURITY CLASSIFICATION OF:			**17. LIMITATION OF ABSTRACT**	**18. NUMBER OF PAGES**	**19a. NAME OF RESPONSIBLE PERSON**
a. REPORT	**b. ABSTRACT**	**c. THIS PAGE**			USAMRMC
U	U	U	UU	245	**19b. TELEPHONE NUMBER** *(include area code)*

Table of Contents

INTRODUCTION:

Apoptosis resistance regulates the pathogenesis, and treatment response of breast tumors. Despite concerted effort towards understanding the molecular basis for apoptosis resistance in breast tumors, progress in this area has been frustratingly slow. Lack of advancement may be attributed in part to the current cell autonomous view of breast cancer etiology and treatment responsiveness. What we now appreciate is that the tissue microenvironment modifies the therapeutic responsiveness of tumors (Taylor et al., 2000; Zahir and Weaver, 2004), and the stroma itself regulates mammary development, homeostasis and transformation and even metastasis (Unger and Weaver, 2003). Alterations in the mammary gland ECM correlate with changes in mammary differentiation, involution (apoptosis) and tumor progression, and culture experiments clearly show that the stromal ECM can modulate mammary epithelial cell (MEC) growth, differentiation and survival and alter apoptotic responsiveness (Lewis et al., 2002; Truong et al., 2003; Zahir and Weaver, 2004). **It is not known how the ECM alters mammary epithelial survival.**

My laboratory has been examining the role of integrin receptors in breast tissue morphology and behavior and malignant transformation and metastasis. Together we have begun to explore how the ECM via its major receptors the integrins modulates mammary tissue homeostasis, invasion and apoptosis responsiveness. We found that the expression of specific integrins including $\alpha5$, $\alpha6$ and $\beta1$ and $\beta4$ expression, organization and activity are consistently altered in primary and metastatic breast tumors and tumorigenic cell lines. Others and we have also determined that perturbing integrin expression and activity can drive malignant behavior of non-malignant and pre-malignant MECs, and that normalizing integrin activity represses expression of the malignant breast phenotype in culture and in vivo (Unger and Weaver, 2003; White et al., 2004) More specific to this proposal our data have shown that integrins including a6b4 integrin can regulate cell survival and modulate the apoptotic responsiveness of mammary tissues to a diverse array of exogenous stimuli including various chemotherapies and immune receptor activators (Weaver et al., 2002; Zahir and Weaver, 2004). We found that integrin-dependent apoptosis resistance and survival are intimately linked to many of the biochemical pathways and mechanisms that regulate tissue organization and specifically tissue polarity. For example, we found that $\alpha6\beta4$ integrin directs mammary epithelial cells to assemble polarized mammary tissue structures that display apoptosis resistance to a wide spectrum of apoptotic insults. We are now exploring the underlying mechanisms whereby integrin expression and/or function becomes altered in breast tumors, how integrin modulate the survival of nonmalignant and transformed mammary epithelial cells, what the molecular link could be between integrin-dependent survival and tissue polarity and the clinical relevance of these findings.

We found that prior to malignant transformation the mammary gland exhibits a 'desmoplastic' response that is associated with an incremental and significant increase in global elastic modulus (stiffness) of the gland and elevated/altered expression of integrins and integrin adhesions (Krouskop et al., 1998; Paszek and Weaver, 2004; Paszek et al., 2005); (unpublished data; refer to previous progress report; data being prepared for manuscript submission). Consistent with results from other laboratories we determined that externally-applied mechanical force regulates the behavior and phenotype of multiple cell types including endothelial, fibroblasts, neurons, and MECs (Bershadsky et al., 2003; Geiger et al., 2001; Grinnell, 2003). Although the mammary gland is not traditionally viewed as a mechanically-regulated tissue, MECs within the ductal tree and alveolus experience passive (isometric) and active mechanical force throughout the lifetime of the mammary gland most notably during development, lactation and involution (Paszek and Weaver, 2004; Plewes et al., 2000; Samani et al., 2003). Similar to other solid tumors, the mammary gland also becomes appreciably stiffer in association with its malignant transformation and mammary epithelial cells within the tumorigenic mammary gland experience an array of additional compression and stress and interstitial associated forces (Kass et al., In progress). During the process of metastasis and once at the metastatic site breast tumor cells also

encounter an array of external mechanical forces that could conceivably influence their behavior and alter their response to treatment. For example, many of the common metastatic sites for breast cancer differ appreciably with respect to their stiffness and biochemical compositions than a normal mammary gland such as bone (very stiff, high vitronectin), in the vasculature (high pulsatile pressures, high fibronectin and fibrin), pleural cavity (very compliant with high fibrin composition but also adjacent fibrotic lung could be quite stiff with a high amount of elastin).

Because physical forces so profoundly influence cell proliferation, survival and differentiation of multiple cell types, we propose that we need to clarify whether and how mechanical cues regulate mammary tissue behavior and apoptosis responsiveness.

Accordingly, we predict that the physical organization of the ECM (which contributes to its mechanical properties) constitutes an independent regulator of mammary epithelial behavior and apoptosis resistance. Delineating the molecular basis for this phenotype will likely have important consequences for tumor therapy. To rigorously test this idea we are in the process of achieving the following specific aims:

Specific Aim 1. To engineer tractable 3D organo-typic model systems that recapitulate the biophysical properties of primary and metastatic breast tumor tissues, and then to use these models to identify and examine putative molecular mechanisms whereby mechanical force could regulate apoptosis resistance in culture and in vivo.

Specific Aim 2. To develop xenograft and transgenic mouse models to test whether ECM stiffness regulates apoptotic responsiveness of mammary epithelia in vivo.

Specific Aim 3. To build a computational model that can predict how changes in ECM compliance could influence integrin-dependent apoptosis responsiveness of mammary epithelia and query this model with clinical data.

Specific Aim 4. To develop non-invasive imaging tools that could be used to monitor changes in ECM stiffness or stiffness-induced changes in mammary tissue phenotype.

Summary of Achievements - Proposal Body:

KEY RESEARCH ACCOMPLISHMENTS:

Task 1: *Engineer tractable 3D organo-type models that recapitulate the biophysical properties of primary and metastatic breast tumor tissues and use these models to dissect candidate molecular mechanisms whereby ECM stiffness could regulate apoptosis resistance in culture and in vivo*

PART A. Development of natural 3D ECM models that recapitulate the biophysical properties of primary normal and malignant metastatic breast tissues.

During the first year of this project we were able to complete many of the objectives outlined for task 1 part A. Our findings were summarized in our first years' progress report. Many of last years results were published and much of the other data are now being prepared for publication (see reportable outcomes). **Included in the current "second years report" we summarize our accomplishments over the first nine months of the second year of the proposal**. With respect to task 1 part A we were able to complete several of the objectives we initiated in the first year, as outlined in our work aims. Although

not outlined as a specific work objective we also exerted considerable effort towards comprehensively characterizing the biochemical and organizational features of a normal and progressively transformed stroma including the composition and organization of the extracellular matrix and the stromas cellular components. A portion of these new data have been presented at National and International meetings and are the subject of a new manuscript under preparation for submission to Cell by the fall of 2007. We maintain that this characterization is critical because it will enable us to design appropriate strategies to manipulate matrix stiffness in vivo to clarify its role in tumor aetiology. In addition understanding what stiffens the gland during malignancy should permit the development of targeted therapies.

To complete the stroma characterization we established productive collaborations with colleagues at the Wistar Institute in Philadelphia, PA (second harmonics imaging) at Boston University (imaging elastography) and Stanford University (lysyl oxidase analysis). These new collaborators have permitted us to set up new technology such as second harmonics imaging that permits visualization of non fixed collagen fibrils in live tissue, imaging elastography to spatially visualize the mechanical properties of the tissues and lysyl oxidase activity analysis, to assess the cross linking potential of cells within the breast stroma. These approaches have permitted us to more comprehensively characterize the biophysical and biochemical properties of the breast stroma. We have also exerted considerable effort towards establishing methodology to construct in house natural cross-linked hydrogels as well as co culture assay systems, so that we can analyze the molecular pathways by which MECs perceive and alter their response to matrix stiffening. Using some of these newly developed experimental matrices we have now been able to identify and characterize in depth the molecular pathways regulated by matrix force and begun to determine their effects on mammary cell behavior.

Using these various new and established experimental approaches, in the past nine months of the second year of this proposal we were able to obtain an improved understanding of the molecular changes that occur in the mammary stroma surrounding the normal and developing breast lesion and identified several key changes that we predict contribute to the stiffening and therefore the transformation behavior of the tissue. The identification of some of the key stromal changes mediating breast tissue stiffening during transformation should permit us to develop new prognostic indicators and even tractable tumor prevention therapies. We also hope that this information will aid in the generation of appropriate culture models for experimental dissection of key molecular pathways linking matrix stiffness to tissue phenotype.

We successfully applied immunostaining of frozen and paraffin sections of developing experimental breast tumors and could detect quantifiable changes in the composition and deposition of various extra cellular matrix proteins and their modifying enzymes including collagen I and lysyl oxidase (see Figures 1 & 2). We could also detect a significant increase in circulating levels of activated lysyl oxidase in transgenic mice with palpable tumors. We applied polarized light and pico serius red staining to analyze collagen alignment and determined that not only is there a significant increase in collagen deposition prior to malignant transformation but that the collagen fibrils become progressively aligned around the mammary ducts. We have initiated studies to generate algorithms to quantify these spatial changes (see Figure 3). Using two photon microscopy to conduct second harmonic imaging we were able to visualize changes in collagen I fibril organization and structure that strongly suggest that collagen I becomes linealized adjacent to the transforming lesion (see Figure 4). We are now in the process of developing and applying ELISA and computational methods to quantify these microscopy-detected changes in matrix organization (these experiments should be completed in the next 6-8 months and will be summarized in next years report). Nevertheless, even in the absence of quantification, our new data suggest that collagen I deposition increases dramatically prior to malignant transformation and that this newly deposited collagen becomes dramatically reorganized and modified coincident with the appearance of elevated lysyl oxidase expression in the stromal fibroblasts and increased circulating

Figure 1. Collagen expression is increased during tumor progression. Histological images of trichrome blue staining in control (non tumorigenic) and Her2/neu transgenic tumors showing dramatically increased collagen deposition in a pre malignant mammary gland and an even further increase following malignant transformation.

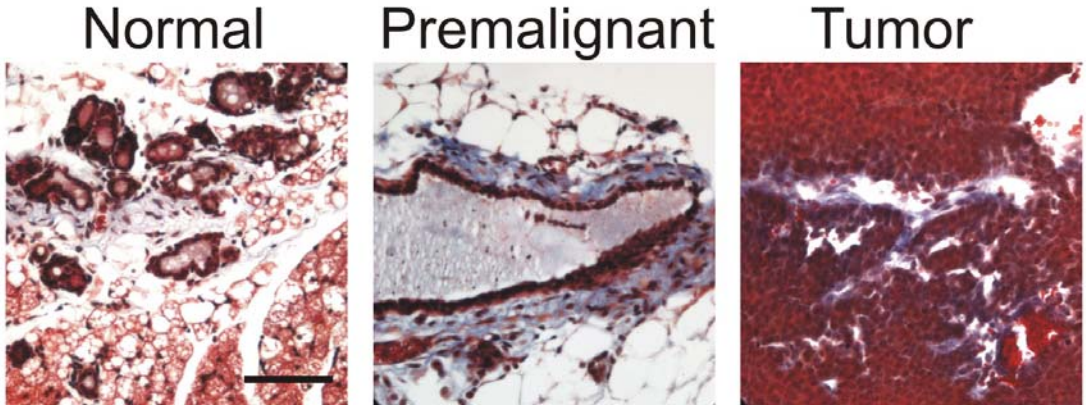

Figure 2. Altered collagen I deposition and organization in vivo during malignant transformation. Left: Phase contrast image (top) and polarized light images (bottom) of picrosirius red and hematocylin staining of normal, premalignant and invasive breast tumors. Right: Quantification of polarized light images shown at bottom, left.

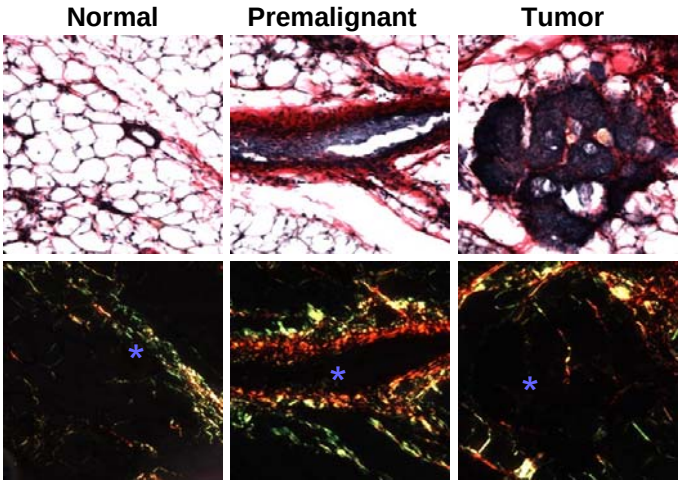

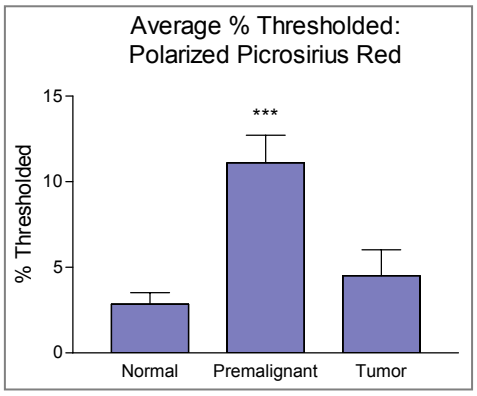

Picrosirius Red /

Figure 3. Lysyl oxidase status in MMTV Fvb mouse with and without breast tumors. Right. Immunostaining showing increased lysyl oxidase expression in stroma of breast tumors. Left. Circulating levels of activated lysyl oxidase increase dramatically coincident with the appearance of palpable breast tumors in FVB MMTV-neu mice.

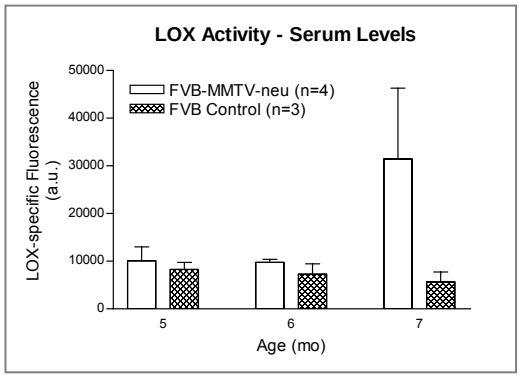

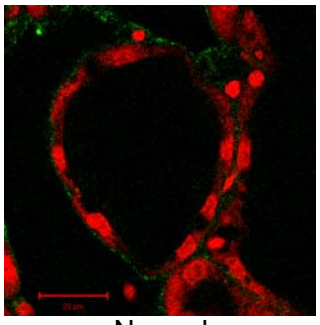

Normal

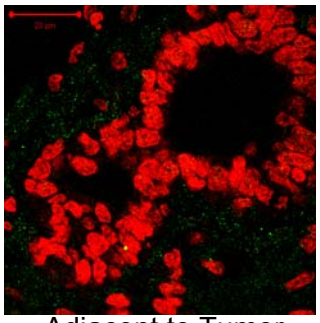

Adjacent to Tumor

Tumor incidence at 7 months

- FVB-MMTV-neu: >85%
- Strain control (FVB) mice: 0%

Propidium Iodide / LOX

Figure 4. Second harmonics imaging reveals relaxed collagens surrounding the normal mammary ducts and their progressive linearization coincident with malignant transformation of the gland. In particular note the strikingly aberrantly organized, linear collagen in the stroma adjacent to the Her2/neu breast tumor.

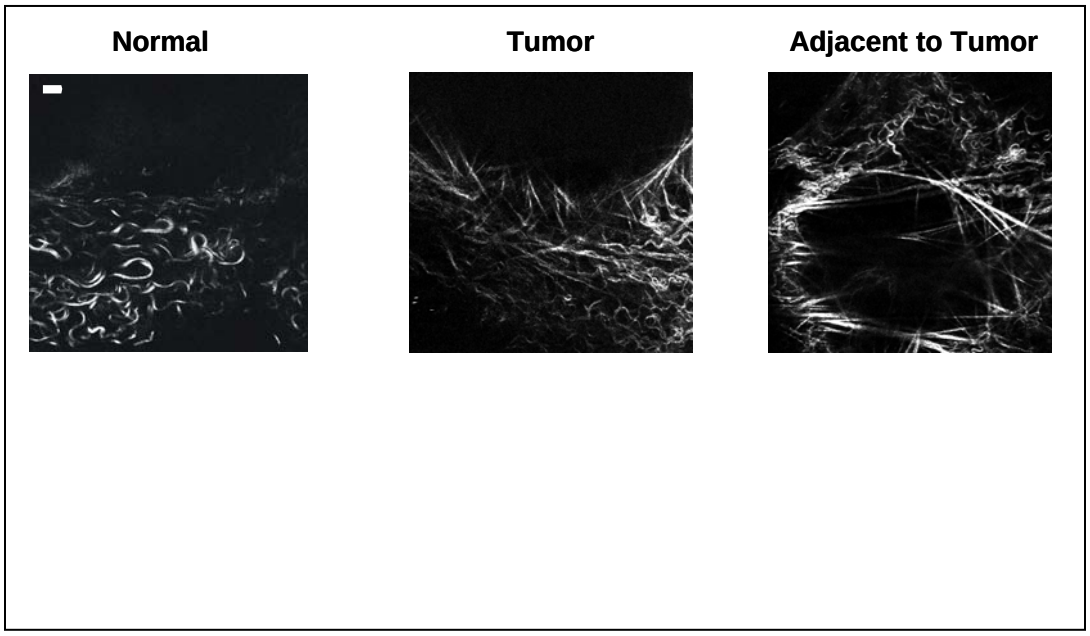

levels in the blood (see Figure 3). Because lysyl oxidase promotes collagen fibril maturation by cross linking the hydroxyl groups and this in turn increases the tensile properties of the collagen we predict that elevated matrix cross linking constitutes an important promoter of matrix stiffening during breast tumor progression. To address this we have initiated studies with an outside institute with expertise in matrix cross linking analysis who uses high high pressure liquid chromatography to analyze the nature of matrix cross links during breast tumorigenesis. Towards this goal we have begun to characterize the specific nature of the cross links that occur in the breast stromal matrix of normal and premalignant breast tissues (see Figure 5). In the next year we intend to acquire the technology to comprehensively analyze collagen cross linking using HPLC as well as mass spectroscopy in house. Regardless, our preliminary studies do indicate that the changes in matrix composition and organization correlate strongly with the progressive stiffening of the tissue as we reported previously using unconfined compression analysis (see Figure 6; see also previous progress report) and in this current report using shear rheology (see Figure 6).

In collaboration with Dr. Katalin Czszar we have been able to successfully construct a recombinant lysyl oxidase that is constitutively active when expressed in fibroblasts and mammary cells. Using this construct we have generated stable murine and human fibroblasts expressing either a constitutively expressed activated LOX or an inducible LOX construct. Data clearly show that ectopically expressed LOX protein is synthesized, secreted and active and that fibroblasts expressing constitutively active LOX stiffen a collagen I matrix by greater than 40% in around 7-10 days (data not shown). More intriguingly, Ras infected "pre-malignant" mammary epithelial cells co cultured in a compliant 3D collagen/BM hydrogel with LOX expressing fibroblasts but not vector expressing fibroblasts, proliferate more and invade into the surrounding 3D hydrogel (collagen I/BM) matrix (see Figure 7). Although we are still in the process of determining if this LOX-mediated invasion is linked specifically to a stiffening of the surrounding matrix, we did find that increasing ribose-mediated matrix cross linking, which also stiffens the matrix by 40% (see Figure 8), promotes MEC proliferation, compromises cell-cell junctional integrity and disrupts basement membrane integrity (see Figure 9; pre requisites for malignant transformation). Indeed, we found that ribose-induced matrix stiffness will cooperate with an oncogene such as Her2/neu to destroy mammary tissue integrity and promote invasion, whereas the Her2/neu oncogene alone is insufficient for cell invasion in 3D hydrogel cultures (see Figures 10 & 11), and malignant transformation of the breast in vivo.

During our first grant cycle we successfully applied non confined compression analysis to measure the bulk “stiffness” or elastic modulus of normal, pre-malignant and transformed breast tissue, the stroma surrounding transgenic breast tumors, and the physical properties of several tissues to which breast tumor cells characteristically metastasize including lung, brain, and liver. Our earlier results were consistent with the notion that a progressive stiffening of the breast tissue precedes and rises further during breast tumorigenesis. We found that each metastatic tissue represents a unique mechanical microenvironment. We now intend to apply a more rigorous characterization of the composition and organization features of the lung which is one of the more frequent sites breast tumors metastasize to. In this regard, we have recently begun to collaborate with Janine Erler to measure circulating lysyl oxidase activity in normal and experimental animal models of breast cancer. We can measure LOX activity in fresh serum samples and preliminary studies suggest that circulating LOX activity increases dramatically coincident with malignant transformation and can be effectively inhibited through treatment with a specific LOX activity inhibitor BAPN (see Figure 12). Whether inhibiting LOX activity will be sufficient to prevent LOX mediated matrix cross linking in vivo has yet to be determined. Also it is not clear what if any effect reducing LOX activity might have on matrix stiffening during malignant transformation. Regardless however, at the time that this proposal was being summarized we had noticed that tumor burden was noticeably reduced in mice that had been treated with the BAPN

Figure 5. DHLNL and HLNL Cross link analysis of matrix in control and early transformed breast lesion.

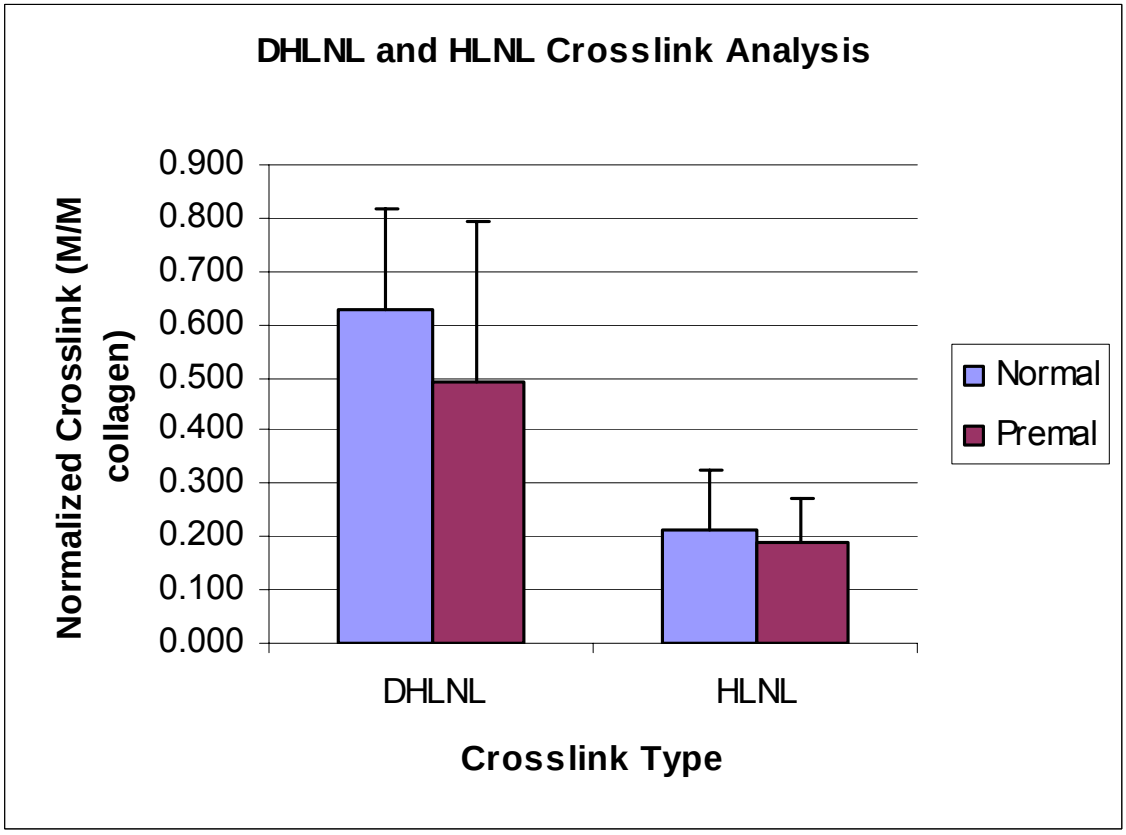

Figure 6 A. Unconfined Compression

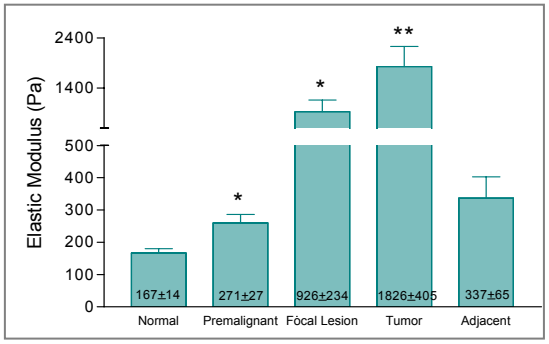

Figure 6 B. Rheology

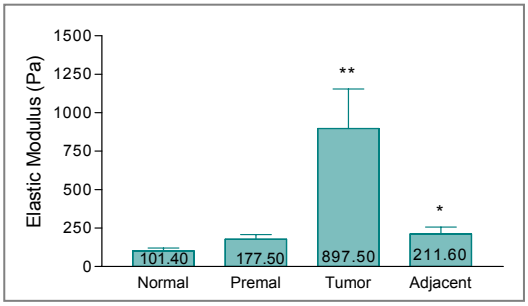

Figure 7. LOX-dependent Matrix Stiffening drives Malignant Transformation *IN CULTURE*

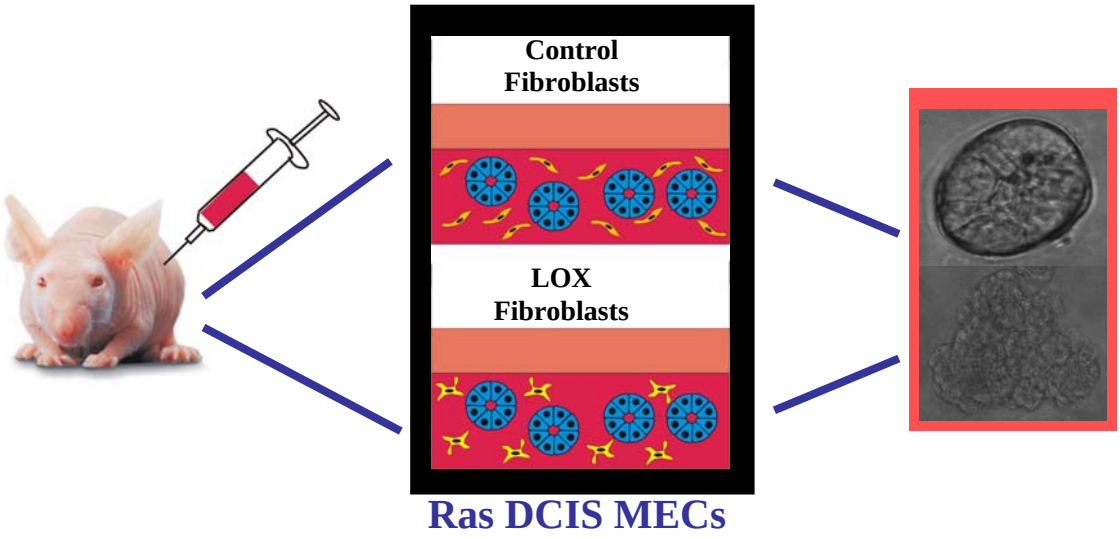

Figure 8. Ribose-induced cross linking of collagen increases the elastic moduls of the matrix and perturbs the morphology of a pre assembled mammary tissue in culture.

- Reducing sugars non-enzymatically crosslink collagen I
- Incrementally stiffens ECM without changing the collagen

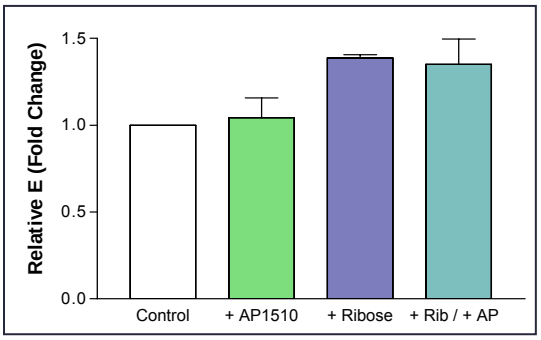

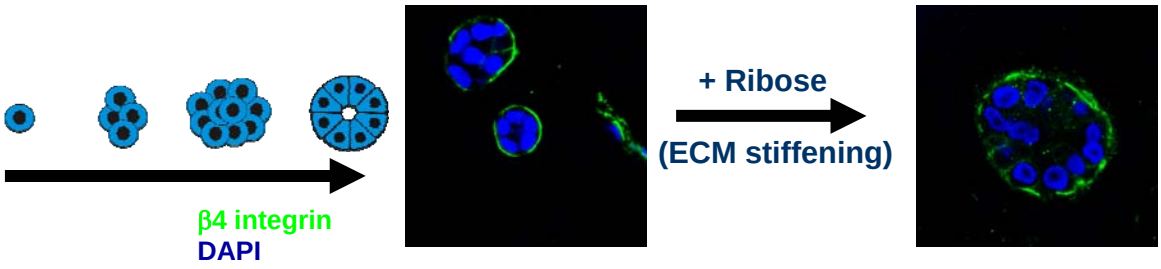

Figure 9. Experimental Setup

1. Allow cells to undergo normal morphogenesis.
2. Stiffen the matrix.
3. Activation of ErbB2.

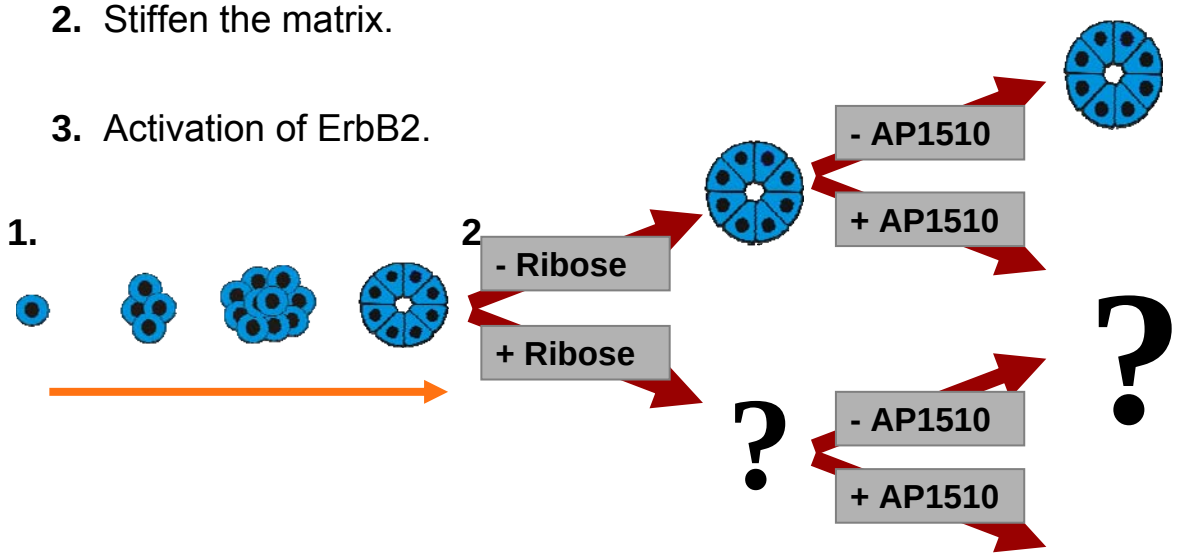

Figure 10. Timed activation of ErbB2 in MEC cultures through receptor homodimerization

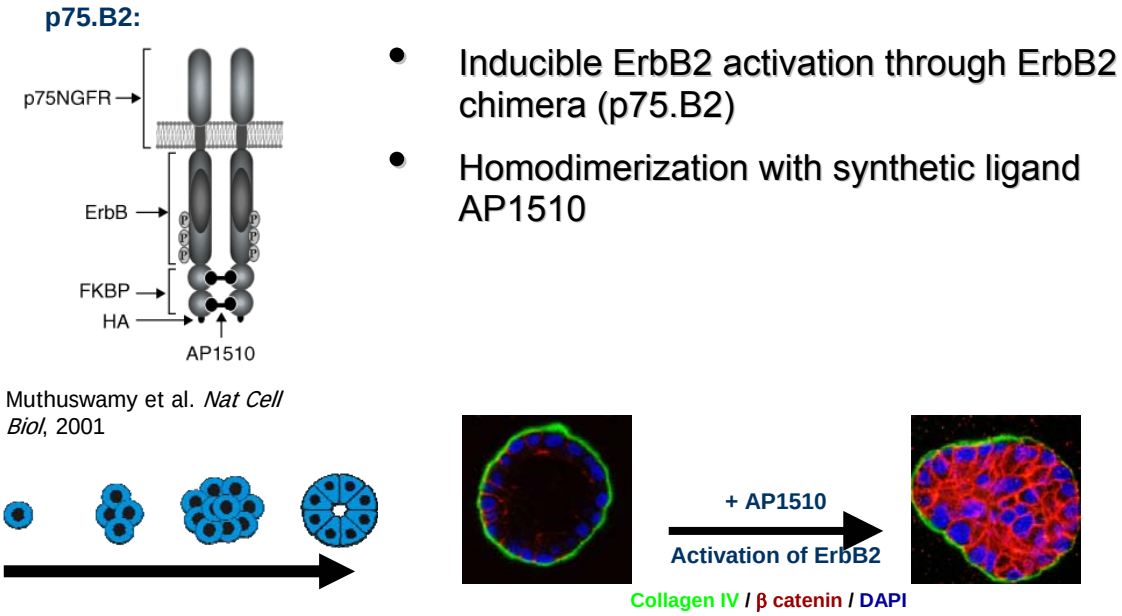

Figure 11. Synergistic interactions between stiffness and oncogenes permit an invasive phenotype in MECs

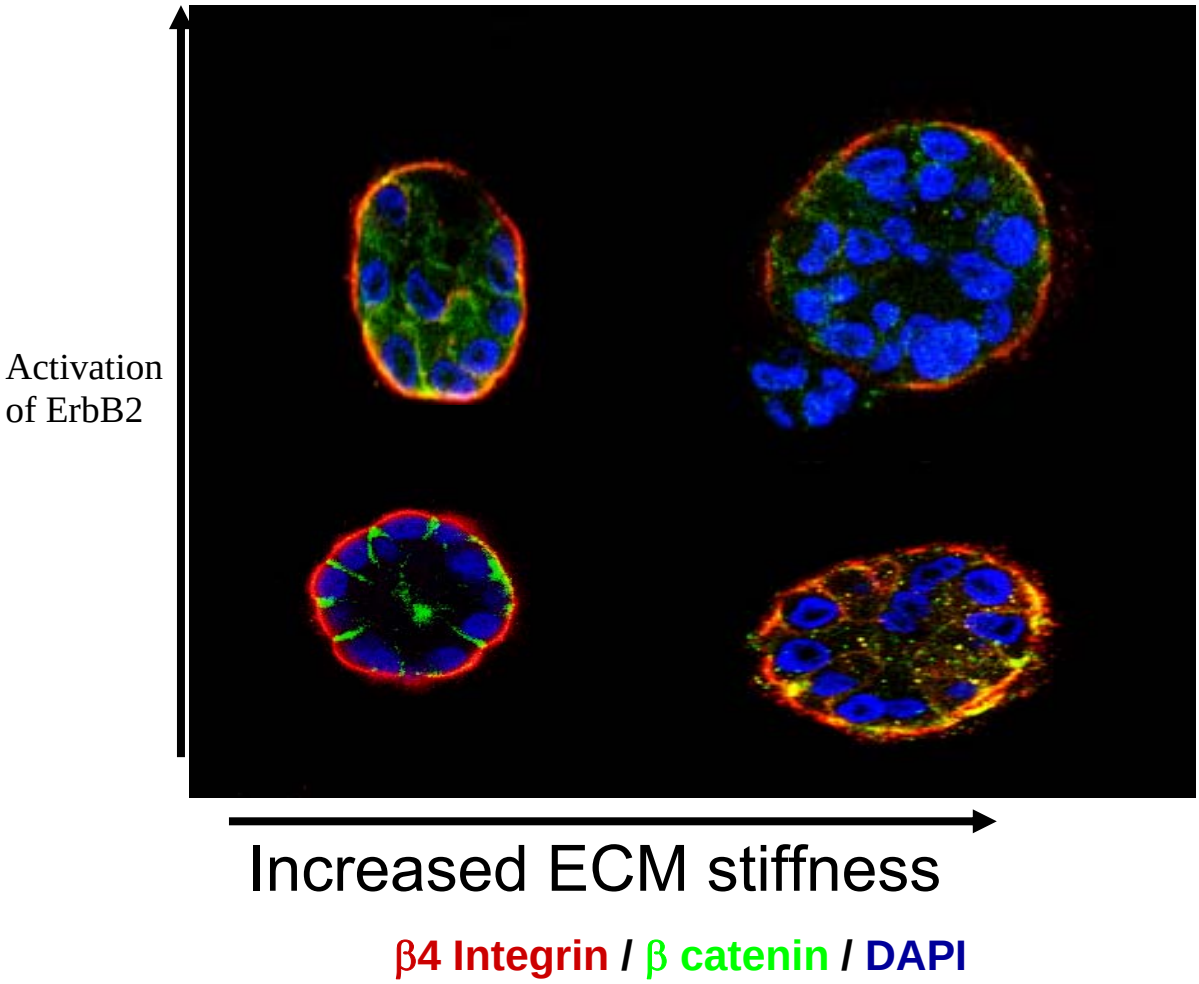

Figure 12. LOX activity is decreased in BAPN-treated animals

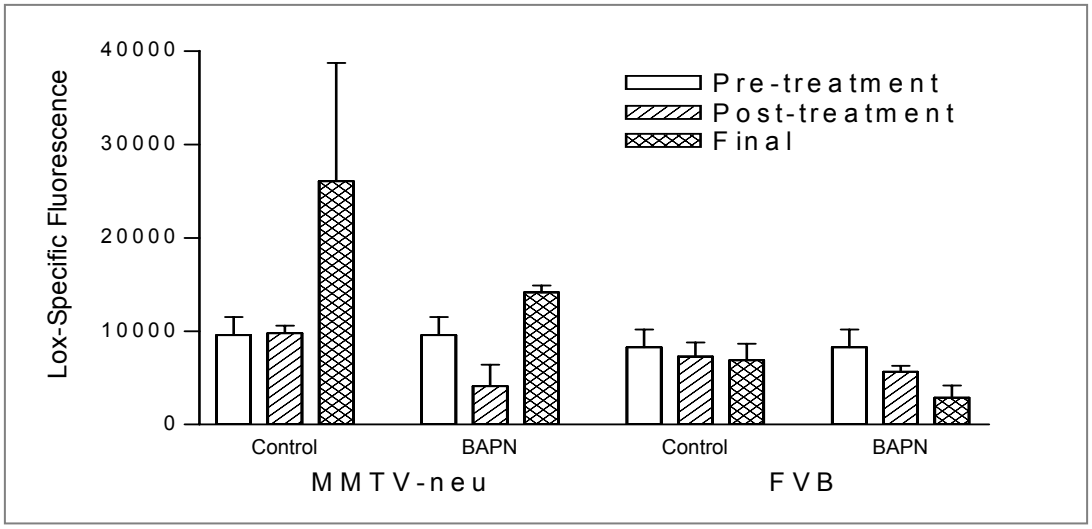

compound to inhibit LOX activity. We anticipate that we should have definitive results to report on this study in our next progress report.

Given the novelty of our observations, we believe that it is critical to establish independent validation measurements using an alternative and more broadly applied method. In the first year and throughout these past 9 months of our second year of funding, we have worked closely with Dr.s Joyce Wong and Susan Margulies to train two bioengineering students to apply shear rheology measurements to 3D hydrogels and freshly explanted tissues. We have also hired two new bioengineering postdoctoral fellows who are also being trained in these measurements. With these combined efforts we have now completed the shear rheology measurements for normal and various stages of malignant transformation of breast tissue from the Her2/neu transgenic mouse model. My group has also successfully applied this method to assess the rheology of 3D natural (collagen, collagen/basement membrane), polyacrylamide gels and self assembling peptide gels. Shear rheology is one of the gold standards used by biomaterials experts to measure the materials properties of gels and tissues and can be applied to hydrogel cultures of living cells because the approach does not need to be corrected for the non-compressibility of water. In the past year we have exploited this method to assess the effect of ribose-mediated cross linking and lysyl oxidase crosslinking on collagen hydrogel rheology (see above). Our latest results confirm and extend our previous compression analysis results, and demonstrate conclusively that mammary gland stiffness increases dramatically prior to malignant transformation (see Figure 6). We could also consistently demonstrate at least a 40% increase in matrix stiffness induced through either chronic (two week) addition of ribose, addition of lysyl oxidase conditioned media (5-10 days) or mediated by fibroblasts expressing a constitutively active lysyl oxidase transgene (data not shown).

However, as was discussed in our first report, we did note that the shear rheology measurements are consistently smaller in magnitude then the unconfined compression results, even after the data have been converted to the elastic modulus.

In addition to observing a progressive increase in the deposition of matrix components such as collagen I and linearization of the collagen fibrils that reveal how heterogeneous the matrix changes are in the transforming breast. Thus while bulk tissue compression and shear rheology measurements are informative they cannot tell us what is happening to matrix generated forces surrounding the transforming breast tissues. Accordingly, we have begun to develop methods to spatially map changes in the extracellular matrix stroma surrounding developing breast tumors. To achieve this goal we have been applying atomic force microscopy indentor analysis (see Figure 13) which can be used to spatially map the physical forces of the cells (rheology) and the surrounding extracellular matrix stroma (stiffness). Using a borrowed AFM machine, and with guidance provided by Drs. Chris Chen and Dennis Discher from the Bioengineering Department at the University of Pennsylvania and Dr. Joyce Wong from the Biomedical Engineering Department at Boston University, we were recently able to successfully apply one dimensional AFM to measure the stiffness of adipocytes and ductal tissue in normal and tumorigenic experimental breast tissue (see Figure 13). This is a major technological breakthrough and significant achievement given the pronounced compliancy of mammary tissue and the fact that very few laboratories world wide have been able to successfully apply AFM measurements to the study of live tissue function/phenotype. Given our success we are in the process of securing funding to obtain our own AFM machine and will use this approach to build a spatial mechanical "map" of a transforming breast tissue. We also intend to apply AFM measurements to characterize the physical characteristics of our experimental gels systems and to monitor effects on the cells rheology in response to alterations in matrix composition and force. We hope to be able to make independent measurements of the rheological properties of mammary cells within the breast tissue and in the context of its metastatic microenvironment. Given that the cells rheological properties are highly responsive to physical cues received from the stroma this is a highly versatile and powerful technique. AFM can also

Figure 13. Atomic force microscopy reveals that the transformed mammary gland is stiffer than the nontransformed mammary gland

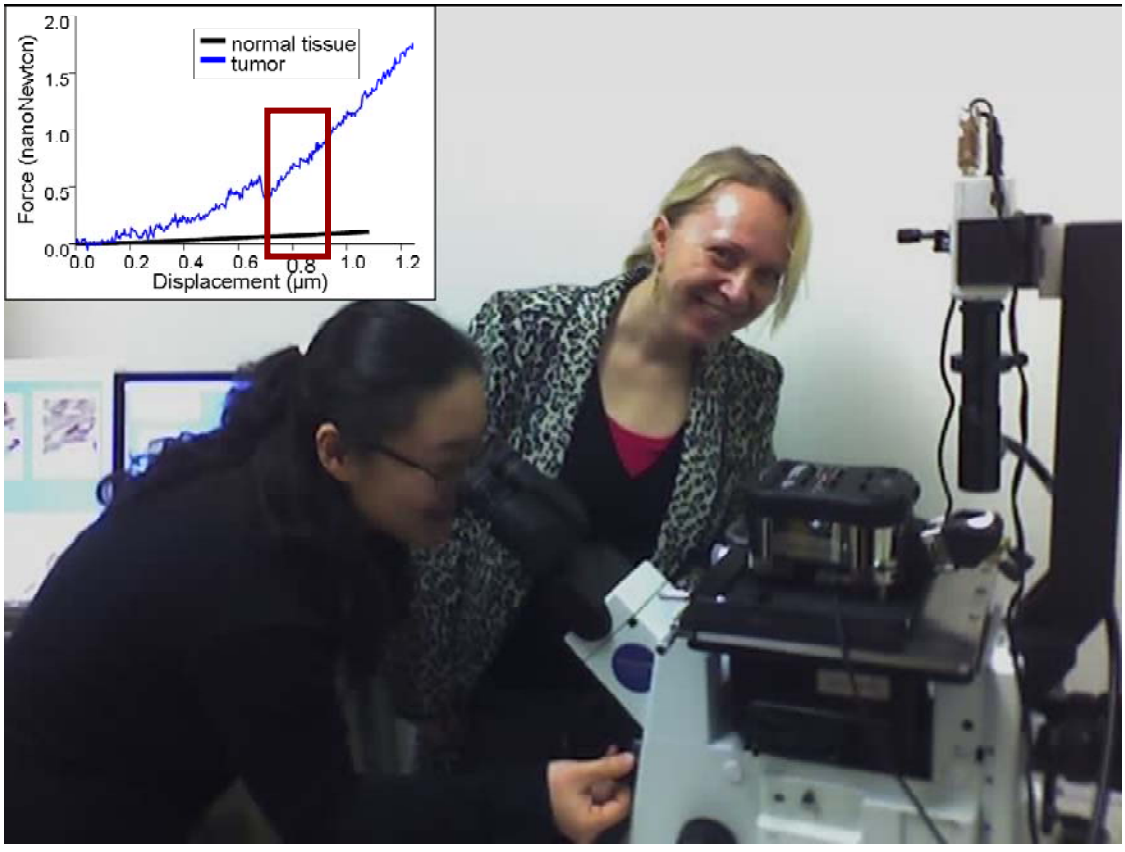

be easily applied as an additional, independent measurement to assess the mechanical properties of our engineered hydrogels. The advantage of AFM measurements is that they will permit us to ascertain with great certainty the physical properties which the cell interacts with on the nanoscale as opposed to basing our conclusions on the bulk properties of the tissue and stroma. For example, second harmonics imaging of 3D collagen/BM hydrogels suggest that invading transformed mammary cells migrate preferentially along spatially oriented collagen fibrils - which are presumably stiffer (see Figure 14). The veracity of this prediction is currently being address. Future AFM work at UCSF will be conducted in collaboration with Dr. Joyce Wong at Boston University, Dr. Chris Chen at UPenn and with Dr. Sanjay Kumar at UC Berkeley.

Our first report summarized our studies illustrating how matrix stiffness mediated through either an increase in collagen concentration or via cross linked poly acrylamide gels disrupted cell-cell adhesions, compromised tissue polarity and promoted MEC proliferation. We showed how matrix force regulates focal adhesion maturation to increase the magnitude and duration of ERK signaling. We further reported that preliminary studies had shown how matrix force can also enhance PI3 kinase signaling and alter JNK to regulate tissue morphology and apoptosis responsiveness of MECs. We have continued with this work and report here that matrix stiffness consistently enhances growth factor dependent activation of PI3 kinase and that this appears to be mediated through alterations of PTEN expression and activity. Thus we could consistently show how matrix stiffness enhances both the activity and duration of epidermal growth factor dependent PI3 kinase activity (as indicated by increased phosphorylation of Akt; see Figure 15). Based upon an investigation of putative pathways implicated in PI3 kinase regulation (Figure 16) we examined the effect of matrix stiffness on mechanically-responsive and integrin-linked pathways that could influence PTEN expression and activity. We found that elevated matrix force is associated with decreased PTEN protein expression and elevated "inhibitory" phosphorylation of PTEN (see Figures 17 & 18). Experiments are now in progress to determine if matrix stiffness alters PTEN expression and/or activity to promote PI3 kinase-dependent mammary tumor invasion. In this regard we could show that matrix force permits Her2/neu-mediated tumor cell invasion in association with enhanced PI3 kinase activity. We are actively exploring how matrix force could alter PTEN expression and activity. Because Src and Src family kinases have previously been shown to modulate PTEN activity and matrix force and integrins can modulate Src expression and activity (Paszek et al., 2005), we will be examining the contribution of Src family kinases and integrin-mediated Src modification. This work will be incorporated into a manuscript together with our in vivo experimental animal work we will be writing and submitting to either Cell or Cancer Cell in the summer of 2007. We anticipate that the work should be submitted for published either in the Fall of 2007 or the Winter of 2008.

We have now essentially completed our first set of studies on the role of matrix stiffness in culture on apoptosis responsiveness of mammary tissues. In our last report, we showed how matrix stiffness will modulate the survival response of mammary tissues to chemo, immune stimuli and gamma irradiation (see figures last report) and that this effect correlated with differences in JNK signaling. We have now completed this work and can show that not only does matrix stiffness modulate the metabolic and apoptotic response of mammary tissues to exogenous death stimuli but matrix force also significantly influences clonogenic survival. Thus irradiated mammary epithelial tissues interacting with a highly compliant matrix show a blunted reduction in metabolism 24 hours after exposure, and reduced apoptosis induction 48 hours post irradiation. Furthermore, treated mammary epithelial cells tested for their clonogenic survival died at similar rates when clonogenic survival assays were conducted on stiff 2D matrices - but survived significantly more when the clonogenic studies were conducted on compliant hydrogels (see Figure 19). These results are extremely important, since the efficacy of virtually ALL new apoptotic reagents under assessment as new clinical cancer therapies are initially assessed for their effects on cell viability, apoptosis and clonogenic survival in cells grown on classic (rigid 2D culture

Figure 14. Second harmonics imaging (Collagen (SHG) red fibers) reveals that matrix force and collagen alignment promote invasive behavior in mammary tissues expressing an activated ErbB2 (10A.B2-GFP green cells).

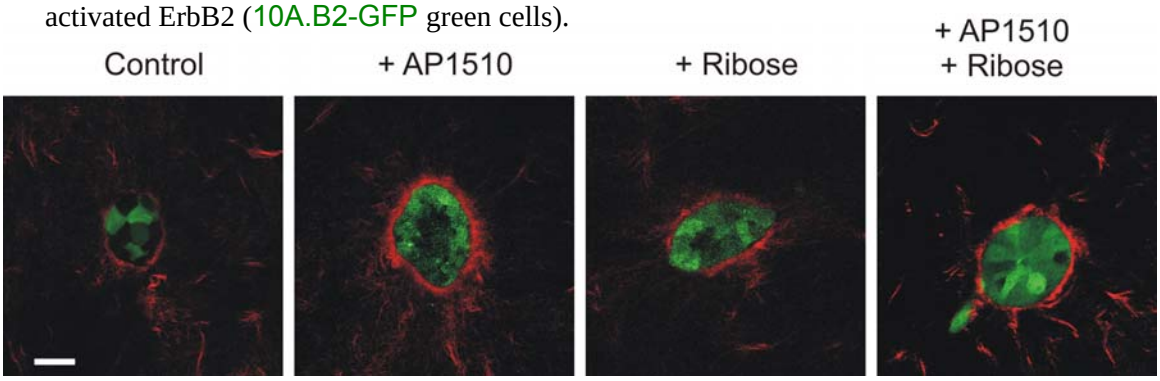

Figure 15. PI3 kinase signaling as indicated by elevated phosphoAkt (activated Akt) increases dramatically and significantly in response to matrix stiffening.

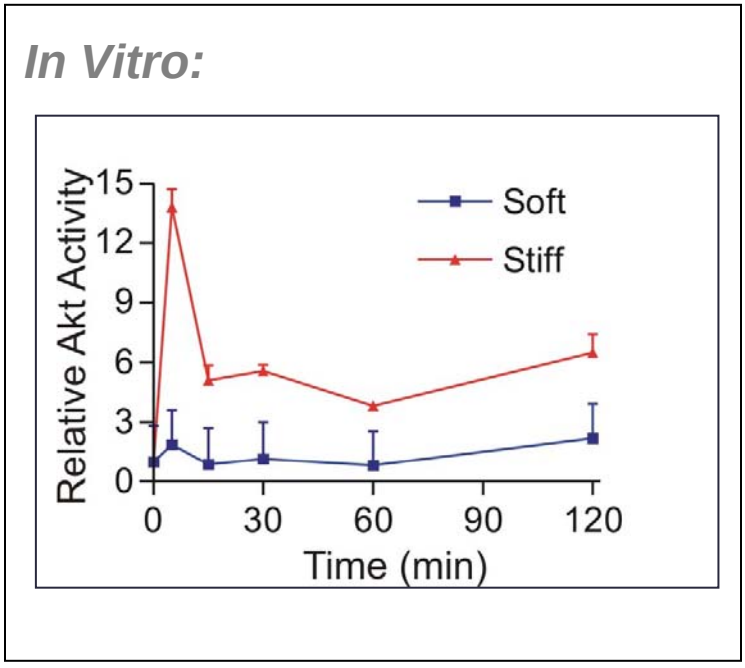

Figure 16. How might matrix force regulate PI3 kinase signaling?

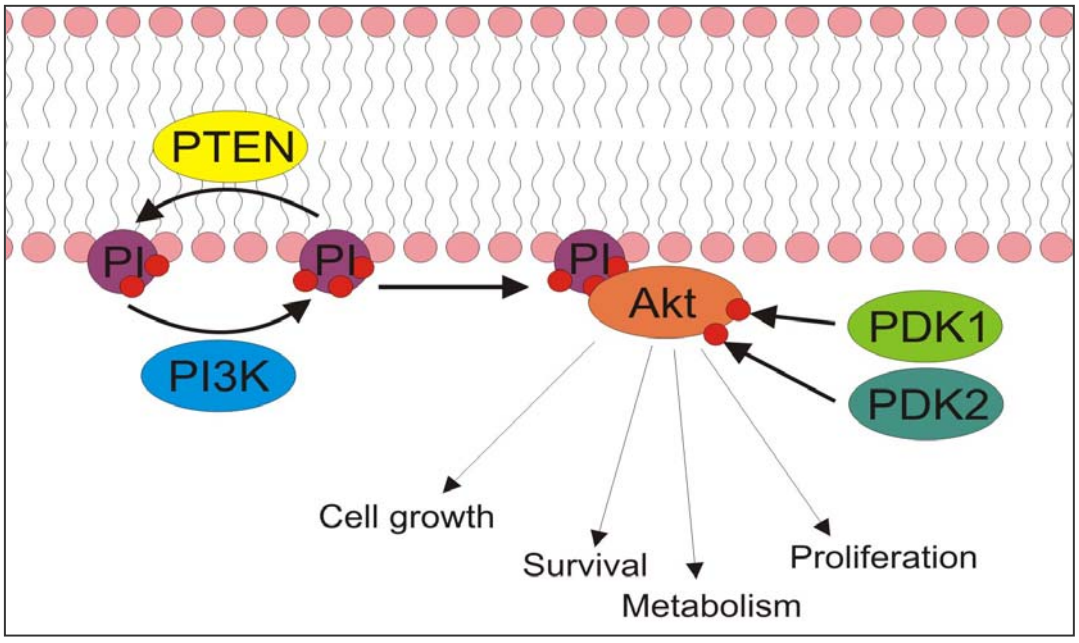

Figure 17. Matrix stiffness leads to a reduction in total PTEN protein and reduced PTEN activity in culture

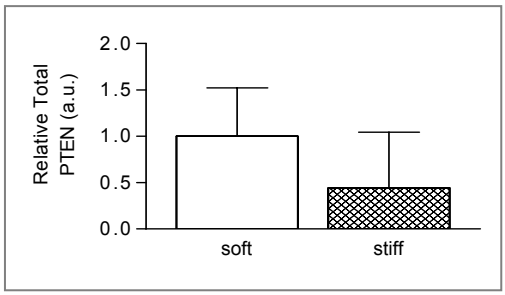

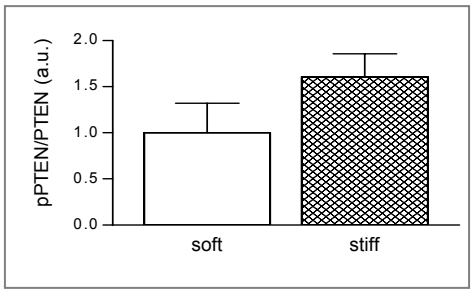

Figure 18. Matrix stiffness cooperates with oncogenes such as ErbB2 to down regulate PTEN expression and activity.

Figure 19. Matrix rigidity regulates the clonogenic survival of mammary epithelial cells exposed to toxic levels of gamma irradiation

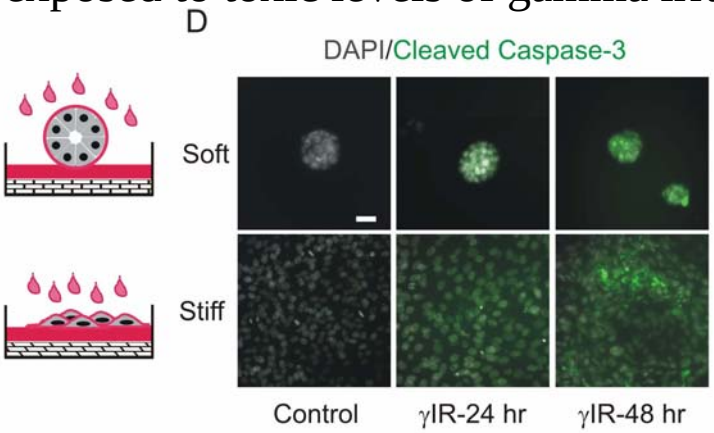

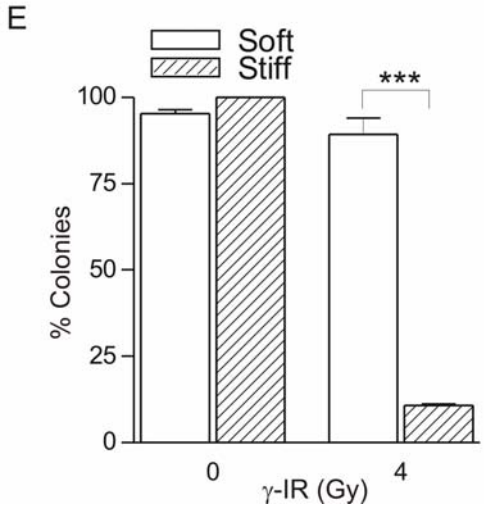

plates). Our work is significant because it clearly shows how the microenvironmental context of the cell modulates its ACUTE and CHRONIC response to a therapy. These observations have strong clinical translation.

Because of the striking phenotype we noted where matrix force can substantially alter the mammary cells responsiveness to therapy we further assessed the effect of force-dependent survival on JNK signaling. We found that force specifically enhances JNK expression and activity (Figure 20) but not p38 expression or activity (data not shown). Moreover we determined that inhibiting JNK prevents apoptosis induction in mammary epithelial cells interacting with a stiff matrix (Figure 21).To more definitively link force and JNK in cell death regulation we used a combination of pharmacological inhibitors as well as dominant negative JNK 1 and JNK 2 (which reduce the activity of endogenous JNK; Figure 21) to establish functional links between JNK signaling, force and apoptotic responsiveness of mammary tissues (see Figure 22). We are now testing whether mammary tissues engineered to ectopically express a constitutively active MEKK (which in turn activates JNK) will survive upon exposure to apoptotic stimuli even when interacting with a compliant matrix. Nevertheless, we could show that cells expressing elevated levels and activity of the RhoGTPase which exhibit high cell contractility and assemble mature focal adhesions even in the absence of matrix stiffness, also have elevated JNK activity and die even when interacting with a compliant matrix (See Figure 23). However, inhibiting RhoGTPase activity through ectopic expression of a dominant negative N19Rho significantly reduced JNK activity and rendered these same tumor structures highly resistant to apoptosis induction (see Figure 23). These results are critical because we previously showed that matrix force alters mammary cell and tissue behavior by increasing the activity of Rho (Paszek et al., 2005). We are now completing the final control experiments required to complete this body of work on force and mammary cell survival and anticipate writing and submitting a manuscript within the next 4-6 months.

Completed validation and characterization of murine fibroblasts expressing a recombinant constitutively active lysyl oxidase

Completed the creation of inducible/repressible constitutively active lysyl oxidase expression constructs (lentiviral)

Initiated work to create human fibroblast lines expressing constitutively active lysyl oxidase

Completed preliminary studies to show that murine fibroblasts expressing a constitutively active lysyl oxidase will increase the stiffness of a collagen I gel by almost 40% in just one week of culture.

Completed reproducible studies using 3D hydrogels composed of collagen I and BM to demonstrate that increasing matrix stiffness of a 3D collagen/BM hydrogel by 40% disrupts mammary tissue integrity and drives growth.

Completed reproducible studies using 3D collagen I/BM hydrogels that show that cross linked stiffening of the matrix will promote malignant transformation and invasion of "pre malignant mammary epithelial cells.

Initiated Atomic Force Microscopy measurements and studies

Preliminary studies completed on the characterization of matrix changes in the breast prior to and following malignant transformation

Figure 20. Matrix stiffness regulates the expression and activity of JNK1&2

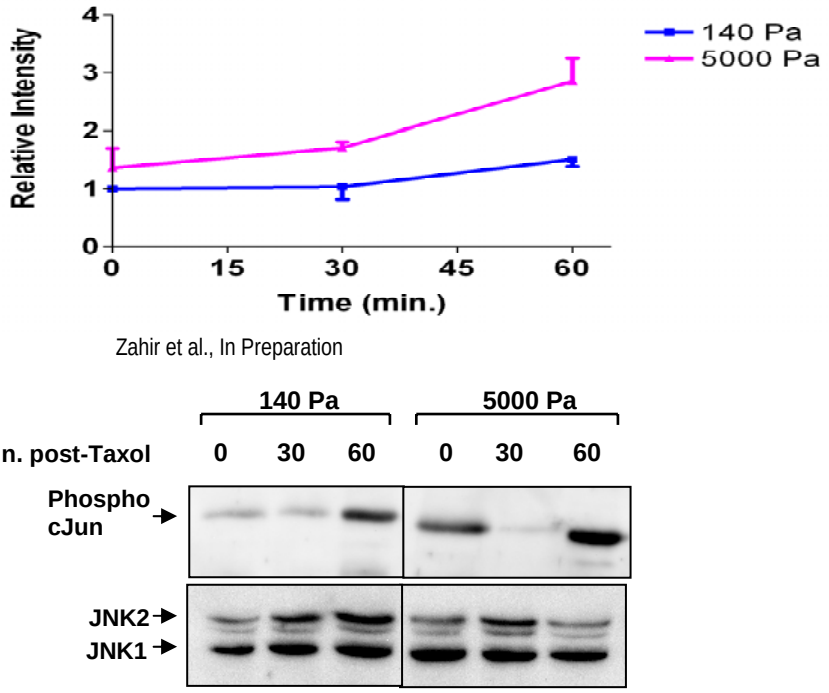

Figure 21. Matrix stiffness regulates JNK expression and activity to modulate mammary epithelial cell survival in response to chemoreagents including Taxol and immune receptor activators such as Trail.

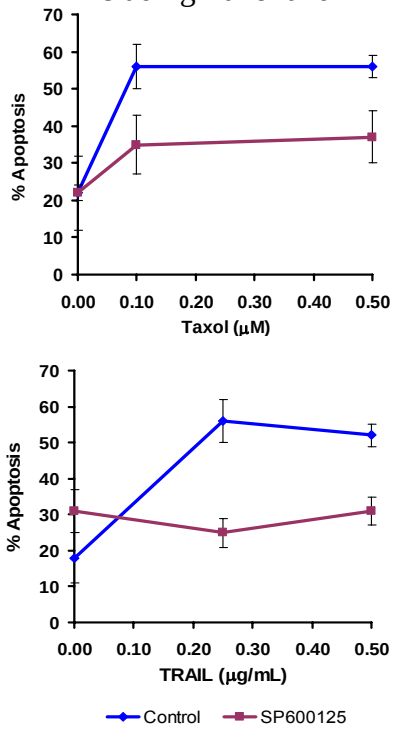

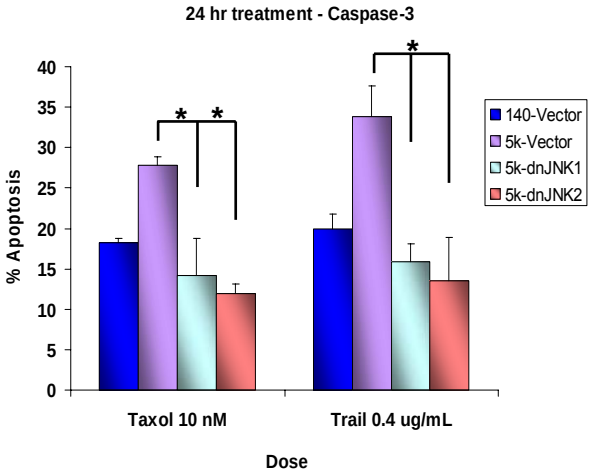

n=3; *p<0.05, **p<0.01

Figure 22. Ectopic expression of dnJNK1 or dnJNK2 reduces JNK activity in human mammary epithelial cells

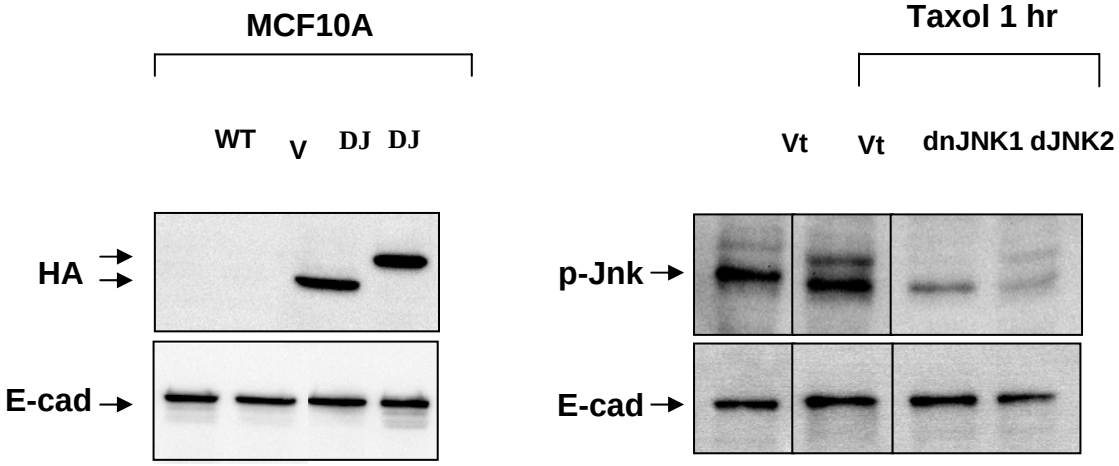

Figure 23. Cells that express elevated Rho activity exhibit enhanced focal adhesion maturation which induces cell contractility and increases JNK activity to permit cell death induction in response to an exogenous death inducer such as taxol or trail. However, reducing Rho activity through ectopic expression of N19Rho normalizes integrin adhesions or inhibiting JNK activity pharmacologically renders the mammary cells apototically resistant.

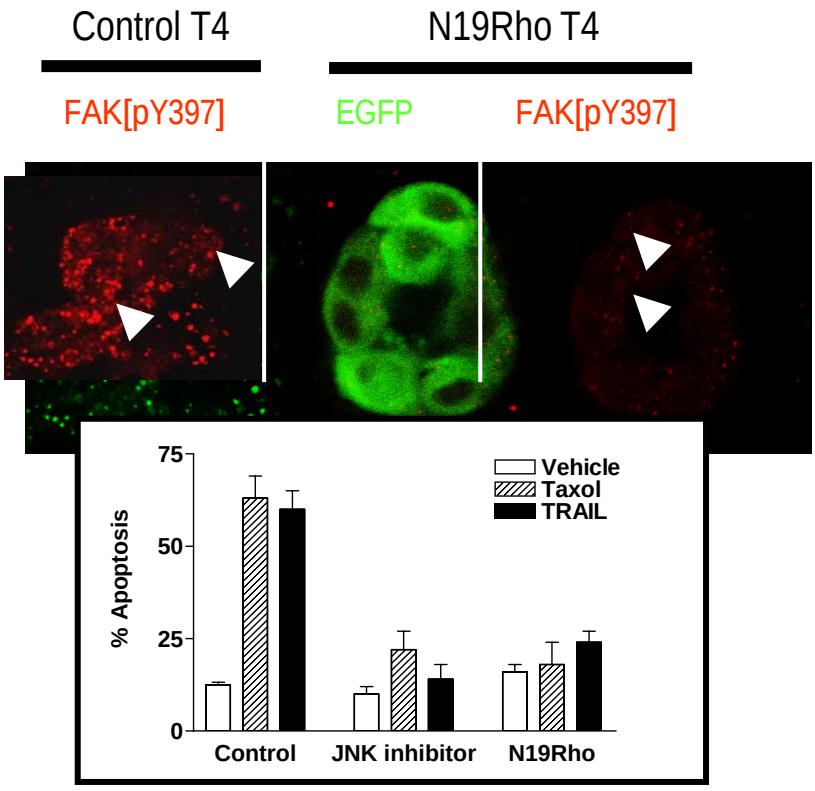

Preliminary studies conducted to assess the orientation and cross linking status of the matrix in the progressively transformed breast

Completed set up of LOX activity assays

Completed analysis of the effect of altering matrix stiffness through increasing matrix concentration and cross linking on mammary tissue aciniar morphogenesis in culture.

Completed preliminary analysis of the effect of increasing matrix stiffness through increasing matrix cross linking on cell proliferation

Completed the analysis of the effect of matrix stiffness on the apoptosis sensitivity of non transformed MECs and mammary acini structures on chemotherapies, immune receptor stimuli and gamma irradiation.

Initiated studies to explore the effect of matrix stiffness through cross linking on mammary epithelial cell survival and apoptosis resistance.

PART B.

Development of alternate synthetic 3D model systems that recapitulate the biophysical and biochemical properties of primary and metastatic breast tumor tissues. Conducted in collaboration with Drs. Wong and Leach at Boston University and University of Maryland, respectively.

In this second year of funding we have continued to develop our synthetic biomaterials to assess the effect of matrix stiffening on mammary tissue behavior in culture and in vivo. We worked together with Dr.s Wong and Leach to learn how to measure and manipulate synthetic matrix stiffness of protein conjugated poly acrylamide gels (PA gel) and peptide conjugated self assembling peptide gels (see earlier report summary). We also worked to establish new protocols to generate PVD synthetic gels cross-linked to RGD and YIGSR and collagens with MMP consensus recognition sites that permit remodelling of the synthetic matrix. We conducted experiments with the protein conjugated poly acrylamide gels over laid with purified extracellular matrix and established a workable range of peptide concentration that yields a comparable increase in matrix stiffness as we found by increasing collagen concentration. Using the peptide gels with and without the addition of reconstitute basement membrane (rBM) or purified laminin or even RGD/YIGSR conjugated gels could show how matrix stiffening modifies mammary tissue morphogenesis (summarized in the first report and published in (Paszek et al., 2005). We have continued our studies with the self assembling RGD/YIGSR conjugated peptide gels. Using the peptide gels with and without the addition of reconstitute basement membrane (rBM) or purified laminin or even RGD/YIGSR conjugated gels we could demonstrate that we could attain the same range of stiffness by increasing peptide concentration as we achieved by increasing collagen I concentration. We also found that mammary epithelial cells survive and can assemble multi cellular structures similar to mammary acini. However we determined that these peptide gels do not appear to support normal morphogenesis as the structures fail to assemble a polarized endogenous basement membrane and many of the structures appeared irregular with distorted lumens and acinar structures. The addition of exogenous rBM, laminin or even the use of RGD/YIGSR conjugated peptides failed to rescue this aberrant phenotype suggesting instead that the presentation of the matrix or the cells inability to turnover and remodel the matrix might be the key issue. Indeed, one of our collaborators has been using similar peptide gels to study effects on angiogenesis and determined that these gels do not support multicellular morphogenesis if the culture conditions require gel remodeling. Such a scenario is not

unfamiliar in the world of synthetic biomaterials which do not easily become remodeled by cells. To avoid such difficulties researchers have incorporated peptides and proteins with proteolytic residues. However, given the expense to synthesize and purified these types of peptides we are opting to develop recombinant proteins that can be proteolytically remodelled (see below).

To further explore the possibility that the absence of or aberrant matrix remodeling compromises mammary morphogenesis we initiated a comprehensive study to compare the effect of different matrices and modified matrix presentation on mammary morphogenesis of nonmalignant mammary cells. This study is close to completion and we present some of our findings here in this report. In this study we compared mammary cells that were embedded completely within a reconstituted highly compliant basement membrane (3D rBM), to those embedded within a highly compliant collagen I/basement membrane (3D Col/rBM), to those grown on top of a compliant rBM with an over lay of rBM (pseudo 3D rBM), to those grown on top of a highly compliant rBM-conjugated PA gels with and without addition of rBM or laminin-1. Although multi-cellular morphogenesis ensued under all conditions, we the structures formed under the pseudo 3D conditions were highly heterogenous in size with many formed acini exhibiting sizes that were 30-50% larger than those structures formed when the MECs were embedded within a compliant matrix. Not only were the structures heterogenous in size but they also had larger lumens and continued to proliferate and die. Because we found that MECs embedded within a compliant matrix (3D) growth arrest coincident with assembly of an endogenous basement membrane we are now exploring the role of matrix presentation and remodeling in mammary morphogenesis. These results are consistent with our observation that MECs completely embedded within the self assembled peptide gels produce matrix proteins but fail to assemble an endogenous basement membrane and do not completely growth-arrest. Current studies are now addressing this question in more detail by looking at the ability of various matrices and their presentation to regulate directed MMP activation and matrix remodeling and to examine the nature of the endogenous basement membrane structure using scanning electron microscopy. In the next six months to a year we hope to complete these studies and then to write up a manuscript for publication. The manuscript will be attached to next years progress report.

Because of the limited use of protein laminated PA gels and the difficulties we have been encountering using self assembled peptides gels have joined forces with Dr.s Wong and Leach to generate synthetic PVD gels with defined biochemical and biophysical properties. As summarized in last years report we made considerable progress with respect to the design and synthesis of the first generation of these synthetic biomaterials. We were able to show that RGD-conjugated PVD and PEG gels are able to support the viability of fibroblasts and smooth muslce cells. The first shipments of unconjugated and RGD and YIGSR-conjugated PVD and PEG gels were received from the Wong and Leach laboratory and experiments were conducted to assess mammary cell viability and adhesion. Initial studies were encouraging and demonstrated that mammary cells can adhere to these surfaces and that the can at least survive short term exposure. However, our recent data suggest that although the mammary cells can adhere well - they fail to spread and assemble focal contacts or mature focal adhesions even under highly stiff conditions. Because these results suggested that insufficient matrix ligand was available we conducted ligand concentration curves assessments. We had no success with these experiments and concluded that the nature of the peptide conjugation is likely influencing how the cells behave. We also noted that the crosslinker itself is not well tolerated by human mammary cells and have spent considerable time and energy identifying new biologically compatible cross linkers. To address the issue of peptide presentation we have opted to begin to design recombinant proteins which we intend to conjugate to the PVD and PEG gels. These types of recombinant proteins are versatile and can be designed to incorporate MMP recognition sites, pro angiogeneic cleavage products and even discoidin ligands (Raeber, Lutolf and Hubbell 2007). We anticipate that within a year we should have a tractable recombinant protein that we can use to generate versatile PEG and PVD gels with tunable stiffnesses.

We noted that the matrix becomes dramatically remodeled during malignant transformation - and that much of this remodeling is associated with a linearization and reorientation of the collagen I fibrils. Collagen reorientation and linearization can increase the apparent rigidity of the matrix that the cell experiences. Accordingly, we have begun to study the effect of heterogeneity of matrix stiffness on cell behavior. In collaboration with Dr. Joyce Wong at Boston University we have set up protocols to test the idea that differences in matrix stiffness drive cell migration to modulate cell invasion and metastasis. Indeed, a critical aspect of breast cancer is the ability of cancer cells to spread from the primary tumor to form metastases in distant locations in the body. It is the metastatic cells and tumors that most frequently acquire resistance to therapy and that result in loss of life. We showed previously that matrix stiffness compromises mammary tissue integrity by destabilizing cell-cell junctions and enhancing cell-ECM interactions to promote cell migration (Paszek et al., 2005). Because an early step in this metastatic process involves cell migration, and we loss of tissue integrity and cell invasion into the parenchyma are pre requisites for tumor metastasis, we have begun to explore the role of matrix force in tumor migration and invasion. To address this Dr. Wong has developed a novel durotaxis migration system that encompasses protein laminated gels with gradients of stiffness and computational algorithms to analyze the cells behavior using real time imaging. Indeed, while growth factors are often considered to be 'chemotactic' agents that drive cell migration, substrata with gradients in substrate compliance have revealed the 'durotactic' potential of cells, i.e. tendency to migrate in response to changes or gradients in substrate stiffness. Consistently, local variations in breast cancer tissue mechanical properties occur *in vivo,* and variations in extracellular matrix stiffness may be an important signal guiding cell behavior *in vivo*. Recent *in vitro* studies showed that fibroblasts and vascular smooth muscle cells (VSMCs) preferentially migrate towards stiffer substrates; however, much of this phenomenon, termed durotaxis, remains ill-defined (Lo et al., 2000). In collaboration with Dr. Joyce Wong at Boston University we conducted initial proof of principal studies using vascular smooth muscle cells on photopolymerized polyacrylamide hydrogels with well-defined gradients of substratum stiffness fabricated using microfluidics. The work with VSMCs demonstrated clearly that cells preferentially migrate with greater persistence towards gradients of increasing matrix stiffness (see Figure 24).

Figure 24 shows the set up of the microfluidic system. We first reported results using this system, but recently, we found that the Hertz model used for nano/microindentation is not appropriate for the soft gels that are generated using photopolymerization (Zaari et al., 2004). This is because the gels are *viscoelastic*, not elastic, which is a key assumption of the Hertz model. We were able to determine the mechanical properties using atomic force microscopy (AFM) in conjunction with tensile testing to correlate micromechanical and macromechanical observations. Baselines for cell spreading, polarization, and random motility were identified using uniform gels with stiffnesses ranging from 5-80 kPa and showed that cell spreading, polarization, and motility—evaluated quantitatively based on a persistent random walk—increased with increasing stiffness. Subsequently, we investigated VSMC response to gradients in stiffness ranging from 0-4 kPa/100 μm. Although morphology on gradient gels correlated with the absolute modulus, durotaxis—evaluated quantitatively as the tactic index for a biased persistent random walk—and orientation with respect to the gradient increased with increasing magnitude of gradient (Wong et al., 2003) (**Figure 25**). Importantly, we have defined this 'durotactic index', which now provides a framework for studying the behavior of breast cancer cells on these gradient substrata. Our observations contribute to the foundation for determining quantitative relationships between scaffold properties and cell response, elucidating insight to normal and pathologic processes, and enabling the rational design of scaffolds to interrogate the role of substrate mechanics on cell behavior.

We now intend to apply these gradient gels and analysis programs to test if this phenomenon also holds true for mammary cell invasion and metastasis. In parallel we will be using AFM to measure the

Figure 24. Schematic of photopolymerization process in microfluidic generator.

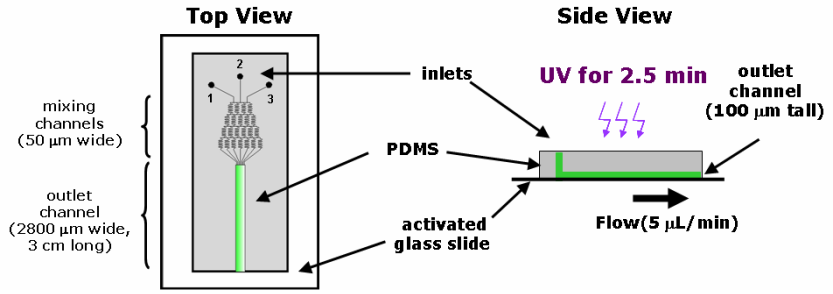

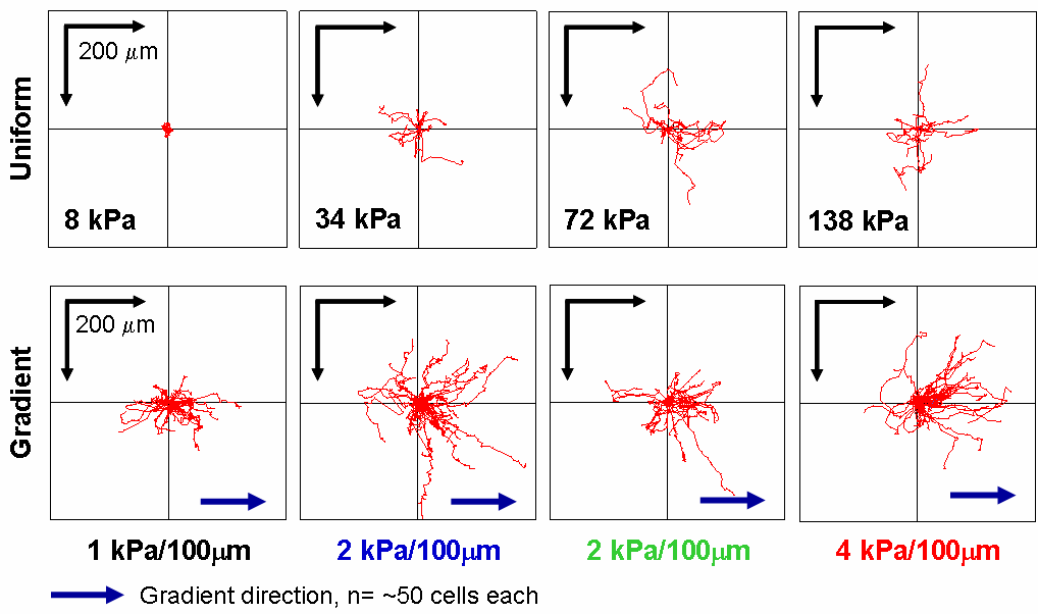

Figure 25. Wind-rose plots of cell tracks from cells on uniform gels (**top row**) and gradient gels (**bottom row**). Each line represents the path followed by an individual cell over the course of the experiment (~20 hours).

nature of the matrix forces surrounding developing breast lesions in experimental animal models. Eventually our goal is to apply these findings and strategies to the study of mammary tumor migration in 3D and then to an analysis of the invasive behavior of primary human tissue samples. Our objective is to determine if our findings could predict tumor metastasis potential in woman with early stages of breast tumors. In this respect, to date there exist little to no reliable molecular or imaging modalities to predict the metastatic potential of early stage primary human breast lesions.

- **Wong Laboratory completed** experiments showing the feasibility of generating photo-activatable PVC gels for easy manipulation of matrix stiffness in 3D.
- **Dr. Jennifer Leach visited the Weaver laboratory** and taught Weaver students and technical associate Dr. Jon Lakins how to polymerize and manipulate the PVC gels
- **Studies have now been completed** by the Weaver laboratory to assess the biocompatibility of self-assembling peptides to assess the effect of matrix stiffness on MEC behavior in 3D.
- **Successful transfer of technology and methods** from the Wong and Cam laboratories to the Weaver laboratory students and technical staff to analyze biophysical properties of gels and tissues using non confined compression and shear rheology.
- **Successful application** of 3D methods to modulate the compliance of self-assembling peptide gels in the Weaver laboratory.
- **Successfully methods establishment** to make reproducible and valid measurement of the biophysical properties of self-assembling peptide gels in the Weaver laboratory.
- **Successfully incorporation** of YIGSR and RGD peptides via stable cross-linking and transfer of self-assembling peptides from the CAM laboratory to the Weaver laboratory to test efficacy for induction of mammary morphogenesis.
- **Successful testing** of YIGSR and RGD peptide conjugated self assembled peptide gels on MEC behavior in 3D
- **Improved method to generate** PVD synthetic gels cross-linked to RGD and YIGSR peptides in Weaver and Wong laboratories.
- **Successful testing of** PVD synthetic gel biocompatibility and behavior on human MECs
- **Completed studies to assess** the gamma radiation sensitivity of single nonmalignant and tumorigenic MECs embedded within compliant rBM gels using short term viability as an end point
- **Completed studies** to assess the effect of matrix compliance on radiation induced cell death
- **Completed studies** to assess the effect of matrix compliance in 2d and 3d on clonogenic survival of normal and transformed MECs
- **Completed studies** to assess the effect of gamma radiation sensitivity of nonmalignant and tumorigenic 3D colonies MECs embedded within compliant rBM gels using short term viability as an end point.
- **Completed studies** to assess the dose dependent effect of gamma radiation on long term MEC survival ex vivo.
- **Initiated studies** to explore the molecular mechanisms whereby matrix compliance modulates the sensitivity of MECs to radiation exposure including an analysis of the role of the RhoGTPase Rho and its downstream target ROCK using pharmacological inhibitors of ROCK and Myosin II and by expressing either dominant negative N19Rho or a constitutively active V14Rho transgene
- **Initiated studies** to explore the role of JNK and MEKK signaling on MEC radiation and chemo and immune receptor sensitivity using dominant negative JNK1 and JNK2 and constitutively active MEKK

Task 2: *Develop xenograft and transgenic mouse models to test whether ECM stiffness regulates apoptotic responsiveness of mammary epithelia in vivo*

PART A. Xenograft studies to test whether ECM stiffness could regulate apoptosis responsiveness of a mammary epithelium in vivo. These studies were conducted in collaboration with Dr. Eric Bernhard from the Radiation Biology Department at the University of Pennsylvania. NOTE: The in vivo radiation studies have been postponed until the culture studies have been completed. We maintain that the culture assays are needed to demonstrate proof of principal that matrix stiffness can in fact regulate the apoptotic responsiveness of mammary tissues and also will to identify dose response criteria and putative molecular pathways that we can then focus on for our in vivo studies.

PART B. Transgenic animal studies designed to test whether ECM stiffness could influence apoptosis regulation in vivo. These studies were conducted in collaboration with Dr.s Gasser and Kissil at the University of Pennsylvania and The Wistar institute respectively.

Based upon our culture studies and published data showing how matrix force influence mammary tissue behavior through modulation of integrin adhesions we have chosen to generate a conditional beta 1 integrin clustering mutant that culture studies demonstrated recapitulates the effect of matrix force and mammary tissue behavior.

As reported in our last yearly summary encouraged by these results we proceeded to design and generate a targeting vector to generate a CRE-LOX inducible V737N beta 1 integrin mouse. We could show that we had successfully generated the targeting vector and proceeded to attempt to generate stable ES cells to generate the mouse. Several ES lines were generated with the targeting vector and initial studies verified that several of these lines do express the transgene and southern blot analysis is under way to verify these findings. Due to the re location of my laboratory we chose to hold off on the generation of the breeder colony until such time as our group had successfully relocated to UCSF in San Francisco and we had established animal protocols and our DOD Scholar award was duly transferred.

However, in lieu of our exciting and encouraging culture results - we opted to conduct xenograft studies to determine if promoting integrin clustering in nonmalignant and pre malignant mammary tissue like structures would promote a tumor like behavior in vivo. Accordingly, we obtained the pre malignant MCF10AT line from collaborators in Michigan. The MCF10AT line was generated from the parental MCF10A nonmalgnant immortalized human mammary epithelial cells through exogenous expression of Ras and following in vivo xenograft manipulations. This line - yields premalignant MECs when injected into nude mice. Analogous to ductal carcinoma in situ, these pre malignant colonies/structures remain embedded within a basement membrane and have a layer of myoepithelial cells around their basal domains. More importantly these structures do not invade into the parenchyma which is a hallmark of malignancy in vivo. When we injected these lines into nude mice we were able to successfully recapitulate this DCIS-like phenotype. More importantly, when we generated MCF10AT lines that expressed the V737N auto clustering beta 1 integrin these cells became fully transformed as evidenced by increased growth, loss of basement membrane deposition and invasion into the surrounding extracellular stroma (see Figure 26). We are still completing the analysis of these studies but are quite encouraged by these results and believe that this heralds well for our future studies using our transgenic V737N mouse model.

Based upon our observations with collagen organization and processing including elevated lysyl oxidase levels prior to transformation in our transgenic mice with stiffer mammary glands - we are also in the midst of designing a targeting vector to generate a conditional lysyl oxidase knockout mouse. We hope that by the next report deadline that we will be able to report the successful design and generation of this targeting vector and hopefully the first founder mice will be generated. However, we also

Figure 26. Integrin clustering via ectopic expression of the V737N b1 integrin in the pre malignant MCF10AT cells promotes malignant transformation in vivo in a xenograft model.

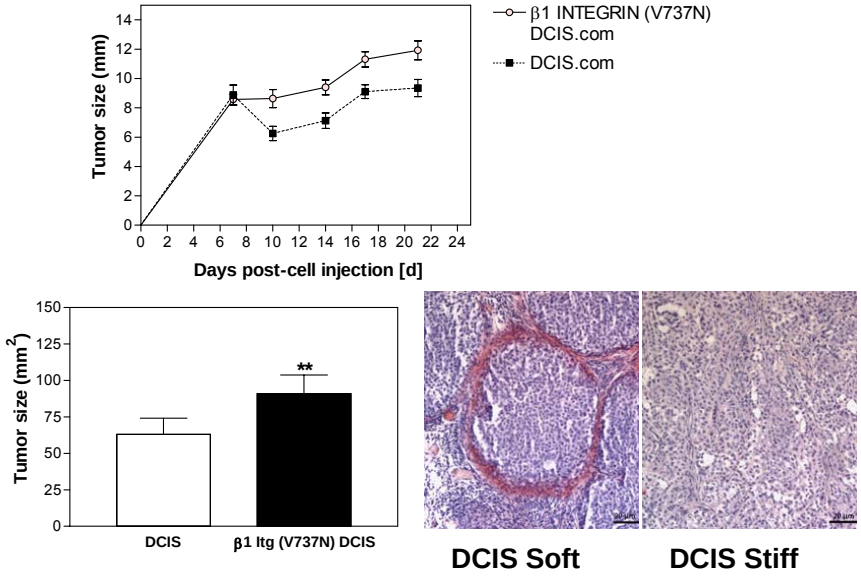

To be continued… CRE-LOX V737N β1 integrin mouse……..

initiated the first of a set of studies in the transgenic Her2/neu mice to ascertain whether or not inhibiting lysyl oxidase activity could reduce matrix stiffness and if so if this would/could inhibit tumorigenesis in vivo. In consultation with Dr. Rebecca Wells we obtained a compound called BAPN which was developed several years ago as a specific lysyl oxidase inhibitor. The inhibitor was generated to treat chronic asthma which is functionally linked and associated with increased lysyl oxidase mediated cross linking of the lung collagens. While these studies were still ongoing at the time that this report was being prepared (i.e. prior to November 2006) - we could already observe a significant reduction in palpable tumors in the BAPN treated transgenic mice. We look forward to analyzing these data and reporting the outcome in the next progress report.

- **Preliminary validation of successful generation** of CRE-LOX β1 integrin cluster mutant expressing mouse embryonic stem cells to create transgenic founder mice using RT-PCR.
- **Xenograft proof of principal experiment** completed to show that ectopic clustering of beta 1 integrin in pre malignant mammary epithelial cells can promote malignant transformation.
- **Obtained BAC vectors** containing lysyl oxidase gene for generating targeting vector for conditional lysyl oxidase knockout mouse
- **Initial design of** lysyl oxidase gene targeting vector for generating conditional lysyl oxidase knockout mouse

Task 3: *Build a computational model that can predict how changes in ECM compliance could influence integrin-dependent apoptosis responsiveness of mammary epithelia and query this model with clinical data*.

PART A. To assemble and generate cell biology and published data required for basic computational model. These studies are currently being conducted in collaboration with Dr. Hammer from the Department of Bioengineering at the University of Pennsylvania and Dr. Tobias at the University of Pennsylvania Bioinformatics Center.

In this second year of funding we have continued with our cell biology experimentation which will be coopted to generate our computational models. In particular we have conducted in depth studies to distinguish the effect of ligand binding with erk, fak and pi3 kinase-dependent signaling. These studies are being incorporated into one of our deterministic models.

- **Successful completion** of analysis of effect of matrix compliance/stiffness on ERK signaling in natural and synthetic matrices of varying compliance
- **Completion of preliminary studies** to assess the effect of varying matrix compliance/stiffness on JNK signaling
- **Completion of preliminary studies** to assess the effect of varying matrix compliance/stiffness on PI3 kinase signaling.

PART B. Generate a simple cell adhesion computational model based upon published values from the literature and data generated using culture models.

We have made excellent progress towards the derivation of in silico deterministic models that recapitulate and predict the behavior of normal and transformed mammary tissue in response to matrix force (stiffness). To begin with we generated a deterministic model that could predict growth factor dependent ERK signaling which is one component of integrin signaling shared with growth factor receptors that we could show is definitively force regulated. This work has been accepted for publication and has been attached to the current progress report. Studies are also nearing completion in which we

have integrated this model with integrin-dependent adhesion and this work should be ready for submission for peer reviewed publication later on in the fall of 2007. We hope to be able to attach our published manuscript for review with next years report. Most importantly, the adhesion/growth factor receptor model is being tested experimentally to determine how it correlates/predicts our experimental data (see above). Thus far we are pleased to report that the in silico model has yielded encouraging results.

- **Successful generation** of in silico deterministic model that predicts growth factor dependent ERK signaling and that concord well with published literature - **publication in press.**

- **Successful generation** of in silico deterministic model that incorporates integrin-dependent adhesion and ligand binding density into the growth factor signaling modality listed above.

- **Progress made towards** incorporating integrin clustering modality into the growth factor/integrin deterministic model

PART C. Incorporate mechanical force values and assumptions into the basic adhesion model.

In parallel with the former two models discussed above we have undertaken the assembly of a highly ambitious deterministic model that incorporate force-dependent integrin clustering, actin cytoskeletal remodeling and erk signaling is being generated. However, this latter model still requires a quite a bit of additional work and will take much longer to yield definitive results. **These are future studies will be reported in future Annual Reports as reportable outcomes.**

PART D. Initiate modeling studies using micro array data sets from the cell culture models developed by my group. These studies are being conducted by the Weaver laboratory in collaboration with Dr. Dan Hammer of the Bioengineering Department at the University of Pennsylvania and Dr. John Tobias in the University of Pennsylvania Bioinformatics Center. These studies have been postponed until such time as we can reproducibly generate tractable 3D synthetic matrices with calibrated stiffness. Once these are available we will once again place a large amount of effort towards achieving this goal.

PART E. Initiate pilot studies to analyze micro array data sets and clinical samples from neoadjuvant breast cancer clinical trial data using a simple model generated using gene data from the culture system. These are studies that will be initiated in a few years.

Task 4: *Develop non-invasive imaging tools that could be used to monitor changes in ECM stiffness or stiffness-induced changes in mammary tissue phenotype.*

PART A. Proof of principal studies for imaging sensitivity using 3D culture models. These are studies that will be initiated in a few years.

PART B. Set up and initiate screening trials with peptide libraries for identification of novel stiffness markers in the ECM.

Originally we envisioned generating novel peptide antibodies that would detect modifications in collagen organization indicative of a stiffer matrix and then apply quantum dot technology and standard imaging approaches to visualize growing tumors in mice. As an alternative however, we have begun to work with Dr. Paul Barbone at Boston University to explore the possibility of using ultrasound imaging

Figure 27A. Reconstructed shear modulus of a thin, inhomogeneous square sheet. (Barbone and Oberai, Physics in Medicine and Biology, 2007) –
Figure 27B. Human breast with small, palpable tumor at arrowhead. (Kruse et al *Phys. Med. Biol* 2000)

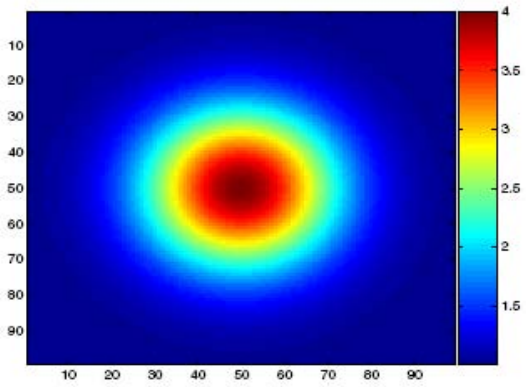

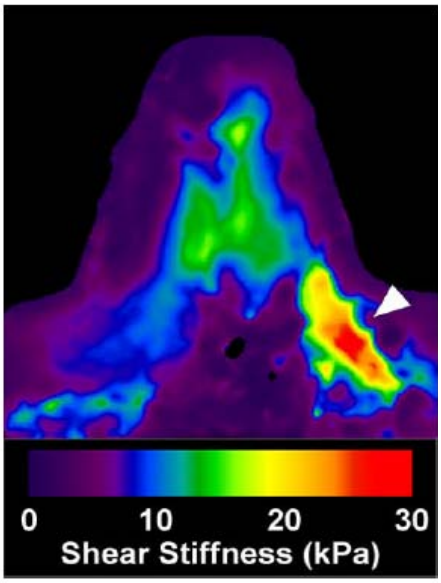

Figure 28. Ultra sound image (left) showing mammary gland embedded within gelatin/magnetic bead matrix. Ultra sound imaging elastography (right) of her2/neu pre malignant breast lesion showing highly stiffened regions (orange to red) within breast tissue.

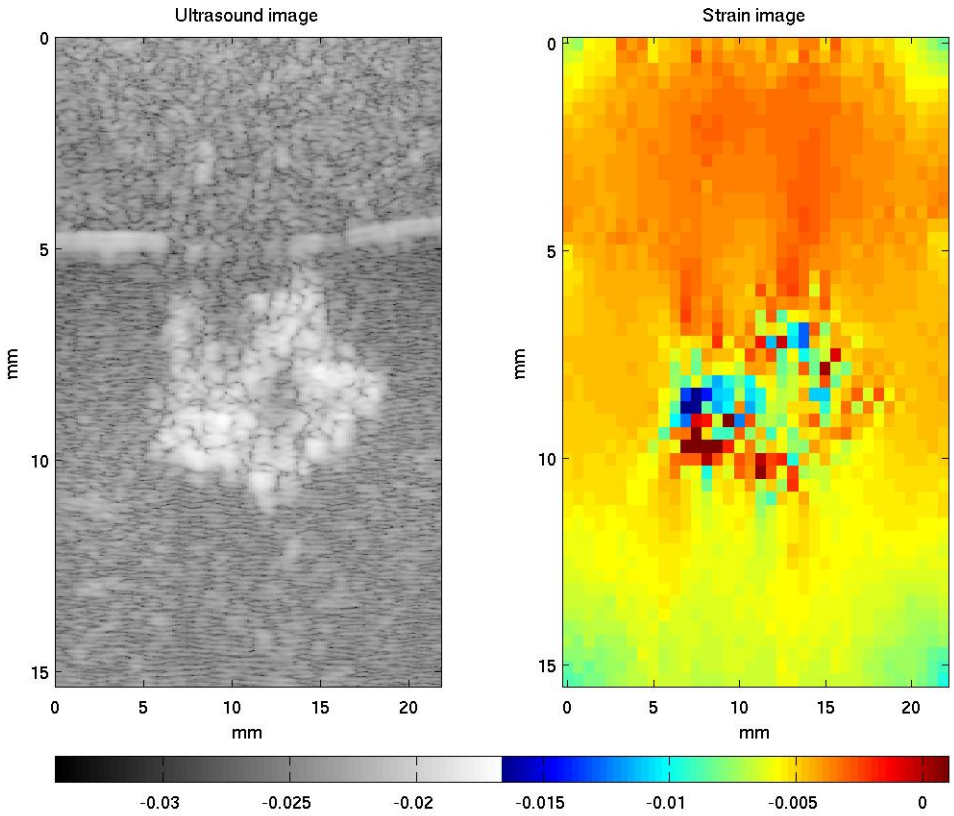

elastography. This approach has been used most successfully to image and characterize breast malignancies in the clinic. In addition to ultra sound imaging elastography MRC elastography has also been successfully used. As a first step we set up collaborations with Dr. Barbone and began to send him mouse mammary glands harboring small but palpable breast tumors. The procedure involves embedding the mammary gland harboring the tumor inside of a gelatin matrix or ghost. The ghost has embedded within it micro beads that provide a stiffness differential the can be used to distinguish the mammary gland stiffness from the surrounding gelatin. Figure 27; left shows a typical phantom image used to calibrate the imaging elastography image. This approach has been used quite successfully for human breast tumors (see Figure 27; right). After a lot of trial and error we were able to successfully embed the gland within the gelatin ghost and obtain rudimentary images (Figure 28). Unfortunately the current software lacks the necessary resolution to accurately analyze mouse breast tumors because the current programs have been designed for much large specimens. Nevertheless, the image illustrates that the principal can be applied to assess the physical properties of breast lesions and the image does show that the mammary gland with the lesion can be detected as an area of increased stiffness. We are confident that once the system and software have been optimized, we will be able to increase the resolution and sensitivity of the approach and hopefully begin to work with hardware specialists to develop a small animal imaging system. While it might seem inappropriate to generate/develop an imaging capability to assess stiffness changes in the transformed breasts of mice - the method if established would help to establish stiffness as a measureable effect of breast tumorigenesis. Once established this type of protocol would be quite important for future work aimed at clarifying mechanisms that regulate breast stiffness and treatment responsiveness. However, we do concede that in all likelihood the work conducted in this grant proposal will end up being applied to excised breast tissue but will hopefully lay the foundation for acquiring the funding required to continue the studies. The phage display library screens to identify antibodies that would/will detect alterations in collagen linked to stiffening have been placed on hold until such time as we can better characterize and quantify which collagen modification drives the stiffening of the breast tissue.

Reportable Outcomes:

A. Manuscripts

1. Johnson, K.R., Leight, J.L., and **Weaver, V.M.** (2007) Demystifying the Effects of a Three-Dimensional Microenvironment in Tissue Morphogenesis. *Methods in Cell Biology:* Vol. 83, 539-577.

2. Hebner, C., **Weaver, V.M**. and Debnath, J. (2008) Modeling Morphogenesis and Oncogenesis In Three Dimensional Breast Epithelial Cultures, *Annual Reviews of Pathology*: Mechanisms of Disease. In Press.

3. Kass, L., Erler, J.T., Dembo, M., **Weaver, V.M.** Matrix form and function regulate mammary tissue behavior. Review article *The International Journal of Biochemistry and Cell Biology*/Cells in Focus. In Press.

4. Yee, K.L., **Weaver, V.M.,** and Hammer, D. (2007) Integrin-mediated Signaling through the MAP-kinase Pathway. *IET Systems Biology*. Accepted.

5. Friedland. J.C., Lakins, J.N., Kazanietz, M.G., Chernoff, J., Boettiger, D. and **Weaver, V.M.** (2007) α6β4 integrin activates Rac-dependent p21-activated kinase 1 to drive NFκ B-dependent apoptosis resistance in 3D mammary acini. *Journal of Cell Science*. In Press.

6. Isenberg, B.C., DiMilla, P.A., Walker, M., Kim, S.Y. and Wong, J.Y. Vascular smooth muscle cell durotaxis depends on substrate stiffness gradient strength. *Biophysical Journal,* Submitted.

B. Abstracts

1. Johnson, K.R., Kass, L., Zahir, N., Gasser, D., Gefen, A., Margulies, S.S., and **Weaver, V.M.** Tissue stiffness cooperates with ErbB2 to drive malignant transformation. IME Symposium, May 2006 (Poster Presentation)

2. Nestor, K.M., Lakins, J.N., Imbalzano, A.N., Nickerson, J.A., and **Weaver, V.M.** Chromatin Remodelers: Forcing the Genome. University of Massachusetts Medical School Worcester, MA, August 2006 (Poster Presentation)

3. Gilbert, P.M., Unger, M.E., Lakins, J.N., Gbegnon, M.K., Clemmer, V., Colligan, T.A., Benezra, M., Naylor, T., Licht, J.D., Boudreau, N.J., Weber, B.L., **Weaver, V.M.** HoxA9 modulates the breast tumor phenotype through BRCA1 regulation. Annual CAMB symposium, Philadelphia, PA, October 2006. (Poster Presentation)

4. Johnson, K.R., Kass, L., Zahir, N., Gasser, D., Gefen, A., Margulies, S.S., and **Weaver, V.M.** Tissue stiffness cooperates with ErbB2 to drive malignant transformation. BMES annual meeting, Chicago, IL, October 2006. (Poster presentation)

5. Kaiser, C., Rozenberg, G., Paszek, M., Dembo, M., Hammer, D., and **Weaver, V.M.** Force, α5β1-integrin and breast cancer metastasis. BMES annual meeting, Chicago, IL, October 2006. (Poster Presentation)

6. Leight, J.L., Friedland, J.C., Zahir, N., Lakins, J.N., and **Weaver, V.M.** Spatial-mechanical regulation of Rac-Pak-JNK survival and breast tumorigenesis. BMES annual meeting, Chicago, IL, October 2006. (Poster Presentation)

7. Yee, K.L., and Hammer, D. A Computational Model of Integrin Clustering and MAPK Activation. BMES annual meeting, Chicago, IL, October 2006. (Poster Presentation)

8. Zahir, N., Leight, J.L., Lakins, J.N., Alston-Mills, B., and **Weaver, V.M.** Force-dependent JNK activation promotes therapeutic responsiveness of a mammary epithelium. BMES annual meeting, Chicago, IL, October 2006. (Poster presentation)

C. Oral Meetings Presentations:

1. **Weaver, V.M.,** Form, Force and Fate, Invited Symposium Speaker, Annual Basic Science Colloquium on Cell Polarity in Morphogenesis and Cancer, Northwestern University, March 24, 2006, Evanston, IL.

2. **Weaver, V.M.** The role of force and matrix organization in malignant transformation, Invited Major Symposium Speaker in the "Tumor Microenvironment session," at the 97th American Association for Cancer Research, April 4, 2006, Washington, DC.

3. JY Wong, Deconstructing the Cell-Biomaterial Interface: Lessons and Challenges in Vascular Tissue Engineering and Targeted Delivery, Keynote Speaker, Biophysical Chemistry Division,

Halifax CSC Meeting 89th Canadian Chemistry Conference and Exhibition, May 2006, Halifax, Nova Scotia, CANADA

4. Gilbert, P.M., Zahir, N., Paszek, M.J., Johnson, K.R., Rozenberg, G.I., Sziemenski, A., and **Weaver, V.M.** Three-dimensional microenvironment and breast cancer progression. In Vitro Biology Meeting, Minneapolis, MN, June 2006.

5. **Weaver, V.M.** Spatial-mechanical regulation of mammary morphogenesis and malignancy, Invited Symposium Speaker, EMBO conference on Breast Cancer, June 6, 2006, Dublin, Ireland.

6. **Weaver, V.M.** Force and the third dimension, Invited Symposium Speaker, Gordon Conference on Signaling by Adhesion Receptors, June 28, 2006, Mount Holyoke College, MA.

7. **Weaver, V.M.**, A Biophysico-Computation Perspective of Breast Cancer Pathogenesis and Treatment Response, Speaker, DOD BCRP LINKS Meeting, July 21, 2006, Baltimore, MD.

8. **Weaver, V.M.** Spatial-Mechanical Regulation of Morphogenesis, Malignancy and Therapeutic Responsiveness, Invited Symposium Speaker, CELLutions SUMMIT, August 16, 2006, Boston, MA.

9. **Weaver, V.M.** Spatial-mechanical Regulation of epithelial morphogenesis and malignancy, Invited Symposium Speaker, HMRI Conference on Translational Cancer Research: Molecular Mechanisms and Implications for Treatment, September 22, 2006, Newcastle City Hall, NSW, Australia.

10. Gilbert, P.M., Unger, M.E., Lakins, J.N., Gbegnon, M.K., Clemmer, V., Colligan, T.A., Benezra, M., Naylor, T., Licht, J.D., Boudreau, N.J., Weber, B.L., **Weaver, V.M.** HoxA9 modulates the breast tumor phenotype through BRCA1 regulation. Annual CAMB symposium, Philadelphia, PA, October 2006.

11. **Weaver, V.M.** Forcing Cell Shape and Fate in the 3rd Dimension, Invited Symposium Speaker, Cell Press/MGH Biology of Shape, October 27, 2006, Barcelona, Spain.

12. **Weaver, V.M.** Force and malignant transformation, Invited Symposium Speaker, 37th International Symposium of the Princess Takamatsu Cancer Research Fund, November 14, 2006, Tokyo, Japan.

D. **Invited Institutional Presentations:**

1. **Weaver, V.M.** A Biophysical Perspective of Mammary Gland Development and Tumorigenesis, Invited Seminar Speaker, The Cancer Institute of New Jersey, February 22, 2006, New Brunswick, NJ.

2. **Weaver, V.M.** Form, Force and Fate, Invited Seminar Speaker, NIH Optical Imaging Special Interest Group (SIG), March 15, 2006, Bethesda, MA.

3. **Weaver, V.M.** Spatial-mechanical Regulation of Mammary morphogenesis, malignancy and tumor therapy, Invited Seminar Speaker, Divisions of Cancer Biology and Molecular Oncology,

Department of Medicine, Evanston Northwestern Research Institute, March 23, 2006, Northwestern University, Evanston, IL.

4. **Weaver, V.M.,** Forcing Cell Fate, Invited Speaker, Department of Oncology, Lombardi Comprehensive Cancer Center, March 31, 2006, Georgetown University, Washington, D.C.

5. Wong, J.Y. Biomaterials for Early Detection and Treatment of Cardiovascular Disease, Invited Speaker, Workshop and Summer School in Cell and Tissue Engineering, July 1-8, 2006, Belgrade, SERBIA.

6. **Weaver, V.M.** Survival and Force in the 3rd Dimension, Invited Seminar Speaker, Peter Mack Cancer Center, September 20, 2006, Melbourne, NSW, Australia.

7. **Weaver, V.M.** Forcing Signaling and Cell Fate in the 3rd Dimension, Invited Graduate Student Seminar Speaker, Cancer Biology/ Tumor Biology Program, October 3, 2006, Stanford, CA.

8. **Weaver, V.M.** Forcing Cell Fate in the 3rd Dimension, Invited Speaker, MARC U*STAR/Howard Hughes Medical Institute Undergraduate Scholars Program Seminar Series, Meyerhoff Scholarship Program, UMBC, October 12, 2006, Maryland, MD.

Progress Summary and Conclusions

In this 9 month period of the second year of funding of this DOD BCRP Era of Hope Scholar award project we have continued to make good progress on all aspects of the work objectives outlined in the original grant proposal. Our most encouraging results pertain to the identification of parameters and pathways potentially linked to matrix remodeling and breast stiffening during malignant transformation. Of these parameters we have identified first increased lysyl oxidase mediated collagen cross linking and integrin clustering and focal adhesion maturation as two key events that precede malignant transformation in the breast and that appear to contribute to tumorigenesis. In the next year we will be gearing up in earnest to test the role of these two molecular changes using combinations of culture models and animal models and manipulations. In this regard, because of the impending relocation to UCSF we have suspended the generation of our transgenic mouse lines until next year. We have almost completed our in vitro studies to explore the role of matrix force in multi drug resistance and have made enouraging progress towards identifying tractable molecular pathways contributing to this phenotype. In the next year or two we hope to elaborate on these molecular signaling pathways using more sophisticated culture models that we are in the process of developing and testing. We also will be moving into animal models. With respect to the generation of engineered natural and synthetic matrices to study the role of force in mammary tumorigenesis we have continued with our work and have identified methods to generate controlled gradients of matrix stiffening that we believe recapitulate the matrix microenvironment in vivo. We continue to develop the technology to manipulate and quantify the biophysical and biochemical properties of these matrices and anticipate that within the next year or two we will have been able to apply these systems both in culture and in vivo to study the role of force in breast tumorigenesis and therapy response. Regarding our in silico modeling efforts - this past year has proved productive with one paper already in press that models growth factor dependent ERK signaling and another one being prepared for publication that incorporates integrin adhesion and clustering into this same model. These established deterministic models are now being tested experimentally and we have begun to generate/calculate an additional model that incorporates the role of matrix mediated physical force and acto myosin generated contractility into these models. However, we realistically believe that the establishment of this latter model will likely take quite a while to perfect. Although we intend to continue with our phage display approach to identify tractable imaging targets that reflect

matrix stiffening in vivo as an alternative approach we have begun to explore the feasibility of using imaging elastography and have made encouraging progress towards this goal. Over the next few years we hope to continue developing this approach in parallel with our quantum dot imaging efforts. Finally, due to the success of the work we have achieved over the past several years I have been recruited to the University of California at San Francisco as the new director for the newly established center for bioengineering and tissue regeneration in the department of surgery. The objective of the center is to foster quantitative approaches to clinically relevant issues including cancer diagnosis and therapy. Mid 2006 I agreed to the offer and relocated my group to UCSF San Francisco December 2006. Accordingly, we are currently in the process of transferring this DOD Scholar award from the University of Pennsylvania to UCSF. It is noteworthy that I have already begun intensive collaborations with several bioengineering colleagues at UCSF, continue collaborating with colleagues in engineering and physics at University of Pennsylvania and have expanded/extended my cross disciplinary research program as the direct result of this new position. In addition, due to the dynamic and highly interactive breast cancer community at UCSF, Stanford and in Berkeley my group now has access to a lively group of colleagues all focused on studying breast cancer. Through my interactions with my colleagues in the San Francisco Bay area my group has already gained access to several highly useful mouse models as well as clinical collaborations. Most importantly, my colleague within the department of Surgery at UCSF is Dr. Laura Esserman with whom I now am in the process of establishing a fruitful and clinically important collaboration.

References:

Bershadsky, A. D., Balaban, N. Q. and Geiger, B. (2003). Adhesion-dependent cell mechanosensitivity. *Annu Rev Cell Dev Biol* **19**, 677-95.

Geiger, B., Bershadsky, A., Pankov, R. and Yamada, K. M. (2001). Transmembrane crosstalk between the extracellular matrix--cytoskeleton crosstalk. *Nat Rev Mol Cell Biol* **2**, 793-805.

Grinnell, F. (2003). Fibroblast biology in three-dimensional collagen matrices. *Trends Cell Biol* **13**, 264-9.

Kass, L., Erler, J. T., Dembo, M. and Weaver, V. M. (In progress). Matrix form and function regulate mammary tissue behavior. In Progress. *The International Journal of Biochemistry and Cell Biology/Cells in Focus*.

Krouskop, T. A., Wheeler, T. M., Kallel, F., Garra, B. S. and Hall, T. (1998). Elastic moduli of breast and prostate tissues under compression. *Ultrason Imaging* **20**, 260-74.

Lewis, J. M., Truong, T. N. and Schwartz, M. A. (2002). Integrins regulate the apoptotic response to DNA damage through modulation of p53. *Proc Natl Acad Sci U S A* **99**, 3627-32.

Lo, C.M., H.B. Wang, M. Dembo, and Wang, Y.L. (2000) Cell movement is guided by the rigidity of the substrate. *Biophys J* **79**, 144-52.

Paszek, M. J. and Weaver, V. M. (2004). The tension mounts: mechanics meets morphogenesis and malignancy. *J Mammary Gland Biol Neoplasia* **9**, 325-42.

Paszek, M. J., Zahir, N., Johnson, K. R., Lakins, J. N., Rozenberg, G. I., Gefen, A., Reinhart-King, C. A., Margulies, S. S., Dembo, M., Boettiger, D. et al. (2005). Tensional homeostasis and the malignant phenotype. *Cancer Cell* **8**, 241-54.

Plewes, D. B., Bishop, J., Samani, A. and Sciarretta, J. (2000). Visualization and quantification of breast cancer biomechanical properties with magnetic resonance elastography. *Phys Med Biol* **45**, 1591-610.

Samani, A., Bishop, J., Luginbuhl, C. and Plewes, D. B. (2003). Measuring the elastic modulus of ex vivo small tissue samples. *Phys Med Biol* **48**, 2183-98.

Taylor, S. T., Hickman, J. A. and Dive, C. (2000). Epigenetic determinants of resistance to etoposide regulation of Bcl-X(L) and Bax by tumor microenvironmental factors. *J Natl Cancer Inst* **92**, 18-23.

Truong, T., Sun, G., Doorly, M., Wang, J. Y. and Schwartz, M. A. (2003). Modulation of DNA damage-induced apoptosis by cell adhesion is independently mediated by p53 and c-Abl. *Proc Natl Acad Sci U S A* **100**, 10281-6.

Unger, M. and Weaver, V. M. (2003). The tissue microenvironment as an epigenetic tumor modifier. *Methods Mol Biol* **223**, 315-47.

Weaver, V. M., Lelievre, S., Lakins, J. N., Chrenek, M. A., Jones, J. C., Giancotti, F., Werb, Z. and Bissell, M. J. (2002). beta4 integrin-dependent formation of polarized three-dimensional architecture confers resistance to apoptosis in normal and malignant mammary epithelium. *Cancer Cell* **2**, 205-16.

White, D.E., Kurpios, N.A., Zuo, D., J.A. Hassell, Blaess, S., Mueller, U., Muller, W.J. (2004) Targeted disruption of beta-1-integrin in a transgenic mouse model of human breast cancer reveals an essential role in mammary tumor induction. **6**, 159-70.

Wong, J.Y., Velasco, A., Rajagopalan, P., and Pham, Q. (2003) Directed movement of vascular smooth muscle cells on gradient compliant hydrogels. *Langmuir*, **19**, 1908-13.

Zaari, N., Rajagopalan, P., Kim, S.K., Engler, A., and Wong, J.Y. (2004) Photopolymerization in microfluidic gradient generators: Microscale control of substrate compliance to manipulate cell response. Advanced Materials, **16**, 2133-37.

Zahir, N. and Weaver, V. M. (2004). Death in the third dimension: apoptosis regulation and tissue architecture. *Curr Opin Genet Dev* **14**, 71-80.

Appendices

Manuscripts

Johnson, K.R., Leight, J.L., and **Weaver, V.M.** (2007) Demystifying the Effects of a Three-Dimensional Microenvironment in Tissue Morphogenesis. Methods in Cell Biology: Vol. 83, 539-577.

Friedland. J.C., Lakins, J.N., Kazanietz, M.G., Chernoff, J., Boettiger, D. and **Weaver, V.M.** (2007) α6β4 integrin activates Rac-dependent p21-activated kinase 1 to drive NFκ B-dependent apoptosis resistance in 3D mammary acini. Journal of Cell Science. In Press.

Yee, K.L., **Weaver, V.M.,** and Hammer, D. (2007) Integrin-mediated Signaling through the MAP-kinase Pathway. IET Systems Biology. In Press.

Kass, L., Erler, J.T., Dembo, M., **Weaver, V.M.** Matrix form and function regulate mammary tissue behavior. Review article The International Journal of Biochemistry and Cell Biology/Cells in Focus. In Press.

Hebner, C., **Weaver, V.M**. and Debnath, J. (2008) Modeling Morphogenesis and Oncogenesis In Three Dimensional Breast Epithelial Cultures, Annual Reviews of Pathology: Mechanisms of Disease. In press.

CHAPTER 23

Demystifying the Effects of a Three-Dimensional Microenvironment in Tissue Morphogenesis

Kandice R. Johnson,[⋆,†] Jennifer L. Leight,[⋆,†] and Valerie M. Weaver[⋆,‡] Au1

[⋆]Institute for Medicine and Engineering
University of Pennsylvania
Philadelphia, Pennsylvania 19104

[†]Department of Bioengineering
University of Pennsylvania
Philadelphia, Pennsylvania 19104

[‡]Department of Pathology
University of Pennsylvania
Philadelphia, Pennsylvania 19104

0091-679X/07 $35.00
DOI: 10.1016/S0091-679X(07)83023-8

Abstract

Tissue morphogenesis and homeostasis are dependent on a complex dialogue between multiple cell types and chemical and physical cues in the surrounding microenvironment. The emergence of engineered three-dimensional (3D) tissue constructs and the development of tractable methods to recapitulate the native tissue microenvironment *ex vivo* has led to a deeper understanding of tissue-specific behavior. However, much remains unclear about how the microenvironment and aberrations therein directly affect tissue morphogenesis and behavior. Elucidating the role of the microenvironment in directing tissue-specific behavior will aid in the development of surrogate tissues and tractable approaches to diagnose and treat chronic-debilitating diseases such as cancer and atherosclerosis. Toward this goal, 3D organotypic models have been developed to clarify the mechanisms of epithelial morphogenesis and the subsequent maintenance of tissue homeostasis. Here we describe the application of these 3D culture models to illustrate how the microenvironment plays a critical role in regulating mammary tissue function and signaling, and discuss the rationale for applying precisely defined organotypic culture assays to study epithelial cell behavior. Experimental methods are provided to generate and manipulate 3D organotypic cultures to study the effect of matrix stiffness and matrix dimensionality on epithelial tissue morphology and signaling. We end by discussing technical limitations of currently available systems and by presenting opportunities for improvement.

I. Introduction

Tissue development depends on coordinated cycles of transcriptionally regulated cell growth, death, and migration that are controlled by exogenous soluble and physical stimuli and spatially dependent cell–matrix and cell–cell adhesion (Barros *et al.*, 1995; Ingber, 2006; Jacobson *et al.*, 1997; Locascio and Nieto, 2001). Regardless of length scale, understanding the molecular basis of tissue-specific differentiation and homeostasis requires an appreciation of adhesion-dependent cell behavior in the context of a three-dimensional (3D) extracellular microenvironment and a complex adhesion-dependent multicellular tissue. Through genetic and biochemical analysis, we have learned much about cell adhesion, including details of adhesion molecule structure and function, and about how various cell adhesion molecules likely mediate cell–extracellular matrix (ECM) interactions and facilitate Au2
cell–cell junctional complexes (Fuchs *et al.*, 1997; Huttenlocher *et al.*, 1998; Springer and Wang, 2004). We have also learned much about how exogenous growth, death, migration, and even mechanical cues activate signaling cascades to influence the fate of individual cells and undifferentiated 2D cell monolayers

(Huttenlocher *et al*., 1995; McBeath *et al*., 2004; Stegemann *et al*., 2005; Thornberry and Lazebnik, 1998; Wang *et al*., 2001). Yet, all too often, experimental conclusions reached from observations of single cells and simplified 2D monolayer cell sheets do not accurately represent how cells behave within 3D tissues *in vivo* (Green *et al*., 1999; Sethi *et al*., 1999). Indeed, developmental models and transgenic animals consistently underscore the importance of studying cell behavior in the correct tissue context. However, live animal experimentation is so inherently complex that systematic assessment of the effect of individual variables, such as cell shape and matrix compliance, on cell behavior is extremely challenging and impractical (Sethi *et al*., 1999; Wang *et al*., 2005). At the interface between *in vivo* studies and 2D culture models are the organotypic culture systems that can faithfully recapitulate various aspects of tissue organization and function *ex vivo*. These organotypic 3D models have been employed with varying degrees of success to clarify some of the mechanisms, whereby biological processes such as adhesion-dependent survival (Weaver *et al*., 2002; Zahir and Weaver, 2004), polarity (O'Brien *et al*., 2002; Wang *et al*., 1998), proliferation (Zink *et al*., 2004), and even epigenetics (Bissell *et al*., 1999; Zink *et al*., 2004) regulate cell behavior as well as novel feedback/regulatory mechanisms (Bissell *et al*., 2002). Organotypic culture models have been effectively applied to study tissue-specific differentiation (Bissell *et al*., 2002), to understand factors controlling stem cell behavior (Hendrix *et al*., 2001), and even microenvironmental control of malignant transformation and tumor dormancy (Margulis *et al*., 2005; Weaver *et al*., 1997). Through the prudent use of organotypic 3D models, critical disparities between the molecular determinants of cell polarity (reviewed in O'Brien *et al*., 2002), apoptosis resistance (Weaver *et al*., 2002), and growth factor responsiveness (Wang *et al*., 1998) in cells incorporated into a 3D tissue and those propagated as 2D monolayers have been revealed (reviewed in O'Brien *et al*., 2002). Yet, while 3D organotypic models can faithfully recapitulate some aspects of tissue behavior *ex vivo*, many of the systems routinely used to study tissue-like behaviors employ crudely defined natural ECM molecules that contribute to considerable experimental variance. In addition, many of the approaches used to assemble 3D tissue-like structures in culture operate by simultaneously modifying multiple variables, including restrictions on cell shape, matrix compliance, biochemical cues and metabolites, and even the spatial orientation of the ECM, thereby obscuring definitive experimental conclusions regarding individual experimental parameters (Kleinman *et al*., 1986; Paszek *et al*., 2005; Wozniak *et al*., 2003). Indeed, the engineering of surrogate tissues and the development of tractable approaches to diagnose and treat chronic-debilitating diseases such as cancer and atherosclerosis require both a comprehensive understanding of tissue-specific behavior at the molecular level and highly reproducible systems. Accordingly, considerable effort has been expended toward developing synthetic biomaterials in which individual material properties such as cell shape, matrix presentation (2D vs 3D), ligand density, and elastic modulus can be precisely modulated (Chen *et al*., 1998; Engler *et al*., 2004; Tan *et al*., 2003; Yamada *et al*., 2003). By applying one of the defined systems in which matrix compliance and ligand density could be

rigorously controlled, the critical role of matrix stiffness and integrin adhesions as a key regulator of multicellular mammary epithelial cell (MEC) tissue morphogenesis and malignant transformation has been highlighted (Paszek and Weaver, 2004; Paszek *et al.*, 2005). In this chapter, we discuss the rationale for applying well-defined 3D organotypic culture assays to study adhesion-dependent cell behavior. We describe the use of 3D MEC organotypic cultures to illustrate how matrix compliance plays a critical role in regulating mammary tissue function and signaling. Finally, we outline experimental methods to generate, manipulate, and study the effect of matrix stiffness and matrix dimensionality on epithelial tissue morphology and signaling, and discuss technical limitations of currently available systems and future opportunities for improvement.

Au3

II. Rationale

A. Stromal–Epithelial Interactions

During embryogenesis, the epithelium originates from the endoderm and ectoderm and develops into a specialized tissue whose primary functions in the organism are to protect and to control permeation or transport. Unlike skin and esophagus, which are stratified epithelia that provide a critical barrier, the secretory epithelium is composed of a simple layer of epithelial cells lining tubes and ducts, whose principal function is to facilitate secretion and transport of biological materials. *In vivo*, the secretory epithelium abuts on and is surrounded by a stroma, which consists of cellular and noncellular components, including ECM molecules, soluble factors, and various stromal cells such as fibroblasts, adipocytes, and endothelial cells. Directly interacting with the epithelium is the basement membrane (BM), which is a specialized, highly organized ECM composed primarily of laminins 1, 5, and 10, collagen IV, entactin, and heparin sulfate proteoglycans. The BM in turn intersects with the interstitial matrix, which consists of collagens I and III, fibronectin, tenascin, elastins, and various proteoglycans including lumican, biglycan, and decorin (Kleinman *et al.*, 1986). Collectively, the various components of the ECM and stroma provide biochemical (composition) and biophysical (structural modification and organization) cues to the epithelium and operate in concert with soluble factors released from the resident stromal cells to maintain the epithelium's organ-specific function. Perturbations in stromal–epithelial interactions and altered epithelial organization are hallmarks of cancer and many chronic degenerative diseases. Moreover, disrupting tissue organization or altering ECM integrity precipitates disease, and restoring tissue structure or proper ECM interactions normalizes tissue behavior (reviewed in Hagios *et al.*, 1998; Jeffery, 2001). Accordingly, the goal of 3D organotypic culture models is to recreate tissue-specific interactions, organizations, functions, and behavior *ex vivo* through prudent control of the biochemical and biophysical properties of the ECM, in order to understand the role of stromal–epithelial interactions and tissue structures in tissue-specific functions.

Mammary gland organotypic culture models have been used effectively to study the role of stromal–epithelial and ECM interactions in tissue-specific differentiation (Debnath *et al*., 2003; Petersen *et al*., 1992; Weaver *et al*., 1996; Wozniak *et al*., 2003). Unlike other tissues, the mammary gland undergoes unique developmental cycles in the adult organism and the gland can be readily accessed and manipulated *in vivo* and in culture. Additionally, reasonable quantities of breast tissue can be isolated and propagated *ex vivo* for culture experiments. As such, much of what we know regarding ECM-dependent epithelial differentiation has been derived from organotypic cultures of primary and immortalized MECs. Early studies demonstrated that MECs grown as 2D monolayers on rigid tissue culture substrates or within a physically constrained collagen I gel fail to assemble tissue-like structures (acini) and differentiate [no detectable expression of differentiated proteins such as whey acidic protein (WAP) or β-casein], despite the availability of appropriate growth factors and lactogenic hormones (reviewed in Roskelley *et al*., 1995). Yet, when the same MECs are grown within unconstrained collagen I gels and allowed to deposit and organize their own endogenous BM, or are embedded within a compliant reconstituted BM (rBM), they are able to assemble multicellular tissue-like structures (acini; reminiscent of terminal ductal lobular units in tissues *in vivo*) and differentiate in response to hormonal cues (expressed β-casein and WAP; reviewed in Roskelley *et al*., 1995; Fig. 1). Further studies using murine and human MECs have also consistently shown that the composition and spatial context of the ECM profoundly influence the responsiveness of an epithelium to exogenous growth, migration, and death stimuli (Wang *et al*., 1998, 2005; Weaver *et al*., 2002). For example, some human luminal epithelial breast tissues *in vivo* express the estrogen receptor (ER) and proliferate in response to hormonal fluctuations in estrogen. When these MECs are isolated and cultured on tissue culture plastic, they spread to form raised ER-negative, 2D cobblestone monolayer colonies that lack estrogenic responsiveness. However, if the isolated MECs are instead grown in the context of a compliant rBM, they retain their ER expression and maintain their estrogenic responsiveness (Novaro *et al*., 2003). Likewise, undifferentiated MECs grown on tissue culture plastic are highly sensitive to exogenous death cues, whereas their rBM-differentiated counterparts exhibit extremely high resistance to multiple apoptotic stimuli (Weaver *et al*., 2002). Analogous observations regarding the importance of biochemical and biophysical ECM cues for epithelial morphogenesis and tissue-specific differentiation have also been reported for thyroid, salivary gland, and kidney epithelia studies (Kadoya and Yamashina, 2005; O'Brien *et al*., 2001; Yap *et al*., 1995).

B. ECM Mechanics and Epithelial Behavior

Many important discoveries have been made concerning the molecular mechanisms by which the ECM influences epithelial behavior, including the requirement of signaling through laminin-dependent ligation of $\alpha 3\beta 1$ and $\alpha 6\beta 4$ integrins. In addition, cooperative ERK-PI3 kinase and RacGTPase-NFκB signaling through

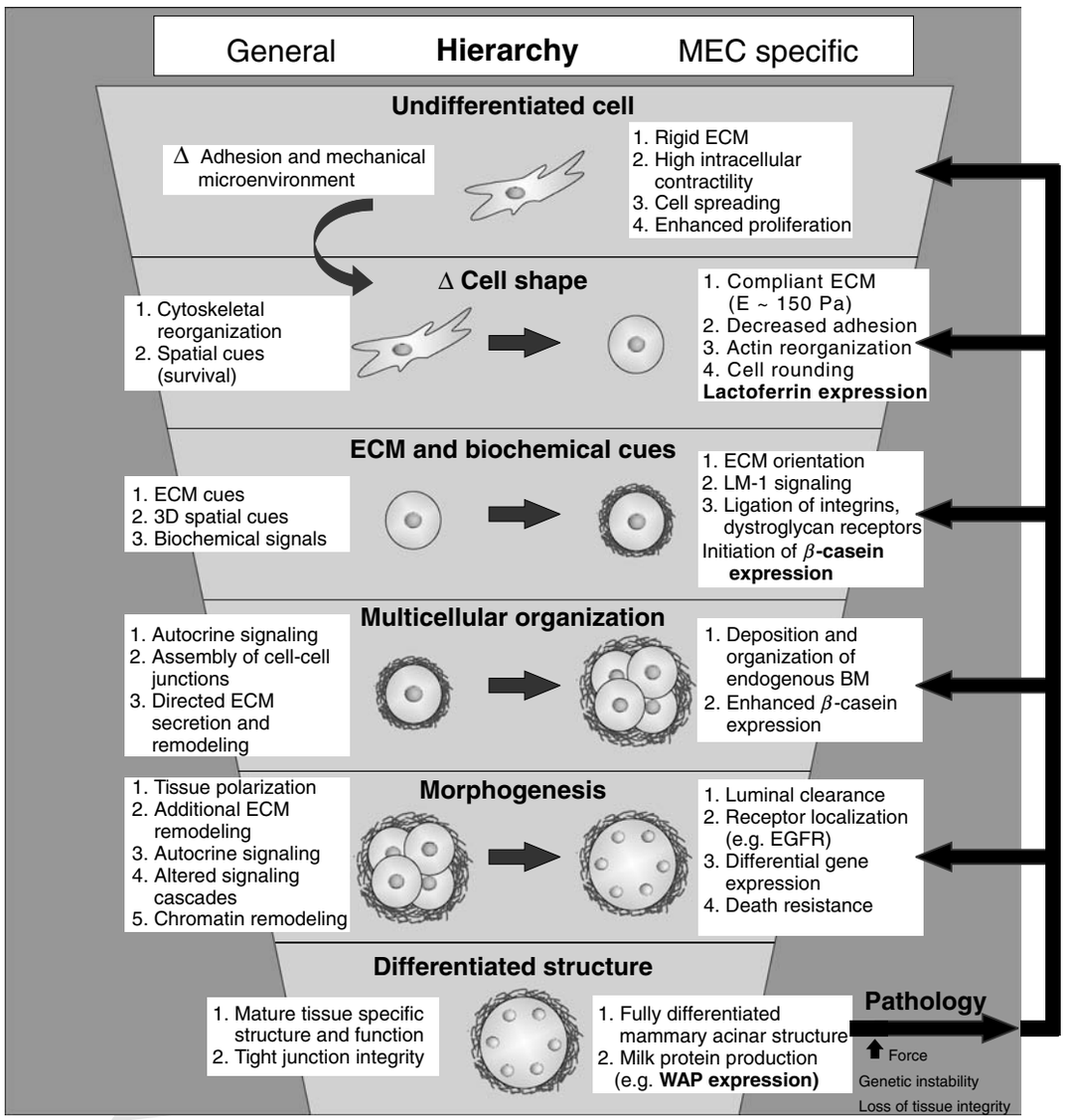

Fig. 1 Biochemical and biophysical cues from the extracellular matrix regulate tissue-specific epithelial differentiation. Illustration depicting ECM regulation of tissue-specific differentiation through a progressively complex hierarchy of adhesion-regulated events functionally linked to changes in cell shape, receptor-initiated biochemical signaling, assembly of multicellular structures, and reciprocal biochemical and physical modification of the ECM microenvironment adjacent to the epithelial tissue. Undifferentiated cell (top): an undifferentiated cell interacting with a highly rigid 2D ECM substratum, such as matrix-coated tissue culture plastic, will adhere rapidly and, if given sufficient ECM ligand, will spread appreciably using multiple adhesion receptors, including integrins, and assemble mature focal Au16

epidermal and insulin growth factor receptors and prolactin-dependent activation of Stat3 have been identified as key biochemical events involved in directing MEC growth, survival, and differentiation (Akhtar and Streuli, 2006; Muschler *et al*., 1999; Paszek *et al*., 2005; Zahir *et al*., 2003). The ECM not only influences epithelial behavior through biochemical signaling but also through the mechanical properties of the microenivornment.

Early studies with constrained versus released collagen gels revealed the importance of ECM mechanics in directing the cell shape of MECs to promote differentiation (Emerman and Pitelka, 1977). MECs plated on constrained collagen gels or gluteraldehyde cross-linked rBM fail to differentiate in response to lactogenic stimuli and instead spread to form a 2D cell monolayer despite appropriate integrin-ECM ligation and growth factor signaling (reviewed in Roskelley *et al*., 1995; Weaver and Bissell, 1999). Furthermore, laminin- and proteoglycan-mediated ligation of dystroglycan (DG) has been strongly implicated as the primary mediator of ECM-directed cell shape fate determination in MECs and as a critical component in establishing a continuous BM (Muschler *et al*., 1999). The hypothesized mechanism seems to depend only on DG's extracellular domain

adhesions. Epithelial cells grown on a rigid 2D matrix proliferate readily to form viable polarized cellular monolayers with adherens and tight junctions as well as prominent focal adhesions. Such cells exhibit robust Rho GTPase activation in response to exogenous stimuli, and require activated PI3 kinase or ERK signaling to survive. Under these conditions, epithelial cells do not assemble 3D tissue-like structures or express differentiated proteins in response to ''differentiation cues.'' Mechanical cues (second tier): an epithelial cell interacting with a highly compliant ECM readily adheres using multiple matrix receptors, including integrins, and assembles small immature focal complexes but fails to spread appreciably. Instead cells interacting with a compliant matrix exhibit profound reorganization of their actin cytoskeleton. MECs grown under these conditions can be induced to express lactoferrin if given the correct exogenous soluble cues. 3D ECM and biochemical cues (third tier): epithelial cells interacting with a highly compliant matrix in three dimensions adhere through multiple adhesion receptors including integrins, syndecans, and DG, and proliferate readily in response to exogenous growth factors. MECs interacting with a highly compliant 3D ECM can be induced to express abundant quantities of the differentiation protein β-casein. Multicellular organization, morphogenesis, and tissue differentiation (fourth to sixth tiers): in response to a 3D compliant ECM, ductal epithelial cells begin to interact with one another and assemble multicellular polarized structures with cell–cell junctions including adherens, scribble, and gap junctions. MECs assembled into multicellular 3D-polarized tissue-like structures begin to deposit and assemble an endogenous basally polarized basement membrane, show enhanced expression of milk protein expression such as β-casein, and exhibit enhanced long-term survival and apoptosis resistance to multiple exogenous stimuli including chemotherapeutics, immune receptor activators, and gamma irradiation. Long term culture of epithelial cells in the context of a 3D compliant ECM permits completion of tissue-like morphogenesis characterized by the assembly of an apically and basally polarized, growth-arrested tissue with a cleared central lumen and spatial restriction of various membrane associated proteins including growth factor receptors. Once a fully polarized and growth-arrested structure has formed, mammary acini can now be induced to express additional milk proteins such as WAP in response to lactogenic hormones. However, in response to an increase in matrix stiffness as occurs following chronic inflammation, injury, or tumorigenesis, or following genetic mutations and oncogene activation, tissue integrity becomes progressively compromised reversing the cell state to a less differentiated condition. In extreme cases, cells can behave analogous to undifferentiated, highly contractile single cells.

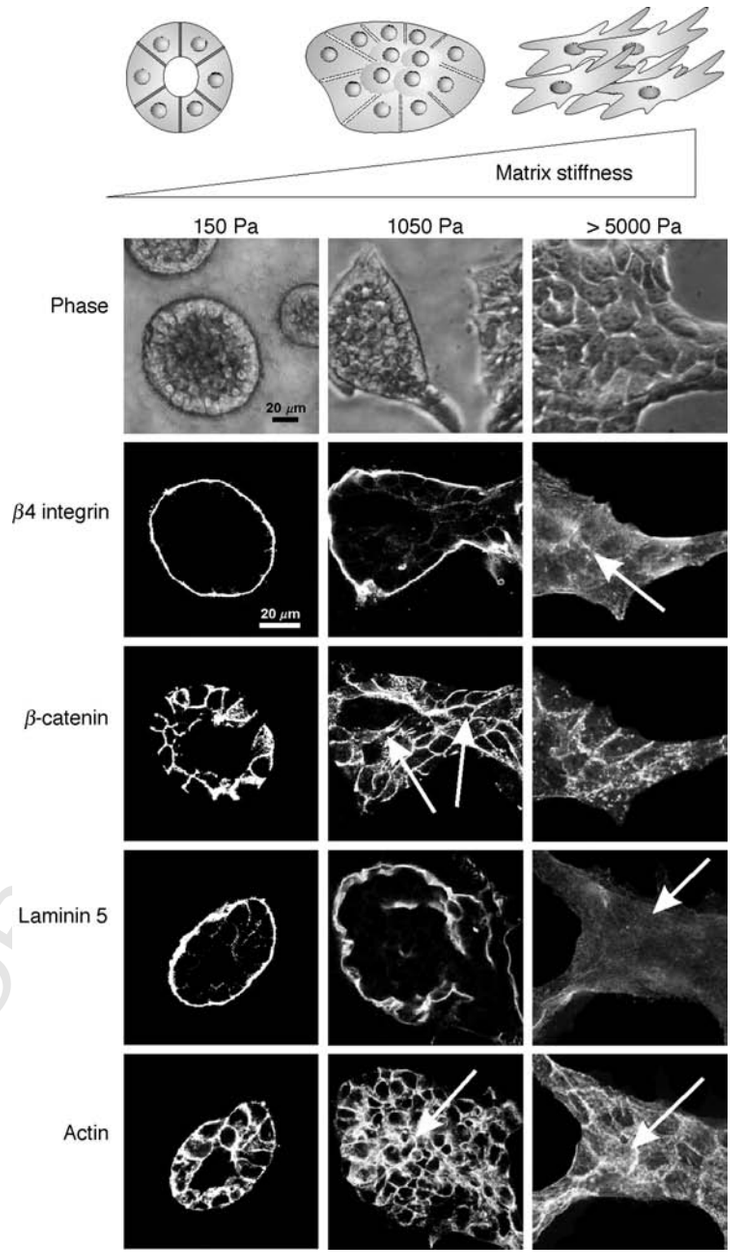

Fig. 2 Matrix stiffness modulates MEC growth and morphogenesis. Phase-contrast and confocal immunofluorescence images of 3D MEC colonies on 3D rBM-cross-linked PA gels of increasing elastic moduli ($E = 150$–5000 Pa) after 20 days, showing progressively disrupted colony morphology as matrix

and to involve DG binding to laminin, which then polymerizes on the cell surface and onto adjacent DG-expressing cells, ultimately establishing a continuous BM. This process of ligation-driven BM assembly is almost certainly in competition with integrin-based and other adhesive processes. The latter seem more mechanosensitive and might dominate on rigid substrates versus soft substrates (Fig. 2).

Although the detailed molecular mechanisms of the mechanosensitivity of MEC differentiation remain to be delineated, recent studies using both nontransformed and transformed human MECs suggest that Rho GTPase-dependent cell contractility regulates adhesion-directed, cell shape-dependent, epithelial tissue-specific functions (Paszek *et al*., 2005). Transformed human mammary epithelial tumor cells propagated on top of constrained collagen I gels assembled aberrant invasive structures with high Rho and ROCK activity, whereas they could form cell aggregates reminiscent of nontransformed tubules when grown on unconstrained collagen I gels (Keely *et al*., 1995). In concert with these *in vitro* observations, transformed mammary tumors were recently shown to exhibit enhanced Rho GTPase activity and exert elevated myosin-dependent cell contractility and aberrant integrin adhesions when compared to nontransformed MECs. Normalizing tumor cell contractility through application of pharmacological inhibitors of Rho, ERK signaling, or myosin could phenotypically revert the malignant phenotype (Paszek *et al*., 2005). Consistent with a critical role for matrix compliance in epithelial behavior, nontransformed MECs grown within highly compliant rBM gels or nonconstrained and compliant collagen I/rBM gels competently assemble polarized, growth-arrested acini-like structures. However, when grown within constrained collagen I/rBM gels or collagen I/rBM gels of higher concentration and stiffness, they form progressively disrupted, disorganized, and continuously proliferating colonies when grown within constrained collagen I/rBM gels or collagen I/rBM gels of higher concentration and stiffness (Paszek *et al*., 2005; see also Sections III.A.1 and III.A.2).

Through the application of defined, synthetic, rBM-cross-linked polyacrylamide gels, it was concluded that matrix stiffness and not matrix density or physical presentation constitutes a critical regulator of multicellular epithelial morphogenesis (Paszek *et al*., 2005; Fig. 2). These studies clearly emphasize the importance of myosin contractility and integrin adhesion maturation as matrix-regulated cell shape and force regulators. They have also identified altered ERK-dependent cell growth and survival, destabilization of cell–cell adhesions, and perturbed matrix assembly, as central mechanisms for further study. Indeed, the proper assembly of an endogenous cell-derived matrix plays a key role in epithelial differentiation, as

stiffness increases (top). Cell–cell adherens junctions are disrupted and luminal clearance is compromised with even a modest increase in the elastic modulus of the matrix ($E = 1050$ Pa central panel; β-catenin and actin). Basal polarity is perturbed (disorganized $\beta 4$ integrin and absence of basally deposited laminin-5) once the matrix stiffness stiffens appreciably ($E > 5000$ Pa; right panel). Scale bar is μm. Adapted from Paszek *et al*. (2005).

Au17

has been illustrated by the necessity of proper laminin–nidogen interactions for mammary tissue differentiation and gene expression in culture (Pujuguet *et al.*, 2000) and for multiple epithelial tissues including the kidney *in vivo* (Willem *et al.*, 2002). Indeed, in lung development, increasing the compliance of the chest wall or decreasing the skeletal muscle fibers that aid in breathing modifies the biophysical properties of the tissue microenvironment by decreasing the applied force to the developing lung, leading to a decrease in lung growth, which further perturbs the tissue ECM and compromises tissue function (reviewed in Liu *et al.*, 1999).

C. 3D Organotypic Model Systems

Key to engineering tissue-specific function is the application of an appropriate ECM in which the biochemical, biophysical, and spatial cues can be defined and controlled. An array of natural ECMs and a growing list of synthetic biomaterials, each with advantages and disadvantages, are available to the experimentalist. Ideally, a comprehensive assessment of what constitutes normal ECM composition, mechanical properties, and organization should be taken into consideration. Unfortunately, our comprehension of these variables has lagged behind, due to the complexity, lack of homogeneity, and anisotropy of biological materials.

rBMs isolated from Engelbreth–Holm–Swarm (EHS) mouse sarcomas have been routinely used to assemble tissue-like structures in culture and have been successfully applied to study mammary, thryoid, salivary gland, lung, and kidney epithelial cell morphogenesis and differentiation, and to distinguish between normal and transformed epithelial cells (Azuma and Sato, 1994; Debnath *et al.*, 2003; Nogawa and Ito, 1995; O'Brien *et al.*, 2001; Petersen *et al.*, 1992; Yap *et al.*, 1995). Similarly, fibrin gels have also been successfully used to assemble 3D normal and transformed tissue-like structures in culture (Alford *et al.*, 1998). However, given that rBM is directly isolated from tissues, the matrix is inherently complex, poorly defined, and subject to complications with lot to lot variability and limitations due to the specific nature of the biochemical and biophysical environment associated with sarcomas. Fibrin gels, while attractive, also suffer from preparation variance. Additionally, fibrin gels are easily proteolyzed by cell-derived MMPs and consequently are not viable for long-term culture experiments. While alternative fibronectin sources that are less proteolytically sensitive have proven useful, these matrices have yet to be routinely applied to epithelial organ culture models.

As an alternative, collagen I gels have been extensively used as a 3D tissue matrix. The application of defined collagen gels to replace the more complex and biologically accurate rBM and fibrin gels has several advantages, including the fact that collagen I is a more biologically defined substrate, is relatively inexpensive to prepare or purchase, and is much more readily available. Because collagen I is the most common protein found in vertebrate animals and is structurally highly conserved, it is generally well tolerated for *in vivo* studies, and multiple cell types readily adhere to this substrate. In addition, the elastic moduli of a collagen I gel can be readily manipulated by varying collagen orientation, fibril cross-linking,

concentration, or even biochemical modification or mutation (Christner *et al.*, 2006; Girton *et al.*, 1999; Martin *et al.*, 1996; Roeder *et al.*, 2002), thereby increasing its biological versatility (Elbjeirami *et al.*, 2003; Grinnell, 2003). The magnitude and directional orientation of externally imposed tension can also be easily manipulated with collagen preparations. For example, through the release of collagen gels from the culture vessel, the isometric tension within the gel can be dramatically reduced (Rosenfeldt and Grinnell, 2000). Collagen gels can also be biochemically modified to facilitate epithelial functionality, as for example through the addition of either rBM, purified laminin, or derivatized peptides (Gudjonsson *et al.*, 2002).

Purified, biologically derived materials, such as rBM and collagen I, have an intrinsic amount of biochemical and biophysical variability due to the inherent variability between animals and preparations. This variability leads to inconsistencies between experiments, as well as a high degree of heterogeneity within single gels. Additionally, the dynamic range of elastic moduli that can be reasonably achieved with these systems is limited by biochemical and biophysical constraints of these unique macromolecules. Therefore, although these materials have proven to be useful for clarifying the general influence of matrix on cell and tissue phenotypes, they are not as tractable for defining precise molecular mechanisms mediating mechanotransduction.

To address the issues listed above, especially control over matrix compliance, we and many others use a system first developed by Pelham and Wang (1997) that involves functionalizing synthetic polyacrylamide gels for cell culture (by cross-linking them with precise concentrations of ECM ligands) as 2D model systems for cell spreading, adhesion, and migration. Polyacrylamide gels represent tractable materials to allow studies of molecular pathways and signaling events of cells grown in various mechanical environments. The mechanical properties of these gels, which have been defined using rheology and atomic force microscopy (Engler *et al.*, 2004; Guo *et al.*, 2006; Yeung *et al.*, 2005; Chapter 22 by Engler *et al.*, this volume), can be manipulated by changing the relative concentration of acrylamide Au4
and the cross-linker, bis-acrylamide, yielding a system with precisely controlled biochemical and biophysical properties. Polyacrylamide is an exemplary material for studying cell behavior, as it is nonreactive, resistant to nonspecific binding and protein adhesion, and optically clear. The most significant downside to the polyacrylamide gel system is that acrylamide is cytotoxic in its monomeric form, which precludes the extension of its use to 3D cultures in which cells are embedded before polymerization. To overcome this limitation, we have used these polyacrylamide gels to reconstitute 3D conditions by overlaying MECs plated on top of rBM-cross-linked polyacrylamide gels with a blanket layer of rBM. Although the cells undergo normal morphogenesis under these conditions, there are some limitations inherent in this unique technique. Namely, and most importantly, this is neither a true 2D nor a complete 3D system, and the cells behave differently than they do in full 3D cultures (Leight *et al.*, unpublished observations). Although this drawback leads to difficulty in interpretation and definition of these experiments, this system

is suitable for approximating the physiological mechanical conditions under which epithelial cells grow and thrive. Alternatively, polyethylene glycol gels combined with bioactive peptides, such as fibronection- and laminin-binding sites, are also attractive biomaterials. However, their 3D organization is significantly different from that found in naturally occurring matrices and *in vivo* in that they typically have a greater matrix density and altered spatial orientation (reviewed in Zhang, 2004). Furthermore, because matrix remodeling is a critical aspect of epithelial morphogenesis, expensive bioactive peptides that can be proteolytically remodeled need to be incorporated into these synthetic biomaterials to permit proper tissue morphogenesis, migration, and to support long-term cell and tissue viability (reviewed in Lutolf and Hubbell, 2005). As an attractive new strategy in the arsenal of synthetic materials, novel matrices that incorporate recombinant natural and synthetic proteins and biopeptides are currently being developed and offer new hope for future applications.

Progress has been made in recapitulating tissue-specific morphology *ex vivo* either for tissue transplantation or for the study of tissue-specific function, but the application of these organotypic model systems to dissect the molecular basis of tissue homeostasis and disease has lagged behind significantly. The failure to exploit current 3D model systems for the study of cell behavior and signaling in the context of a tissue-like microenvironment and structure resides primarily in the lack of appropriate, cost-effective, easy, and reproducible strategies to manipulate, analyze, and assess cell function, signaling, and gene expression in these model systems. We have been studying the effect of cell shape, matrix compliance, adhesion, and dimensionality on cell behavior at the molecular levels, and here we provide a detailed description of the methods we have successfully used to do so.

III. Methods

A. Engineered Cell/Tissue Explants

1. Natural matrices: rBM
   a. On ice, evenly coat the bottom of a tissue culture plastic dish with ice-cold rBM and incubate the dishes at 37 °C for 10–20 min to permit gel polymerization (see Table I for volume).
   b. Prepare a single-cell suspension of trypsinized/washed cells in log-phase growth, and adjust the final cell concentration to 1×10^6 cells/ml media.
   c. Aliquot cell suspension into individual tubes, adjusting cell number to desired total gel volume [see step (g)].
   d. Centrifuge individual tubes to pellet cells (5 min, $180 \times g$ rcf).
   e. Aspirate the supernatant from the cell pellet, leaving 5% of the media behind.

Table I
Matrix Volume (μl) Per Well Size

	Underlay (μl)	Embed (μl)
60 mm	1250	4250
35 mm	450	1400
12-well	200	700
4-well	100	300
24-well	100	300
48-well	50	175
96-well	20	60

f. Resuspend the cells in the remaining media by vigorously tapping the side of the tube, and place the tube on ice (note: do not vortex).
g. Add desired volume (Table I) plus an additional 10% of ice-cold rBM, and resuspend cells by gentle pipetting, taking care to avoid bubbles and keep the tube cold.
h. Transfer the cell/gel solution to the precoated tissue culture chambers, ensuring that the surface is covered with a uniform layer of cell/gel solution. Incubate at 37 °C for 20–30 min to permit gel polymerization.
i. Gently add complete growth media to the cultures until the gels are fully covered, taking care not to disrupt the gels. Incubate cultures in humidified chambers (37 °C) for desired length of time with media changes every 2–3 days.

2. Natural matrices: collagen I
   a. Prepare collagen/rBM solution following an adapted version of the protocol published by BD (BD Biosciences—Discovery Labware, Catalog No. 354236 Product Specification Sheet).
      i. Place the following on ice: acid-solubilized rat tail collagen I, sterile 10× phosphate-buffered saline (PBS), sterile deionized, distilled water (ddH_2O), sterile 1-N sodium hydroxide (NaOH), and an empty sterile tube marked "Final Collagen Solution."
      ii. Calculate the desired volumes required for the experiment. (Note: Prepare 20% extra volume to account for material loss during experimental manipulations. See Table I for suggested total volumes.):

$$\text{Volume of } 10\times \text{PBS} = \frac{\text{Total final volume}}{10}$$

$$\text{Volume of collagen} = \frac{\text{Total final volume} \times \text{Final collagen concentration}}{\text{Stock collagen concentration}}$$

$$\text{Volume of 1-N NaOH} = \text{Volume of collagen} \times 0.023$$

$$\text{Volume of dd}H_2O = \text{Final volume} - \text{Volume of collagen} - \text{Volume of } 10 \times \text{PBS} - \text{Volume of 1-N NaOH} - \text{Volume of rBM}$$

iii. To the tube marked "Final Collagen Solution," add the desired volumes of sterile ice-cold 10× PBS, 1-N NaOH, and ddH_2O, then mix.

iv. To the tube marked "Final Collagen Solution," add the acid-solubilized collagen [from step (ii)], and mix gently by pipetting several times, taking care to keep the solution ice cold and to minimize air bubble formation. (Note: Do not over mix the gel solution, or the materials properties of the final gel will be altered.)

v. Neutralize the pH to 7.2–7.6 by titrating, drop-wise with 1-N NaOH until the solution turns a slight shade of reddish-purple indicated by the phenol red dye. Mix gently after the addition of each drop.

vi. If desired, add an appropriate amount of rBM to the gel solution and leave on ice until required. The collagen solution can be used immediately or held on ice for 2–3 h.

b. Place the desired tissue culture dish on ice, and coat the bottom of each well with a thin layer of the collagen/rBM gel solution. Incubate the plate at 37 °C for 10–20 min to permit gel polymerization (see Table I for volume).

c. Prepare a single-cell suspension of trypsinized/washed cells in log-phase growth, and adjust the final cell concentration to 1×10^6 cells/ml media.

d. Aliquot cell suspension into individual tubes, adjusting cell number to the desired gel volume [see step (h)].

e. Centrifuge individual tubes to pellet cells (5 min, 180 × *g* rcf).

f. Aspirate the supernatant from the cell pellet, leaving 5% of the media behind.

g. Resuspend the cells in the remaining media by vigorously tapping the side of the tube and place the tube on ice (note: do not vortex).

h. Add desired volume plus an additional 10% of ice-cold collagen/rBM solution, and resuspend cells by gentle pipetting, taking care to avoid bubbles and to maintain the tube cold.

i. Transfer the cell/gel solution to the precoated tissue culture chambers ensuring that the surface is covered with a uniform layer of cell/gel solution. Incubate at 37 °C for 20–30 min to permit gel polymerization.

j. After polymerization, release the gel from the sides of the dish by running a small sterile spatula around the edge.

k. Gently add complete growth media to the cultures until the gels are fully covered, taking care not to disrupt the gels. Incubate cultures in humidified chambers (37 °C) for desired length of time with media changes every 2–3 days.

Anticipated results: Because the cells are seeded as single entities, it is possible to monitor the various stages of morphogenesis. Within 24 h all of the cells should be actively dividing, and by 48 h cell doublets should have formed with detectable polarized deposition of laminin-5 ECM protein and E-cadherin and β-catenin localized at cell–cell junctions. By 72–96 h cell proliferation should approach 60–85% [assessed by 5-bromo-2-deoxyuridine (BrdU) incorporation] and basal/apical tissue polarity should be established (determined by basal localization of β4 integrin and basal deposition of laminin-5). Within 10 days, fully embedded MECs within a compliant 3D rBM or collagen/rBM gel should have assembled small, essentially uniform, growth-arrested, polarized acini (Petersen *et al.*, 1992; Weaver *et al.*, 2002). Tissue morphology can be easily assessed by monitoring morphogenesis using immunofluoresence and morphometric assessment markers (Sections III.E.1 and III.E.2; Debnath *et al.*, 2003; Paszek *et al.*, 2005; Weaver *et al.*, 1997). [Note: Cells grown on top of rBM as opposed to those completely embedded tend to form larger and more heterogeneous spheroids and exhibit slightly delayed lumenal clearance and growth arrest dynamics (Leight *et al.*, unpublished observations). In addition, cells embedded within collagen/rBM gels of increasing elastic modulus ($E > 675$ Pa) form larger nonpolarized structures that lack a central lumen (Paszek *et al.*, 2005)].

3. Synthetic matrices: functionalized polyacrylamide gels [Note: For immunofluorescence techniques, small (18–25 mm) coverslips can be used. For total RNA and protein isolation, larger (50 mm) coverslips should be used. The cell number should be optimized for the experiment performed, based on the degree of cell spreading and proliferation anticipated. For example, at least 750,000 cells are needed for total RNA and protein isolation, while significantly less is required for immunofluorescence visualization.]

a. Flame coverslip quickly and let cool.
b. Using a cotton swab, evenly and thoroughly coat the coverslip with 0.1-N NaOH. Air dry the coverslips until a filmy coat appears.
c. Using a p100 pipette tip, spread an even but thin coat of silane onto the surface of the coverslip (refer to Table II for amount). Allow the silane coating to dry (room temperature, 5–10 min), and place the coated coverslips silane-side up in a Petri dish. (Note: Do not incubate longer than 20 min.) Au5
d. Wash the coverslips thoroughly with ddH_2O (minimum 3×; 10 min each), tapping the dish vigorously to remove excess liquid.
e. Incubate the coverslips in 70% glutaraldehyde (1:140; v:v in PBS) at room temperature for 30 min.

Table II
Amount of Each Solution to Add During Steps (c), (o), (q), and (s) When Using the Stated Coverslip Size

	Silane	Acrylamide solution	rBM solution	Ethanolamine
18-mm circle	20	20	300	300
25-mm circle	30	30	450	450
50-mm circle	100	190	900	900

All values listed are in microliters. Au18

Table III
Recipes of 1-ml Polyacrylamide Gel Solutions for Given Elastic Modulus (Yeung *et al.*, 2005)

Elastic modulus (Pa)	140	400	1050	5000	60,000
Acrylamide (%)	3	3	3	5.5	10
Bis-acrylamide (%)	0.04	0.05	0.1	0.15	0.5
40% Acrylamide (μl)	75	75	75	137.5	250
2% Bis-acrylamide (μl)	20	25	50	75	250
0.5-M HEPES, pH 4.22 (μl)	100	100	100	100	100
TEMED (μl)	0.5	0.5	0.5	0.5	0.5
ddH_2O (μl)	648.9	643.9	618.9	541.4	243.9

f. Wash the coverslips thoroughly with ddH_2O (minimum 3×; 5–10 min each).
g. Arrange the coverslips face-up to dry.
h. After fully drying, the activated coverslips can be used immediately or stored for several weeks in a dry place. (Note: If the coverslips turn a rust-brown color, they should not be used as this is indicative of excess silane reacting with glutaraldehyde.)
i. In a microcentrifuge tube, mix the solutions required for gel preparation (see Table III for recipe).
j. In another microcentrifuge tube, weigh 5.6 mg of *N*-succinimidyl ester of acrylamidohexanoic acid (N6 cross-linker) per 1 ml of final desired solution. This compound can incorporate into the polyacrylamide gel, rendering it reactive with amine groups of proteins.
k. Add 70 μl of 200 proof ethanol and 80-μl ddH_2O (per 1 ml of final solution) to the N6 cross-linker. Briefly, sonicate in a sonicating water bath (average peak power = 45 W), or vortex at highest setting until fully dissolved.
l. Add 844.4 μl of gel solution to the cross-linker/ethanol solution, and vortex.

m. Degas the gel solution using a vacuum flask or chamber for at least 30 min.

n. While the solutions are being degassed, evenly coat an additional set of equivalent-sized coverslips with Rain-x. Allow the Rain-x coating to dry at room temperature for 5–10 min, then gently buff the coverslip using a Kimwipe.

o. Place the activated coverslips face-up on a secured piece of paraffin.

p. Add 10 μl of freshly made 5% ammonium persulphate (w:v in ddH_2O) per 1 ml of fully degassed acrylamide solution, mix well, and quickly dispense the desired volume of solution onto each activated coverslip (refer to Table III for volumes). Carefully place the Rain-x treated coverslip on top without trapping air bubbles and allow the gel solution to polymerize at room temperature for 25–60 min. (Note: Gel polymerization is indicated by retraction of the gel from the edge of the coverslip. Do not allow them to set for longer than 60 min, or the gel will dehydrate.)

q. While the gels are polymerizing, prepare a surface amenable to placing the gels on ice by covering the top surface of polystyrene tissue culture dishes with parafilm. (Note: The size is dependent on the size of the coverslips.)

r. Place the parafilm-affixed dishes on ice, and prepare the rBM solution for coating the coverslips. In a prechilled conical tube, prepare a solution of 140-μg/ml rBM, 5-mM EDTA, in 50-mM HEPES buffer, pH 8.0. (Note: Be sure to keep on ice to prevent polymerization of rBM.)

s. After the polyacrylamide gels have fully polymerized, carefully remove the top Rain-x-coated coverslip using a razorblade, taking care not to scratch the gel surface. Rinse each gel with ice-cold ddH_2O. If using 18- and 25-mm coverslips, place the coverslips gel-side on the parafilm-affixed dishes on ice. Immediately dispense the appropriate amount of rBM solution onto the gel (Table III). For 50-mm coverslips, pipette the appropriate amount of rBM solution (Table III) directly onto the paraffin-affixed dishes, and place the rinsed gels face down on top of the solution. Avoid trapping air bubbles under the coverslip. Incubate coverslips on ice for 2 h.

t. While the coverslips are incubating, prepare the ethanolamine solution (1:100 v:v; 50-mM HEPES, pH 8.0) and chill the solution on ice.

u. Following incubation, individually rinse each gel in ice-cold ddH_2O and wipe the parafilm-affixed dishes dry. Following the method in step (s), incubate the coverslips with ethanolamine on ice for 30 min to quench the unreacted N6 cross-linker (refer to Table III for volumes).

v. Soak the prepared gels in ice-cold PBS. In a sterile tissue culture hood, move the gels to sterile tissue culture dishes and store for up to 3 days in sterile 2-mM sodium azide/PBS at 4 °C.

w. Prior to cell plating, rinse each gel thoroughly in sterile PBS (minimum 3×), and leave the gels fully immersed in sterile PBS while preparing single-cell suspensions.

x. Prepare a single-cell suspension of trypsinized/washed cells in log-phase growth, and adjust the final cell concentration to 1×10^6 cells/ml media.

y. Aliquot cell suspension into individual tubes, adjusting cell number to desired concentration.

z. Centrifuge individual tubes to pellet cells (5 min, $180 \times g$ rcf).

aa. Aspirate the supernatant from the cell pellet, leaving 5% of the media behind.

bb. Resuspend the cells in the remaining media by vigorously tapping the side of the tube and place the tube on ice (note: do not vortex).

cc. Resuspend the cell suspension in cold growth medium, supplemented with 500-ng/ml fungizone, 50-μg/ml gentamicin sulfate, and 1:100 penicillin/streptomycin (stock concentration: 10,000 units penicillin/ml and 10,000-μg streptomycin/ml).

dd. Pipette the desired cell number onto each gel taking care to ensure an even distribution of cells across the gel surface, and allow the cells to adhere. (Note: The length of time for cells to adhere to the gel surface varies between cell types and needs to be optimized for each experiment.)

ee. To facilitate 3D morphogenesis, after complete cell adhesion (minimum 6–8 h), cover cells in media containing 0.2-mg/ml rBM, and incubate cells for desired number of days. Change the culture media including 0.2-mg/ml rBM, fungizone, gentamicin, and penicillin/streptomycin, the following day and then every other day until termination of experiment.

Anticipated results: After 14 days in culture, MECs plated on top of functionalized polyacrylamide gels with a rBM blanket layer, similar to cells overlaid on rBM gels (Debnath *et al.*, 2003), form larger acini than their counterparts embedded within natural matrices. Analogous to cells grown within a natural matrix or grown on top of rBM with an overlay of rBM, by day 4, cells grown on the rBM PA gels should have acquired detectable cell–cell E-cadherin/β-catenin junctions as well as basal and apical polarity. Thus, by day 4, the cells should be highly proliferative but have acquired basal polarity, detectable by basally localized β4 integrin and deposition of a laminin-5- and collagen IV-rich endogneous BM as well as apically localized cortical actin. Studies have revealed that while the growth rate of MCF10As plated on soft ($E = 140$ Pa) and stiff ($E = 5000$ Pa) rBM-functionalized polyacrylamide gels are similar, cells interacting with a matrix stiffer than 1000 Pa fail to fully growth arrest. We have previously shown that MECs plated with a 3D rBM blanket layer on soft rBM-functionalized polyacrylamide gels undergo normal morphogenesis, while morphogenesis is perturbed in those plated on a stiff gel under the same conditions (Paszek *et al.*, 2005; Fig. 2).

A protocol outlining basic immunofluorescence techniques for each cell culture method is described in the Section III.E, for the visualization of characteristics indicative of morphogenesis. A comparison detailing morphogenetic characteristics of all of the described methods is currently in progress (Leight *et al.*, unpublished observations).

B. Isolation of Bulk Proteins

1. Natural matrices: rBM (Note: This protocol is for isolating proteins from 1-ml rBM gels. Adjust volumes stated if necessary.)

a. Prepare 25-ml of ice-cold Dulbecco's PBS solution (DPBS) containing 5-mM EDTA (EDTA/DPBS).
b. Supplement 25% of the EDTA/DPBS solution as prepared above with a cocktail of serine and cysteine protease and tyrosine phosphatase inhibitors. (Note: See Section IV for specific reagents and concentrations.)
c. Place culture on ice and gently aspirate off the medium.
d. Add 3 ml of the protease inhibitor/EDTA/DPBS solution prepared in step (b) to the culture dish, and pipette up and down using a p1000 pipette until a uniform suspension is obtained, avoiding the formation of insoluble foam.
e. Transfer the solubilized rBM gel solution to a 15-ml conical tube on ice.
f. Repeat steps (d) to (f) once, collecting all of the solubilized rBM into the conical tube.
g. Angle the conical tubes in a box of ice. Secure the tube and box of ice on a rocker and rock at 4 °C for 45–60 min.
h. Place 24 nonstick microcentrifuge tubes on ice, and aliquot the cell/rBM solution evenly among the tubes.
i. Centrifuge tubes at 4 °C for 10 min (3200 × *g* rcf).
j. Aspirate the supernatant, leaving 5% of the media behind.
k. Add 500 μl of the EDTA/DPBS solution to one tube, scraping the pellet against the side of the tube to resuspend the pellet. Mix well, and transfer to the next tube. Continue to scrape, mix, and transfer the solution to combine a total of four tubes into one.
l. Repeat steps (i) to (k) until the original 24 tubes are combined into one.
m. Centrifuge final tube at 4 °C for 15 min (21,000 × *g* rcf).
n. Prepare the lysis buffer, supplementing it with a cocktail of serine and cysteine protease and tyrosine phosphatase inhibitors.
o. Carefully aspirate the supernatant, and resuspend the pellet in 100–300 μl of lysis buffer (see note in Section IV), depending on the size of the pellet and the amount of protein expected.
p. Incubate on ice for 30 min.

q. Sonicate the lysis solution on ice with three pulses of 10 sec each, at an output power of 8 W, pausing for 30 sec between each pulse for the sample to cool down.
r. Centrifuge final tube at 4 °C for 10 min (10,500 × *g* rcf).
s. Transfer the supernatant to a clean microcentrifuge tube and fast freeze on dry ice. Store at −80 °C.

2. Natural matrices: collagen I (Note: This protocol is for isolating proteins from 1-ml collagen/rBM gels. Adjust volumes stated if necessary.)

a. Prepare 10 ml of ice-cold collagen release solution: 2-mg/ml collagenase, 2-mg/ml trypsin, and 5% fetal bovine serum in DMEM:F12. Keep on ice until needed and warm the amount needed just prior to experimentation. (Note: The trypsin should be EDTA-free or cell cadherin junctions will be disrupted.)
b. Gently aspirate medium from the 3D culture.
c. Add 2.5 ml of the collagen release solution and 500 μl of full-strength dispase and incubate at 37 °C for 10–15 min. (Note: The dispase should be prewarmed to 37 °C.)
d. Pipette up and down vigorously using a p1000 pipette to disrupt the gel. Incubate at 37 °C for 10–15 min.
e. Repeat step (d) until pipetting is easy and the colonies fall freely.
f. Transfer the solubilized gel solution to a 15-ml conical tube.
g. Centrifuge tubes for 5 min at 180 × *g* rcf.
h. Aspirate the supernatant, leaving 5% of the media behind.
i. Resuspend the pellet in 5-ml DMEM:F12 with 10% fetal bovine serum. Pellet by centrifugation for 5 min at 180 × *g* rcf.
j. Repeat steps (h) and (i) three times to thoroughly wash the pellet.
k. Aspirate the supernatant, leaving 5% of the media behind.
l. Resuspend the pellet in 5-ml ice-cold DMEM:F12. Pellet by centrifugation (4 °C, 5 min; 180 rcf).
m. Repeat steps (k) and (l) three times to thoroughly wash the pellet.
n. Aspirate the supernatant.
o. Prepare lysis buffer, supplementing it with a cocktail of serine and cysteine protease and tyrosine phosphatase inhibitors. (Note: See Section IV for specific reagents and concentrations.)
p. Carefully aspirate the supernatant, and resuspend the pellet in 100–300 μl of lysis buffer, depending on the size of the pellet and the amount of protein expected.
q. Incubate on ice for 30 min.
r. Sonicate the lysis solution on ice with three pulses of 10 sec each at an output power of 8 W, pausing for 30 sec between each pulse for the sample to cool down.

s. Centrifuge final tube at 4 °C for 10 min (10,500 × *g* rcf).

t. Transfer the supernatant to a clean microcentrifuge tube, and fast freeze on dry ice. Store at −80 °C.

3. Synthetic matrices: functionalized polyacrylamide gels (Note: This protocol is for 50-mm polyacrylamide gels.)

a. Prepare the lysis buffer, supplementing it with a cocktail of serine and cysteine protease and tyrosine phosphatase inhibitors. (Note: See Section IV for specific reagents and concentrations.)

b. Aspirate the medium from the gels and rinse with ice-cold DPBS.

c. Aspirate the DPBS from each plate and invert the lids of 60-mm tissue culture dishes onto ice.

d. Remove the coverslip from the plate, and very carefully wipe the edges clean with a cotton swab and/or Kimwipe to remove any cells adhered to the glass or edges of the gel to eliminate cell variability.

e. Pipette 250 μl of lysis buffer into the lid of the tissue culture plate.

f. Place the coverslip gel-side down onto the lysis buffer and incubate on ice for 5 min.

g. With a cell scraper, push the coverslip down and carefully scrape the coverslip against the lid of the culture plate for at least 5 min.

h. Squeeze the excess buffer from underneath the glass and remove the coverslip from the lid.

i. Transfer the solution into a microcentrifuge tube.

j. Incubate on ice for 30 min.

k. Sonicate the lysis solution on ice with three pulses of 10 sec each at an output power of 8 W, pausing for 30 sec between each pulse for the sample to cool down.

l. Centrifuge final tube at 4 °C for 10 min (10,500 × *g* rcf).

m. Transfer the supernatant to a clean microcentrifuge tube and fast freeze on dry ice. Store at −80 °C.

C. Isolation of Bulk mRNA

1. Natural matrices: rBM

a. Prepare a 3-ml solution/ml of rBM of 4-M guanidine thiocyanate; 25-mM sodium citrate–citric acid, pH 7.0; 0.5% (w:v) *N*-laurylsarcosine, sodium salt; 100-mM 2-mercaptoethanol. (Note: The 2-mercaptoethanol should be added fresh each time.)

b. Aspirate culture media and add 3-ml guanidine thiocyanate/mercaptoethanol solution as prepared above for each milliliter of rBM.

c. Using a p1000 pipette, pipette the solution up and down to solubilize the rBM.

d. Transfer the solubilized solution to an RNase-free polypropylene tube.
e. Add 1/10 volume {note: for steps (e) through (g), 1 volume refers to the sum of the residual culture volume [from step (b)] and the guanidine thiocyanate/mercaptoethanol volume} of DEPC-treated 2-M acetic acid–sodium acetate, pH 4.0, and mix thoroughly by vortexing at the highest setting. (Note: Be sure to obtain a completely homogeneous solution before proceeding to the next step.)
f. In a fume hood, add 1 volume of 0.1-M citrate, pH 4.3 buffered/saturated phenol, and mix thoroughly by vortexing at the highest setting. (Note: Protective safety attire should be worn. Be sure to obtain a completely homogeneous solution before proceeding to the next step.)
g. In a fume hood, add 2/10 volume of 49:1 (v:v) chloroform:isoamyl alcohol. Incubate at room temperature for 5–10 min. Then, briskly shake the tube by hand 8–10 times. Do not vortex here. (Note: A milky solution should form.)
h. Place the tube on ice for at least 15 min. The emulsion should break into two phases at this point, with a clear aqueous layer forming on top of a milky organic layer.
i. Centrifuge at 4 °C for 30 min (3200 × *g* rcf) to clarify the upper aqueous phase.
j. Transfer the upper aqueous phase to a clean RNase-free tube, taking care to avoid disturbing the interface, and add equal volume (the volume of the aqueous phase) of isopropanol, prechilled to −20 °C. Mix well and incubate at −20 °C for 2 h to overnight to precipitate the RNA.
k. Pellet RNA by centrifugation at 4 °C for 30 min (21,000 × *g* rcf).
l. Carefully aspirate the supernatant, being careful not to disturb the loosely adherent pellet.
m. Add 500 μl of very cold (−20 °C) 75% (v:v) ethanol in DEPC-treated ddH_2O, and immediately pellet the total RNA by centrifugation at 4 °C for 15 min (21,000 × *g* rcf).
n. Repeat steps (l) and (m) six times to thoroughly wash the pellet and incubate the last wash in −20 °C 75% ethanol overnight.
o. Pellet total RNA by centrifugation at 4 °C for 15 min (21,000 × *g* rcf), and carefully aspirate the supernatant.
p. Air dry the pellet at room temperature until the pellet appears glassy (usually 10–15 min, depending on the volume of residual ethanol).
q. Dissolve the RNA pellet in DEPC-treated ddH_2O. The volume depends on the expected amount of total RNA. (Note: When starting with 250,000 preformed spheroids, the expected RNA yield usually ranges between 10 and 15 μg.) Incubate on ice for 30 min to 1 h to thoroughly solubilize RNA.
r. Store at −80 °C until required.

2. Natural matrices: collagen I
   a. Aspirate culture medium. Use a flamed RNase-free razor blade to cut the collagen gel into small pieces for easier RNA extraction, taking care to remove residual medium released prior to gel solubilization.
   b. Add 3 ml of the prepared guanidine thiocyanate/mercaptoethanol solution (as described in C.1) per 1 ml of collagen, and allow to solubilize for 5 min at room temperature on a rocking platform.
   c. Follow steps (C.1.e) to (C.1.s) to extract the total RNA.
3. Synthetic matrices: functionalized polyacrylamide gels
   a. Prepare a solution of 4-M guanidine thiocyanate; 25-mM sodium citrate–citric acid, pH 7.0; 0.5% (w:v) *N*-laurylsarcosine, sodium salt; 100-mM 2-mercaptoethanol. (Note: The 2-mercaptoethanol should be added fresh each time.)
   b. Invert the lids of 60-mm tissue culture dishes on the bench top. Add 600 μl of the prepared guanidine thiocyanate/mercaptoethanol solution for each 50-mm polyacrylamide gel to each lid.
   c. Remove the coverslip from the culture dish, and very carefully wipe the edges clean with a cotton swab and/or Kimwipe to remove any cells adhered to the glass or edges of the gel to eliminate cell variability.
   d. Place the coverslip gel-side down onto the guanidine thiocyanate/mercaptoethanol solution, and incubate on ice for 5 min.
   e. With a cell scraper, push the coverslip down and carefully scrape the coverslip against the lid of the culture plate for at least 5 min.
   f. Squeeze excess buffer from underneath the glass and remove the coverslip from the lid.
   g. Transfer the solution to an RNase-free polypropylene tube and follow steps outlined in (C.1.e) to (C.1.r) to extract the total RNA.

D. Rapid Protein Isolation Techniques

1. Synthetic matrices: functionalized polyacrylamide gels (Note: This protocol is for isolating Rac-GTP. For rapid isolation of other proteins, the assay will be similar, but may need to be modified and/or optimized. At least 600 μg of total protein is needed. Adjust the number and size of gels to obtain enough protein.)
   a. Prepare glutathione-sepharose beads for glutathione-*S*-transferase-tagged p21-binding domain of Pak1 (GST-PBD) binding.
      i. Centrifuge 1 ml of 50% glutathione-sepharose slurry at 4 °C for 30 sec (21,000 $\times$ *g* rcf).
      ii. Aspirate the supernatant and add 500-μl MLB (Section I.1). Pellet by centrifugation at 4 °C for 30 sec (21,000 $\times$ *g* rcf).

iii. Repeat step (ii) three times to wash the beads.
iv. Aspirate the supernatant and resuspend the sepharose beads in an equal volume of MLB (500 μl) to produce a 50% slurry.
v. Incubate the 20- to 30-μl GST-PBD with 20- to 30-μl sepharose slurry (4 °C; 20 min).

b. Supplement MLB with a cocktail of serine and cysteine protease and tyrosine phosphatase inhibitors. (Note: See Section IV for specific reagents and concentrations.)
c. Aspirate the medium from the gels and rinse with ice cold DPBS.
d. Aspirate the DPBS from each plate and invert the lids of 60-mm tissue culture plates onto ice.
e. Remove the coverslip from the plate, and very carefully wipe the edges clean with a cotton swab and/or Kimwipe to remove any cells adhered to the glass or edges of the gel to eliminate cell variability.
f. Pipette 350- to 400-μl MLB into the lid of the tissue culture plate.
g. Place the coverslip gel-side down onto the lysis buffer and incubate on ice for 5 min.
h. With a cell scraper, push the coverslip down and carefully scrape the coverslip against the lid of the culture plate for at least 5 min.
i. Squeeze the excess buffer from underneath the glass and remove the coverslip from the lid.
j. Pipette the MLB solution into a microcentrifuge tube, combining like samples.
k. Centrifuge the tubes at 4 °C for 5 min (10,500 $\times$ *g* rcf).
l. Transfer at least 800 μl of lysate into the tube containing GST-PBD. Leave at least 50 μl of lysate for determining total Rac separately.
m. Gently rock the solution at 4 °C for 60 min.
n. Collect the GST-PBD-Rac mixture by centrifugation at 4 °C for 30 sec (21,000 $\times$ *g* rcf).
o. Carefully aspirate the supernatant and resuspend the beads in 500 μl of ice-cold MLB.
p. Centrifuge at 4 °C for 30 sec (21,000 $\times$ *g* rcf).
q. Repeat steps (o) and (p) three times.
r. Resuspend the beads in 15 μl of sample loading buffer for electrophoresis and vortex briefly. Heat the samples to 95 °C for 10 min. (Note: Visually confirm that the sample loading buffer penetrates the beads before heating.)
s. Centrifuge the solution at room temperature for 30 sec (21,000 $\times$ *g* rcf).
t. Fast freeze the samples in a dry ice/ethanol bath and store at −80 °C.

E. Immunofluorescence

1. Natural matrices: rBM
   a. Aspirate cell culture medium, and wash in DPBS (containing Ca^{2+} and Mg^{2+}), if cultures were grown in serum.
   b. Add equal-volume neutralized collagen solution [see step (A.2.a) for directions, omitting ddH_2O] and mix thoroughly. (Note: Collagen is added to strengthen the matrix and permits easier cryosectioning.)
   c. Incubate the gels at 37 °C for 30 min to polymerize.
   d. If desired, sections can be triton-extracted prior to fixation to facilitate cytoskeletal and nuclear visualization.
      i. Prepare ice-cold cytoskeletal extraction buffer (see Section IV for details) containing Triton X-100 (0.005%; v:v) and 5-mM EGTA, supplemented with protease and phosphatase inhibitors.
      ii. Add equal-volume extraction buffer and incubate at room temperature for 30 min.
   e. Fix with 2% paraformaldehyde (pH 7.4) at 4 °C overnight.
   f. Rinse cultures with PBS/glycine at 4 °C (minimum 3×, 5 min each).
   g. Incubate cultures with 18% sucrose-1× PBS/glycine at 4 °C for 3 h.
   h. Incubate cultures with 30% sucrose-PBS/glycine at 4 °C for 3 h.
   i. Rinse cultures with PBS/glycine at 4 °C for 5 min.
   j. Add OCT Tissue Tek compound for cryosection, and rapidly freeze on a bed of dry ice and ethanol or in liquid nitrogen. Store culture blocks at −80 °C until required.
   k. Prepare activated gelatin-coated microscope slides:
      i. Autoclave (121 °C, 30 min) 0.5-g gelatin in 25-ml ddH_2O and cool to room temperature.
      ii. Add 0.05-g chromium potassium sulfate dissolved in 75 ml of ddH2O to precooled gelatin solution.
      iii. Store at 4 °C until required.
   l. Prepare microscope slides for tissue culture sections:
      i. To minimize antibody solution requirement, generate a hydrophobic incubation ring on a microscope slide. This can be done using a hydrophobic (wax) pen to draw small rings slightly larger than the tissue samples to be stained. Additionally, this can be achieved by melting paraffin at 95 °C around the circumference of a microcentrifuge tube or the lid of a 15-ml conical tube lid, and then gently, but firmly placing the tube on the slide. Incubate the slide on a heating block at 58 °C for 1 min. Carefully, remove the tube/lid from the slide while the slide is on the heating block, and let the paraffin solidify at room temperature.

ii. Evenly coat the interior of the paraffin ring with activated 0.5% gelatin, and air dry at room temperature overnight.

m. Using a cryostat, cut frozen sections of 3D tissue blocks (5–20 μm), and transfer sections to the gelatin-coated paraffin ring. Store the slides at −80 °C until required.

n. For immunostaining, remove sections from freezer, thaw, and air dry at room temperature for 5–20 min.

o. Rehydrate sections in IF buffer at room temperature for 20 min.

p. Incubate sections in blocking buffer at room temperature for 1 h or at 4 °C overnight in a humidified chamber.

q. Incubate sections in primary antibody solution at room temperature for 1–2 h or at 4 °C overnight in a humidified chamber.

r. Wash sections in IF buffer at room temperature, minimum three times for 15 min each.

s. Incubate in secondary antibody in IF buffer at room temperature for 45 min. (Note: If the secondary antibody is fluorescent, keep slides under foil.)

t. Wash sections in IF buffer at room temperature, minimum three times for 10 min each.

u. To visualize nuclei, counterstain with 1-μg/ml DAPI in PBS/glycine at room temperature for 5 min.

v. Rinse each gel in PBS/glycine at room temperature, minimum three times for 5 min each.

w. Aspirate residual liquid from the gels and mount sections with mounting media. Leave under foil to dry at room temperature for 15–30 min. Secure with nail polish when dry.

x. Store at −20 °C until visualization.

2. Natural matrices: collagen I

   a. Follow the steps outlined in Section III.E.1 , omitting steps (b) and (c).

3. Synthetic matrices: functionalized polyacrylamide gels

   a. Aspirate cell culture medium and rinse cells grown in serum with DPBS (containing Ca^{2+} and Mg^{2+}).

   b. Fix with 2% paraformaldehyde, pH 7.4 at room temperature for 30 min.

   c. Rinse with IF buffer at room temperature, minimum three times for 5 min each.

   d. With fine tip forceps, remove the coverslip from the cell culture dish, and place the coverslips gel-side on a secured piece of paraffin.

   e. Follow protocol outlined in steps (Section III.E.1.p) to (Section III. E.1.v).

f. Aspirate residual liquid from the gels and mount gels onto microscope slides with mounting media. Leave under foil to air dry at room temperature for 15–30 min. Secure with nail polish when dry.

g. Store at $-20\,^{\circ}C$ until visualization.

IV. Materials

A. Engineering Tissue Explants

1. Natural matrices: rBM
   a. Wet ice
   b. rBM, BD Biosciences BD Matrigel™ [Note: As there is inherent lot-to-lot variability, each lot should be tested prior to use. When deciding which lots to choose, we prefer lots that have endotoxin levels less than 2 units/ml and protein concentrations ranging from 9 to 12 mg/ml. Additionally, we have found that MECs behave similarly in Matrigel and Growth Factor Reduced Matrigel (both from BD), although this should be tested for each cell line. Each lot should be tested for compatibility with the various cell lines by looking for changes in morphology in 3D cultures and ensuring low background nucleic acid and IgG levels that would interfere with RNA isolation and immunofluorescence procedures. It should be noted also that the rheological properties of commercially available rBM preparations can also vary from $E = 50$ to 200 Pa (unpublished observations).]
   c. Cell culture supplies (medium, trypsin, trypsin-inhibiting agent)
2. Natural matrices: collagen I/rBM
   a. Wet ice
   b. Acid-solubilized rat tail collagen I [Note: Although this protocol is designed for acid-solubilized rat tail collagen I, we have previously used acid-solubilized bovine dermal collagen I (ICN Biomedicals Catalog No. 152394) and acid-solubilized rat tail collagen I (BD Labware Catalog No. 354236) to embed MECs in 3D ECM gels. As there is inherent lot variability, each lot should be tested prior to use to determine the appropriate concentration and gelling time for each system. Additionally, the elastic modulus of the gels can be manipulated by varying the concentration of collagen I ($E = 20$–1800 Pa; Leight *et al.*, unpublished observations). We have found that the elastic modulus varies between lots, so each lot should be tested prior to experimentation (unpublished observation).]
   c. 10× DPBS containing 1.33-g/ml Ca^{2+} and 1.0-g/ml Mg^{2+}, supplemented with phenol red.

d. Deionized, distilled water (ddH_2O)
e. 1-N sodium hydroxide (NaOH)
f. rBM
g. Cell culture supplies (medium, trypsin, trypsin-inhibiting agent)
h. Small sterile spatula

3. Synthetic matrices: functionalized polyacrylamide gels (Note: When possible, presterilized materials should be used.)

a. Bunsen burner
b. Coverslips (No. 1 thickness, hydrolytic class 1 borosilicate coverslips, Fisher; see note in Section III regarding the size of the coverslip required.)
c. Cotton swabs
d. 0.1-N NaOH
e. 3-Aminopropyltrimethoxysilane, 97%, Sigma Aldrich
f. Glutaraldehyde, 70%, Sigma Aldrich
g. PBS
h. ddH_2O
i. 40% Acrylamide
j. 2% Bis-acrylamide
k. 0.5-M *N*-(2-hydroxyethyl)-piperazine-*N*′-2-ethanesulfonic acid (HEPES buffer), pH 4.22
l. *N,N,N*′,*N*′-Tetramethylethylenediamine (TEMED)
m. *N*-Succinimidyl ester of acrylamidohexanoic acid (N6 cross-linker) [Note: The N6 cross-linker can be synthesized following the protocol outlined in Pless *et al*. (1983).]
n. 200-Proof ethanol
o. Rain-X™ (available at automobile part store).
p. Parafilm™
q. Ammonium persulfate (APS)
r. 50-mM HEPES buffer, pH 8.0
s. 0.5-M ethylenediaminetetraacetic acid (EDTA), pH 8.0
t. rBM
u. Ethanolamine, Sigma Aldrich
v. Sterile PBS
w. Sodium azide
x. Cell culture supplies (medium, trypsin, trypsin-inhibiting agent)
y. Cell culture antibiotics and antimycotics [fungizone (amphotericin B, Sigma Aldrich), gentamicin sulfate (Gibco™, penicillin G/streptomycin sulfate)]

B. Isolation of Bulk Proteins

1. Natural matrices and synthetic matrices
   a. DPBS (for rBM and functionalized polyacrylamide gels only)
   b. 0.5-M EDTA, pH 8.0 (for rBM and functionalized polyacrylamide gels only)
   c. Collagenase, Roche Applied Sciences (for collagen/rBM gels only)
   d. Trypsin (for collagen/rBM gels only)
   e. Dispase, BD Biosciences (for collagen/rBM gels only)
   f. Fetal bovine serum (for collagen/rBM gels only)
   g. DMEM:F12 (for collagen/rBM gels only)
   h. Wet ice
   i. Serine and cysteine protease and tyrosine phosphatase inhibitor cocktail: 2-μg/ml aprotinin (Roche Applied Sciences), 1-μg/ml leupeptin (Sigma Aldrich), 1-μg/ml E-64 (Sigma Aldrich), 50-mM sodium fluoride, 10-μg/ml pepstatin A (Sigma Aldrich), 0.5-mM benzamidine (Sigma Aldrich), 1-mM sodium orthovanadate, 1-mM Pefabloc SC (Roche Applied Sciences). [Note: Activate 125-mM sodium orthovanadate with 100-mM hydrogen peroxide at room temperature for 20 min just prior to use (Zhang *et al*., 2005). Add activated sodium orthovanadate and Pefabloc SC to solution just prior to use.]
   j. Appropriate lysis buffer (Note: The choice of lysis buffer is dependent on the nature of the protein to be studied and should be optimized for each experiment. Radioimmunoprecipitation assay (RIPA) and Laemmli buffers are common choices. RIPA buffer enables suitable extraction of cytoplasmic proteins, while Laemmli buffer is effective for membrane-bound and nuclear proteins.)
      i. RIPA buffer: 50-mM Tris–HCl pH 8.0, 50-mM sodium chloride, 0.5% (w:v) sodium deoxycholate, 1% IGEPAL® CA-630 (Sigma Aldrich), 0.1% (w:v) SDS
      ii. Laemmli buffer: 33.3-mM Tris–HCl pH 8.0, 50-mM EDTA, 2% (w:v) SDS
   k. Cell scraper, Sigma Aldrich
   l. Dry ice

C. Isolation of Bulk mRNA

1. Natural matrices and synthetic matrices
   a. Diethyl pyrocarbonate (DEPC)-treated ddH_2O (Note: Prepare by adding 1-ml DEPC (Sigma Aldrich) to 500-ml ddH_2O in a glass bottle. Mix vigorously, and incubate overnight in a fume hood, leaving the cap slightly loose. Autoclave for 45 min at 121 °C, 20 psig, and store at room temperature.)

b. 4-M guanidine thiocyanate; 25-mM sodium citrate–citric acid, pH 7.0; 0.5% (w:v) *N*-laurylsarcosine (ICN Biomedicals), sodium salt; in DEPC-treated ddH_2O
c. 2-Mercaptoethanol
d. DEPC-treated 2-M acetic acid–sodium acetate, pH 4.0 (Note: Prepare by adding 4.022-ml glacial acetic acid to 31-ml ddH_2O. Adjust the pH to 4.0 with 2-M sodium acetate. Add 2 μl/ml total volume of DEPC. Mix well and incubate at room temperature overnight. Autoclave for 15 min at 121 °C, 18 psig, and store at room temperature.)
e. 0.1-M citrate, pH 4.3 buffered/saturated phenol, Sigma Aldrich
f. 49:1 (v:v) Chloroform:isoamyl alcohol
g. Wet ice
h. Isopropanol
i. 75% Ethanol in DEPC-treated ddH_2O

D. Rapid Protein Isolation Techniques

1. Synthetic matrices: functionalized polyacrylamide gels
   a. MLB: 25-mM HEPES, pH 7.5; 150-mM sodium chloride; 1% Igepal CA-630; 10-mM $MgCl_2$; 1-mM EDTA; 10% glycerol
   b. Serine and cysteine protease and tyrosine phosphatase inhibitor cocktail: 2-μg/ml aprotinin (Roche Applied Sciences), 1-μg/ml leupeptin (Sigma Aldrich), 1-μg/ml E-64 (Sigma Aldrich), 50-mM sodium fluoride, 10-μg/ml pepstatin A (Sigma Aldrich), 0.5-mM benzamidine (Sigma Aldrich), 1-mM sodium orthovanadate, 1-mM Pefabloc SC (Roche Applied Sciences) [Note: Activate 125-mM sodium orthovanadate with 100-mM hydrogen peroxide at room temperature for 20 min just prior to use (Zhang *et al*., 2005). Add activated sodium orthovanadate and Pefabloc SC to solution just prior to use.]
   c. Sample loading buffer: 0.25-M Tris, pH 6.8; 50% (v:v) glycerol; 2% (w:v) sodium dodecyl sulfate (SDS); 50-μl/ml 2-mercaptoethanol in ddH_2O, supplemented with bromophenol blue
   d. Wet ice
   e. Ice-cold DPBS
   f. Glutathione-sepharose slurry, Sigma Aldrich

E. Immunofluorescence

1. Natural matrices and synthetic matrices
   a. DPBS (containing 1.33-g/ml Ca^{2+} and 1.0-g/ml Mg^{2+})
   b. Wet ice
   c. Acid-solubilized rat tail collagen I

d. 10× DPBS with Ca^{2+} and Mg^{2+}, supplemented with phenol red
e. ddH_2O
f. 1-N NaOH
g. 1.5× Cytoskeletal extraction buffer: 150-mM sodium chloride; 450-mM sucrose; 15-mM piperazine-1,4-bis(2-ethanesulfonic acid) (PIPES) buffer, pH 6.7; 5-mM magnesium chloride in ddH_2O
h. Triton X-100
i. Serine and cysteine protease and tyrosine phosphatase inhibitor cocktail: 2-μg/ml aprotinin, 1-μg/ml leupeptin, 1-μg/ml E-64, 50-mM sodium fluoride, 10-μg/ml pepstatin, 0.5-mM benzamidine, 1-mM sodium orthovanadate, 1-mM Pefabloc SC (Note: Activate sodium orthovanadate with hydrogen peroxide just prior to use. Add activated sodium orthovanadate and Pefabloc SC to solution just prior to use.)
j. 2% (w:v) Paraformaldehyde, pH 7.4
k. PBS/glycine (1× PBS, supplemented with 75-mg/ml glycine)
l. Dry ice
m. 0.5% (w:v) Porcine gelatin (Sigma Aldrich) in ddH_2O, supplemented with 0.5-mg/ml chromium potassium sulfate
n. Microscope slides
o. Paraffin
p. IF buffer: 7.6-mg/ml sodium chloride, 1.9-mg/ml sodium phosphate, 0.4-mg/ml potassium phosphate monobasic, 0.5-mg/ml sodium azide, 1-mg/ml bovine serum albumin, 0.2% (v:v) Triton X-100, 0.05% (v:v) Tween 20 in ddH_2O
q. Blocking buffer: 10% normal goat serum, 0.13-mg/ml appropriate Fab fragments, in IF buffer
r. Primary and secondary antibodies
s. Aluminum foil
t. 4′,6-Diamidino-2-phenylindole (DAPI), Sigma Aldrich
u. Mounting medium (e.g., Vectashield Mounting Medium®, Vector)
v. Nail polish

V. Discussion

Epithelial tissues are highly complex, organized 3D structures that evolve incrementally during development to generate these specialized functional tissues through spatially and temporally controlled stromal–epithelial interactions. The tissue microenvironment of the epithelium is composed of multiple stromal cell types, and these cellular components, together with the epithelium, are embedded

within a proteinaceous ECM. It is the combination of cellular and ECM interactions, operating through controlled biochemical and physical cues, that ultimately regulates epithelial cell fate and function. The goal of an epithelial experimentalist is to recreate at least some of the intricate relationships that exist between the various cell types and the ECM *in vivo*, but in a simple format in culture, such that the recreated system is more amenable to molecular studies without severely compromising the epithelial cell's normal tissue behavior. The idea is that experimental observations made using such "contrived but simplified systems" will ultimately be distilled into the critical information that is necessary to systematically engineer surrogate tissues for replacement therapy or to develop tractable treatments to prevent and cure various diseases. Toward this lofty goal, considerable research has been successfully directed at determining how each individual cell variable and microenvironmental component influences epithelial cell behavior (Mostov *et al*., 2005; Paszek *et al*., 2005; Petersen *et al*., 1992).

Despite the efforts, our understanding of what controls the epithelial cells' behavior within the complex 3D tissue-like structure and how combinations of microenvironmental cues might cooperate to influence epithelial function remains rudimentary at best. Moreover, although we and others have been successful in generating functional data using these "crude" systems, it remains difficult to isolate specific responses to allow the identification of the precise molecular mechanisms linked to the generation of a given tissue phenotype. For example, MECs grown within a 3D rBM simultaneously and acutely change their shape, matrix adhesion, cell contractility, and signaling, as well as growth factor and apoptosis responsiveness, as compared to MECs interacting with a 2D rigid substrate (Debnath *et al*., 2003; Wang *et al*., 1998; Weaver *et al*., 2002). To address this difficulty, tractable culture models that reproducibly reconstruct individual aspects of tissue organization and function and that encompass controllable homotypic and heterotypic cell–cell interactions and ECM cues are needed. Preferably, these newly engineered culture systems will be amenable to precise biochemical and physical manipulation and will be sufficiently robust and versatile for routine experimentation. Additionally, they should be inexpensive and lend themselves to easy and reproducible manipulation.

Conventional organotypic systems are often expensive, labor intensive to generate, and suffer from experimental inconsistencies. It is now feasible to synthesize biocompatible matrices to study the effect of individual parameters, such as matrix binding and ECM orientation, receptor expression and activity, cell shape, matrix compliance, and even ECM dimensionality through a combination of nonreactive hydrogels with cell-adhesive sites. Recombinant synthetic proteins have also been used to promote specific adhesion and to foster cell-specific degradation and remodeling of the matrix by incorporating proteolytically degradable peptide sequences. We and others have applied similar strategies to successfully study the phenotypic behavior of individual cells in response to various physical, architectural, and biochemical cues including issues pertaining to the regulation of cell survival (Buckley *et al*., 1999; Capello *et al*., 2006; Chen *et al*., 1997; Friedland

et al., unpublished observations), migration (Gobin and West, 2002; Wong *et al*., 2003), stem cell fate (McBeath *et al*., 2004), differentiation (Bokhari *et al*., 2005; Mauck *et al*., 2006), and growth regulation (Bokhari *et al*., 2005; Georges *et al*., 2006; Paszek *et al*., 2005). However, such specialized systems have limited application for studying cell behavior in multicellular structures and 3D tissues and have only sparingly been applied to the study of heterotypic cell–cell interactions (Georges *et al*., 2006). Moreover, many of the currently available synthetic biomaterials exhibit incompatible material properties such as high stiffness, elevated matrix density, and random matrix presentation that render them less than suitable for the study of epithelial tissue morphogenesis (reviewed in Zhang, 2004). To address these concerns, newer generations of biomaterials are currently being developed, including highly compliant synthetic matrices generated using combinations of polyethylene glycol and methylcellulose conjugated with various bioactive peptides and MMP-cleavable proteins (Leach JB, personal communication), polyethylene glycol gels with functionalized recombinant proteins (Rizzi and Hubbell, 2005), electrically spun collagen gels with precisely controlled orientations (Matthews *et al*., 2002), and synthetic gels with gradients of ECM compliance that recreate durotactic-directed cell migration during development, wound closure, and tumor metastasis (Lo *et al*., 2000; Wong *et al*., 2003; Zaari *et al*., 2004). Au6
The application of these novel materials together with the availability of pluripotent and tissue-specific stem cells provide encouragement that we are at least moving closer to our idealized model systems, to begin to elucidate the mechanisms regulating multicellular epithelial tissue-specific structure and function.

In addition to these important considerations, it is recognized that tissues develop progressively and evolve through reciprocal and dynamic dialogues between the cellular and stromal components and tissue milieu, and this temporal relationship must also provide the mature tissue with physiological advantages that need to be identified and assessed. For example, although bioengineers have been able to successfully reconstruct blood vessels that are phenotypically and functionally identical to differentiated arteries *in vivo*, the engineered vessels rapidly fatigue when transplanted into a host *in vivo*. One must also consider that our ultimate goal should be the engineering of complex 3D microenvironments that are amenable to dynamic physical and biochemical modification. When seeded with pluripotent and tissue-specific stem cells, they should allow systematic development *ex vivo* of viable, live tissues to be used for routine and faithful experimentation and for various clinical applications. Clearly, we have our work cut out for us.

Acknowledgments

We thank J. C. Friedland and J. N. Lakins for their contributions. This work was supported by NIH grants CA078731 and BRP HL6438801A1 (to V.M.W.) and T32HL00795404 (to K.R.J.), DOD grants W81XWH-05-1-330 and DAMD17-01-1-0367 (to V.M.W.), and a NSF graduate fellowship (to J.L.L.).

References

Akhtar, N., and Streuli, C. H. (2006). Rac1 links integrin-mediated adhesion to the control of lactational differentiation in mammary epithelia. *J. Cell Biol.* **5,** 781–793.

Alford, D., Baeckstrom, D., Geyp, M., Pitha, P., and Taylor-Papadimitriou, J. (1998). Integrin-matrix interactions affect the form of the structures developing from human mammary epithelial cells in collagen or fibrin gels. *J. Cell Sci.* **111**(Pt. 4), 521–532. Au7

Azuma, M., and Sato, M. (1994). Morphogenesis of normal human salivary gland cells *in vitro*. *Histol. Histopathol.* **4,** 781–790.

Barros, E. J., Santos, O. F., Matsumoto, K., Nakamura, T., and Nigam, S. K. (1995). Differential tubulogenic and branching morphogenetic activities of growth factors: Implications for epithelial tissue development. *Proc. Natl. Acad. Sci. USA* **10,** 4412–4416.

Bissell, M. J., Radisky, D. C., Rizki, A., Weaver, V. M., and Petersen, O. W. (2002). The organizing principle: Microenvironmental influences in the normal and malignant breast. *Differentiation* **9–10,** 537–546.

Bissell, M. J., Weaver, V. M., Lelievre, S. A., Wang, F., Petersen, O. W., and Schmeichel, K. L. (1999). Tissue structure, nuclear organization, and gene expression in normal and malignant breast. *Cancer Res.* **59**(7 Suppl.), 1757–1763s; discussion 1763s–1764s. Au8

Bokhari, M. A., Akay, G., Zhang, S., and Birch, M. A. (2005). The enhancement of osteoblast growth and differentiation *in vitro* on a peptide hydrogel-polyHIPE polymer hybrid material. *Biomaterials* **25,** 5198–5208.

Buckley, S., Driscoll, B., Barsky, L., Weinberg, K., Anderson, K., and Warburton, D. (1999). ERK activation protects against DNA damage and apoptosis in hyperoxic rat AEC2. *Am. J. Physiol.* **1**(Pt. 1), L159–L166.

Capello, A., Krenning, E. P., Bernard, B. F., Breeman, W. A., Erion, J. L., and de Jong, M. (2006). Anticancer activity of targeted proapoptotic peptides. *J. Nucl. Med.* **1,** 122–129.

Chen, C. S., Mrksich, M., Huang, S., Whitesides, G. M., and Ingber, D. E. (1997). Geometric control of cell life and death. *Science* **5317,** 1425–1428.

Chen, C. S., Mrksich, M., Huang, S., Whitesides, G. M., and Ingber, D. E. (1998). Micropatterned surfaces for control of cell shape, position, and function. *Biotechnol. Prog.* **3,** 356–363.

Christner, P. J., Gentiletti, J., Peters, J., Ball, S. T., Yamauchi, M., Atsawasuwan, P., Beason, D. P., Soslowsky, L. J., and Birk, D. E. (2006). Collagen dysregulation in the dermis of the Sagg/+mouse: A loose skin model. *J. Invest. Dermatol.* **3,** 595–602.

Debnath, J., Muthuswamy, S. K., and Brugge, J. S. (2003). Morphogenesis and oncogenesis of MCF-10A mammary epithelial acini grown in three-dimensional basement membrane cultures. *Methods* **3,** 256–268.

Elbjeirami, W. M., Yonter, E. O., Starcher, B. C., and West, J. L. (2003). Enhancing mechanical properties of tissue-engineered constructs via lysyl oxidase crosslinking activity. *J. Biomed. Mater. Res. A.* **3,** 513–521.

Emerman, J. T., and Pitelka, D. R. (1977). Maintenance and induction of morphological differentiation in dissociated mammary epithelium on floating collagen membranes. *In Vitro* **13,** 316–328.

Engler, A., Bacakova, L., Newman, C., Hategan, A., Griffin, M., and Discher, D. (2004). Substrate compliance versus ligand density in cell on gel responses. *Biophys. J.* **1**(Pt. 1), 617–628.

Fuchs, E., Dowling, J., Segre, J., Lo, S. H., and Yu, Q. C. (1997). Integrators of epidermal growth and differentiation: Distinct functions for beta 1 and beta 4 integrins. *Curr. Opin. Genet. Dev.* **5,** 672–682.

Georges, P. C., Miller, W. J., Meaney, D. F., Sawyer, E. S., and Janmey, P. A. (2006). Matrices with compliance comparable to that of brain tissue select neuronal over glial growth in mixed cortical cultures. *Biophys. J.* **8,** 3012–3018.

Girton, T. S., Oegema, T. R., and Tranquillo, R. T. (1999). Exploiting glycation to stiffen and strengthen tissue equivalents for tissue engineering. *J. Biomed. Mater. Res.* **1,** 87–92.

Gobin, A. S., and West, J. L. (2002). Cell migration through defined, synthetic ECM analogs. *FASEB J.* **7,** 751–753.

Green, S. K., Frankel, A., and Kerbel, R. S. (1999). Adhesion-dependent multicellular drug resistance. *Anticancer Drug Des.* **2,** 153–168.

Grinnell, F. (2003). Fibroblast biology in three-dimensional collagen matrices. *Trends Cell Biol.* **5,** 264–269.

Gudjonsson, T., Ronnov-Jessen, L., Villadsen, R., Rank, F., Bissell, M. J., and Petersen, O. W. (2002). Normal and tumor-derived myoepithelial cells differ in their ability to interact with luminal breast epithelial cells for polarity and basement membrane deposition. *J. Cell Sci.* **115**(Pt. 1), 39–50. Au9

Guo, W. H., Frey, M. T., Burnham, N. A., and Wang, Y. L. (2006). Substrate rigidity regulates the formation and maintenance of tissues. *Biophys. J.* **6,** 2213–2220.

Hagios, C., Lochter, A., and Bissell, M. J. (1998). Tissue architecture: The ultimate regulator of epithelial function? *Philos. Trans. R. Soc. Lond., B. Biol. Sci.* **1370,** 857–870.

Hendrix, M. J., Seftor, E. A., Meltzer, P. S., Gardner, L. M., Hess, A. R., Kirschmann, D. A., Schatteman, G. C., and Seftor, R. E. (2001). Expression and functional significance of VE-cadherin in aggressive human melanoma cells: Role in vasculogenic mimicry. *Proc. Natl. Acad. Sci. USA* **14,** 8018–8023.

Huttenlocher, A., Lakonishok, M., Kinder, M., Wu, S., Truong, T., Knudsen, K. A., and Horwitz, A. F. (1998). Integrin and cadherin synergy regulates contact inhibition of migration and motile activity. *J. Cell Biol.* **2,** 515–526.

Huttenlocher, A., Sandborg, R. R., and Horwitz, A. F. (1995). Adhesion in cell migration. *Curr. Opin. Cell Biol.* **5,** 697–706.

Ingber, D. E. (2006). Mechanical control of tissue morphogenesis during embryological development. *Int. J. Dev. Biol.* **2–3,** 255–266.

Jacobson, M. D., Weil, M., and Raff, M. C. (1997). Programmed cell death in animal development. *Cell* **3,** 347–354.

Jeffery, P. K. (2001). Remodeling in asthma and chronic obstructive lung disease. *Am. J. Respir. Crit. Care Med.* **10**(Pt. 2), S28–S38.

Kadoya, Y., and Yamashina, S. (2005). Salivary gland morphogenesis and basement membranes. *Anat. Sci. Int.* **2,** 71–79.

Keely, P. J., Fong, A. M., Zutter, M. M., and Santoro, S. A. (1995). Alteration of collagen-dependent adhesion, motility, and morphogenesis by the expression of antisense alpha 2 integrin mRNA in mammary cells. *J. Cell Sci.* **108**(Pt. 2), 595–607. Au10

Kleinman, H. K., McGarvey, M. L., Hassell, J. R., Star, V. L., Cannon, F. B., Laurie, G. W., and Martin, G. R. (1986). Basement membrane complexes with biological activity. *Biochemistry* **2,** 312–318.

Liu, M., Tanswell, A. K., and Post, M. (1999). Mechanical force-induced signal transduction in lung cells. *Am. J. Physiol.* **4**(Pt. 1), L667–L683.

Lo, C. M., Wang, H. B., Dembo, M., and Wang, Y. L. (2000). Cell movement is guided by the rigidity of the substrate. *Biophys. J.* **1,** 144–152.

Locascio, A., and Nieto, M. A. (2001). Cell movements during vertebrate development: Integrated tissue behaviour versus individual cell migration. *Curr. Opin. Genet. Dev.* **4,** 464–469.

Lutolf, M. P., and Hubbell, J. A. (2005). Synthetic biomaterials as instructive extracellular microenvironments for morphogenesis in tissue engineering. *Nat. Biotechnol.* **1,** 47–55.

Margulis, A., Zhang, W., Alt-Holland, A., Crawford, H. C., Fusenig, N. E., and Garlick, J. A. (2005). E-cadherin suppression accelerates squamous cell carcinoma progression in three-dimensional, human tissue constructs. *Cancer Res.* **5,** 1783–1791.

Martin, R. B., Lau, S. T., Mathews, P. V., Gibson, V. A., and Stover, S. M. (1996). Collagen fiber organization is related to mechanical properties and remodeling in equine bone. A comparison of two methods. *J. Biomech.* **12,** 1515–1521.

Matthews, J. A., Wnek, G. E., Simpson, D. G., and Bowlin, G. L. (2002). Electrospinning of collagen nanofibers. *Biomacromolecules* **2,** 232–238.

Mauck, R. L., Yuan, X., and Tuan, R. S. (2006). Chondrogenic differentiation and functional maturation of bovine mesenchymal stem cells in long-term agarose culture. *Osteoarthr. Cartil.* **2,** 179–189.

McBeath, R., Pirone, D. M., Nelson, C. M., Bhadriraju, K., and Chen, C. S. (2004). Cell shape, cytoskeletal tension, and RhoA regulate stem cell lineage commitment. *Dev. Cell* **4,** 483–495.

Mostov, K., Brakeman, P., Datta, A., Gassama, A., Katz, L., Kim, M., Leroy, P., Levin, M., Liu, K., Martin, F., O'Brien, L. E., Verges, M., *et al.* (2005). Formation of multicellular epithelial structures. *Novartis Found. Symp.* **269,** 193–200; discussion 200–205, 223–230. Au11, 12

Muschler, J., Lochter, A., Roskelley, C. D., Yurchenco, P., and Bissell, M. J. (1999). Division of labor among the alpha6beta4 integrin, beta1 integrins, and an E3 laminin receptor to signal morphogenesis and beta-casein expression in mammary epithelial cells. *Mol. Biol. Cell* **9,** 2817–2828.

Nogawa, H., and Ito, T. (1995). Branching morphogenesis of embryonic mouse lung epithelium in mesenchyme-free culture. *Development* **4,** 1015–1022.

Novaro, V., Roskelley, C. D., and Bissell, M. J. (2003). Collagen-IV and laminin-1 regulate estrogen receptor alpha expression and function in mouse mammary epithelial cells. *J. Cell. Sci.* **116**(Pt. 14), 2975–2986. Au13

O'Brien, L. E., Jou, T. S., Pollack, A. L., Zhang, Q., Hansen, S. H., Yurchenco, P., and Mostov, K. E. (2001). Rac1 orientates epithelial apical polarity through effects on basolateral laminin assembly. *Nat. Cell Biol.* **9,** 831–838.

O'Brien, L. E., Zegers, M. M., and Mostov, K. E. (2002). Opinion: Building epithelial architecture: Insights from three-dimensional culture models. *Nat. Rev. Mol. Cell Biol.* **7,** 531–537.

Paszek, M. J., and Weaver, V. M. (2004). The tension mounts: Mechanics meets morphogenesis and malignancy. *J. Mammary Gland Biol. Neoplasia* **4,** 325–342.

Paszek, M. J., Zahir, N., Johnson, K. R., Lakins, J. N., Rozenberg, G. I., Gefen, A., Reinhart-King, C. A., Margulies, S. S., Dembo, M., Boettiger, D., Hammer, D. A., and Weaver, V. M. (2005). Tensional homeostasis and the malignant phenotype. *Cancer Cell.* **3,** 241–254.

Pelham, R. J., Jr., and Wang, Y. (1997). Cell locomotion and focal adhesions are regulated by substrate flexibility. *Proc. Natl. Acad. Sci. USA* **25,** 13661–13665.

Petersen, O. W., Ronnov-Jessen, L., Howlett, A. R., and Bissell, M. J. (1992). Interaction with basement membrane serves to rapidly distinguish growth and differentiation pattern of normal and malignant human breast epithelial cells. *Proc. Natl. Acad. Sci. USA* **19,** 9064–9068.

Pless, D. D., Lee, Y. C., Roseman, S., and Schnaar, R. (1983). Specific cell adhesion to immobilized glycoproteins demonstrated using new reagents for protein and glycoprotein immobilization. *J. Biol. Chem.* **258,** 2340–2349.

Pujuguet, P., Simian, M., Liaw, J., Timpl, R., Werb, Z., and Bissell, M. J. (2000). Nidogen-1 regulates laminin-1-dependent mammary-specific gene expression. *J. Cell. Sci.* **113**(Pt. 5), 849–858. Au14

Rizzi, S. C., and Hubbell, J. A. (2005). Recombinant protein-co-PEG networks as cell-adhesive and proteolytically degradable hydrogel matrixes. Part I: Development and physicochemical characteristics. *Biomacromolecules* **3,** 1226–1238.

Roeder, B. A., Kokini, K., Sturgis, J. E., Robinson, J. P., and Voytik-Harbin, S. L. (2002). Tensile mechanical properties of three-dimensional type I collagen extracellular matrices with varied microstructure. *J. Biomech. Eng.* **2,** 214–222.

Rosenfeldt, H., and Grinnell, F. (2000). Fibroblast quiescence and the disruption of ERK signaling in mechanically unloaded collagen matrices. *J. Biol. Chem.* **5,** 3088–3092.

Roskelley, C. D., Srebrow, A., and Bissell, M. J. (1995). A hierarchy of ECM-mediated signalling regulates tissue-specific gene expression. *Curr. Opin. Cell Biol.* **5,** 736–747.

Sethi, T., Rintoul, R. C., Moore, S. M., MacKinnon, A. C., Salter, D., Choo, C., Chilvers, E. R., Dransfield, I., Donnelly, S. C., Strieter, R., and Haslett, C. (1999). Extracellular matrix proteins protect small cell lung cancer cells against apoptosis: A mechanism for small cell lung cancer growth and drug resistance *in vivo*. *Nat. Med.* **6,** 662–668.

Springer, T. A., and Wang, J. H. (2004). The three-dimensional structure of integrins and their ligands, and conformational regulation of cell adhesion. *Adv. Protein Chem.* **2,** 9–63. Au15

Stegemann, J. P., Hong, H., and Nerem, R. M. (2005). Mechanical, biochemical, and extracellular matrix effects on vascular smooth muscle cell phenotype. *J. Appl. Physiol.* **6,** 2321–2327.

Tan, J. L., Tien, J., Pirone, D. M., Gray, D. S., Bhadriraju, K., and Chen, C. S. (2003). Cells lying on a bed of microneedles: An approach to isolate mechanical force. *Proc. Natl. Acad. Sci. USA* **4,** 1484–1489.

Thornberry, N. A., and Lazebnik, Y. (1998). Caspases: Enemies within. *Science* **5381,** 1312–1316.

Wang, F., Weaver, V. M., Petersen, O. W., Larabell, C. A., Dedhar, S., Briand, P., Lupu, R., and Bissell, M. J. (1998). Reciprocal interactions between beta1-integrin and epidermal growth factor receptor in three-dimensional basement membrane breast cultures: A different perspective in epithelial biology. *Proc. Natl. Acad. Sci. USA* **25,** 14821–14826.

Wang, H. B., Dembo, M., Hanks, S. K., and Wang, Y. (2001). Focal adhesion kinase is involved in mechanosensing during fibroblast migration. *Proc. Natl. Acad. Sci. USA* **20,** 11295–11300.

Wang, W., Goswami, S., Sahai, E., Wyckoff, J. B., Segall, J. E., and Condeelis, J. S. (2005). Tumor cells caught in the act of invading: Their strategy for enhanced cell motility. *Trends Cell Biol.* **3,** 138–145.

Weaver, V. M., and Bissell, M. J. (1999). Functional culture models to study mechanisms governing apoptosis in normal and malignant mammary epithelial cells. *J. Mammary Gland Biol. Neoplasia* **2,** 193–201.

Weaver, V. M., Fischer, A. H., Peterson, O. W., and Bissell, M. J. (1996). The importance of the microenvironment in breast cancer progression: Recapitulation of mammary tumorigenesis using a unique human mammary epithelial cell model and a three-dimensional culture assay. *Biochem. Cell Biol.* **6,** 833–851.

Weaver, V. M., Lelievre, S., Lakins, J. N., Chrenek, M. A., Jones, J. C., Giancotti, F., Werb, Z., and Bissell, M. J. (2002). Beta4 integrin-dependent formation of polarized three-dimensional architecture confers resistance to apoptosis in normal and malignant mammary epithelium. *Cancer Cell* **3,** 205–216.

Weaver, V. M., Petersen, O. W., Wang, F., Larabell, C. A., Briand, P., Damsky, C., and Bissell, M. J. (1997). Reversion of the malignant phenotype of human breast cells in three-dimensional culture and *in vivo* by integrin blocking antibodies. *J. Cell Biol.* **1,** 231–245.

Willem, M., Miosge, N., Halfter, W., Smyth, N., Jannetti, I., Burghart, E., Timpl, R., and Mayer, U. (2002). Specific ablation of the nidogen-binding site in the laminin gamma1 chain interferes with kidney and lung development. *Development* **11,** 2711–2722.

Wong, J. Y., Velasco, A., Rajagopalan, P., and Pham, Q. (2003). Directed movement of vascular smooth muscle cells on gradient-compliant hydrogels. *Langmuir* **19,** 1908–1913.

Wozniak, M. A., Desai, R., Solski, P. A., Der, C. J., and Keely, P. J. (2003). ROCK-generated contractility regulates breast epithelial cell differentiation in response to the physical properties of a three-dimensional collagen matrix. *J. Cell Biol.* **3,** 583–595.

Yamada, K. M., Pankov, R., and Cukierman, E. (2003). Dimensions and dynamics in integrin function. *Braz. J. Med. Biol. Res.* **8,** 959–966.

Yap, A. S., Stevenson, B. R., Keast, J. R., and Manley, S. W. (1995). Cadherin-mediated adhesion and apical membrane assembly define distinct steps during thyroid epithelial polarization and lumen formation. *Endocrinology* **10,** 4672–4680.

Yeung, T., Georges, P. C., Flanagan, L. A., Marg, B., Ortiz, M., Funaki, M., Zahir, N., Ming, W., Weaver, V., and Janmey, P. A. (2005). Effects of substrate stiffness on cell morphology, cytoskeletal structure, and adhesion. *Cell Motil. Cytoskeleton* **1,** 24–34.

Zahir, N., Lakins, J. N., Russell, A., Ming, W., Chatterjee, C., Rozenberg, G. I., Marinkovich, M. P., and Weaver, V. M. (2003). Autocrine laminin-5 ligates alpha6beta4 integrin and activates RAC and NFkappaB to mediate anchorage-independent survival of mammary tumors. *J. Cell Biol.* **6,** 1397–1407.

Zahir, N., and Weaver, V. M. (2004). Death in the third dimension: Apoptosis regulation and tissue architecture. *Curr. Opin. Genet. Dev.* **1,** 71–80.

Zhang, S. (2004). Beyond the Petri dish. *Nat. Biotechnol.* **2,** 151–152.

Zhang, X., Huang, J., and McNaughton, P. A. (2005). NGF rapidly increases membrane expression of TRPV1 heat-gated ion channels. *EMBO J.* **24,** 4211–4223.

Zink, D., Fischer, A. H., and Nickerson, J. A. (2004). Nuclear structure in cancer cells. *Nat. Rev. Cancer* **9,** 677–687.

Author Query

Methods in Cell Biology, 83
Article No.: Chapter 23

ELSEVIER

Dear Author,

During the preparation of your manuscript for typesetting some questions have arisen. These are listed below. Please check your typeset proof carefully and mark any corrections in the margin of the proof or compile them as a separate list. This form should then be returned with your marked proof/list of corrections to Elsevier Science.

Disk use

In some instances we may be unable to process the electronic file of your article and/or artwork. In that case we have, for efficiency reasons, proceeded by using the hard copy of your manuscript. If this is the case the reasons are indicated below:

☐ Disk damaged ☐ Incompatible file format ☐ LaTeX file for non-LaTeX journal

☐ Virus infected ☐ Discrepancies between electronic file and (peer-reviewed, therefore definitive) hard copy.

☐ Other: .....

We have proceeded as follows:

☐ Manuscript scanned ☐ Manuscript keyed in ☐ Artwork scanned

☐ Files only partly used (parts processed differently:.....)

Bibliography

If discrepancies were noted between the literature list and the text references, the following may apply:

☐ The references listed below were noted in the text but appear to be missing from your literature list. Please complete the list or remove the references from the text.

☐ Uncited references: This section comprises references which occur in the reference list but not in the body of the text. Please position each reference in the text or, alternatively, delete it. Any reference not dealt with will be retained in this section.

Query Refs.	Details Required	Author's response
AU1	Please check the change for correctness.	
AU2	As per style, ''Abbreviations'' are not listed in the chapter rather they are integrated into the text at the first occurrence.	
AU3	Time-specific term ''recently'' which ''date'' a volume has been deleted. Please check the change for accuracy (in all such cases).	
AU4	The style for cross-citation of chapters is ''Chapter No. by Author(s), this volume.'' Kindly check the change for accuracy (in all such cases).	
AU5	Please check the change to maintain consistency throughout the chapter and volume.	
AU6	Reference ''Zaari et al. (2004)'' is not provided in the reference list. Please provide with complete bibliographic details.	
AU7	Please check the inserted volume number.	

AU8	Please check the inserted volume number.	
AU9	Please check the inserted volume number.	
AU10	Please check the inserted volume number.	
AU11	As per style et al. is allowed only after 12 author names. Please check the inserted author names.	
AU12	Please check the inserted volume number.	
AU13	Please check the inserted volume number.	
AU14	Please check the inserted volume number.	
AU15	Please provide volume number.	
AU16	Please check the change for accuracy.	
AU17	Please check the change to maintain consistency throughout the volume.	
AU18	Please check the change for accuracy.	
AU19	please check the chapter running head for accuracy.	

α6β4 integrin activates Rac-dependent p21-activated kinase 1 to drive NFκ B-dependent apoptosis resistance in 3D mammary acini

Julie C. Friedland[1,3,4], Johnathon N. Lakins[1,2], Marcelo G. Kazanietz[4], Jonathan Chernoff[5] , David Boettiger[3] and Valerie M. Weaver[1,2,6]

[1]Department of Surgery, University of California San Francisco, San Francisco, CA, 94143

[2]Center for Bioengineering and Tissue Regeneration, University of California San Francisco, San Francisco, CA 94143

[3]Department of Microbiology, University of Pennsylvania, Philadelphia, PA 19104

[4]Department of Pharmacology, University of Pennsylvania, Philadelphia, PA 19104

[5]Fox Chase Cancer Center, Philadelphia, PA, 19111

[6]Address correspondence to:

Valerie M. Weaver,
University of California, San Francisco
Department of Surgery
Center for Bioengineering and Tissue Regeneration
S1364C, Box 0456
513 Parnassus Avenue
San Francisco, CA 94143-0456
Email: **weaverv@surgery.ucsf.edu**
Telephone: (415) 476-3826
Fax: (415) 476-3985

Running header: MECs resist death via β4 integrin, Rac, Pak and NFκ B.

Keywords: α6β4 integrin, Rac, Pak1, NFκ B, apoptosis resistance, mammary epithelial cells

Word count: 70,027 with spaces

Summary

Malignant transformation and multi-drug resistance are linked to apoptosis resistance, yet the molecular mechanisms enhancing tumor cell survival remain poorly understood. Because the stroma can influence tumor behavior by regulating tissue phenotype, we explored the role of extracellular matrix-mediated tissue organization in epithelial survival. Here we report that elevated (α6)β4 integrin-dependent Rac-Pak1 signaling drives apoptosis resistance in mammary acini by facilitating stress-induced NFκ B p65 stimulation through activation of Pak1. We determined that inhibiting Pak1 through ectopic expression of N17Rac or PID compromises NFκ B activation to render mammary acini death sensitive, and that apoptosis resistance can be restored in these structures by over-expressing a wild type NFκ B p65. We further observed that acini expressing elevated levels of Pak1 can activate p65 and survive death induction, even in the absence of activated Rac, but will die if their NFκ B activation is inhibited through expression of IκBαM. Accordingly we conclude that mammary epithelial tissues can resist apoptotic stimuli through NFκ B activation and that this effect is mediated through increased α6β4 integrin-dependent-Rac-Pak1 signaling. Our data emphasize the importance of extracellular matrix context in mammary tissue survival, and implicate α6β4 integrin-dependent Rac-stimulation of Pak1 as a key mediator of apoptosis-resistance in breast tumors.

Introduction

Apoptosis is essential for tissue development and homeostasis and is required for efficient tumor therapy (Fernandez et al., 2002; Igney and Krammer, 2002; Zakeri and Lockshin, 2002). Aberrant regulation of cell death contributes to the pathogenesis of various diseases in adult tissues, including cancer and neuro-degeneration. Moreover, defects in apoptosis regulation and cell death execution have been implicated in the pathogenesis of treatment resistant tumors (Fulda and Debatin, 2004; Sethi et al., 1999; Zahir and Weaver, 2004). Yet, while we know much about the molecular machinery and events driving apoptosis execution at the cellular level, by comparison we know little about how cell death decisions are controlled in three-dimensional (3D) tissues.

In vivo epithelial cells exist within an organized, 3D tissue that is mediated by cell-cell and cell-extracellular matrix (ECM) interactions, and driven by dynamic soluble and insoluble microenvironmental cues (Barros et al., 1995; Bissell and Radisky, 2001; Unger and Weaver, 2003). Similar to tissues *in vivo*, mammary epithelial cells (MECs) incorporated into 3D tissue-like structures (acini) in culture exhibit a markedly enhanced survival phenotype, characterized by increased resistance to diverse death stimuli, as compared to non-differentiated MECs grown as two dimensional (2D) monolayers (Weaver et al., 2002). The increased death resistance behavior displayed by 3D multi-cellular structures (spheroids) has been functionally-linked to the enhanced cell-cell associations and altered cell-ECM interactions found in these tissues (Bates et al., 1994; Hermiston and Gordon, 1995; Kirshner et al., 2003; Santini et al., 2000; Zahir and Weaver, 2004). Cell adhesion can promote the viability of cells grown as non-differentiated monolayers by changing the activity or expression of Bcl2 family member dimers, or by increasing Erk, PI3 kinase and Akt signaling to inhibit mitochondrial-dependent death, modify cellular metabolism and sustain cell proliferation (Matter and Ruoslahti, 2001; Plas and Thompson, 2002; Vander Heiden et al., 2001). Cell-ECM interactions and integrin engagement

can also protect monolayers of cells from exogenous death stimuli by tempering death receptor signaling and altering cell cycle dynamics (Dalton, 2003; Sethi et al., 1999). Interestingly, ECM-ligated epithelial cells incorporated into 3D spheroids exhibit increased resistance to exogenous death cues when compared to epithelial cells interacting with the same ECM ligand in 2D (i.e. plated on top of the same ECM ligand; Igney and Krammer, 2002; Tsai et al., In preparation). It is not clear whether the improved survival of 3D spheroids is linked to increased activity of known adhesion-dependent anti-apoptotic signaling or if additional adhesion-regulated, death-resistance mechanisms become engaged in 3D spheroids.

3D spheroids often exhibit reduced cell growth, altered cell cycle regulation, hypoxia, compromised drug accessibility, increased matrix deposition, and modified cell adhesion, and these features are thought to increase the death resistance phenotype of these structures (Kuh et al., 1999; Sminia et al., 2003; Tannock et al., 2002); Delcommenne and Streuli, 1995). We reported that α6β4 integrin and tissue polarity mediate apoptosis resistance in 3D mammary acini in the absence of hypoxia and irrespective of the cells growth status, by permitting stress-dependent NFκ B activation (Weaver et al., 2002). The importance of α6β4 integrin-NFκ B activation in apoptosis resistance of 3D spheroids is underscored by the clinical finding that aggressive and treatment resistant solid tumors frequently show constitutive activation of NFκ B (Baldwin, 2001; Sovak et al., 1997), and activated NFκ B protects epithelial cells *in vivo* from death induced through radiation treatment, immune stimuli and chemotherapy exposure (Baeuerle and Baltimore, 1996; Baldwin, 2001). In addition, high grade tumors with a poor clinical prognosis often express increased levels of α6β4 integrin and secrete abundant quantities of laminin-5 (Davis et al., 2001; Jones et al., 1997; Taylor-Papadimitriou et al., 1993), and elevated α6β4 integrin has been functionally-associated with tumor metastasis, a process that requires apoptosis resistance (Lipscomb et al., 2005; Mercurio and Rabinovitz, 2001; Gupta and Massague, 2006). We showed that laminin-ligated α6β4 integrin can enhance anchorage-

independent survival in 3D mammary spheroids by facilitating epidermal growth factor (EGF)-dependent activation of Rac and NFκ B (Zahir et al., 2003). Consistently, Rac levels and activity are often elevated in aggressive human epithelial tumors *in vivo* (Fritz et al., 1999), and Rac has been strongly implicated in tissue morphogenesis and polarity (O'Brien et al., 2001; Akhtar and Streuli, 2006). These findings implicate but do not prove that α6β4 integrin-Rac-NFκ B activity mediates apoptosis resistance in tissues. To explore this possibility we asked if α6β4 integrin polarized 3D mammary acini resist diverse exogenous apoptosis stimuli through Rac-dependent NFκ B activation, and if so how.

Using two non-malignant human MEC models and a reconstituted laminin-rich, basement membrane (rBM) (Debnath et al., 2003; Johnson et al., In Press; Weaver et al., 1997), we grew MECs on top of rBM and compared their death-resistance behavior to that of mammary acini embedded within rBM (3D). We could show that laminin-ligated α6β4 integrin confers apoptosis resistance to 3D mammary acini by increasing the activity of Rac and p21-activated kinase 1 (Pak1 signaling) to permit stress-induced NFκ B activation. Our findings emphasize the importance of matrix context in cell death regulation, and implicate α6β4 integrin-dependent Rac-Pak1-NFκ B signaling in the pathogenesis of treatment resistant tumors.

Results

α6β4 integrin regulates apoptosis resistance and Rac activity

When compared to cells grown as 2D monolayers, epithelial cells assembled into 3D spheroids exhibit enhanced apoptosis resistance that is analogous to that found in multi-drug, immune and radiation resistant tumors *in vivo* (Desoize and Jardillier, 2000). 3D spheroids are typically multi-layered with a hypoxic core and cells incorporated into these structures display growth patterns that appear to depend upon their location within the spheroid (reviewed in Zahir and Weaver, 2004; Santini et al., 2000). Accordingly, the increased survival behavior of 3D spheroids has been largely attributed to compromised drug penetrance, altered cell cycle dynamics, or hypoxia

(Kuh et al., 1999; Sminia et al., 2003; Tannock et al., 2002). In contrast, we could show that rBM-generated 3D acini of S1 HMT-3522 and MCF10 nonmalignant MECs, consisting of a single layer of non-hypoxic cells interacting directly with the rBM (Weaver et al., 2002), and that display proliferative phenotypes similar to their BM-ligated counterparts grown as 2D monolayers (data not shown), are consistently more resistant to immune receptor stimuli such as Trail (Fig 1A; top), chemotherapy treatments including Taxol (Fig 1A; bottom) and gamma irradiation exposure (not shown).

We previously reported that the apoptosis resistant phenotype of 3D mammary acini is functionally-dependent upon laminin-ligation of α6β4 integrin and NFκ B activation (data not shown; Weaver et al., 2002). Laminin-ligated α6β4 integrin regulates Rac (Russell et al., 2003; Zahir et al., 2003), and Rac can promote anchorage-independent cell survival (Zahir et al., 2003; Jacquier et al., 2006). We found that the level of GTP-Rac is significantly elevated in BM-ligated 3D MEC acini as compared to BM-ligated 2D MEC monolayers, consistent with the idea that a 3D spheroid could acquire death resistance through elevated adhesion-dependent survival signaling, (Fig. 1B; quantified in 1C). We additionally observed that ectopic expression of a tail less EGFP-tagged β4 integrin, that competes with the endogenous wild type β4 integrin to heterodimerize with α6 integrin at the membrane, and that efficiently supports laminin-ligation, but does permit hemidesmosome formation or α6β4 integrin-dependent signaling (Zahir et al., 2003; Spinardi et al., 1995) significantly reduced Rac activity in rBM-ligated 2D (data not shown; Zahir et al., 2003) and 3D cultures of MECs (Figure 1D; quantified in 1E). Because we demonstrated that expression of the tail less β4 integrin compromises tissue polarity and renders 3D MEC acini sensitize to exogenous death stimuli (immune receptor and chemotherapy induced), and Rac can regulate tissue polarity (Akhtar and Streuli, 2006; O'Brien et al., 2001) and cell survival (Zahir et al., 2003) these observations indicate that the elevated laminin-α6β4

integrin-dependent Rac activity displayed by 3D mammary acini could contribute to their enhanced apoptosis resistance phenotype.

Rac activity is necessary for apoptosis resistance

To examine the functional link between apoptosis resistance and Rac in 3D mammary acini we reduced GTP-Rac levels through stable retroviral expression of a dominant-negative EGFP-tagged N17Rac (Fig. 2A). Consistent with the idea that elevated Rac activity contributes to apoptosis resistance, ectopic expression of N17Rac substantially reduced GTP-Rac levels (Fig. 2B; quantified in C) and the activity of its effector Pak1 in 3D mammary acini (Fig. 2D; quantified in 2E). Reducing Rac and Pak activity also significantly sensitized the 3D mammary acini to apoptosis induced in response to immune-receptor ligation and chemo-reagent treatment (Trail and Taxol-induced apoptosis; Fig. 2F).

Interestingly, although decreasing Rac activity sensitized the 3D mammary acini to death induction, N17 Rac expression did not overtly compromise tissue integrity (Fig. 3A; compare top row left phase contrast image to middle image) nor did it appear to impede polarity (Fig. 3A; compare first column of confocal images to second column), as illustrated by basally-localized β4 integrin, basal deposition of laminin-5 and collagen IV, and maintenance of cellular adhesions, as indicated by cell-cell localized scribble (Fig. 3A; left) and co-localized E cadherin and β-catenin (data not shown). Because tissue polarity has been linked to apoptosis resistance in mammary tissues (Weaver et al., 2002), and Rac has been strongly implicated in mammary morphogenesis (Akhtar and Streuli, 2006) and polarity (O'Brien et al., 2001) we further explored of the effect of Rac on tissue polarity. To begin with we assessed the efficiency of N17Rac to reduce GTP-Rac in mammary 3D MEC acini as compared to 2D monolayers. Somewhat surprisingly, whereas N17Rac effectively reduced GTP-Rac by greater than 80% in MECs grown as 2D rBM-ligated monolayers (Fig. 2B; quantified in 2C), despite similar expression of the transgene, N17Rac could only reduce Rac activity in 3D MEC acini by 40% (Fig. 3B;

quantified in 3C). Nevertheless, a 40% reduction in GTP-Rac was sufficient to sensitize 3D MEC acini to death stimuli, even in the absence of an effect on tissue polarity. These data imply that while Rac mediates apoptosis resistance of 3D spheroids, it apparently does so through a mechanism independent from that controlling tissue polarity.

Rac elicits its cellular actions by activating a plethora of downstream effectors, each with different activation and turnover dynamics. Accordingly, we reasoned that the Rac-effector pathways driving survival might be distinct from those that mediate tissue polarity. To test this possibility we treated pre formed death-resistant acini with pharmacologic inhibitors of RhoGTPase, including the general inhibitor Toxin A and the specific Rac inhibitor NSC23766. We found that directly inhibiting Rac activity with Toxin A (see Appendix 1) or with NSC23766 (Fig. 3D) substantially sensitized 3D mammary acini to death induction induced through either immune receptor stimuli or chemotherapy treatment. More importantly, and consistent with previous data implicating Rac in polarity, reducing Rac activity to less than 10% was sufficient to disrupt mammary tissue integrity (Fig 3A; compare phase contrast images top left to far right showing control acini and NSC23766 treated structures), and to compromise tissue polarity, as illustrated by loss of basal β4 integrin localization, perturbed deposition of laminin-5 and collagen IV and aberrant distribution of scribble (Fig. 3A; compare confocal images in first column to the last column). While these results confirm that Rac does regulate tissue polarity, they also imply that the molecular mechanism(s) whereby Rac mediates apoptosis resistance and polarity in tissues are likely mediated through distinct effector pathways.

To further explore the functional link between Rac, tissue polarity and apoptosis resistance in 3D mammary acini we ectopically expressed the Rac-specific GAP, β2-Chimerin, which accelerates the hydrolysis of GTP from Rac, without influencing Cdc42 or RhoA GTP activity (Caloca et al., 2003). Monolayers of non-differentiated MECs and rBM-differentiated 3D mammary acini infected with adenoviral β2-Chimerin showed uniform and sustained (8

days) expression of an HA-tagged β2-Chimerin transgene (Fig. 4A & E middle images), that was associated with a significant reduction in Rac activity (Fig. 4B; quantified in 4C) and increased death sensitivity in the 3D mammary acini (Fig. 4D). Yet again however, while β2-Chimerin expression substantially reduced Rac activity and reduced death resistence, acini integrity (Fig. 4E; compare phase contrast images of control to β2-Chimerin expressing acini; top row) and polarity, (demonstrated by the maintenance of basally-localized β4 integrin; Fig. 4E; compare confocal images of control to β2-Chimerin expressing acini) remained essentially intact. Collectively these data indicate that the elevated GTP-Rac observed in 3D mammary acini promotes apoptosis resistance through a pathway that is independent from that directing polarity.

p21-activated kinase 1 activity is necessary and sufficient for Rac-mediated apoptosis resistance in 3D mammary acini

The Rho GTPase Rac regulates cell behavior by stimulating the activity of multiple molecular effectors, including members of the Pak family (Boettner and Van Aelst, 1999; Schmitz et al., 2000; Van Aelst and D'Souza-Schorey, 1997). Paks are important modulators of tissue development and homeostasis, they can repress anoikis (Menard et al., 2005) and they have been implicated in malignant transformation (Qu et al., 2001; Wang et al., 2006). Consistent with an important role for Paks in mediating apoptosis resistance in MEC acini, we found that total levels of Pak1 and activated Pak1 rise significantly following rBM-induced tissue differentiation (acini formation) in both MCF10A (Fig. 5A; quantified in B) and HMT-3522 S1 (data not shown) nonmalignant MECs. In contrast, we noted that the specific activity of Pak4 decreased (Fig. 5A) and Pak3 protein was non-detectable (Fig. 5A). Pak1 activity was also significantly reduced in 3D mammary acini expressing the tail less β4 integrin (Fig. 5C; quantified in D), which we showed also abrogates Rac activity (Fig. 1D; quantified in E). Moreover, inhibiting GTP-Rac through N17Rac expression, which sensitizes 3D mammary acini to apoptosis stimuli (Fig. 3D), concomitantly decreased Pak1 activity (data not shown). Whereas a constitutively active

adenoviral V12Rac could effectively restore Pak activity and apoptosis resistance to increasingly cytotoxic doses of Trail and Taxol in N17Rac death-sensitized mammary acini (Fig. 5E), infection with V12RacH40, which harbors a mutation that prevents the activated Rac from interacting with and stimulating Pak, could not (Fig. 5F). Indeed, direct inhibition of Pak activity through ectopic expression of the Pak inhibitor domain (PID) rendered 3D mammary acini sensitive to death stimulation by Trail (Fig. 5G) and Taxol (not shown). Furthermore, infection with a wild-type adenoviral Pak1 (Pak1 WT) restored apoptosis resistance to the death-sensitive N17Rac expressing acini, analogous to the resistance achieved through expression of the constitutively active V12Rac (Fig. 5H). These findings strongly implicate Rac-dependent Pak1 activity as a necessary and sufficient mediator of α6β4 integrin-dependent apoptosis resistance in 3D mammary acini.

Rac activates Pak1 and mediates apoptosis resistance in 3D mammary acini by stimulating NFκ B

Having established a functional link between Rac, Pak, and apoptosis resistance, we sought to delineate the molecular mechanism(s) whereby Rac activated Pak1 could promote apoptosis resistance in 3D mammary acini. Pak can regulate cell survival by inhibiting the activity of the pro apoptotic Bcl2 family member Bad (Cotteret et al., 2003). Yet, whereas GTP-Rac and Pak activity were consistently and significantly elevated in the death resistant 3D mammary acini, Bad levels and activity remained unaltered between BM-ligated 2D and 3D MECs (data not shown). This suggests Pak1 must be driving death resistance through an alternative mechanism. Paks can activate NFκ B to mediate cell survival (Frost et al., 2000), and we showed that α6β4 integrin-polarized 3D mammary acini resist apoptosis induction through NFκ B activation (Weaver et al., 2002). Consistently, we could show that incubating 3D mammary acini with the membrane-soluble peptide SN50, which inhibits activation of NFκ B, but not its nonfunctional peptide SN50M, prevented nuclear translocation of p65 NFκ B (data

not shown; Zahir et al., 2003), and increased the sensitivity of the structures to death stimuli such as Trail (Fig. 6A). In addition, inhibiting nuclear translocation of p65 (and the subsequent activation of NFκ B), through treatment of the acini with SN50, also prevented exogenously-expressed Pak1 from conferring apoptosis resistance to N17Rac-expressing, death-sensitized mammary acini (Fig. 6B). Indeed, while control mammary acini survived and exhibited high levels of nuclear p65 following Trail treatment, mammary structures with PID-reduced Pak activity had low to non-detectable nuclear p65 in response to Trail (Fig. 6C; quantified in 6D) and died 24 hours following treatment (Fig. 6E). Finally, we found that the apoptotically-sensitized 3D mammary acini that constitutively expressed N17Rac showed lower levels of nuclear p65 following Trail treatment, but that nuclear p65 levels were restored following ectopic expression of a wild type Pak1 adenoviral construct (Fig. 6C; quantified in 6D).

To more directly implicate Pak activation of NFκ B in the apoptosis resistance phenotype of 3D mammary acini, we prepared populations of MECs stably expressing a retroviral wild type p65, which promotes constitutive activation of NFκ B. MEC acini ectopically expressing p65 showed constitutive expression of nuclear p65 (Appendix 3), that was not diminished by either reducing cellular GTP-Rac or decreasing Pak activity through co expression of N17Rac or PID. More importantly, constitutive activation of NFκ B prevented apoptosis induction in 3D mammary acini treated with Trail even when they had reduced Rac or Pak activity (Fig. 6E). Furthermore, co expression of the NFκ B signaling pathway super repressor IκBαM, which prevents NFκ B activation and inhibits nuclear translocation of p65, permitted death induction in 3D polarized mammary acini, even when these acini were engineered to express elevated levels of Pak1 (Fig. 6F). These data indicate that Rac-mediated activation of Pak1 supports apoptosis resistance in 3D mammary acini by regulating NFκ B activation. However, because we also determined that inhibiting Rac and Pak1 through expression of N17Rac reduced phospho Bad levels, and increasing Pak levels increased Bad phosphorylation (see appendix), we cannot rule

out the possibility that Rac-Pak-dependent modulation of Bad activity additionally contributes to the increased survival phenotype of 3D mammary acini (Fig. 7). Nevertheless, we suggest that mammary acini likely resist apoptotic stimuli primarily through enhanced α6β4 integrin-dependent Rac-Pak1-NFκ B activation (Fig. 7).

Discussion

Using a rBM assay and two non-malignant, immortalized MEC lines, HMT-3522 S-1 and MCF10A, we could show that a polarized 3D mammary acini resists diverse exogenous apoptotic stimuli including immune-receptor stimuli and chemotherapeutics by promoting Pak1-mediated NFκ B activation. We determined that α6β4 integrin signaling in 3D mammary acini is necessary to elevate the activity of Rac and Pak1 and that Pak1 facilitates stress-dependent NFκ B-activation to drive apoptosis resistance. Although α6β4 integrin can support epithelial survival through ERK and PI3 kinase (Bachelder et al., 1999), and PI3 kinase can activate Rac (Shaw et al., 1997), we found that the activity of ERK and PI3 kinase is significantly diminished in 3D mammary acini, and that inhibiting the activity of these kinases fails to sensitize mammary acini to apoptotic stimuli (data not shown; Zahir et al., 2003). Although we have no explanation for this finding, transgenic and 3D organoid experiments suggest that Akt may be more critical for regulating cellular metabolism and tumor invasion in 3D tissues *in vivo* (Boxer et al., 2006; Hutchinson et al., 2004; Irie et al., 2005; Ju et al., 2007). Consistently, studies that have linked α6β4 integrin-dependent survival to ERK and PI3 kinase signaling were conducted using transformed breast cells grown as 2D monolayers, whereas our studies showing that α6β4 integrin-dependent survival depends upon elevated Rac and Pak1 and NFk B were conducted in nonmalignant 3D mammary acini that were generated by embedding the cells within a compliant rBM. The compliance of hydrogels such as the rBM used in our experiments is similar in physical consistency to that of the stroma found in tissues *in vivo* and both of these stroma are significantly softer than the rigid tissue culture plastic or borosilicate glass surfaces frequently

used for traditional signal transduction experiments. Indeed, others and we showed that matrix stiffness profoundly alters ERK and RhoGTPase activity and signaling (Engler et al., 2006; McBeath et al., 2004; Paszek et al., 2005). Whether matrix compliance could modify the molecular mechanisms whereby matrix adhesion regulates cell survival is under investigation.

Similar to metastatic tumors *in vivo*, tumor cells grown as 3D spheroids can rapidly acquire multi-drug resistance in response to acute drug treatment (Durand and Olive, 2001; Kerbel, 1994; Sutherland and Durand, 1972). Although the molecular mechanisms regulating treatment resistance of 3D spheroids has been attributed to reduced drug penetrance (Jain, 1987; Tong et al., 2004), hypoxia (Sminia et al., 2003) and altered cell growth or cell cycle regulation (St Croix et al., 1996), we found that the viability of the drug-treated 3D polarized, apoptotically-resistant mammary acini was not modified by varying cell proliferation, that the structures were not hypoxic, and that the acini could resist even high doses of gamma irradiation, where penetrance is not an issue (shown by increased apoptosis resistance and high clonogenic survival; unpublished observations). Instead, our data are consistent with the notion that apoptosis resistance of 3D acini is linked to increased (integrin-dependent) adhesion signaling, similar to the enhanced survival phenotype documented for myeloma, cervical, lung and lymphoid tumor cells exposed to pro-death stimuli (Dalton, 2003; Damiano et al., 1999; Sethi et al., 1999; Whitacre and Berger, 1997), and the elevated drug resistance behavior of integrin-ligated monolayers of tumors and 3D spheroids (Damiano et al., 1999; Kerbel et al., 1996; Narita et al., 1998; Santini et al., 2000). To explain this adhesion-mediated resistance, we showed that laminin-mediated ligation of α6β4 integrin promotes immune-receptor and multi-drug resistance in mammary acini by permitting stress-induced activation of NFκ B (Weaver et al., 2002), and that α6β4 integrin permits epidermal growth factor-dependent activation of Rac to stimulate NFκB and mediate anchorage-independent survival of MECs (Zahir et al., 2003). Our current findings extend our earlier observations to demonstrate that laminin-ligated α6β4 integrin

enhances Rac and Pak activity in 3D mammary acini to permit stress-dependent NFk B activation and increase survival, independent of its effects on tissue polarity. Although we do not know how α6β4 integrin modulates tissue polarity, we did find that α6β4 integrin regulates GTP-Rac, and in accordance with previous work, that Rac regulates tissue morphology and polarity (Akhtar and Streuli, 2006; O'Brien et al., 2001); Fig. 3A). However, given that we could functionally distinguish between Rac-dependent survival through Pak and tissue polarity regulation, we suggest that the Rac-activated effectors regulating tissue polarity are distinct from those that promote cell survival. In this regard, we determined that Rac regulates Pak activity to support apoptosis resistance in mammary acini, but that modulating Pak expression and activity had no effect on tissue integrity or polarity. Clearly, additional experiments are required to identify the Rac effectors directing tissue polarity, and to determine whether these pathways are α6β4 integrin-regulated.

It is not yet clear why α6β4 integrin is able to enhance Rac and Pak activity more effectively in 3D epithelial structures as compared to 2D epithelial monolayers. However, increased integrin engagement, altered integrin and Rac turnover and modifications in matrix adhesion composition, and differences in matrix compliance and tissue architecture are all plausible explanations for this phenotype. Consistently, others and we have determined that matrix stiffness increases the activity of Rho to promote focal adhesion assembly (Bershadsky et al., 2006; Paszek et al., 2005), and that Rac activity is inhibited by matrix stiffness and increased significantly in MECs interacting with a compliant substrate (unpublished observations). RhoGTPase targeting and function can also be modified by tissue morphology and matrix compliance. For example, the localization of activated Rac becomes restricted to tight junctions following epithelial polarization (Chen and Macara, 2005), PTEN localizes activated cdc42 to stimulate αPKC-dependent lumen formation in polarized kidney epithelial cysts (Martin-

Belmonte et al., 2007), and we found that matrix stiffness disrupts tissue polarity to re-localize GTP-Rac and promote cell invasion (unpublished observations).

Rac is often over expressed in tumors of the breast (Fritz et al., 1999), it can support anchorage independent growth of MECs (Bouzahzah et al., 2001; Zahir et al., 2003) and Rac protects MDCK cells from anoikis (Coniglio et al., 2001). Depleting Rac in glioblastoma cells and breast cancer cells also strongly inhibits invasion (Chan et al., 2005). Rac elicits its pleiotrophic effects on cell function by interacting with and activating a plethora of cellular targets including the Pak family of signaling molecules. Paks facilitate growth factor signaling and interact with multiple downstream effectors to alter cell growth, survival, migration and differentiation (Bokoch, 2003; Puto et al., 2003; Vadlamudi and Kumar, 2003; Wang et al., 2002) and Paks can promote the tumorigenic behavior of cells (Menard et al., 2005; Schurmann et al., 2000; Tang et al., 1997). For example, Rac-dependent Pak activation drives cell migration and tumor invasion (Alahari, 2003; Alahari et al., 2004; Brown et al., 2005), and Paks can enhance cell survival (Gnesutta et al., 2001; Johnson and D'Mello, 2005; Qu et al., 2001). We showed that the specific activity of Pak1 increases dramatically and significantly in apoptotically-resistant mammary acini, and that Pak1 is essential for immune-receptor and drug-induced death because it permits stress-dependent NFκ B activation (Fig. 6C, D). Our results are consistent with experiments showing how Pak4 sustains anchorage-independent cell survival by stimulating NFκ B (Cammarano and Minden, 2001), and extend these observations to demonstrate that Pak1 can render cells resistant to diverse exogenous apoptotic stimuli also through NFκ B regulation. Activated Pak can also prevent apoptosis by inducing the phosphorylation of BAD on Ser-112 to prevent mitochondria-mediated activation of executioner caspases (Cotteret et al., 2003; Deacon et al., 2003; Gnesutta et al., 2001; Schurmann et al., 2000), and we could establish a correlation between Bad phosphorylation, apoptosis resistance and Pak activity (Appendix 2). Yet, we found that neither Bad expression nor phosphorylation

increase in association with elevated death resistance in 3D MEC acini, despite finding that Rac and Pak activity were significantly higher in these same structures. Thus, while we cannot rule out the possibility that decreased Bad phosphorylation also contributes to Rac-Pak-dependent apoptosis resistance it seems more likely that Pak-induced NFκ B activation is the more predominant anti-apoptotic mechanism.

We could establish a functional link between laminin-mediated activation of α6β4 integrin and Rac-dependent activation of Pak1, and β4 integrin and laminins are frequently elevated in tumors (Davis et al., 2001) they cooperate to drive invasion and metastasis (Jones et al., 1997; Lipscomb and Mercurio, 2005; Lipscomb et al., 2005), and their co-expression is associated with a poor prognosis in breast cancer patients (Tagliabue et al., 1998). Our data offer an explanation for these findings and additionally may explain why Paks are often over-expressed in tumors (Vadlamudi and Kumar, 2003) and why hyper-activation of Pak1 so efficiently drives mammary gland tumor formation (Wang et al., 2006). Indeed, NFκ B expression increases during malignant transformation of the breast (Kim et al., 2000), is implicated in mammary tumor pathogenesis (Sovak et al., 1997), breast tumor metastasis (Nakshatri et al., 1997), and resistance to chemical, immune and radiation therapy (Baeuerle and Baltimore, 1996; Baldwin, 2001; Weaver et al., 2002). Moreover, Rac-Pak-dependent NFκ B activation can drive Kaposi sarcoma-associated malignant transformation (Dadke et al., 2003). Regardless, by linking matrix-dependent Rac-Pak activation to NFκ B-dependent apoptosis resistance our findings underscore the importance of identifying pharmacological Pak inhibitors that could be used as tractable anti-tumor therapies.

Materials and Methods

Antibodies and Reagents

We used commercial EHS matrix (Matrigel™; Collaborative Research) for the reconstituted basement membrane (rBM) assays. Primary antibodies used in these studies were as follows: β4 integrin, clone 3E1 (Chemicon); Phospho-Bad (Ser136), Bad, cleaved caspase 3, Phospho-Pak1 (Thr423)/Pak2 (Thr402), Pak1, Pak 3, Pak 4, Phospho-Pak4 (Ser474)/Pak5 (Ser602)/Pak6 (Ser560), rabbit sera (all from Cell Signaling); E-cadherin, clone 36, and Rac1, clone 102 (BD Biosciences); HA.11, clone 16B12 (Covance); and NFκ B p65, rabbit sera (Santa Cruz Biotechnology Inc.). The secondary antibodies used were as follows: HRP-conjugated anti-rabbit and mouse (Amersham Laboratories); and Alexa Fluor 488 and 555-conjugated anti-mouse and rabbit IgGs (Molecular Probes). Reagents used in the studies were as follows: Rho GTPase inhibitor toxin A *Clostridium difficile* (10 mM in DMSO; Calbiochem); and Rac1 inhibitor NSC23766 (50 mM in H_2O; Calbiochem); NFκB SN50, active cell-permeable inhibitory peptide (50 μM in H_2O), NFκB SN50M, inactive cell-permeable control peptide (50 μM in H_2O), Trail (approximately 0.5 mg/ml), and Taxol (20 mM in DMSO; Biomol); Etoposide (10-100 μM in DMSO; TopoGen Inc.); Live/Dead Viability Cytotoxicity Kit (Molecular Probes); and the *In Situ* Cell Death Detection Kit (TUNEL; Roche).

Cell Culture

The HMT-3522 and MCF10A mammary epithelial cells (MECs) were grown and maintained exactly as previously described (Paszek et al., 2005).

Flow Cytometry

Live cells were isolated, re-suspended in Dulbecco's PBS with 0.5% Fetal Bovine Serum and immediately sorted for high eGFP expression on a FACScan™ (Becton Dickinson). All manipulations were conducted at 4°C.

Immunofluorescence analysis

Cells were directly fixed using 100% methanol, and samples were incubated with primary antibody followed by either Alexa Fluor 488 or 555-conjugated secondary antibody. Nuclei were counterstained with diaminophenylindole (DAPI; Sigma-Aldrich). Cells were visualized using a Bio-Rad MRC 1024 laser scanning confocal microscope attached to a Nikon Diaphot 200 microscope. Images were recorded at 60x magnification.

Apoptosis assay

Apoptosis was assayed via immuno-detection of activated caspase 3. Percent apoptosis was quantified as the number of cells positive for activated caspase 3 divided by the total number of cells. The minimum number of cells scored was 200-300 per experimental condition. Results were confirmed using Live/Dead and TUNEL assay. Cells were visualized using a fluorescence microscope (Olympus model U-LH100HGAPO).

Adenoviral and Retroviral constructs and studies

EGFP-tagged N17Rac1 has been described previously (Russell et al., 2003). Stable MEC populations expressing eGFP-tagged N17Rac1 were antibiotic selected, FACS sorted and visually-confirmed through immunofluorescence microscopy (Zahir et al., 2003). IκBαM and p65 cloned into PLZRS (provided by P. Khavari, Stanford Medical Center) were used directly. Adenovirus Tet, V12Rac, V12Rac H40, PID, Pak1 WT, and HA-tagged β2-Chimerin have been described previously (Beeser et al., 2005; Tang et al., 1999; Yang et al., 2005), and were expanded and virus was purified by cesium chloride banding (He et al., 1998). 3D MEC tissue structures were generated using a polyHEMA/rBM suspension culture (Roskelley et al., PNAS 1995), and polarized acini were then isolated in PBS/10mM EDTA, infected with adenovirus (15 minutes; 37°C) and transgene expression was confirmed by immunofluoresence microscopy and immunoblot and Rac GTPase activity assay. 24 hours following adenoviral infection, the acini

were embedded within a 3D rBM and then assayed for resistance to apoptotic stimuli (Trail; 0.1-2 μg/ml; 24 hours; 37°C), as described above.

Immunoblot analysis

Cells were lysed in RIPA buffer containing protease and phosphatase inhibitors and equal quantities of protein were separated on reducing SDS-PAGE gels, and immunoblotted for protein, as previously described (Zahir et al., 2003).

Rac GTPase Assay

Rac GTPase activity was assessed in cell extracts (G protein lysis buffer: 25 mM Hepes, pH 7.5, 150 mM NaCl, 1% Igepal CA-630, 10 mM MgCl2, 1 mM EDTA, 10% glycerol, 1 mM pefabloc SC, 1 μg/ml leupeptin, 5 μg/ml aproptinin, 1 mM sodium orthovanadate, and 1 mM sodium fluoride) prepared from PBS-washed (4°C), equalized cell numbers plated as 2D monolayers on rBM-coated tissue culture plastic (24 hours) or as 3D tissue-like acini structures within rBM (10-12 days). Cell lysates were centrifuged (5 minutes; 20,817 RCF; 4°C), and supernatants were mixed with GST-PBD and incubated with glutathione-sepharose beads (Amersham Biosciences; 60 minutes; 4°C). Cleared lysates were then washed (3x lysis buffer), and bound protein was eluted with Laemmli buffer and separated on a 12% SDS–PAGE gel. Active Rac was detected by immunoblotting with anti-Rac antibody, and specific activity was calculated by normalizing densitometric values of Pak-associated Rac to total Rac and E-cadherin, as previously described (Zahir et al., 2003).

Acknowledgments

We thank G. Rozenberg for assistance with the confocal microscopy and J. Meinkoth and R. Assoian for helpful comments. This work was supported by grants from the National Cancer Institute CA078731 and Department of Defense DAMD17-01-100368, 1703-1-0496 and W81X WH-05-1-330 to V.M. Weaver, National Institutes of Health GM-57388 to D. Boettiger, National Cancer Institute CA 117884 to J. Chernoff, and DAMD17-01-1-0367 to J.N. Lakins.

References

Akhtar, N. and Streuli, C. H. (2006). Rac1 links integrin-mediated adhesion to the control of lactational differentiation in mammary epithelia. *J Cell Biol* **173**, 781-93.

Alahari, S. K. (2003). Nischarin inhibits Rac induced migration and invasion of epithelial cells by affecting signaling cascades involving PAK. *Exp Cell Res* **288**, 415-24.

Alahari, S. K., Reddig, P. J. and Juliano, R. L. (2004). The integrin-binding protein Nischarin regulates cell migration by inhibiting PAK. *Embo J* **23**, 2777-88.

Bachelder, R. E., Ribick, M. J., Marchetti, A., Falcioni, R., Soddu, S., Davis, K. R. and Mercurio, A. M. (1999). p53 inhibits alpha 6 beta 4 integrin survival signaling by promoting the caspase 3-dependent cleavage of AKT/PKB. *J Cell Biol* **147**, 1063-72.

Baeuerle, P. A. and Baltimore, D. (1996). NF-kappa B: ten years after. *Cell* **87**, 13-20.

Baldwin, A. S. (2001). Control of oncogenesis and cancer therapy resistance by the transcription factor NF-kappaB. *J Clin Invest* **107**, 241-6.

Barros, E. J., Santos, O. F., Matsumoto, K., Nakamura, T. and Nigam, S. K. (1995). Differential tubulogenic and branching morphogenetic activities of growth factors: implications for epithelial tissue development. *Proc Natl Acad Sci U S A* **92**, 4412-6.

Bates, R. C., Buret, A., van Helden, D. F., Horton, M. A. and Burns, G. F. (1994). Apoptosis induced by inhibition of intercellular contact. *J Cell Biol* **125**, 403-15.

Beeser, A., Jaffer, Z. M., Hofmann, C. and Chernoff, J. (2005). Role of group A p21-activated kinases in activation of extracellular-regulated kinase by growth factors. *J Biol Chem* **280**, 36609-15.

Bershadsky, A. D., Ballestrem, C., Carramusa, L., Zilberman, Y., Gilquin, B., Khochbin, S., Alexandrova, A. Y., Verkhovsky, A. B., Shemesh, T. and Kozlov, M. M. (2006). Assembly and mechanosensory function of focal adhesions: experiments and models. *Eur J Cell Biol* **85**, 165-73.

Bissell, M. J. and Radisky, D. (2001). Putting tumours in context. *Nat Rev Cancer* **1**, 46-54.

Boettner, B. and Van Aelst, L. (1999). Rac and Cdc42 effectors. *Prog Mol Subcell Biol* **22**, 135-58.

Bokoch, G. M. (2003). Biology of the p21-activated kinases. *Annu Rev Biochem* **72**, 743-81.

Bouzahzah, B., Albanese, C., Ahmed, F., Pixley, F., Lisanti, M. P., Segall, J. D., Condeelis, J., Joyce, D., Minden, A., Der, C. J. et al. (2001). Rho family GTPases regulate mammary epithelium cell growth and metastasis through distinguishable pathways. *Mol Med* **7**, 816-30.

Boxer, R. B., Stairs, D. B., Dugan, K. D., Notarfrancesco, K. L., Portocarrero, C. P., Keister, B. A., Belka, G. K., Cho, H., Rathmell, J. C., Thompson, C. B. et al. (2006). Isoform-specific requirement for Akt1 in the developmental regulation of cellular metabolism during lactation. *Cell Metab* **4**, 475-90.

Brown, M. C., Cary, L. A., Jamieson, J. S., Cooper, J. A. and Turner, C. E. (2005). Src and FAK kinases cooperate to phosphorylate paxillin kinase linker, stimulate its focal adhesion localization, and regulate cell spreading and protrusiveness. *Mol Biol Cell* **16**, 4316-28.

Caloca, M. J., Wang, H. and Kazanietz, M. G. (2003). Characterization of the Rac-GAP (Rac-GTPase-activating protein) activity of beta2-chimaerin, a 'non-protein kinase C' phorbol ester receptor. *Biochem J* **375**, 313-21.

Cammarano, M. S. and Minden, A. (2001). Dbl and the Rho GTPases activate NF kappa B by I kappa B kinase (IKK)-dependent and IKK-independent pathways. *J Biol Chem* **276**, 25876-82.

Chan, A. Y., Coniglio, S. J., Chuang, Y. Y., Michaelson, D., Knaus, U. G., Philips, M. R. and Symons, M. (2005). Roles of the Rac1 and Rac3 GTPases in human tumor cell invasion. *Oncogene* **24**, 7821-9.

Chen, X. and Macara, I. G. (2005). Par-3 controls tight junction assembly through the Rac exchange factor Tiam1. *Nat Cell Biol* **7**, 262-9.

Coniglio, S. J., Jou, T. S. and Symons, M. (2001). Rac1 protects epithelial cells against anoikis. *J Biol Chem* **276**, 28113-20.

Cotteret, S., Jaffer, Z. M., Beeser, A. and Chernoff, J. (2003). p21-Activated kinase 5 (Pak5) localizes to mitochondria and inhibits apoptosis by phosphorylating BAD. *Mol Cell Biol* **23**, 5526-39.

Dadke, D., Fryer, B. H., Golemis, E. A. and Field, J. (2003). Activation of p21-activated kinase 1-nuclear factor kappaB signaling by Kaposi's sarcoma-associated herpes virus G protein-coupled receptor during cellular transformation. *Cancer Res* **63**, 8837-47.

Dalton, W. S. (2003). The tumor microenvironment: focus on myeloma. *Cancer Treat Rev* **29 Suppl 1**, 11-9.

Damiano, J. S., Cress, A. E., Hazlehurst, L. A., Shtil, A. A. and Dalton, W. S. (1999). Cell adhesion mediated drug resistance (CAM-DR): role of integrins and resistance to apoptosis in human myeloma cell lines. *Blood* **93**, 1658-67.

Davis, T. L., Cress, A. E., Dalkin, B. L. and Nagle, R. B. (2001). Unique expression pattern of the alpha6beta4 integrin and laminin-5 in human prostate carcinoma. *Prostate* **46**, 240-8.

Deacon, K., Mistry, P., Chernoff, J., Blank, J. L. and Patel, R. (2003). p38 Mitogen-activated protein kinase mediates cell death and p21-activated kinase mediates cell survival during chemotherapeutic drug-induced mitotic arrest. *Mol Biol Cell* **14**, 2071-87.

Debnath, J., Muthuswamy, S. K. and Brugge, J. S. (2003). Morphogenesis and oncogenesis of MCF-10A mammary epithelial acini grown in three-dimensional basement membrane cultures. *Methods* **30**, 256-68.

Desoize, B. and Jardillier, J. (2000). Multicellular resistance: a paradigm for clinical resistance? *Crit Rev Oncol Hematol* **36**, 193-207.

Durand, R. E. and Olive, P. L. (2001). Resistance of tumor cells to chemo- and radiotherapy modulated by the three-dimensional architecture of solid tumors and spheroids. *Methods Cell Biol* **64**, 211-33.

Engler, A. J., Sen, S., Sweeney, H. L. and Discher, D. E. (2006). Matrix elasticity directs stem cell lineage specification. *Cell* **126**, 677-89.

Fernandez, Y., Gu, B., Martinez, A., Torregrosa, A. and Sierra, A. (2002). Inhibition of apoptosis in human breast cancer cells: role in tumor progression to the metastatic state. *Int J Cancer* **101**, 317-26.

Fritz, G., Just, I. and Kaina, B. (1999). Rho GTPases are over-expressed in human tumors. *Int J Cancer* **81**, 682-7.

Frost, J. A., Swantek, J. L., Stippec, S., Yin, M. J., Gaynor, R. and Cobb, M. H. (2000). Stimulation of NFkappa B activity by multiple signaling pathways requires PAK1. *J Biol Chem* **275**, 19693-9.

Fulda, S. and Debatin, K. M. (2004). Apoptosis signaling in tumor therapy. *Ann N Y Acad Sci* **1028**, 150-6.

Gnesutta, N., Qu, J. and Minden, A. (2001). The serine/threonine kinase PAK4 prevents caspase activation and protects cells from apoptosis. *J Biol Chem* **276**, 14414-9.

Gupta, G. P. and Massague, J. (2006). Cancer metastasis: building a framework. *Cell* **127**, 679-95.

He, T. C., Zhou, S., da Costa, L. T., Yu, J., Kinzler, K. W. and Vogelstein, B. (1998). A simplified system for generating recombinant adenoviruses. *Proc Natl Acad Sci U S A* **95**, 2509-14.

Hermiston, M. L. and Gordon, J. I. (1995). In vivo analysis of cadherin function in the mouse intestinal epithelium: essential roles in adhesion, maintenance of differentiation, and regulation of programmed cell death. *J Cell Biol* **129**, 489-506.

Hutchinson, J. N., Jin, J., Cardiff, R. D., Woodgett, J. R. and Muller, W. J. (2004). Activation of Akt-1 (PKB-alpha) can accelerate ErbB-2-mediated mammary tumorigenesis but suppresses tumor invasion. *Cancer Res* **64**, 3171-8.

Igney, F. H. and Krammer, P. H. (2002). Death and anti-death: tumour resistance to apoptosis. *Nat Rev Cancer* **2**, 277-88.

Irie, H. Y., Pearline, R. V., Grueneberg, D., Hsia, M., Ravichandran, P., Kothari, N., Natesan, S. and Brugge, J. S. (2005). Distinct roles of Akt1 and Akt2 in regulating cell migration and epithelial-mesenchymal transition. *J Cell Biol* **171**, 1023-34.

Jacquier, A., Buhler, E., Schafer, M. K., Bohl, D., Blanchard, S., Beclin, C. and Haase, G. (2006). Alsin/Rac1 signaling controls survival and growth of spinal motoneurons. *Ann Neurol* **60**, 105-17.

Jain, R. K. (1987). Transport of molecules across tumor vasculature. *Cancer Metastasis Rev* **6**, 559-93.

Johnson, K. and D'Mello, S. R. (2005). p21-Activated kinase-1 is necessary for depolarization-mediated neuronal survival. *J Neurosci Res* **79**, 809-15.

Johnson, K. R. (In Press). Demystifying Three-Dimensional Force and Tissue Morphogenesis. *Methods in Cell Biology: Cell Mechanics*.

Jones, J. L., Royall, J. E., Critchley, D. R. and Walker, R. A. (1997). Modulation of myoepithelial-associated alpha6beta4 integrin in a breast cancer cell line alters invasive potential. *Exp Cell Res* **235**, 325-33.

Ju, X., Katiyar, S., Wang, C., Liu, M., Jiao, X., Li, S., Zhou, J., Turner, J., Lisanti, M. P., Russell, R. G. et al. (2007). Akt1 governs breast cancer progression in vivo. *Proc Natl Acad Sci U S A* **104**, 7438-43.

Kerbel, R. S. (1994). Impact of multicellular resistance on the survival of solid tumors, including micrometastases. *Invasion Metastasis* **14**, 50-60.

Kerbel, R. S., St Croix, B., Florenes, V. A. and Rak, J. (1996). Induction and reversal of cell adhesion-dependent multicellular drug resistance in solid breast tumors. *Hum Cell* **9**, 257-64.

Kim, D. W., Sovak, M. A., Zanieski, G., Nonet, G., Romieu-Mourez, R., Lau, A. W., Hafer, L. J., Yaswen, P., Stampfer, M., Rogers, A. E. et al. (2000). Activation of NF-kappaB/Rel occurs early during neoplastic transformation of mammary cells. *Carcinogenesis* **21**, 871-9.

Kirshner, J., Chen, C. J., Liu, P., Huang, J. and Shively, J. E. (2003). CEACAM1-4S, a cell-cell adhesion molecule, mediates apoptosis and reverts mammary carcinoma cells to a normal morphogenic phenotype in a 3D culture. *Proc Natl Acad Sci U S A* **100**, 521-6.

Kuh, H. J., Jang, S. H., Wientjes, M. G., Weaver, J. R. and Au, J. L. (1999). Determinants of paclitaxel penetration and accumulation in human solid tumor. *J Pharmacol Exp Ther* **290**, 871-80.

Lipscomb, E. A. and Mercurio, A. M. (2005). Mobilization and activation of a signaling competent alpha6beta4integrin underlies its contribution to carcinoma progression. *Cancer Metastasis Rev* **24**, 413-23.

Lipscomb, E. A., Simpson, K. J., Lyle, S. R., Ring, J. E., Dugan, A. S. and Mercurio, A. M. (2005). The alpha6beta4 integrin maintains the survival of human breast carcinoma cells in vivo. *Cancer Res* **65**, 10970-6.

Martin-Belmonte, F., Gassama, A., Datta, A., Yu, W., Rescher, U., Gerke, V. and Mostov, K. (2007). PTEN-mediated apical segregation of phosphoinositides controls epithelial morphogenesis through Cdc42. *Cell* **128**, 383-97.

Matter, M. L. and Ruoslahti, E. (2001). A signaling pathway from the alpha5beta1 and alpha(v)beta3 integrins that elevates bcl-2 transcription. *J Biol Chem* **276**, 27757-63.

McBeath, R., Pirone, D. M., Nelson, C. M., Bhadriraju, K. and Chen, C. S. (2004). Cell shape, cytoskeletal tension, and RhoA regulate stem cell lineage commitment. *Dev Cell* **6**, 483-95.

Menard, R. E., Jovanovski, A. P. and Mattingly, R. R. (2005). Active p21-activated kinase 1 rescues MCF10A breast epithelial cells from undergoing anoikis. *Neoplasia* **7**, 638-45.

Mercurio, A. M. and Rabinovitz, I. (2001). Towards a mechanistic understanding of tumor invasion--lessons from the alpha6beta 4 integrin. *Semin Cancer Biol* **11**, 129-41.

Nakshatri, H., Bhat-Nakshatri, P., Martin, D. A., Goulet, R. J., Jr. and Sledge, G. W., Jr. (1997). Constitutive activation of NF-kappaB during progression of breast cancer to hormone-independent growth. *Mol Cell Biol* **17**, 3629-39.

Narita, T., Kimura, N., Sato, M., Matsuura, N. and Kannagi, R. (1998). Altered expression of integrins in adriamycin-resistant human breast cancer cells. *Anticancer Res* **18**, 257-62.

O'Brien, L. E., Jou, T. S., Pollack, A. L., Zhang, Q., Hansen, S. H., Yurchenco, P. and Mostov, K. E. (2001). Rac1 orientates epithelial apical polarity through effects on basolateral laminin assembly. *Nat Cell Biol* **3**, 831-8.

Paszek, M. J., Zahir, N., Johnson, K. R., Lakins, J. N., Rozenberg, G. I., Gefen, A., Reinhart-King, C. A., Margulies, S. S., Dembo, M., Boettiger, D. et al. (2005). Tensional homeostasis and the malignant phenotype. *Cancer Cell* **8**, 241-54.

Plas, D. R. and Thompson, C. B. (2002). Cell metabolism in the regulation of programmed cell death. *Trends Endocrinol Metab* **13**, 75-8.

Puto, L. A., Pestonjamasp, K., King, C. C. and Bokoch, G. M. (2003). p21-activated kinase 1 (PAK1) interacts with the Grb2 adapter protein to couple to growth factor signaling. *J Biol Chem* **278**, 9388-93.

Qu, J., Cammarano, M. S., Shi, Q., Ha, K. C., de Lanerolle, P. and Minden, A. (2001). Activated PAK4 regulates cell adhesion and anchorage-independent growth. *Mol Cell Biol* **21**, 3523-33.

Russell, A. J., Fincher, E. F., Millman, L., Smith, R., Vela, V., Waterman, E. A., Dey, C. N., Guide, S., Weaver, V. M. and Marinkovich, M. P. (2003). Alpha 6 beta 4 integrin regulates keratinocyte chemotaxis through differential GTPase activation and antagonism of alpha 3 beta 1 integrin. *J Cell Sci* **116**, 3543-56.

Santini, M. T., Rainaldi, G. and Indovina, P. L. (2000). Apoptosis, cell adhesion and the extracellular matrix in the three-dimensional growth of multicellular tumor spheroids. *Crit Rev Oncol Hematol* **36**, 75-87.

Schmitz, A. A., Govek, E. E., Bottner, B. and Van Aelst, L. (2000). Rho GTPases: signaling, migration, and invasion. *Exp Cell Res* **261**, 1-12.

Schurmann, A., Mooney, A. F., Sanders, L. C., Sells, M. A., Wang, H. G., Reed, J. C. and Bokoch, G. M. (2000). p21-activated kinase 1 phosphorylates the death agonist bad and protects cells from apoptosis. *Mol Cell Biol* **20**, 453-61.

Sethi, T., Rintoul, R. C., Moore, S. M., MacKinnon, A. C., Salter, D., Choo, C., Chilvers, E. R., Dransfield, I., Donnelly, S. C., Strieter, R. et al. (1999). Extracellular matrix proteins protect small cell lung cancer cells against apoptosis: a mechanism for small cell lung cancer growth and drug resistance in vivo. *Nat Med* **5**, 662-8.

Shaw, L. M., Rabinovitz, I., Wang, H. H., Toker, A. and Mercurio, A. M. (1997). Activation of phosphoinositide 3-OH kinase by the alpha6beta4 integrin promotes carcinoma invasion. *Cell* **91**, 949-60.

Sminia, P., Acker, H., Eikesdal, H. P., Kaaijk, P., Enger, P., Slotman, B. and Bjerkvig, R. (2003). Oxygenation and response to irradiation of organotypic multicellular spheroids of human glioma. *Anticancer Res* **23**, 1461-6.

Sovak, M. A., Bellas, R. E., Kim, D. W., Zanieski, G. J., Rogers, A. E., Traish, A. M. and Sonenshein, G. E. (1997). Aberrant nuclear factor-kappaB/Rel expression and the pathogenesis of breast cancer. *J Clin Invest* **100**, 2952-60.

Spinardi, L., Einheber, S., Cullen, T., Milner, T. A. and Giancotti, F. G. (1995). A recombinant tail-less integrin beta 4 subunit disrupts hemidesmosomes, but does not suppress alpha 6 beta 4-mediated cell adhesion to laminins. *J Cell Biol* **129**, 473-87.

St Croix, B., Florenes, V. A., Rak, J. W., Flanagan, M., Bhattacharya, N., Slingerland, J. M. and Kerbel, R. S. (1996). Impact of the cyclin-dependent kinase inhibitor p27Kip1 on resistance of tumor cells to anticancer agents. *Nat Med* **2**, 1204-10.

Sutherland, R. M. and Durand, R. E. (1972). Radiosensitization by nifuroxime of the hypoxic cells in an in vitro tumour model. *Int J Radiat Biol Relat Stud Phys Chem Med* **22**, 613-8.

Tagliabue, E., Ghirelli, C., Squicciarini, P., Aiello, P., Colnaghi, M. I. and Menard, S. (1998). Prognostic value of alpha 6 beta 4 integrin expression in breast carcinomas is affected by laminin production from tumor cells. *Clin Cancer Res* **4**, 407-10.

Tang, Y., Chen, Z., Ambrose, D., Liu, J., Gibbs, J. B., Chernoff, J. and Field, J. (1997). Kinase-deficient Pak1 mutants inhibit Ras transformation of Rat-1 fibroblasts. *Mol Cell Biol* **17**, 4454-64.

Tang, Y., Yu, J. and Field, J. (1999). Signals from the Ras, Rac, and Rho GTPases converge on the Pak protein kinase in Rat-1 fibroblasts. *Mol Cell Biol* **19**, 1881-91.

Tannock, I. F., Lee, C. M., Tunggal, J. K., Cowan, D. S. and Egorin, M. J. (2002). Limited penetration of anticancer drugs through tumor tissue: a potential cause of resistance of solid tumors to chemotherapy. *Clin Cancer Res* **8**, 878-84.

Taylor-Papadimitriou, J., D'Souza, B., Berdichevsky, F., Shearer, M., Martignone, S. and Alford, D. (1993). Human models for studying malignant progression in breast cancer. *Eur J Cancer Prev* **2 Suppl 3**, 77-83.

Tong, R. T., Boucher, Y., Kozin, S. V., Winkler, F., Hicklin, D. J. and Jain, R. K. (2004). Vascular normalization by vascular endothelial growth factor receptor 2 blockade induces a pressure gradient across the vasculature and improves drug penetration in tumors. *Cancer Res* **64**, 3731-6.

Unger, M. and Weaver, V. M. (2003). The tissue microenvironment as an epigenetic tumor modifier. *Methods Mol Biol* **223**, 315-47.

Vadlamudi, R. K. and Kumar, R. (2003). P21-activated kinases in human cancer. *Cancer Metastasis Rev* **22**, 385-93.

Van Aelst, L. and D'Souza-Schorey, C. (1997). Rho GTPases and signaling networks. *Genes Dev* **11**, 2295-322.

Vander Heiden, M. G., Plas, D. R., Rathmell, J. C., Fox, C. J., Harris, M. H. and Thompson, C. B. (2001). Growth factors can influence cell growth and survival through effects on glucose metabolism. *Mol Cell Biol* **21**, 5899-912.

Wang, R. A., Zhang, H., Balasenthil, S., Medina, D. and Kumar, R. (2006). PAK1 hyperactivation is sufficient for mammary gland tumor formation. *Oncogene* **25**, 2931-6.

Wang, W., Wyckoff, J. B., Frohlich, V. C., Oleynikov, Y., Huttelmaier, S., Zavadil, J., Cermak, L., Bottinger, E. P., Singer, R. H., White, J. G. et al. (2002). Single cell behavior in metastatic primary mammary tumors correlated with gene expression patterns revealed by molecular profiling. *Cancer Res* **62**, 6278-88.

Weaver, V. M., Lelievre, S., Lakins, J. N., Chrenek, M. A., Jones, J. C., Giancotti, F., Werb, Z. and Bissell, M. J. (2002). beta4 integrin-dependent formation of polarized three-dimensional architecture confers resistance to apoptosis in normal and malignant mammary epithelium. *Cancer Cell* **2**, 205-16.

Weaver, V. M., Petersen, O. W., Wang, F., Larabell, C. A., Briand, P., Damsky, C. and Bissell, M. J. (1997). Reversion of the malignant phenotype of human breast cells in three-dimensional culture and in vivo by integrin blocking antibodies. *J Cell Biol* **137**, 231-45.

Whitacre, C. M. and Berger, N. A. (1997). Factors affecting topotecan-induced programmed cell death: adhesion protects cells from apoptosis and impairs cleavage of poly(ADP-ribose)polymerase. *Cancer Res* **57**, 2157-63.

Yang, C., Liu, Y., Leskow, F. C., Weaver, V. M. and Kazanietz, M. G. (2005). Rac-GAP-dependent inhibition of breast cancer cell proliferation by {beta}2-chimerin. *J Biol Chem* **280**, 24363-70.

Zahir, N., Lakins, J. N., Russell, A., Ming, W., Chatterjee, C., Rozenberg, G. I., Marinkovich, M. P. and Weaver, V. M. (2003). Autocrine laminin-5 ligates alpha6beta4 integrin and activates RAC and NFkappaB to mediate anchorage-independent survival of mammary tumors. *J Cell Biol* **163**, 1397-407.

Zahir, N. and Weaver, V. M. (2004). Death in the third dimension: apoptosis regulation and tissue architecture. *Curr Opin Genet Dev* **14**, 71-80.

Zakeri, Z. and Lockshin, R. A. (2002). Cell death during development. *J Immunol Methods* **265**, 3-20.

Figure Legends

Figure 1. Tissue differentiation is associated with an increase in (α6)β4 integrin-dependent Rac activity and enhanced apoptosis resistance. (A) Dose response curves showing that nonmalignant HMT-3522 S1 and MCF10A MECs acquire apoptosis resistance to chemotherapeutics including Taxol and immune receptor activators such as Trail following their rBM-induced differentiation into 3D polarized acini. Percent apoptosis was calculated by scoring the number of activated caspase 3-positive cells 48 hours after treatment divided by the total cell number. MECs were either plated on top of a 1:100 diluted rBM for 48-96 hours (2D) or differentiated by embedment within rBM for 10-12 days (3D) followed by exposure to increasing doses of apoptotic stimuli. (B) Representative immunoblot of immunoprecipitated Pak-associated Rac (GTP-Rac), total Rac (Rac), and E-cadherin in MECs plated either on top (2D) as monolayers or within (3D) rBM to assemble acini. Data indicate that total Rac decreases appreciably following rBM-induced differentiation whereas GTP-loaded Rac increases dramatically. (C) Average relative specific activity of Rac in 3D mammary acini calculated by densitometric analysis of immunoblots of GTP-Rac divided by total cellular Rac following E-cadherin normalization, as shown in B. (D) Representative immunoblot of GTP-Rac, total Rac (Rac), and E-cadherin in vector control and β4 integrin tailless (β4Δcyto) 3D mammary acini grown within rBM (10-14 days). Data illustrate that Rac activity diminishes significantly in mammary acini that express a signaling-defective tailless β4 integrin. (E) Average relative specific activity of Rac in control mammary acini versus mammary tissues expressing the tailless β4 integrin calculated as above in C and shown in D. Results are the mean ± S.E.M. of three to five separate experiments. *, $p \leq 0.05$; **, $p \leq 0.01$; ***, $p \leq 0.001$.

Figure 2. Rac activity is necessary for apoptosis resistance in 3D mammary acini. (A) FACS® analysis showing increased EGFP expression in MECs expressing the EGFP-tagged N17

Rac (P4) as compared to vector control MEC's (P3). (B) Representative immunoblot of GTP-Rac, Rac, and E-cadherin in vector control MECs grown as 2D monolayers as compared to the MECs expressing eGFP-tagged N17 Rac. Data illustrate that N17Rac significantly reduces GTP-Rac levels in MECs. (C) Average relative specific activity of Rac in MECs calculated by densitometric analysis of immunoblots of GTP-Rac divided by total cellular Rac following E-cadherin normalization of data illustrated in B. (D) Representative immunoblot of phospho-Pak1 and total Pak1 in 2D monolayer cultures of control MECs and MECs expressing EGFP-tagged N17Rac demonstrating how loss of Rac activity also reduces Pak1 activity. (E) Bar graph depicting the average fold reduction of Pak1 activity in MECs expressing EGFP-N17Rac as compared to control MECs. (F) Dose response curves of percent apoptosis, as determined by calculating the number of activated caspase 3-positive cells divided by the total cell number, showing how 3D rBM polarized mammary acini with reduced Rac activity are now more sensitive to both chemotherapeutic (Taxol) and receptor-mediated (Trail) apoptotic stimuli. Results are the mean ± S.E.M. of three to five separate experiments. *, $p \leq 0.05$; **, $p \leq 0.01$.

Figure 3. Rac-mediates apoptosis resistance and tissue polarity through distinct mechanisms. (A) (top) Phase contrast, and confocal immunofluoresence images of colonies of control mammary acini (left panel; control), acini expressing EGFP-tagged N17Rac (middle panel; N17Rac) and acini treated with the Rac1 inhibitor NSC23766 (right panel; NSC23766) stained for β4 integrin, laminin-5, collagen IV and scribble (red). Data show that expression of N17Rac does not effect either tissue integrity (compare control phase contrast images of acini to N17Rac expressing acini; top), or tissue polarity (lower images; evidenced by similar basally-localized b4 integrin; deposition of laminin-5 and collagen IV and intact cell-cell localized scribble; compare images of control acini to those expressing N17Rac). However, treatment of acini with the Rac inhibitor NSC23766 disrupted acini integrity (compare phase contrast images of control to NSC23766-treated acini), and severely perturbed tissue polarity, as evidenced by

disturbed localization of β4 integrin, laminin-5 and collagen IV and scribble (compare images of control to NSC23766-treated acini). Bar, 50 μm. Results are the mean ± S.E.M. of three to five separate experiments. *, $p \leq 0.05$; **, $p \leq 0.01$.

Figure 4. GAP-dependent Rac inactivation sensitizes mammary acini to death induction. (A) Representative immunoblot showing non-detectable amounts of HA expressed in vector control MECs and high levels in MECs expressing an exogenous HA-tagged β2-Chimerin. (B) (top) Phase contrast and (bottom) immunofluorescence images of 3D poly-HEMA rBM generated vector control MEC colonies (left) and MEC colonies expressing HA-tagged β2-Chimerin (right; red) illustrating robust and uniform expression of the transgene 48 hours following adenoviral infection. Bar, 50 μm. (C) Representative immunoblot showing GTP-Rac, Rac, and E-cadherin levels in vector control MECs compared to β2-Chimerin expressing MECs. (D) Average relative specific activity of GTP-loaded Rac illustrating reduced Rac activity in MEC expressing exogenous β2-Chimerin as compared to vector control MECs. (E) Bar graph illustrating increased percent apoptosis induced by treatment with Trail (1 μg/ml) in 3D rBM differentiated MECs with reduced Rac activity mediated by expression of either the Rac GAP β2-Chimerin or dominant-negative N17Rac. Percent apoptosis was calculated by scoring the number of activated caspase 3-positive MECs divided by the total number of MECs 24 hours following apoptosis treatment. Similar results were obtained following treatment with chemotherapeutic agents (data not shown). (F) Confocal immunofluorescence images of polarized β4 integrin (green) localization in vector control (left) and 3D rBM MEC acini despite the expression of exogenous β2-Chimerin and a significant reduction of Rac activity in the differentiated colonies. Bar, 50 μm. Results are the mean ± S.E.M. of three separate experiments. *, $p \leq 0.05$; **, $p \leq 0.01$.

Figure 5. Rac-dependent Pak1 activity is necessary and sufficient for apoptosis resistance of mammary acini. (A) Representative immunoblots of phospho-Pak1, total Pak1, Pak-3, phospho-Pak4, total Pak4, and E-cadherin in rBM-ligated MECs plated as 2D monolayers or 3D mammary acini. Data indicate that Pak1 activity is significantly higher, Pak4 activity is substantially lower and Pak3 is non-detectable in 3D mammary acini as compared to 2D monolayers of MECs. (B) Quantification of averaged experimental data shown in A of Pak1 specific activity, calculated by densitometric analysis of immunoblots of Phospho-Pak1 divided by total Pak1 after normalization to E-cadherin. Similar results were obtained for HMT-3522 S1 and MCF10A nonmalignant MECs. (C) Representative immunoblots of phospho-Pak1 and total Pak1 in 3D mammary acini expressing the tailless β4 integrin (β4Δcyto) as compared to control acini. Data demonstrate that Pak1 activity but not expression is regulated by (α6)β4 integrin signaling. (D) Quantification of averaged experimental data shown in C of Pak1 specific activity calculated as described above in B. (E) Dose response curves illustrating percent apoptosis induced in 3D mammary acini following 24 hours of treatment with increasing concentrations of Trail (left) and Taxol (right), calculated by scoring the number of caspase 3-positive cells divided by the total number of cells. Mammary acini with reduced Rac activity were sensitized to Trail and Taxol-induced apoptosis (N17Rac/Vector) their death resistance phenotype was restored following ectopic expression of V12Rac. (F) Bar graphs illustrating how expression of V12Rac restores apoptosis resistance to Trail treatment in N17Rac expressing 3D mammary acini, whereas expression of V12Rac H40 which cannot activate Pak does not. Percent apoptosis was calculated by scoring the number of activated caspase 3-positive cells divided by the total number of cells. (G) Bar graph demonstrating that inhibiting Pak activity, by expressing PID significantly sensitizes mammary acini to Trail-induced death, analogous to that mediated by N17Rac. (H) Bar graph showing how expression of wild type Pak1 can restore resistance to

Trail treatment to 3D mammary acini expressing N17Rac (N17Rac). Results are the mean ± S.E.M. of three to five separate experiments. *, $p \leq 0.05$; **, $p \leq 0.01$.

Figure 6. Pak permits NFκ B activation to mediate apoptosis resistance in mammary acini. (A) Bar graph indicating how inhibiting NFκ B activation by treating mammary acini with SN50 peptide permits Trail-induced apoptosis. MECs were grown in rBM for 10 days and treated with SN50 or inactive, scrambled SN50M peptide. Polarized acini were treated with Trail (1 μg/ml) and after 24 hours the acini were stained and quantified for activated caspase 3. (B) Bar graph illustrating how ectopically-expressed wild type Pak1 can restore apoptosis resistance to N17Rac expressing mammary acini treated with Trail (N17Rac) but the acini remain death sensitive if NFk B activation is prevented by pre-incubation with SN50. 3D mammary acini were infected with adenovirus, pre-incubated for 24 hours with either SN50 to inhibit NFκB activation or its non-active analogue SN50M, and treated with Trail (1 μg/ml) for 24 hours. Percent apoptosis for (A) and (B) was calculated by scoring the number of activated caspase 3-positive cells divided by the total cell number. (C) Confocal immunofluoresence microscopy images showing NFκ B p65 nuclear translocation in response to Trail treatment (90 min) in 3D mammary acini expressing either vector (Control), the Pak activity inhibitor (PID), N17Rac (N17Rac), or N17Rac and wild type Pak1 (N17Rac/Pak1 WT). Note the presence of high nuclear levels of p65 in response to Trail stimulation in control and N17Rac/Pak1 WT expressing mammary tissues and decreased levels in acini with reduced Rac or Pak activity. Bar, 10 μm. (D) Quantification of nuclear p65 in 50-100 representative images as shown in C. (E) Bar graph showing how expression of a wild type p65 transgene restores Trail-induced death-resistance to apoptotically-sensitized N17Rac and PID expressing mammary acini. (F) Bar graph showing how inhibiting NFκ B activation through expression of the IκBαM super repressor permits Trail-dependent

death induction in 3D mammary acini despite elevated levels of Pak1. Results are the mean ± S.E.M. of three separate experiments. * $p \leq 0.05$; ** $p \leq 0.01$; *** $p \leq 0.001$.

Figure 7. Schemata illustrating proposed mechanism whereby α6β4 integrin regulates Rac and Pak to mediate Bad and NFκ B-dependent apoptosis resistance in mammary acini. Nonmalignant MECs differentiate into polarized tissue-like structures that assemble an endogenous laminin-5 BM. Laminin-ligation of α6β4 integrin stimulates Rac to drive tissue polarity and promote apoptosis resistance in 3D mammary acini through Pak-dependent NFk B activation and Bad phosphorylation.

Figure legends for Appendix

Appendix 1. Pharmacological inhibition of Rac perturbs tissue polarity and sensitizes mammary acini to death induction. (A) Representative confocal immunofluorescence images of β4 integrin (green) in control and Toxin A treated MEC acini showing that inhibiting Rho GTPase activity disrupts the polarity of rBM-differentiated mammary tissue structures. Bar, 50 μm. (B) Dose response curves of percent death, calculated using the Live/Dead assay, induced following treatment with increasing doses of the chemotherapeutic agents Etoposide and Taxol. Results demonstrate how inhibiting Rho GTPase activity compromised both acini polarity and apoptosis resistance. Similar data were obtained following treatment with Doxirubicin and Camptothecin (data not shown). Results are the mean ± S.E.M. of at least three separate experiments of duplicates. *, $p \leq 0.05$.

Appendix 2. Rac-dependent Pak activation regulates Bad phosphorylation. (A) Representative immunoblots of phospho-Bad, total Bad, and E-cadherin in 3D control, N17Rac and N17Rac/wild type Pak1 expressing 3D mammary acini. Data indicate that Rac-dependent

Pak1 activity regulates Phospho Bad levels. (B) Quantification of experimental data shown in A of phosphorylation-mediated Bad activity inhibition, calculated by densitometric analysis of immunoblots of Phospho-(inactivated)-Bad divided by total Bad after normalization to E-cadherin.

Appendix 3. Transgene manipulation of NFk B in 3D mammary acini. (A) Confocal immunoflouresence images of elevated nuclear (DAPI) p65 (green) in 3D control mammary acini and N17 expressing acini ectopically expressing p65. Data indicate that elevated expression of p65 increases nuclear p65 in 3D mammary acini even in the absence of Rac activity. (B) Representative immunoblots of total cellular NFκ B p65 and E cadherin in control and N17Rac infected mammary acini and acini ectopically expressing p65 or IκBαM. (C) Quantification of immunoblots shown in B depicting relative p65 levels normalized to total cellular E cadherin expressed in control and N17Rac infected mammary acini and acini expressing p65 or IκBαM.

Fig. 1

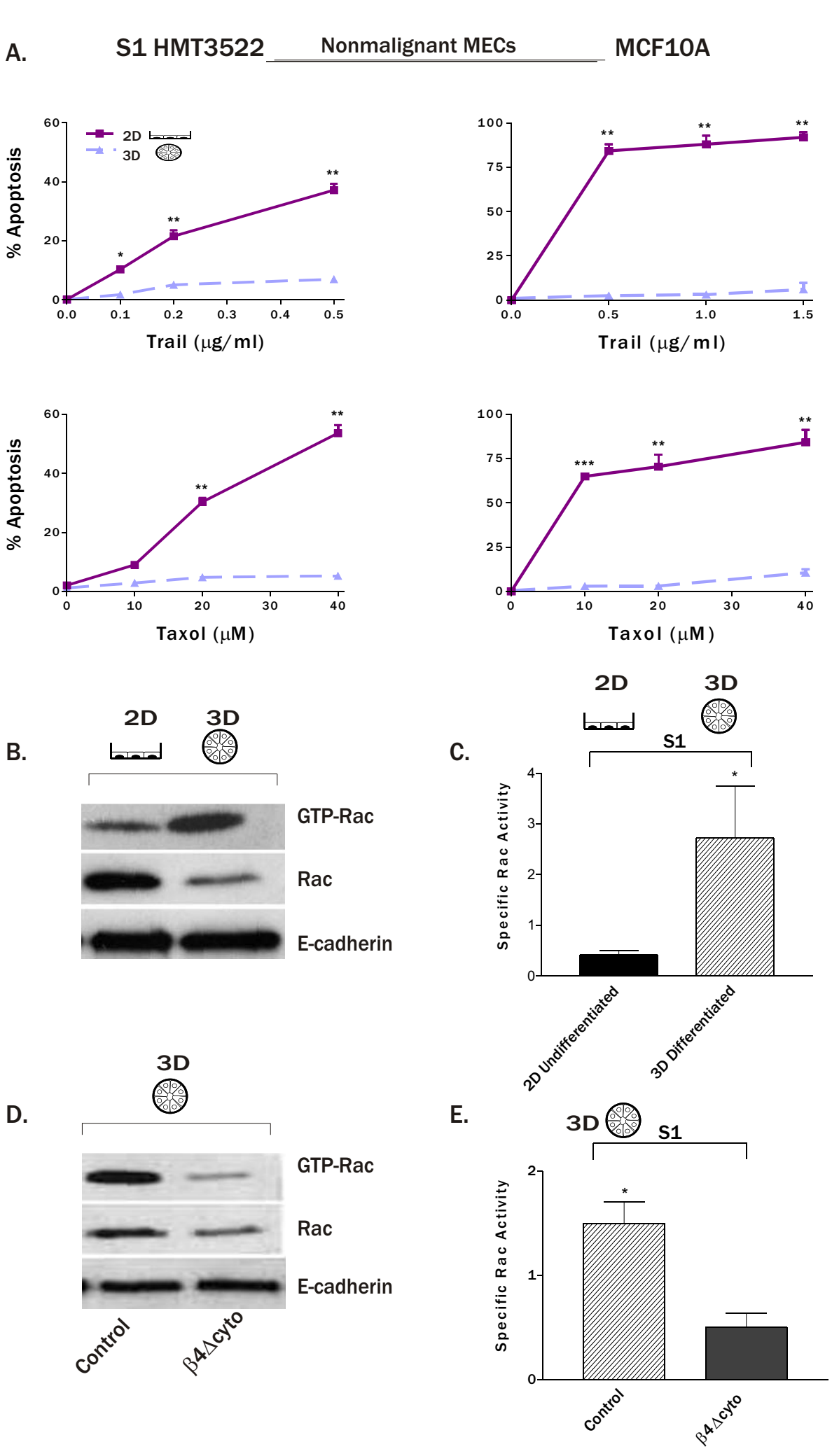
A.
S1 HMT3522
Nonmalignant MECs
MCF10A
% Apoptosis
2D
3D
Trail (μg/ml)
Taxol (μM)
B.
GTP-Rac
Rac
E-cadherin
C.
S1
Specific Rac Activity
2D Undifferentiated
3D Differentiated
D.
Control
β4Δcyto
E.

Fig. 2

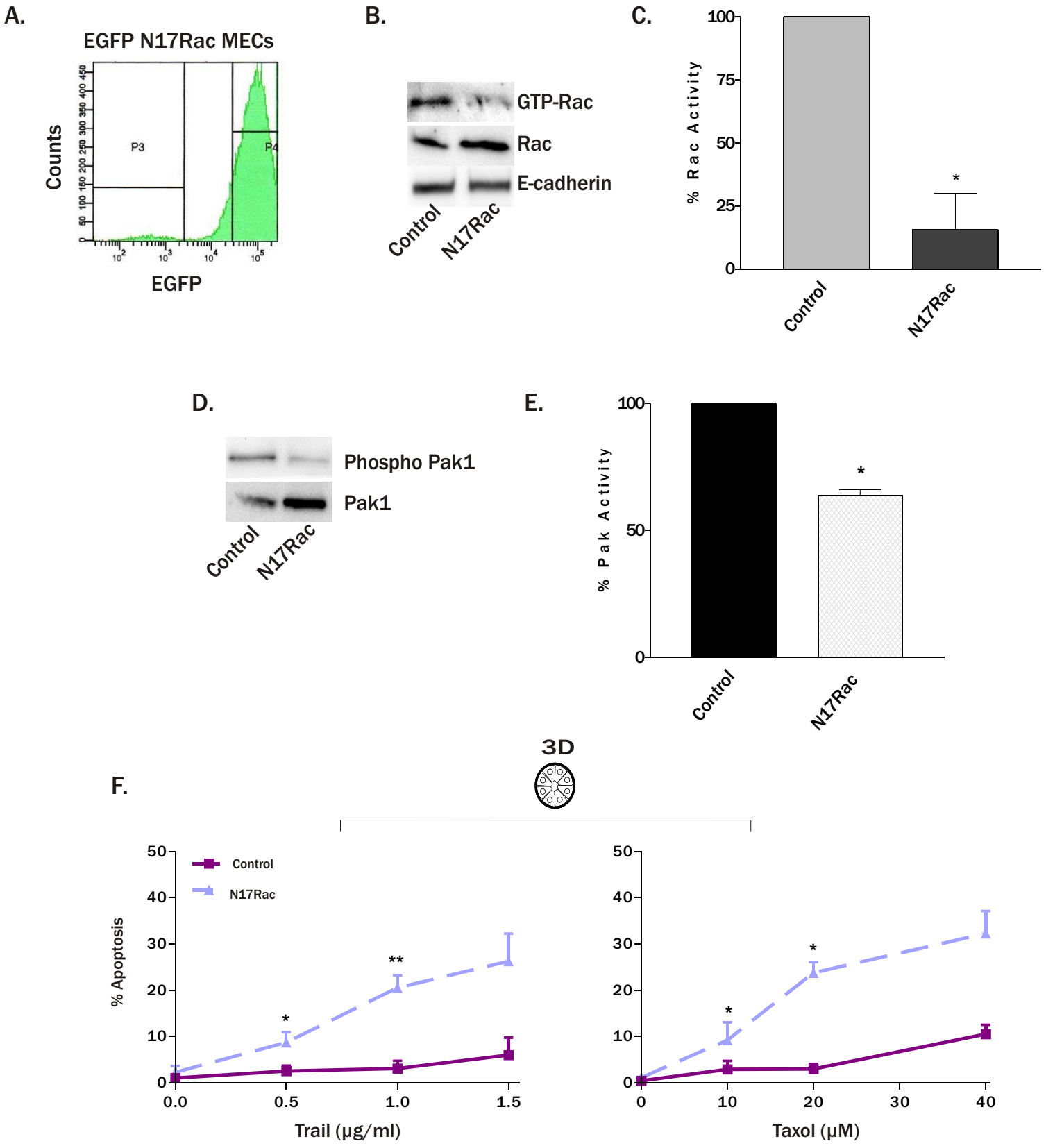
A.
EGFP N17Rac MECs
Counts
P3
P4
EGFP
B.
GTP-Rac
Rac
E-cadherin
Control
N17Rac
C.
% Rac Activity
100
75
50
25
0
*
Control
N17Rac
D.
Phospho Pak1
Pak1
Control
N17Rac
E.
% Pak Activity
100
50
0
*
Control
N17Rac
F.
3D
Control
N17Rac
% Apoptosis
50
40
30
20
10
0
*
**
0.0
0.5
1.0
1.5
Trail (µg/ml)
*
*
0
10
20
30
40
Taxol (µM)

Fig. 3

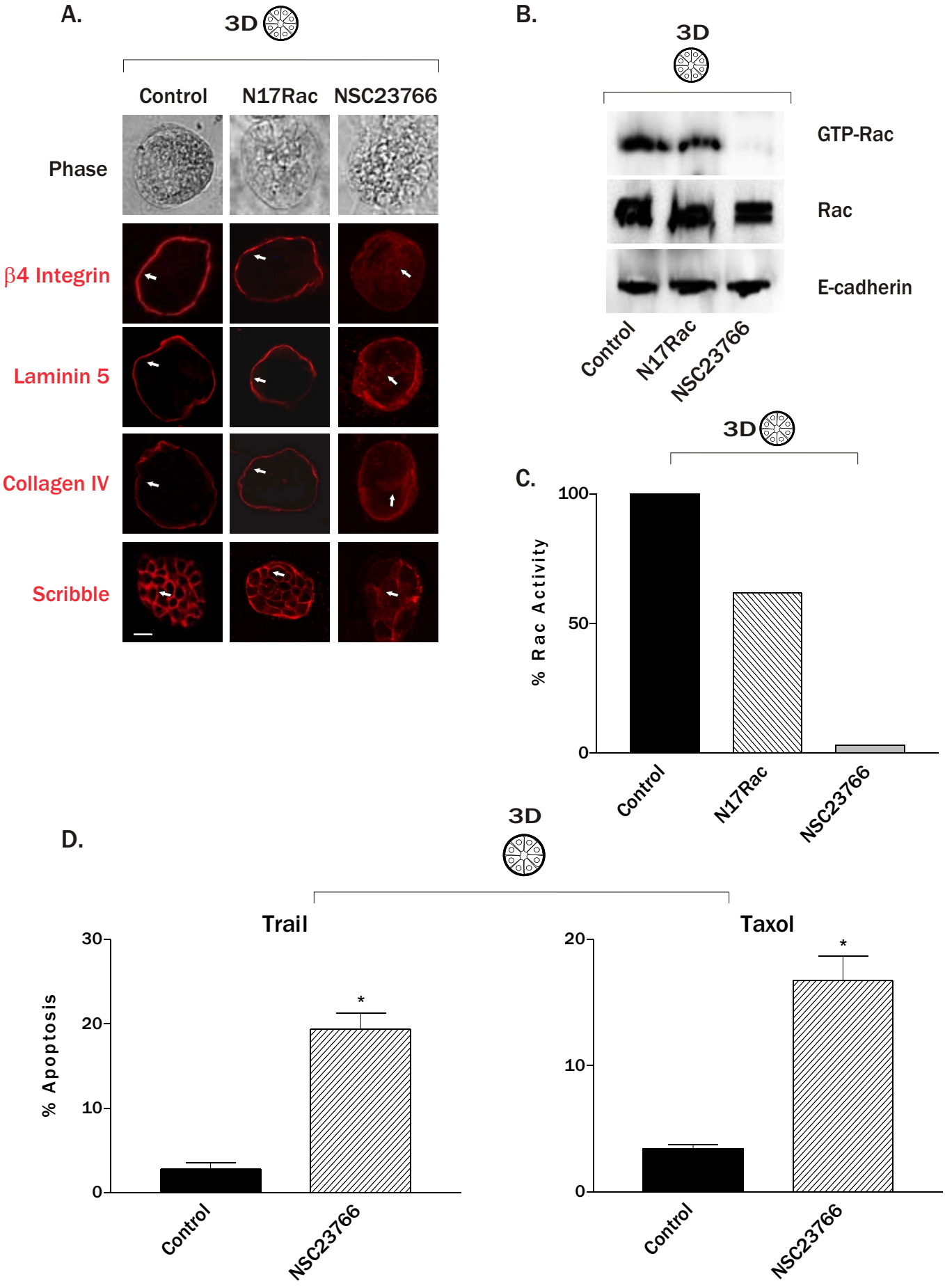
A.
3D
Control
N17Rac
NSC23766
Phase
β4 Integrin
Laminin 5
Collagen IV
Scribble
B.
3D
GTP-Rac
Rac
E-cadherin
Control
N17Rac
NSC23766
C.
3D
% Rac Activity
100
50
0
Control
N17Rac
NSC23766
D.
3D
Trail
% Apoptosis
30
20
10
0
*
Control
NSC23766
Taxol
20
10
0
*
Control
NSC23766

Fig. 4

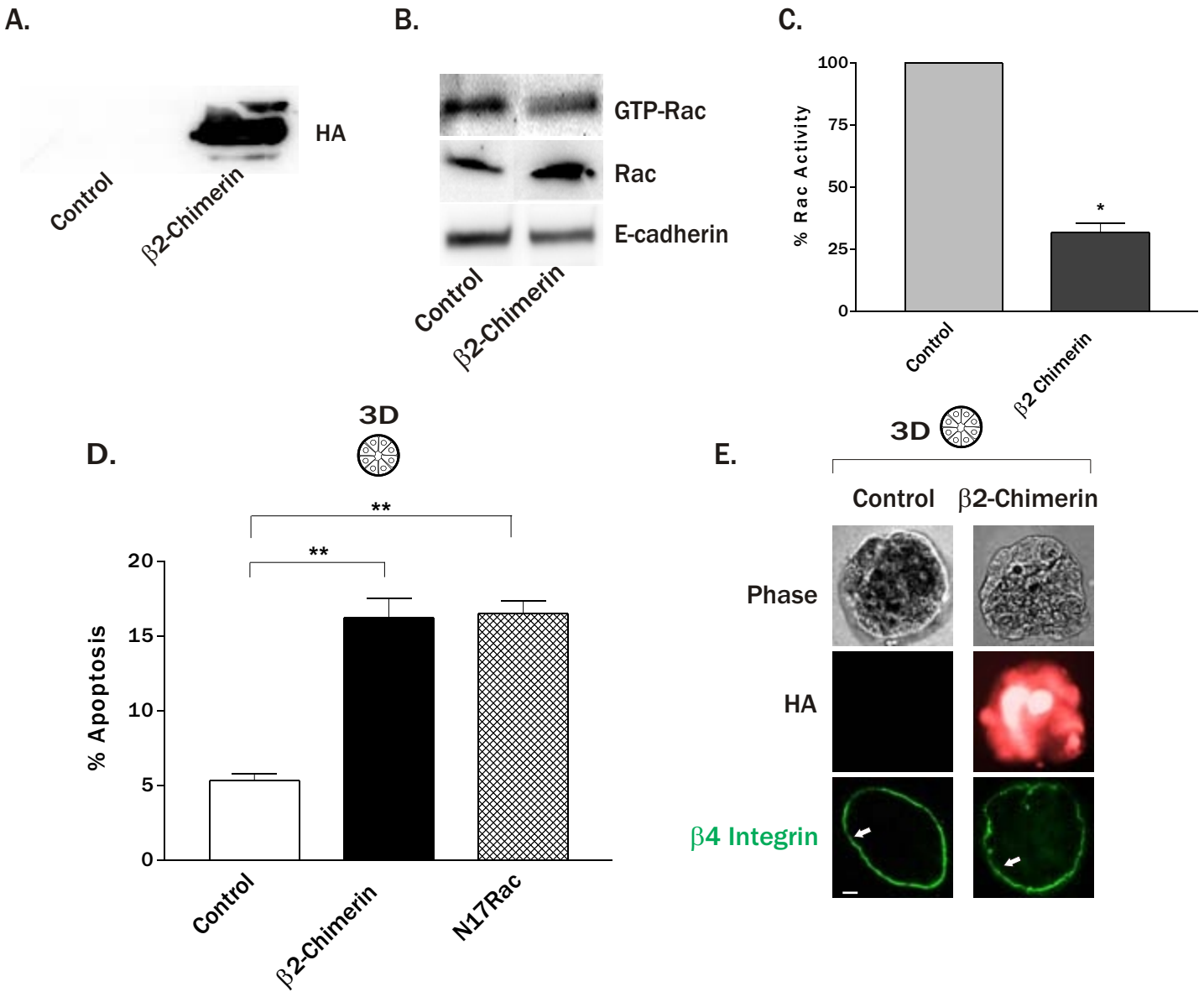
A.
HA
Control
β2-Chimerin
B.
GTP-Rac
Rac
E-cadherin
Control
β2-Chimerin
C.
% Rac Activity
100
75
50
25
0
*
Control
β2 Chimerin
D.
3D
% Apoptosis
20
15
10
5
0
**
**
Control
β2-Chimerin
N17Rac
E.
3D
Control
β2-Chimerin
Phase
HA
β4 Integrin

Fig. 5

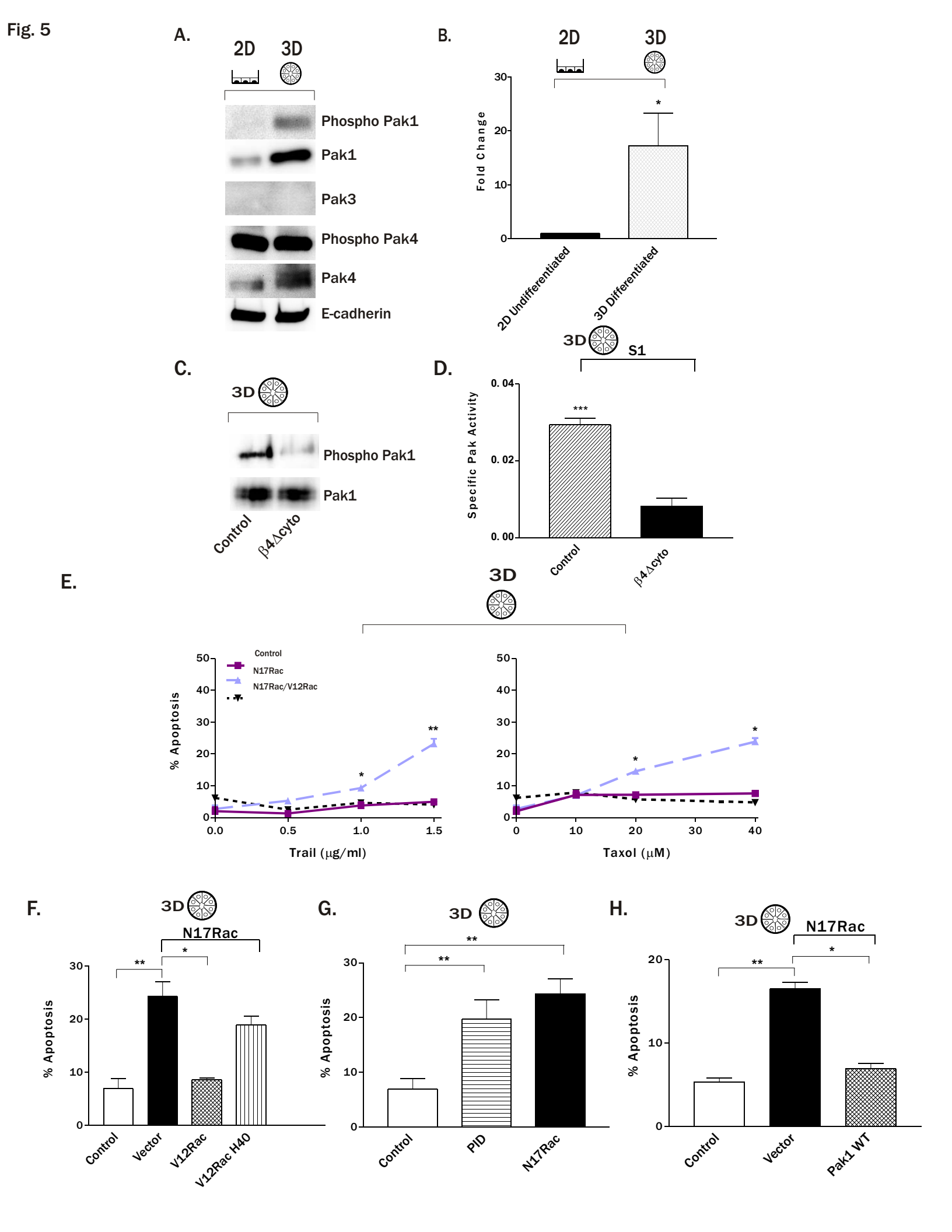
A.
2D
3D
Phospho Pak1
Pak1
Pak3
Phospho Pak4
Pak4
E-cadherin
B.
2D
3D
Fold Change
30
20
10
0
*
2D Undifferentiated
3D Differentiated
C.
3D
Phospho Pak1
Pak1
Control
β4Δcyto
D.
3D
S1
Specific Pak Activity
0. 04
0. 02
0. 00
***
Control
β4Δcyto
E.
3D
Control
N17Rac
N17Rac/V12Rac
% Apoptosis
50
40
30
20
10
0
0.0
0.5
1.0
1.5
Trail (μg/ml)
0
10
20
30
40
Taxol (μM)
F.
3D
N17Rac
% Apoptosis
Control
Vector
V12Rac
V12Rac H40
G.
3D
% Apoptosis
Control
PID
N17Rac
H.
3D
N17Rac
% Apoptosis
Control
Vector
Pak1 WT

Fig. 6

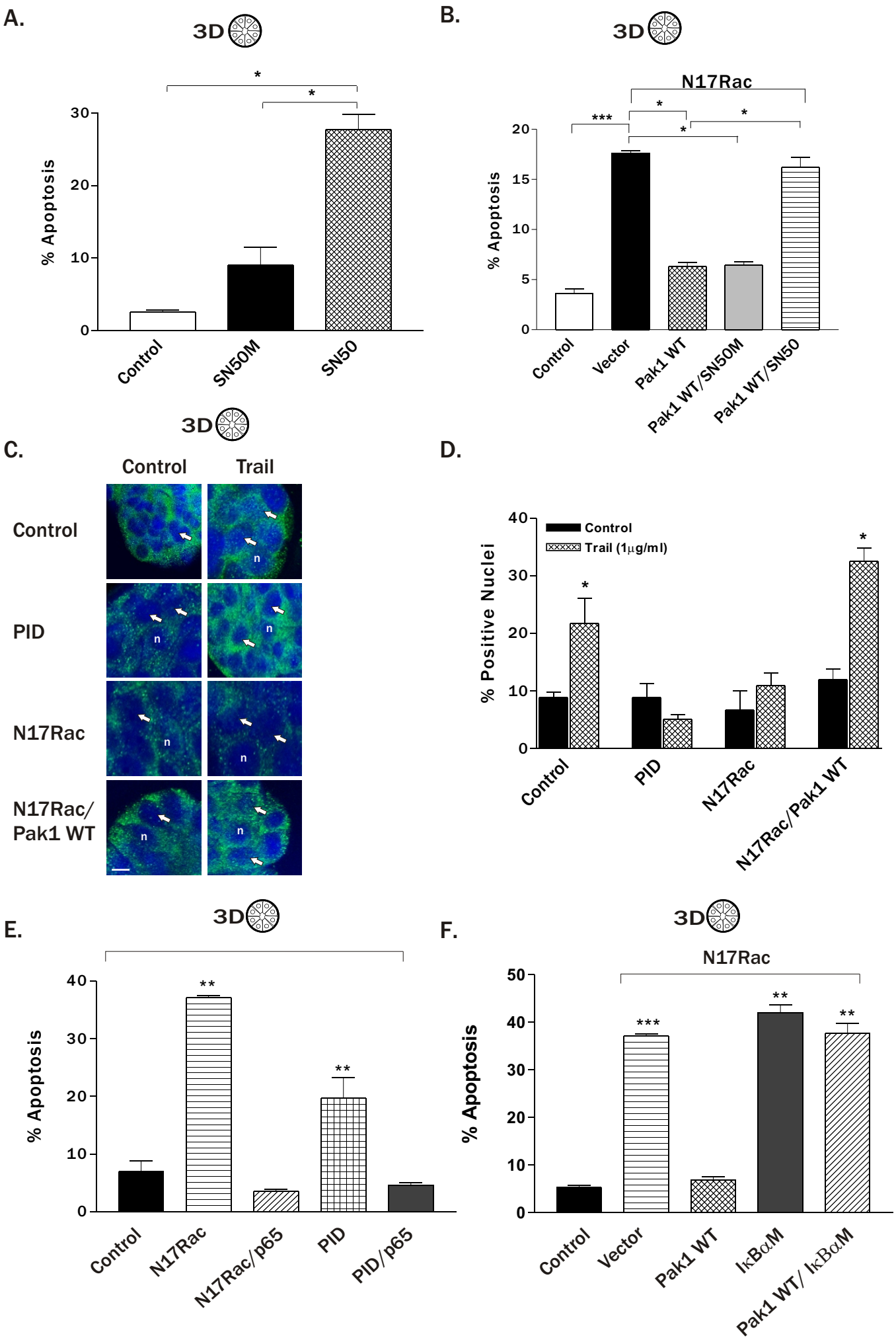
A.
3D
% Apoptosis
Control
SN50M
SN50
B.
3D
N17Rac
% Apoptosis
Control
Vector
Pak1 WT
Pak1 WT/SN50M
Pak1 WT/SN50
C.
3D
Control
Trail
Control
PID
N17Rac
N17Rac/
Pak1 WT
D.
% Positive Nuclei
Control
Trail (1μg/ml)
Control
PID
N17Rac
N17Rac/Pak1 WT
E.
3D
% Apoptosis
Control
N17Rac
N17Rac/p65
PID
PID/p65
F.
3D
N17Rac
% Apoptosis
Control
Vector
Pak1 WT
IκBαM
Pak1 WT/ IκBαM

Fig. 7

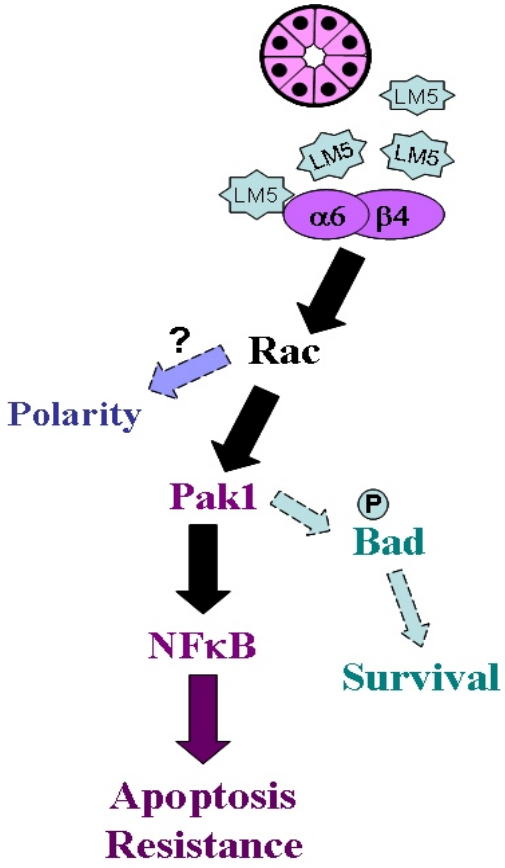
LM5
LM5
LM5
LM5
α6
β4
?
Rac
Polarity
Pak1
P
Bad
NFκB
Survival
Apoptosis
Resistance

Fig. S-1

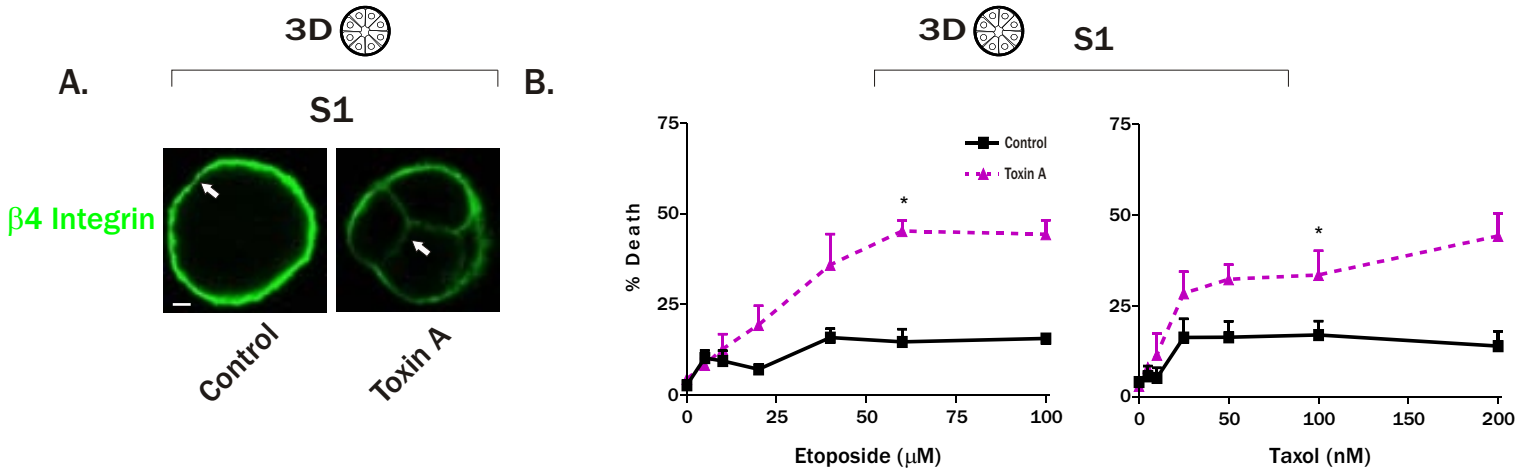
3D
A.
S1
β4 Integrin
Control
Toxin A
B.
3D
S1
% Death
Control
Toxin A
Etoposide (μM)
Taxol (nM)

Fig. S-2

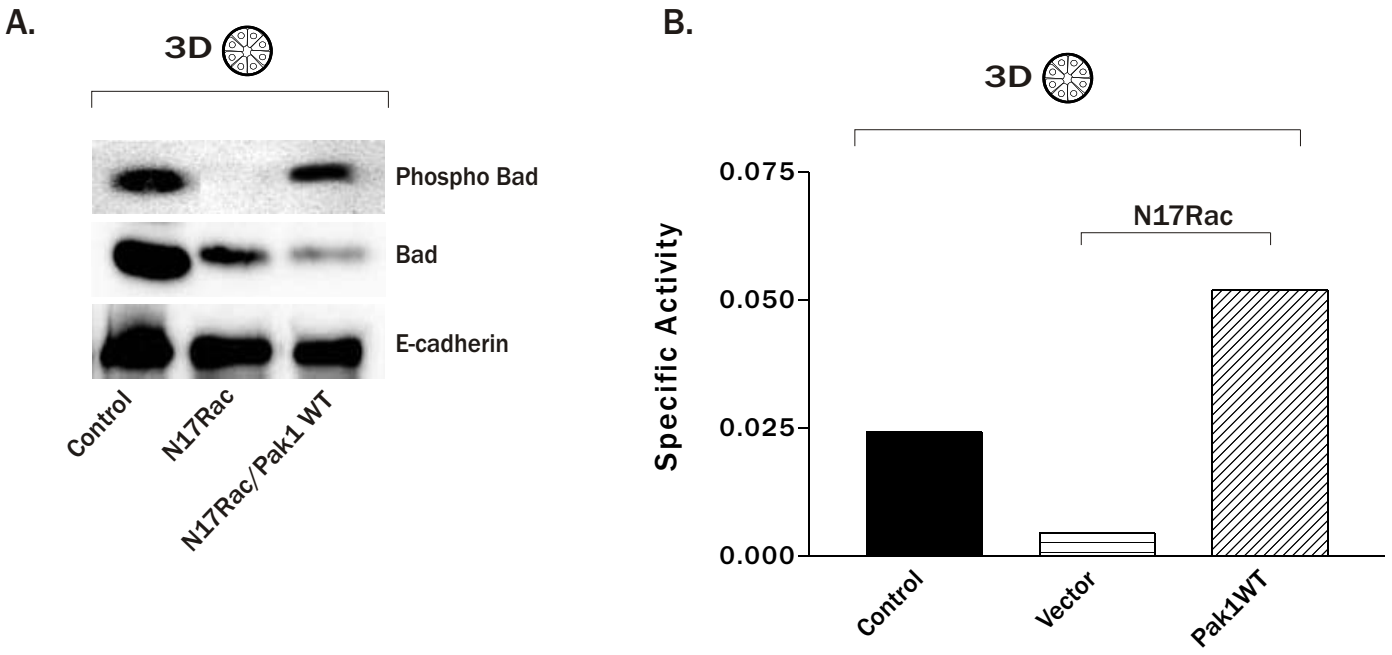
A.
3D
Phospho Bad
Bad
E-cadherin
Control
N17Rac
N17Rac/Pak1 WT
B.
3D
N17Rac
Specific Activity
0.075
0.050
0.025
0.000
Control
Vector
Pak1WT

Fig. S-3

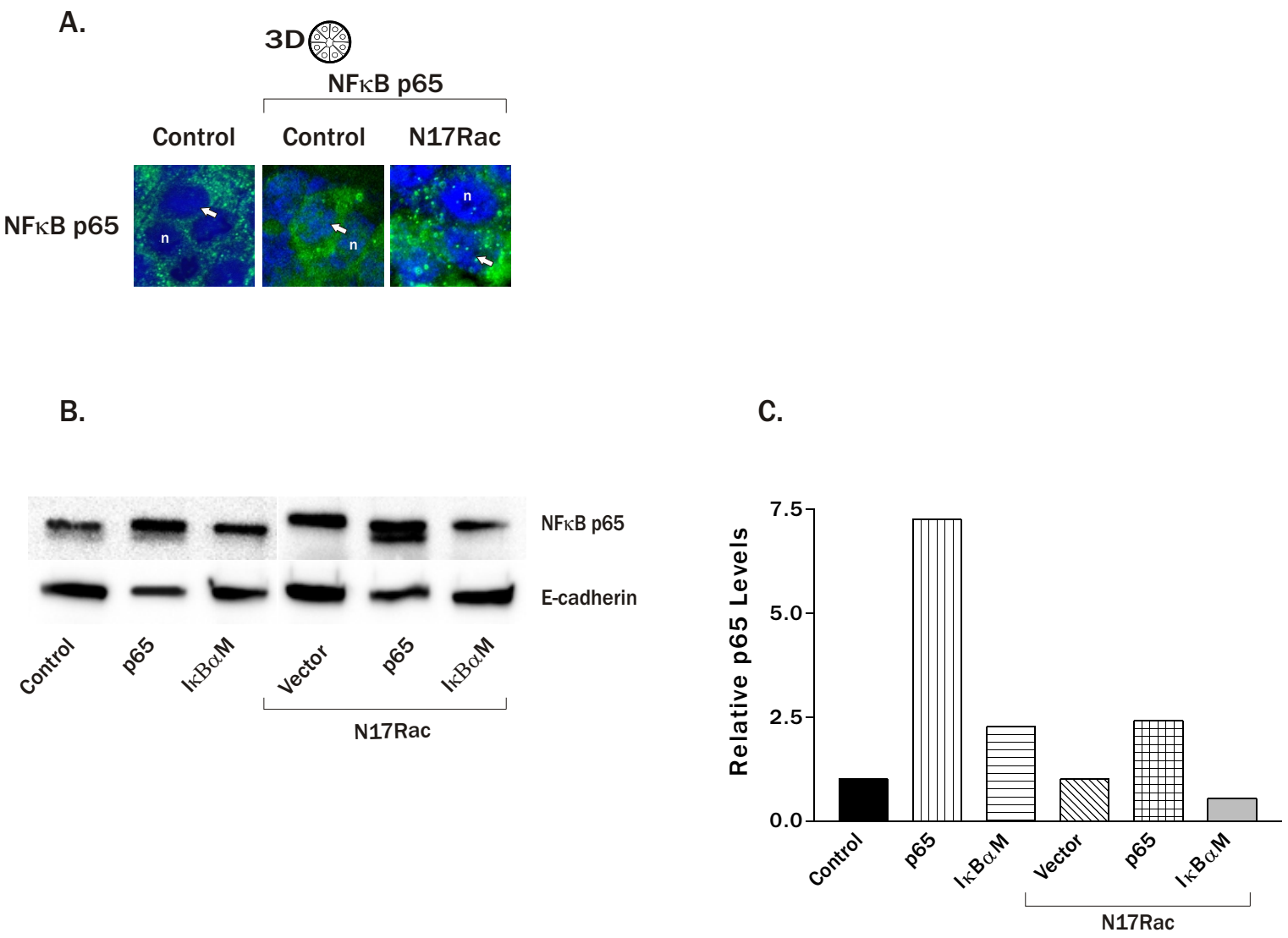
A.
3D
NFκB p65
Control
Control
N17Rac
NFκB p65
n
n
n
B.
NFκB p65
E-cadherin
Control
p65
IκBαM
Vector
p65
IκBαM
N17Rac
C.
Relative p65 Levels
7.5
5.0
2.5
0.0
Control
p65
IκBαM
Vector
p65
IκBαM
N17Rac

Integrin-mediated Signaling through the MAP-kinase Pathway

Ka Lai Yee, Valerie M. Weaver, and Daniel A. Hammer

Correspondence Address:

Daniel A. Hammer
240 Skirkanich Hall
210 S 33rd St.
Dept of Bioengineering
University of Pennsylvania
Philadelphia, PA 19104

Email: hammer@seas.upenn.edu

Abstract

The MAP kinase cascade, leading to ERK activation, is a key regulator of cell growth and proliferation. The effects of ERK are mediated by differences in ERK signaling dynamics, including magnitude and duration. In vivo, ERK signaling, is stimulated by both growth factors and adhesion signals. Here, a model for adhesion-mediated ERK activation is presented. Outputs of the model such as ERK and FAK activation, as well as responses to different ligand densities, are matched to published experimental data. The model then serves as a basis for understanding how adhesion may contribute to ERK signaling through changes in the dynamics of FAK activation. The main parameters influencing ERK are determined through screening analyses and parameter variation. With these parameters, key points in the pathway that give rise to changes in downstream signaling dynamics are identified. In particular, we propose that oncogenic Raf and Ras promote cell growth by increasing the magnitude and duration, respectively, of ERK activity.

1 Introduction

The MAP kinase cascade is an important signaling pathway associated with tumorigenic behavior. In cancerous cells, the pathways that regulate proliferation are disrupted so that cells experience unchecked growth. A major factor in proliferation is the increased activity of the MAPK cascade, which can be caused by increased external stimuli or mutations along the pathway that promote pathway activation [1]. The MAPK involved in growth regulation is extracellular-regulated kinase (ERK). Upon double phosphorylation by MEK, ERKPP translocates to the nucleus and induces gene transcription by phosphorylation of transcription factors [2]. One of ERK's targets is fos, a member of the AP-1 transcription factor heterodimer [3]. AP-1 family transcription factors induce the transcription of cyclin D1, which promotes cell cycle entry [4, 5]. Modeling this pathway to gain an understanding of how specific elements give rise to different ERK signaling dynamics is an important step towards regulating signal transduction, and ultimately cell behavior, *in vivo*.

The signaling pathway that culminates in ERK activation is initiated by extracellular stimuli such as adhesion to the extracellular matrix or growth factors. Cell adhesion activates ERK by binding of $\alpha 5\beta 1$ integrins at the cell surface to extracellular matrix proteins such as fibronectin [6, 7]. Integrins activate ERK via a pathway involving Shc, Grb2, Sos, the GTPase Ras, and focal adhesion kinase (FAK) [5, 6, 8]. Epidermal growth factor (EGF) binding to its receptor is also known to activate ERK through the same Shc-Grb2-Sos-Ras pathway as integrins [9-11]. Though integrins may activate ERK in the absence of growth factors, cells *in vivo* are exposed to both adhesion signals and growth factor signals. In addition, there is cross talk between growth factor and integrin activated pathways to ERK activation at different levels of the pathway [12-14]. This cross-talk likely gives rise to distinctive ERK activation signals that

can regulate different behaviors [12]. For example, ERK activity stimulated by growth factors and adhesion independently is transient, whereas ERK activity in adherent, growth factor stimulated cells is sustained. Moreover, the cell cycle protein cyclin D1 is only induced by sustained ERK signals [5, 15].

The MAPK cascade and activation by EGF have been previously explored with deterministic, computational models. A basic model of the Shc-Grb2-Sos-Ras pathway activated by EGF was described by Kholodenko [16]. A more comprehensive model of ERK activation in response to EGF stimulation has also been examined [17]. In that model, EGF receptor-ligand binding and dimerization initiates the traditional Shc-Grb2-Sos-Ras pathway that leads into the MAPK cascade. More recently, Chapman and Asthagiri undertook an exploration of MAPK cascade dynamics [18]. Their work demonstrated that adjusting rate constants and protein or phosphatase concentrations controls ERK activation dynamics. Similarly, Hornberg and colleagues [19] applied control analysis to the model developed by Schoeberl, identifying specific proteins that are important in EGF-mediated ERK signaling.

As a first step towards developing a model of ERK activation by both EGF and integrins, a computational model for integrin activation of ERK is presented in this paper. In this model, the ERK signaling pathway is initiated by $\alpha 5\beta 1$ integrin binding to its extracellular ligand fibronectin. The model successfully simulates experimental FAK and ERK activation time courses. Semi-quantitative data on FAK and ERK activation after adhesion [20] are used to verify the results of the model. After matching simulated signals to experimental results, the pathways were explored to gain insight into specific characteristics that contribute to ERK activation dynamics. To systematically explore the set of parameters used in the model, a screening method developed by Morris [21] was used to identify the key parameters that affect

different characteristics of the output signal, such as overall dynamics, maximum value, and time to reach maximum.

2 Methodology

2.1 Biological Considerations

The signaling events culminating in ERK activation are modeled as a set of differential equations. The protein-protein interactions included in the pathway were chosen based on published pathways and experimental data and are illustrated in Figure 1a. The full pathway and a list of reactions and rate constants are provided in the Supplementary Materials Spreadsheet.

The Integrin/FAK activation portion of the model deals with receptor-ligand binding as a cell spreads on fibronectin. The cell-surface contact area begins at zero and increases according to an experimentally determined profile [22] (see Supplementary Materials). The increase in contact area regulates the transport of receptors and ligands into the contact area where binding occurs. Integrin-fibronectin binding is modeled according to the Bell model for receptor-ligand binding [23]. Because integrin clustering is a complex process involving the many cytoskeletal proteins and the transduction for force, clustering is modeled as dimerization of receptor-ligand pairs (see Supplementary Materials). We assume only dimerized receptor-ligand pairs are able to recruit FAK, which becomes autophosphorylated at tyrosine 397 (FAKP)[24].

Src activation occurs after cell adhesion, though it is unclear how adhesion signals regulate the Src activation machinery [25]. Activation begins with the dephosphorylation of cytoplasmic Src at tyrosine 527. The protein then undergoes a conformational change and translocates to the membrane [26]. To be fully active, Src undergoes an intermolecular autophosphorylation at Y416. However, fully active Src can be re-phosphorylated and dephosphorylated, thereby cycling it from active to inactive conformations [27-29]. This module

is linked to the rest of the pathway by the ability of Src to phosphorylate its substrate FAK at Y925 [30]. Src and FAK are both capable of phosphorylating Shc [9, 11, 31]. This interaction leads into the same sequence of signaling events activated by the EGF receptor, ultimately resulting in activation of the MAPK cascade [32, 33].

Evidence suggests that integrins may also activate ERK through a FAK independent pathway [9]. Such a pathway likely involves Fyn, a member of the Src kinase family, and the alpha integrin subunit [34]. Because of limited experimental data on this pathway, this model focuses on the FAK dependent pathways to ERK activation.

2.2 Model Parameters

Rate constants and protein concentrations were either found in literature or estimated based on known constants for similar reactions. For protein interactions without published binding constants, K_d's, k_f's, and k_r's were estimated from available peptide binding data. For example, binding constants for Src and FAKP in the Src activation module were estimated with rate constants for Src SH2 domain binding to the pYEEI peptide, which is similar to the autophosphorylation site for FAK [35, 36]. Most binding events in this pathway involve SH2-phosphotyrosine and SH3-PXXP binding [37, 38].

During integrin activation of FAK, k_1 is the rate of dimerization of receptor-ligand pairs while k_p and k_m are the forward and backward rate constants for FAK binding to receptor-ligand dimers and subsequent autophosphorylation. k_1 is a phenomenological rate constant assigned a value of $0.01s^{-1}$, which corresponds to maximum levels of FAK activation. Decreasing k_1 will decrease the final magnitude of FAK activation without significantly changing the kinetics. Values for k_p and k_m were estimated to obtain a variety of time scales for FAK autophosphorylation, which are discussed in the Results section. The Src activation module also

contains the phenomenological rate constant k_t, which represents the rate of Src transport from the cytoplasm to the membrane by the cytoskeleton [39]. Because these steps are not easily modeled, they are lumped into the transport rate k_t; k_t is set at 0.1 s^{-1}, at which the rate of cytoskeletal transport is maximal. Rate constants for the phosphatase and kinase reactions in Src activation were obtained from literature [40-42]. Subsequent analyses of FAK and downstream signaling focus on the relative effects of different parameter values on kinetics and magnitude, so that the conclusions drawn are valid regardless of the specific phenomenological constants used.

Initial protein concentrations were obtained from Schoeberl [17] and were varied over several orders of magnitude to explore their effects on signal dynamics. The constant concentrations of phosphatases were also estimated based on these initial values .The initial conditions specify protein concentrations for FAK, Src, Shc, Grb2, Sos, MEK, and ERK. All other protein species present in the system at any given time are derived from these proteins and have an initial concentration of zero.

The resulting set of equations with initial conditions was solved in MATLAB 6.5 using the ODE15s solver.

3 Results

3.1 Kinetics of FAK and ERK Activation

Asthagiri [20] has shown that activation of ERK by adhesion occurs before maximal FAK activation. Simulations of ERK and FAK activation showed similar behavior (Figure 2). Over a range of FAK recruitment rates (k_p), the ERK activation peak consistently occurs ahead of full FAK activation. Since FAK is the only means by which ERK is activated in this model, early and therefore relatively low levels of FAK activation are sufficient for stimulating the MAP kinase cascade. For FAK to achieve sufficient levels of activation to stimulate the MAPK

cascade at early times, it was found that the total level of FAK must be higher than that of downstream effectors such as Sos, the activator of the MAPK cascade. For example, a peak magnitude of 1.4nM ERKPP at t=2800s requires the amount of total FAK to be nearly 22 times the amount of Sos. As a result, it is assumed that the amount of FAK is in excess of other signaling proteins in the system. Lastly, sustained FAK activation does not necessarily result in sustained ERK activation, implying that FAK serves as an initial stimulus for ERK activation, but the duration of ERK activation is also regulated by downstream factors that will be discussed.

3.2 FAK and ERK Activation in Response to Ligand Density

Fibronectin density is one of the most readily controllable experimental parameters in the system and has been shown to affect both the magnitude and kinetics of ERK activation [20]. As ligand density increases, the magnitude of the ERKPP peak also increases while the peak occurs faster. The effects of ligand density were successfully replicated *in silico* for similar fibronectin densities, assuming a high receptor density of 7.89×10^{10} molecules/cm^2 (~1.5×10^6/cell) (Figure 3a). Not surprisingly, changes in ligand density had substantial effects on ERKPP dynamics only when ligand density is non-saturating ($R_t > L_t$), thus requiring a high assumed receptor density. Furthermore, the linear correlation between the ligand density and initial rates of FAK and ERK activation observed by Asthagiri [20] was also seen in simulations (Figure 3b). At saturating ligand densities, the linear correlation fails.

3.3 Exploration of Signaling Dynamics

3.3.1 The relationship between FAK and ERK Activation

The effects of ligand density on ERK raise the question of how the signal is transduced downstream. Since FAK is a major mediator between adhesion-based signals and downstream signaling, it is reasonable to examine the effects of ligand density on FAK activation to

understand how such changes can affect ERK. Because FAK is in excess of ligand and receptor binding sites, the magnitude of FAKP is directly proportional to ligand density while the time required to reach maximal FAKP is unchanged. As shown in Figure 3a, increases in ligand density correspond to increases in ERKPP magnitude and decreases in the time to reach maximum. To determine whether such effects are specific to changes in the magnitude of FAKP, we considered the effects of changes in the time to reach maximal FAKP by changing the total amount of FAK. Increased levels of FAK drive the rate of its activation, resulting in increased kinetics without changing the magnitude of FAKP. Figure 4a shows that equivalent increases in ligand density and FAK decrease the time of the ERKPP peak similarly. Figure 4a also illustrates that ligand density has a more pronounced affect on ERKPP magnitude than does FAK. In order to better compare the effects of magnitude and kinetics directly, FAK activation dynamics are expressed as an initial rate of activation (Figure 4b). If the effects of FAKP magnitude and kinetics are equivalent, each initial rate calculated from either ligand density or total FAK changes should correspond to a unique change in ERK activation dynamics. However, the curves for ERKPP dynamics differ depending on ligand density or total FAK changes, indicating that the effects are parameter-specific. In fact, ligand density, via changes in the magnitude of FAKP, appears to be a stronger regulator of ERKPP dynamics than total FAK, which changes the kinetics of FAKP. Furthermore, the differing curves in response to ligand density and FAK imply that the initial rate of FAKP is not the sole determinant of ERKPP dynamics and that other factors affected by these two parameters are also playing a role. Moreover, FAK-independent pathways are not likely the source of these factors since their contributions to ERK activation are only on the order of 10^{-19}-10^{-18} M. Regardless of these factors, the relationship between ERKPP

and initial rate is non-linear and plateaus as the initial rate increases. Thus, the effects of Fn density and FAK will attenuate as these two factors reach saturation.

3.3.2 Ras and Raf as Regulators of ERK Activity

To better understand the behavior of the system, parameters that play a key role in regulating the dynamics of the ERK signal were identified by parameter variations. The duration of ERK activation is found to be particularly sensitive to the concentrations of Ras and Raf. Testing Raf concentrations over an order of magnitude from 10 nM to 100 nM produced ERKPP signals with a range of durations (Figure 5a). At or above a [Raf] of 100 nM, the ERKPP signal is a sharp peak at approximately 5 minutes, which falls off quickly by 30 minutes. As [Raf] is decreased, the ERKPP signal duration increases until a sustained signal is obtained at 10 nM. Between 20 nM and 60 nM, very small changes in Raf concentration can give rise to significant changes in signal duration. For example, a 25% concentration decrease from 40 nM to 30 nM results in a signal duration increase of nearly 45%. For high [Raf], the ERKPP signal is very similar to that obtained by Asthagiri [20]. Similarly, the duration of the ERKPP signal increases with increasing levels of Ras (Figure 5b). While the changes in ERKPP are not as sensitive to small changes in [Ras], large increases in [Ras] do yield significant prolongation of ERK activation.

The sensitivity of ERKPP to Raf and Ras originates at the locus of intersection between the RasGTP/GDP cycle and the MAPK cascade (Figure 1b), where RasGTP binds and activates Raf, forming Raf*. The fast drop off in signaling that forms the peak in ERKPP signals results from the depletion of RasGTP available for interaction with Raf. When RasGTP is depleted, no more Raf can be activated causing the Raf* and subsequently ERKPP signals to fall off, resulting in the formation of a peak. Therefore, as [Raf] increases, the velocity of the Raf-RasGTP binding

reaction also increases, thereby increasing the rate at which RasGTP is depleted. Similarly, Sydor [43] has shown that the Raf-Ras complex has an extremely short lifetime, after which Raf is released for downstream signaling. The resulting Ras species, denoted RasGTP*, is no longer capable of activating Raf and will undergo GTP hydrolysis catalyzed by GAPs, which are recruited to focal adhesions after integrin-ligand binding [44, 45]. In the case of high [Raf], Ras accumulates as RasGTP*, suggesting that the Raf-RasGTP reaction is much faster than the action of GAPs in recycling Ras. Thus, nearly 80% of Ras accumulates in the GTP* form and is not recycled fast enough to the RasGTP form to prevent depletion. As [Raf] is reduced, the rate of RasGTP conversion to RasGTP* is more comparable to the rate of recycling to RasGTP. Depletion of RasGTP is delayed and an increasingly sustained ERKPP signal is obtained. An increase in [Ras], conversely, increases the amount of RasGTP available, prolonging the ERKPP signal.

3.4 Sensitivity Analysis

3.4.1 Morris Screening

To systematically identify key parameters involved in ERK signaling, the Morris screening method [21] was applied to the model. The Morris method allows for the effects of a particular parameter variation to be seen in the context of different values for every other parameter, as opposed to fixing all other parameters. The result of the model is a measure of the effect each parameter has on the output signal. For the dynamics of ERK activation, the effect of each parameter on the overall ERK time course as measured by the norm of the change in output, time to reach maximum, peak magnitude, and 3 specific time points were calculated. These values were normalized by the relative change in input values. However, because parameters were sampled over a log uniform distribution, the fractional change remains constant between

parameters. Morris runs were performed until at least the top 20% of parameters converged (n = 160).

The main parameters involved in regulating ERK activation are rate constants associated with the MAPK cascade. However, of the factors that could be readily manipulated experimentally, Ras and Raf fall within the top 15% of key parameters for several measures of ERK dynamics, confirming the effects on ERKPP signal duration described above (Table 1). Out of 106 parameters, Ras ranked second in importance for the time of the ERKPP peak, 16th based on overall time course and 29th based on a late time point that indicates signal duration. Similarly, Raf ranks 4th in determining the time of the ERKPP peak and 7th in early activation. Both Ras and Raf also fall within the top 20% of parameters affecting the magnitude of ERK activation, ranking 18th and 19th respectively. Interestingly, RasGAP ranks first out of all parameters for the time of the ERK activation peak, again highlighting the importance of the RasGDP/GTP cycle in regulating ERK activation dynamics. Receptor density also falls within the top 15% of key parameters affecting the ERKPP signal. Moreover, integrin density and contact area, which determines the total amount of fibronectin available, are ranked 7th and 5th respectively as regulators of the kinetics of ERK activation. FAK is also identified as a key parameter in ERK activation kinetics, supporting the idea that initial FAK signaling contributes significantly to the activation of ERK. Integrin density, and not fibronectin density, was likely identified in the Morris screening because of the relative values the two parameters used. Depending on the values of receptor and ligand density, the rate limiting density will be identified as the more important parameter. As a result, the importance of integrin density also points to the importance of fibronectin density in modulating the magnitude and kinetics of ERKPP.

3.4.2 One-at-a-time Parameter Variation

In order to gauge the robustness of the model to changes in parameters, one-at-a-time parameter variations were performed while holding every other parameter fixed at their assumed values. Parameters were varied over 3 orders of magnitude above and below their assumed values and the range over which the conclusions drawn in the results section held qualitatively was determined (Figure 6). The model is found to be robust and tolerant of significant changes in many parameters. Parameters 24 to 64 and 85 to 105 refer to reactions involved in Src activation, Shc phosphorylation, and recruitment of both Grb2 and Sos. Even many of the MAP kinase cascade reaction rates, including some that were identified as key regulators by Morris screening (ex. 81, 79, 74, 83, 82, etc), do not limit the qualitative conclusions drawn from the model.

4 Discussion

This model for the integrin activation of ERK successfully replicated experimentally observed behavior for FAK and ERK activation, as well as changes in ERK activation in response to fibronectin density. Application of the Morris method to the model allowed the identification of key parameters contributing to ERKPP dynamics. Thus, the model serves as a tool for understanding and identifying characteristics of the pathway that contribute to different ERKPP behavior. The insights gained by such models are important steps to ultimately controlling signaling pathways in vivo.

The ability of the model to replicate experimentally measured time courses for FAK and ERK in response to adhesion on fibronectin is an important foundation for understanding the adhesion specific parameters that might contribute to ERK activation. The appearance of an early peak for ERKPP is not surprising as long as there is an excess of FAK, which serves as an early stimulus for ERKPP. Factors affecting FAKP magnitude, such as fibronectin density, are found to be stronger regulators of ERKPP dynamics that those affecting only FAKP kinetics. However,

the effects of ligand density are not solely dependent on the initial rate of FAK activation, but are likely transduced downstream by additional pathways. While additional western blot time courses have been published, we chose a semi-quantitative time course for the purposes of comparing to simulated results. Deviations between the experimental data used here and other available data may be due to a myriad of differences including cell type and experimental procedure.

The simplified integrin clustering model used is shown to be sufficient for predicting the effects of ligand density on ERK activation. The model based on dimerization predicts that increases in ligand density will increase the magnitude of FAK activation, which has been shown by Garcia and Boettiger [46]. Changes in the magnitude of FAK activation are then translated into changes in the kinetics and magnitude of ERK activation. While k_p and k_m may alter the time at which FAK activation reaches its maximum, the ultimate magnitude, as specified by ligand density will not be affected. Changes in k_1 may also affect the magnitude of FAK activation, but the relative changes that result from ligand density variations will remain the same. More generally, the magnitude of FAK activation increases with ligand density regardless of the assumed value of k_1 or k_p and k_m. As a result, changes in downstream signaling that originate with ligand density will also remain the same qualitatively. Future work should include a more detailed model of the integrin clustering process so that the roles of additional parameters involved in clustering can be tested.

Raf and Ras were identified as key regulators of ERK signaling magnitude and duration, in agreement with the control analysis performed by Hornberg [19]. Furthermore, the behavior of proteins involved in RasGDP/GTP cycling reveal that Raf and Ras may function as a key checkpoint in the MAPK cascade because of the relative kinetics of RasGDP/GTP cycling and

Ras-Raf binding, which allow for the formation of transient and sustained ERKPP signals. However, the main effects of the Raf oncogene may not be mediated by this particular characteristic of the signaling pathway, as was suggested by Hornberg. Increases in [Raf] result in increasing magnitudes of ERK activation, but increasingly transient activation signals. For cell cycle progression and uncontrolled growth, one would expect that increasingly the levels of oncogenic Raf would instead lead to sustained signaling. On the other hand, this model shows that increases in the level of the oncogene Ras result in more sustained ERK signals, though larger changes in the Ras concentration are required. This is consistent with the role of Ras as an oncogene that promotes tumorigenic behavior. Moreover, the behavior of the Raf/Ras checkpoint suggests that mutations in Ras that affect the GDP/GTP cycling, such as its affinity for GAPs or GTPases may be a mechanisms for modulating cell behavior. Therefore, the oncogenic effects of Raf may be mediated mainly by changes in the magnitude of ERK activation, whereas the effects of Ras are more likely to involve changes in signal duration.

This is consistent with Roovers' and Assoian's [5] suggestion that cell cycle progression requires a large transient ERK activation that will induce p21cip expression in the early G1 phase followed by a sustained mid-level activation that promotes cyclin D1 expression and stops the induction of p21cip by late G1 phase. It has also been shown that p21cip is induced by high levels of Raf [47, 48]. Our results would suggest that an ideal combination of Raf and Ras levels could create cell growth promoting ERK activities. To determine these levels, Raf and Ras concentrations were varied and their effects on the magnitude and duration of ERK activation were observed (Figure 7). While the concentrations plotted are model-specific, the trends hold regardless of parameter values. Increasing Ras concentration promotes transition of ERK activity from transient to sustained behavior. Here, transient and sustained behavior refer to initial ERK

activation that falls to less than a 1/3 and between 1/3 and 2/3 of initial activation respectively. At low [Raf], a plateau in ERK activation may form into addition to transient and sustained behavior for certain [Ras]. Also, the magnitude of ERK activity is found to significantly decrease with [Raf] so that cell cycle progression might be inhibited regardless of the signal duration. When both Raf and Ras concentrations are high, ERK activation exhibited a large magnitude initial peak that fell off to sustained mid-level activation. This behavior is consistent with cell cycle progression. This may correspond to cells in which both Raf and Ras oncogenes are over-expressed or contain activating mutations. Thus, both Raf and Ras may act together to promote cell growth. Raf contributes to the magnitude of the signal, bringing the initial transient activation of ERK to levels that allow for induction of p21cip, while Ras primarily extends the duration of ERK, sustaining mid-level activation for long times. .

It has been suggested that the peak in ERK activation arises from negative feedback, which turns off the ERK activation signal [49-51]. Feedback, either positive or negative, has not been included in this system. While negative feedback may occur, we have shown that the Raf/Ras checkpoint can also play a role in regulating signal duration, particularly in controlling the fall off of the ERK activation signal. In fact, for certain Raf and Ras concentrations, the transient activity of ERK decreases rapidly, but does not approach zero, instead remaining at some lower level of ERK activation. In such cases, a negative feedback might be an important mechanism for shutting down the remaining ERK activity.

Src and Shc represent parallel pathways by which the MAPK cascade can be activated by FAK. As the model is run now, the Shc pathway dominates signaling to ERK. While it is possible for Src to be the main contributor to ERK activation, that assumption is not explored in detail in this paper. However, the overall effects seen in this paper were confirmed in a pathway

in which the levels of Shc are significantly reduced so as to allow the Src pathway to dominate [data not shown].

Though our model is robust and sufficient for predicting ERK activation by adhesion, a complete model of ERK activation should take into account the contributions of both growth factors and adhesion. Crosstalk between growth factor and adhesion signaling are vital for producing high magnitude, sustained ERK activation. In this paper, a model for adhesion-based activation is presented. Future work will involve the addition of the growth-factor mediated pathway. Coupled with the detailed model of clustering described above, the model not only complements experimental systems in which signaling in adhesive, growth factor stimulated cells is measured, but is also a means for exploring the cross-talk between growth factors and receptors.

Acknowledgments

This work was supported by a grant from Department of Defense W81XWH-05-1-330 to D. Hammer and V.M. Weaver.

1. Hanahan D and Weinberg RA. The hallmarks of cancer. Cell 2000; 100(1):57-70.

2. Aplin AE and Juliano RL. Regulation of nucleocytoplasmic trafficking by cell adhesion receptors and the cytoskeleton. J Cell Biol 2001; 155(2):187-91. Epub 2001 Oct 15.

3. Shaulian E and Karin M. AP-1 in cell proliferation and survival. Oncogene 2001; 20(19):2390-400.

4. Marshall C. How do small GTPase signal transduction pathways regulate cell cycle entry? Current Opinion in Cell Biology 1999; 11(6):732-736.

5. Roovers K and Assoian RK. Integrating the MAP kinase signal into the G1 phase cell cycle machinery. Bioessays 2000; 22(9):818-26.

6. Danen EH and Yamada KM. Fibronectin, integrins, and growth control. J Cell Physiol 2001; 189(1):1-13.

7. Renshaw MW, Ren XD, Schwartz MA. Growth factor activation of MAP kinase requires cell adhesion. Embo J 1997; 16(18):5592-9.

8. Giancotti FG and Ruoslahti E. Integrin signaling. Science 1999; 285(5430):1028-32.

9. Barberis L, Wary KK, Fiucci G, Liu F, Hirsch E, Brancaccio M, et al. Distinct roles of the adaptor protein Shc and focal adhesion kinase in integrin signaling to ERK. Journal of Biological Chemistry 2000; 275(47):36532-36540.

10. Schlaepfer DD and Hunter T. Integrin signalling and tyrosine phosphorylation: just the FAKs? Trends Cell Biol 1998; 8(4):151-7.

11. Wary KK, Mainiero F, Isakoff SJ, Marcantonio EE, Giancotti FG. The adaptor protein Shc couples a class of integrins to the control of cell cycle progression. Cell 1996; 87(4):733-43.

12. Assoian RK and Schwartz MA. Coordinate signaling by integrins and receptor tyrosine kinases in the regulation of G1 phase cell-cycle progression. Current Opinion in Genetics & Development 2001; 11(1):48-53.

13. Giancotti FG. Integrin signaling: specificity and control of cell survival and cell cycle progression. Current Opinion in Cell Biology 1997; 9(5):691-700.

14. Schwartz MA and Ginsberg MH. Networks and crosstalk: integrin signalling spreads. Nature Cell Biology 2002; 4(4).

15. Roovers K, Davey G, Zhu X, Bottazzi ME, Assoian RK. Alpha5beta1 integrin controls cyclin D1 expression by sustaining mitogen-activated protein kinase activity in growth factor-treated cells. Mol Biol Cell 1999; 10(10):3197-204.

16. Kholodenko BN, Demin OV, Moehren G, Hoek JB. Quantification of short term signaling by the epidermal growth factor receptor. J Biol Chem 1999; 274(42):30169-81.

17. Schoeberl B, Eichler-Jonsson C, Gilles ED, Muller G. Computational modeling of the dynamics of the MAP kinase cascade activated by surface and internalized EGF receptors. Nat Biotechnol 2002; 20(4):370-5.

18. Chapman S and Asthagiri AR. Resistance to signal activation governs design features of the MAP kinase signaling module. Biotechnol Bioeng 2004; 85(3):311-22.

19. Hornberg JJ, Binder B, Bruggeman FJ, Schoeberl B, Heinrich R, Westerhoff HV. Control of MAPK signalling: from complexity to what really matters. Oncogene 2005; 24(36):5533-5542.

20. Asthagiri AR, Nelson CM, Horwitz AF, Lauffenburger DA. Quantitative relationship among integrin-ligand binding, adhesion, and signaling via focal adhesion kinase and extracellular signal-regulated kinase 2. Journal of Biological Chemistry 1999; 274(38):27119-27.

21. Morris MD. Factorial Sampling Plans For Preliminary Computational Experiments. Technometrics 1991; 33(2):161-174.

22. Giannone G, Dubin-Thaler BJ, Dobereiner HG, Kieffer N, Bresnick AR, Sheetz MP. Periodic lamellipodial contractions correlate with rearward actin waves. Cell 2004; 116(3):431-43.

23. Bell GI. Models for the specific adhesion of cells to cells. Science 1978; 200(4342):618-27.

24. Parsons JT. Focal adhesion kinase: the first ten years. J Cell Sci 2003; 116(8):1409-1416.

25. Aplin AE, Howe A, Alahari SK, Juliano RL. Signal transduction and signal modulation by cell adhesion receptors: the role of integrins, cadherins, immunoglobulin-cell adhesion molecules, and selectins. Pharmacol Rev 1998; 50(2):197-263.

26. Kaplan KB, Bibbins KB, Swedlow JR, Arnaud M, Morgan DO, Varmus HE. Association of the Amino-Terminal Half of C-Src with Focal Adhesions Alters Their Properties and Is Regulated by Phosphorylation of Tyrosine-527. Embo Journal 1994; 13(20):4745-4756.

27. Bjorge JD, Jakymiw A, Fujita DJ. Selected glimpses into the activation and function of Src kinase. Oncogene 2000; 19(49):5620-35.

28. Boerner RJ, Kassel DB, Barker SC, Ellis B, DeLacy P, Knight WB. Correlation of the phosphorylation states of pp60c-src with tyrosine kinase activity: the intramolecular pY530-SH2 complex retains significant activity if Y419 is phosphorylated. Biochemistry 1996; 35(29):9519-25.

29. Cole P, Burn P, Takacs B, Walsh C. Evaluation of the catalytic mechanism of recombinant human Csk (C- terminal Src kinase) using nucleotide analogs and viscosity effects. J. Biol. Chem. 1994; 269(49):30880-30887.

30. Schlaepfer DD and Hunter T. Focal adhesion kinase overexpression enhances ras-dependent integrin signaling to ERK2/mitogen-activated protein kinase through interactions with and activation of c-Src. J Biol Chem 1997; 272(20):13189-95.

31. Schlaepfer DD, Jones KC, Hunter T. Multiple Grb2-mediated integrin-stimulated signaling pathways to ERK2/mitogen-activated protein kinase: summation of both c-Src- and focal adhesion kinase-initiated tyrosine phosphorylation events. Mol Cell Biol 1998; 18(5):2571-85.

32. Downward J. The GRB2/Sem-5 adaptor protein. FEBS Lett 1994; 338(2):113-7.

33. Howe AK and Juliano RL. Distinct mechanisms mediate the initial and sustained phases of integrin-mediated activation of the Raf/MEK/mitogen-activated protein kinase cascade. J Biol Chem 1998; 273(42):27268-74.

34. Wary KK, Mariotti A, Zurzolo C, Giancotti FG. A requirement for caveolin-1 and associated kinase Fyn in integrin signaling and anchorage-dependent cell growth. Cell 1998; 94(5):625-34.

35. Ladbury JE, Lemmon MA, Zhou M, Green J, Botfield MC, Schlessinger J. Measurement of the binding of tyrosyl phosphopeptides to SH2 domains: a reappraisal. Proc Natl Acad Sci U S A 1995; 92(8):3199-203.

36. Payne G, Shoelson SE, Gish GD, Pawson T, Walsh CT. Kinetics of p56lck and p60src Src homology 2 domain binding to tyrosine-phosphorylated peptides determined by a competition assay or surface plasmon resonance. Proc Natl Acad Sci U S A 1993; 90(11):4902-6.

37. Kaneko T, Kumasaka T, Ganbe T, Sato T, Miyazawa K, Kitamura N, et al. Structural insight into modest binding of a non-PXXP ligand to the signal transducing adaptor molecule-2 Src homology 3 domain. J Biol Chem 2003; 278(48):48162-8. Epub 2003 Sep 16.

38. Matsuda M, Ota S, Tanimura R, Nakamura H, Matuoka K, Takenawa T, et al. Interaction between the Amino-terminal SH3 Domain of CRK and Its Natural Target Proteins. J. Biol. Chem. 1996; 271(24):14468-14472.

39. Fincham VJ, Unlu M, Brunton VG, Pitts JD, Wyke JA, Frame MC. Translocation of Src kinase to the cell periphery is mediated by the actin cytoskeleton under the control of the Rho family of small G proteins. Journal of Cell Biology 1996; 135(6 Pt 1):1551-64.

40. Wang D, Esselman WJ, Cole PA. Substrate Conformational Restriction and CD45-catalyzed Dephosphorylation of Tail Tyrosine-phosphorylated Src Protein. J. Biol. Chem. 2002; 277(43):40428-40433.

41. Wang J and Walsh CT. Mechanistic studies on full length and the catalytic domain of the tandem SH2 domain-containing protein tyrosine phosphatase: analysis of phosphoenzyme levels and Vmax stimulatory effects of glycerol and of a phosphotyrosyl peptide ligand. Biochemistry 1997; 36(10):2993-9.

42. Zhang Z. Kinetic and mechanistic characterization of a mammalian protein- tyrosine phosphatase, PTP1. J. Biol. Chem. 1995; 270(19):11199-11204.

43. Sydor JR, Engelhard M, Wittinghofer A, Goody RS, Herrmann C. Transient Kinetic Studies on the Interaction of Ras and the Ras-Binding Domain of c-Raf-1 Reveal Rapid Equilibration of the Complex. Biochemistry 1998; 37(40):14292-14299.

44. Hecker TP, Ding Q, Rege TA, Hanks SK, Gladson CL. Overexpression of FAK promotes Ras activity through the formation of a FAK/p120RasGAP complex in malignant astrocytoma cells. Oncogene 2004; 23(22):3962-3971.

45. Sharma SV. Rapid recruitment of p120RasGAP and its associated protein, p190RhoGAP, to the cytoskeleton during integrin mediated cell-substrate interaction. Oncogene 1998; 17(3):271-281.

46. Garcia AJ and Boettiger D. Integrin-fibronectin interactions at the cell-material interface: initial integrin binding and signaling. Biomaterials 1999; 20(23-24):2427-2433.

47. Sewing A, Wiseman B, Lloyd AC, Land H. High-intensity Raf signal causes cell cycle arrest mediated by p21Cip1. Mol. Cell. Biol. 1997; 17(9):5588-5597.

48. Woods D, Parry D, Cherwinski H, Bosch E, Lees E, McMahon M. Raf-induced proliferation or cell cycle arrest is determined by the level of Raf activity with arrest mediated by p21Cip1. Mol. Cell. Biol. 1997; 17(9):5598-5611.

49. Dougherty MK, Muller J, Ritt DA, Zhou M, Zhou XZ, Copeland TD, et al. Regulation of raf-1 by direct feedback phosphorylation. Molecular Cell 2005; 17(2):215-224.

50. Sundberg-Smith LJ, Doherty JT, Mack CP, Taylor JM. Adhesion stimulates direct PAK1/ERK2 association and leads to ERK-dependent PAK1 Thr(212) phosphorylation. Journal Of Biological Chemistry 2005; 280(3):2055-2064.

51. Brummer T, Naegele H, Reth M, Misawa Y. Identification of novel ERK-mediated feedback phosphorylation sites at the C-terminus of B-Raf. Oncogene 2003; 22(55):8823-8834.

<Separate Section>

Supplementary Materials

General rate equations

A differential equation for the rate of concentration change of each protein species present in the system was written using rates of species formation and reaction. The full list of equations and rate constants in the model is contained in the Supplemental Materials.

Cell-Surface Contact Area during Spreading

The increase in contact area over time during cell spreading was modeled based on experimental data from Giannone (1). The experimental data was fit using an equation for area as a function of time:

(1) $$A(t) = A_{\max} e^{-t/85}\left[-1 + e^{t/85} - \frac{t}{85} - \frac{t^2}{14450} - \frac{t^3}{3684750}\right],$$

where A_{max}, the maximum cell-surface contact area is equal to 1.9×10^{-5} cm^2.

Integrin-Fibronectin Binding

For integrin-fibronectin binding, the Bell model (2) that describes binding between ligand and receptors diffusing in the plane of the membrane was used. In this model, however, the ligand was assumed to be immobile because surface adsorbed fibronectin is not free to diffuse. After integrin-fibronectin binding, the model for integrin clustering assumes that receptor ligand pairs (RL) dimerize and subsequently recruit FAK to the RL dimer. Because there is little quantitative data on FAK's response after integrin-ligand binding, FAK recruitment and phosphorylation are modeled with one reaction governed by forward and reverse rates that are fit

to experimental time courses of FAK activation. This process was modeled with the following set of equations,

(2) $$R + L \longleftrightarrow RL$$

(3) $$RL + RL \longleftrightarrow RL - RL$$

(4) $$RL - RL + FAK \longleftrightarrow RL - RL - FAKP$$
$$RL - RL - FAKP + FAK \leftrightarrow FAKP - RL - RL - FAKP$$

where Eq 2 has forward and reverse rate constants of k_f and k_r, Eq 3 has a forward rate constant of k_1, and Eq 4 has forward and reverse rate constants k_p and k_m. The receptor-ligand binding rate constants k_f and k_r were obtained from Takagi (3) and converted from three- dimensional to two dimensional rate constants for the case of immobilized ligand and membrane-diffusive receptors. The method for this conversion is described by English and Hammer (4). Fibronectin was assumed to have a negligible diffusion constant compared to integrins. The diffusion constant for membrane-bound integrins was assumed to be 10^{-10} cm^2/s. The diffusion constant for integrins in solution was estimated from the Stokes-Einstein equation, assuming a radius of 5nm and cytoplasmic viscosity. The encounter distance was assumed to be .75 nm.

Modeling Src Activation

The steps that bridge extracellular stimulation with the initial de-phosphorylation of Src at tyrosine 527 have not yet been elucidated, but involve some signaling mechanism that activates a phosphatase, in this model SHP, and causes it to de-phosphorylate it. Because these steps are still largely unknown, SHP activation was assumed to be proportional to FAK activation. The proportionality constant was set so that SHP concentration was 3.5 times the magnitude of FAK activation in order to make the maximum SHP concentration comparable to that for the other phosphatases and kinases involved in the Src activation reactions.

Decomposition of Src-FAKP Binding

To estimate the kinetics of the Src-FAKP binding, the enzymatic reaction was broken down into binding and catalytic steps:

$$(4)\ Src + FAKP \leftrightarrow Src - FAKP \rightarrow Src - FAKP - P$$

k_1 and k_2 are the forward and reverse binding constants respectively and k_{cat} is the catalytic rate constant. k_1 was calculated from published Michaelis-Menten data (5) using the equation

$$(4)\ K_m = \frac{k_2 + k_{cat}}{k_1}$$

assuming that k_2 is $1 \times 10^{-2}\ s^{-1}$.

1. Giannone G, Dubin-Thaler BJ, Dobereiner HG, Kieffer N, Bresnick AR, Sheetz MP. Periodic lamellipodial contractions correlate with rearward actin waves. Cell 2004;116(3):431-43.
2. Bell GI. Models for the specific adhesion of cells to cells. Science 1978;200(4342):618-27.
3. Takagi J, Strokovich K, Springer TA, Walz T. Structure of integrin alpha5beta1 in complex with fibronectin. Embo J 2003;22(18):4607-15.
4. English TJ, Hammer DA. Brownian adhesive dynamics (BRAD) for simulating the receptor-mediated binding of viruses. Biophys J 2004;86(6):3359-72.
5. Boerner RJ, Kassel DB, Barker SC, Ellis B, DeLacy P, Knight WB. Correlation of the phosphorylation states of pp60c-src with tyrosine kinase activity: the intramolecular pY530-SH2 complex retains significant activity if Y419 is phosphorylated. Biochemistry 1996;35(29):9519-25.

Supplementary Material Spreadsheet

Table 1 List of differential equations for model.

Table 2 Model parameters.

Figure Legends

Figure 1 (a) Signaling pathways for ERK Activation by Adhesion. (b) Ras cycle of GDP/GTP Binding.

Figure 2 FAK and ERK activation over a range of k_p, assuming that $K_d=k_m/k_p=1066$ is constant. Experimentally observed time courses (Asthagiri) are also plotted.

Figure 3 (a) ERK Activation in response to changes in fibronectin density. (b) Initial rates of FAK and ERK activation with ligand density. Initial rates were calculated from 470-480s, which falls within the linear phase of activation. The onset of the linear phase is subject to a time lag due to the clustering process.

Figure 4 (a) Fold changes in ERK activation dynamics as a function of fold changes in ligand density and total FAK. All fold changes are normalized to the starting values ($53/um^2$ and $2x10^6$ respectively). (b) Fold changes in ERK activation dynamics as function of the initial rate of FAK activation. Initial rates in response to changes in ligand density and total FAK were calculated based on the dynamics of FAK activation from t=470-480s, where the signal is linear.

Figure 5 (a) ERK activation in response to [Raf]. [Ras] is assumed to be 1.072×10^{-5} M. (b). ERK activation in response to [Ras]. Raf is assumed to be 3.76×10^{-7} M.

Figure 6 Parameter ranges over which qualitative results hold. Parameters were varied one at a time over 6 orders of magnitude while holding all other fixed. Changes in parameter are expressed as $\log_{10}$ of the fold change. The parameters that correspond to each parameter number along the x-axis are listed in the Supplementary Materials.

Figure 7 Effects of Raf and Ras concentrations on ERK activity. Concentrations of Ras and Raf are expressed as multiples of the minimum plotted values (5×10^{-7} M and 1×10^{-8} M respectively). The magnitude of ERK, expressed as a percentage of the maximal ERK activation, is also plotted for different values of Raf (■). The shaded regions represent an initial transient activation followed by sustained mid level signaling at 33-66% of maximum (red "sustained"), sustained high level signaling at 66-100% of maximum (green "plateau), a decrease to less than 33% of maximal signal within 6 hours (blue "transient"), or a decrease to less than 33% of maximum between 6 and 12 hours (yellow "transition").

Table 1. Experimentally controllable parameters identified by Morris screening within the top 85th percentile of parameters important for ERK activation. Each parameter's rank out of the total 106 parameters is included in parentheses. PP1, PP2, and PP3 refer to phosphatases for Raf, MEK, and ERK respectively. CA denotes contact area.

Figure 1

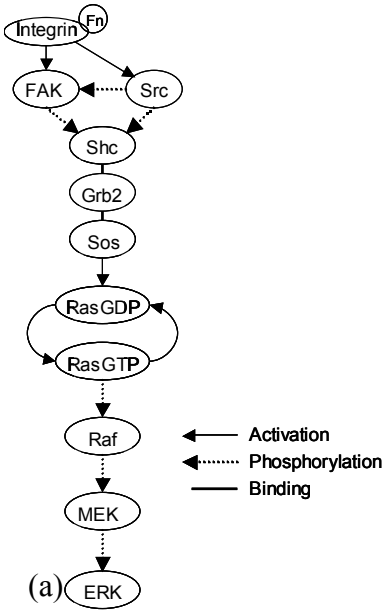
Integrin
Fn
FAK
Src
Shc
Grb2
Sos
RasGDP
RasGTP
Raf
MEK
ERK
Activation
Phosphorylation
Binding

(a)

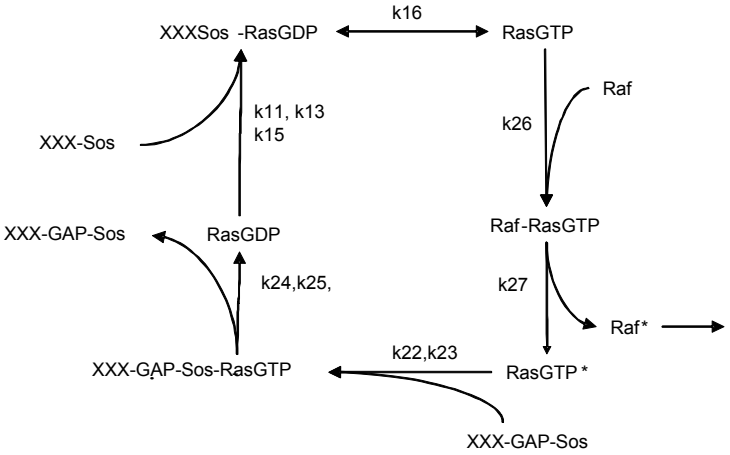
XXXSos -RasGDP
k16
RasGTP
Raf
k26
XXX-Sos
k11, k13
k15
XXX-GAP-Sos
RasGDP
Raf-RasGTP
k24,k25,
k27
Raf*
k22,k23
XXX-GAP-Sos-RasGTP
RasGTP*
XXX-GAP-Sos

(b)

Figure 2

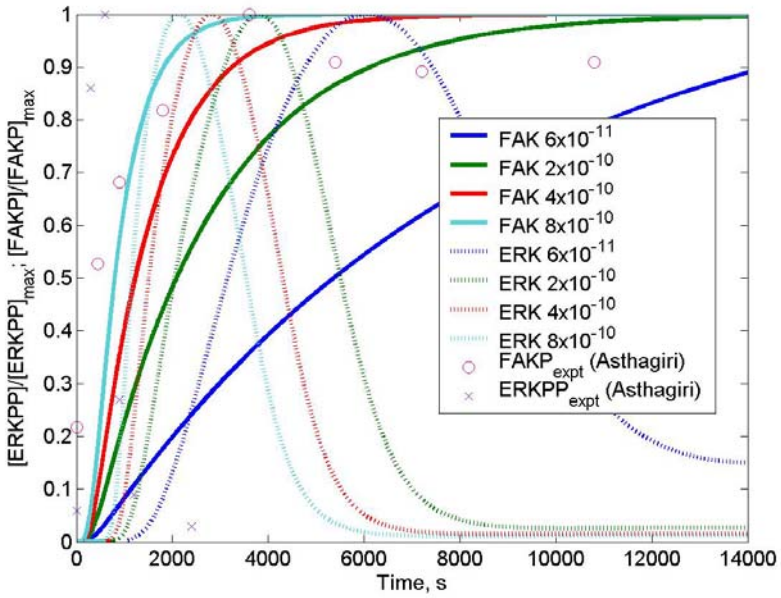
[ERKPP]/[ERKPP]max; [FAKP]/[FAKP]max
Time, s
FAK 6x10-11
FAK 2x10-10
FAK 4x10-10
FAK 8x10-10
ERK 6x10-11
ERK 2x10-10
ERK 4x10-10
ERK 8x10-10
FAKPexpt (Asthagiri)
ERKPPexpt (Asthagiri)

Figure 3

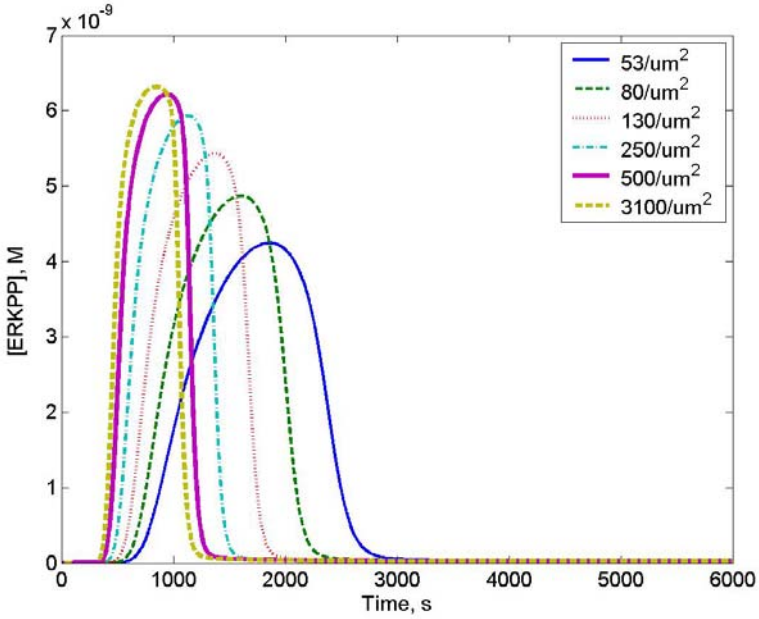
x 10^-9
7
6
5
4
3
2
1
0
[ERKPP], M
0
1000
2000
3000
4000
5000
6000
Time, s
53/um^2
80/um^2
130/um^2
250/um^2
500/um^2
3100/um^2

(a)

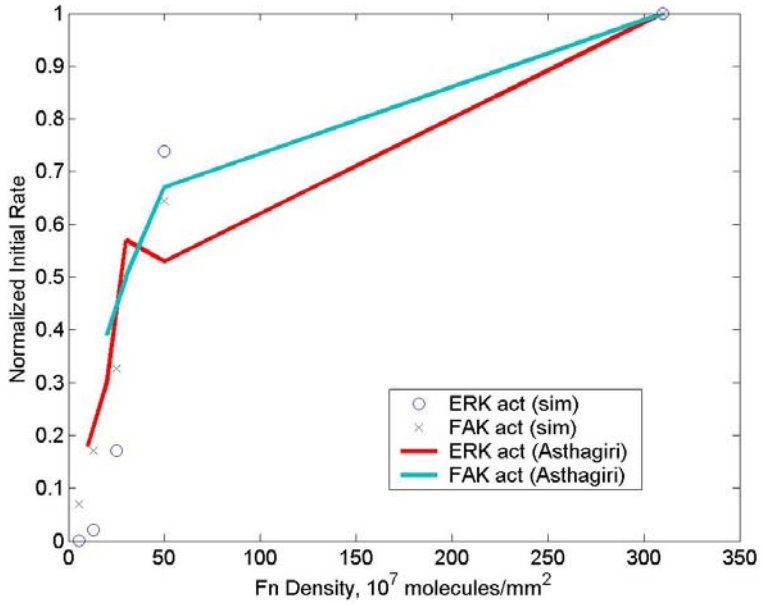
Normalized Initial Rate
Fn Density, 10^7 molecules/mm^2
ERK act (sim)
FAK act (sim)
ERK act (Asthagiri)
FAK act (Asthagiri)

(b)

Figure 4

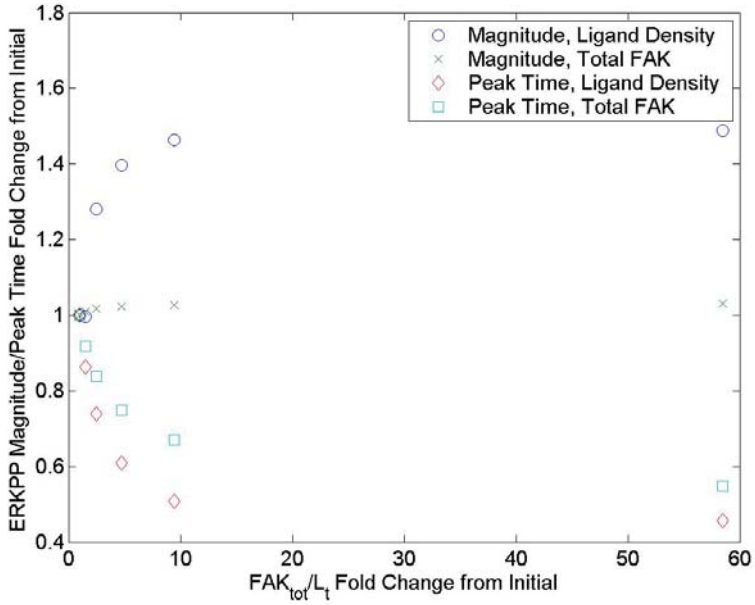
ERKPP Magnitude/Peak Time Fold Change from Initial
FAK_{tot}/L_t Fold Change from Initial
Magnitude, Ligand Density
Magnitude, Total FAK
Peak Time, Ligand Density
Peak Time, Total FAK

(a)

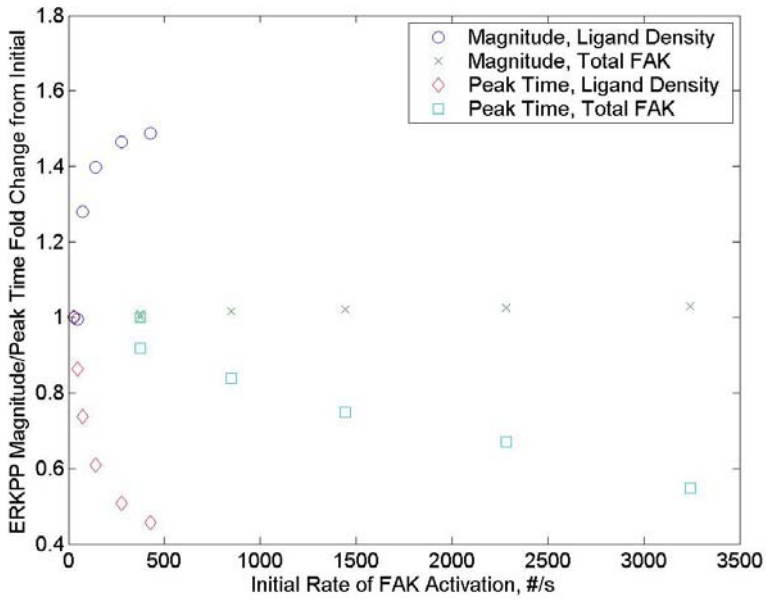
Magnitude, Ligand Density
Magnitude, Total FAK
Peak Time, Ligand Density
Peak Time, Total FAK
ERKPP Magnitude/Peak Time Fold Change from Initial
Initial Rate of FAK Activation, #/s
1.8
1.6
1.4
1.2
1
0.8
0.6
0.4
0
500
1000
1500
2000
2500
3000
3500

(b)

Figure 5

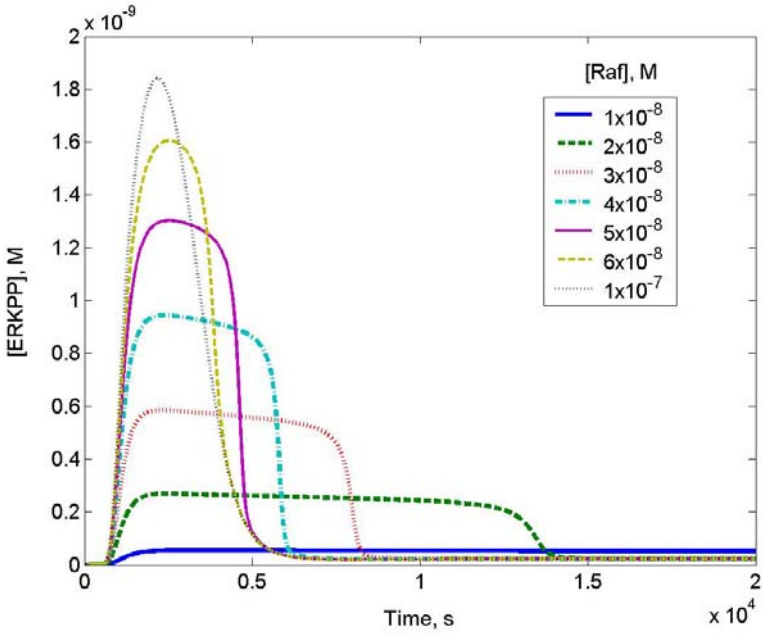
x 10^-9
[Raf], M
1x10^-8
2x10^-8
3x10^-8
4x10^-8
5x10^-8
6x10^-8
1x10^-7
[ERKPP], M
Time, s
x 10^4
2
1.8
1.6
1.4
1.2
1
0.8
0.6
0.4
0.2
0
0.5
1
1.5

(a)

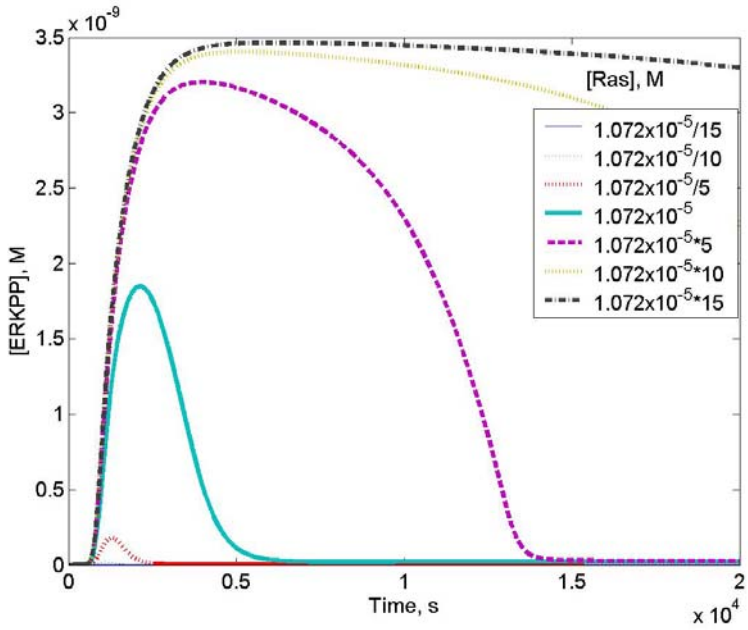
x 10^-9
3.5
3
2.5
2
1.5
1
0.5
0
[ERKPP], M
0
0.5
1
1.5
2
Time, s
x 10^4
[Ras], M
1.072x10^-5/15
1.072x10^-5/10
1.072x10^-5/5
1.072x10^-5
1.072x10^-5*5
1.072x10^-5*10
1.072x10^-5*15

(b)

Figure 6

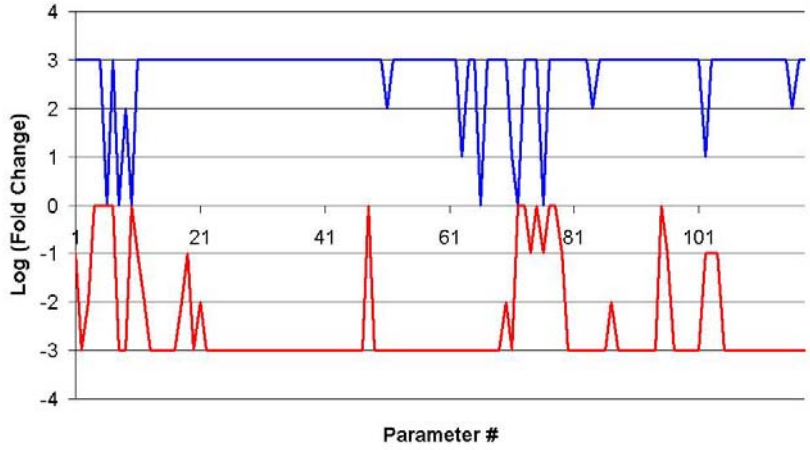
4
3
2
1
0
-1
-2
-3
-4
Log (Fold Change)
1
21
41
61
81
101
Parameter #

Figure 7

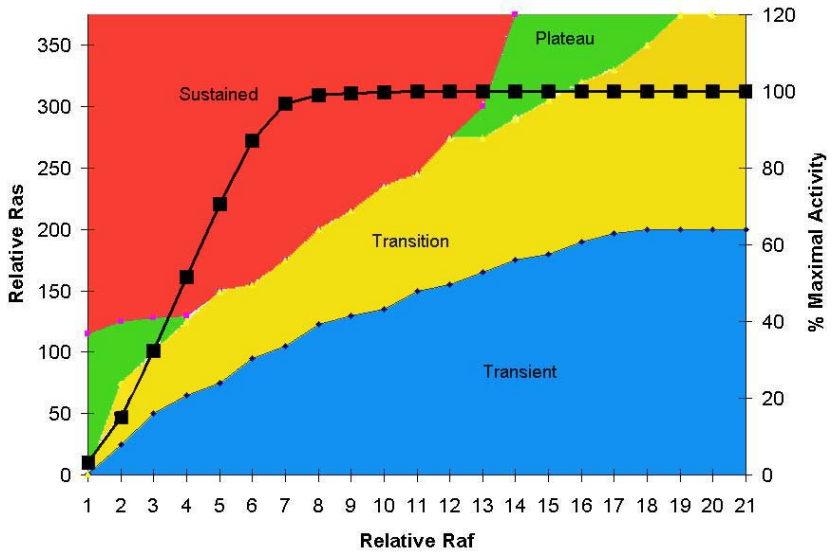
Plateau
Sustained
Transition
Transient
Relative Ras
% Maximal Activity
Relative Raf
0
50
100
150
200
250
300
350
0
20
40
60
80
100
120
1 2 3 4 5 6 7 8 9 10 11 12 13 14 15 16 17 18 19 20 21

Table 1

ERKPP Behavior	Experimentally Controllable Parameters within 85th Percentile
Overall Time Course	PP3 (2), ERK (3), PP2 (7), MEK (8), PP1 (9), Raf (12), Rt (15), Ras (16)
Time to max	RasGAP (1), Ras (2), MEK (3), Raf (4), CA (5), PP2 (6), Rt (7), FAK (11), Grb2 (16)
t1=1500s	PP3 (2), ERK (3), PP2 (5), Raf (7), PP1 (9), Grb2 (11), MEK (14)
t2=4000s	PP3 (2), ERK (3), PP2 (5), MEK (8), Ras (10), Rt (11), PP1 (13)
t3=15000s	ERK (2), PP3 (4), MEK(6), PP2 (7), PP1 (10)
Maximum Value	PP3(2), ERK (3), PP2 (6), PP1 (8), Grb2 (10), MEK (11), Rt (12)

Revised Version

Review article The International Journal of Biochemistry and Cell Biology/ Cells in Focus

Title: **Extracellular matrix composition and organization regulate mammary tissue development and tumorigenesis**

Authors: Laura Kass[1], Janine T. Erler[2], Micah Dembo[3], Valerie M. Weaver[1,4,5]

Affiliation: [1] Department of Surgery, University of California, San Francisco, San Francisco, CA 94143, USA; 2 Department of Radiation Oncology, Stanford University School of Medicine, Stanford, CA 94305, USA; [3]Department of Biomedical Engineering, Boston University; Boston, MA 02215; [4]Center for Bioengineering and Tissue Regeneration, Departments of Surgery & Anatomy, University of California, San Francisco, San Francisco, CA 94143, USA

[5]Corresponding Author: Dr. Valerie M. Weaver
Department of Surgery
University of California, San Francisco
513 Parnassus Ave, Rm. S1364C, Box 0456
San Francisco, CA 94143, USA
Tel: +1 415 476-3826
Fax: +1 415 476-3985
E-mail: WeaverV@surgery.ucsf.edu

Key words: mammary epithelial cells, extracellular matrix, matrix stiffness, integrins

Abbreviations: ECM: extracellular matrix, MMP(s): metalloproteinase(s), EGFR: epidermal growth factor receptor, ERα: estrogen receptor alpha, PRL: prolactin, BM: basement membrane, MEC: mammary epithelial cell, 2D or 3D: two- or three-dimensions, TIMPs: tissue inhibitors of metalloproteinase(s), Stat5: signal transducers and activators of transcription protein 5, LOX: lysyl oxidase.

Abstract

Stromal-epithelial interactions regulate mammary gland development and are critical for the maintenance of tissue homeostasis. The extracellular matrix, which is a proteinaceous component of the stroma, regulates mammary epithelial growth, survival, migration and differentiation through a repertoire of transmembrane receptors, of which integrins are the best characterized. Integrins modulate cell fate by reciprocally transducing biochemical and biophysical cues between the cell and the extracellular matrix, facilitating processes such as embryonic branching morphogenesis and lactation in the mammary gland. During breast development and cancer progression the extracellular matrix is dynamically altered such that its composition, turnover, processing and orientation change dramatically. These modifications influence mammary epithelial cell shape, and modulate growth factor and hormonal responses to regulate processes including branching morphogenesis and alveolar differentiation. Malignant transformation of the breast is also associated with significant matrix remodeling and a progressive stiffening of the stroma that can enhance mammary epithelial cell growth, perturb breast tissue organization, and promote cell invasion and survival. In this review we discuss the role of stromal-epithelial interactions in normal and malignant mammary epithelial cell behavior. We specifically focus on how dynamic modulation of the biochemical and biophysical properties of the extracellular matrix elicit a dialogue with the mammary epithelium through transmembrane integrin receptors to influence tissue morphogenesis, homeostasis and malignant transformation.

Cell Facts.

- Stromal-epithelial interactions regulate mammary epithelial cell growth and differentiation during embryonic and postnatal development.
- The spatial organization and composition of the extracellular matrix influence mammary epithelial cell behavior.
- Alterations in extracellular matrix receptor expression can enable malignant transformation of the mammary epithelial cells
- Differences in the biophysical properties of the extracellular matrix due to an increase in deposit and/or cross-linking can induce the malignant transformation of mammary epithelial cells.

1. Introduction:

The mammary gland is a dynamic tissue derived from the epidermis that achieves full maturity in the adult. The development of the mammary ductal tree depends on stromal-epithelial interactions, and these interactions are important in embryonic and postnatal evolvement. The stroma not only modulates the normal development of the mammary gland but actively participates in malignant transformation of the tissue. Mammary ducts consist of luminal cells associated with myoepithelial cells surrounded by the basement membrane (BM) that separates the epithelium from the stroma. The stromal compartment is composed of mesenchymal cells (fibroblasts, blood cells and leukocytes) and extracellular matrix (ECM) (laminin, fibronectin, collagen, proteoglycans, etc.), which influence mammary development. In this short review, we focus on how the ECM modulates mammary epithelial growth and differentiation in embryonic development, postnatal ductal growth, branching morphogenesis, and

carcinogenesis. Of the myriad of ECM-mammary epithelial cell interactions, integrin signaling will be discussed in more detail. The biochemical and biophysical cues from the extracellular stroma that guide mammary epithelial morphogenesis, homeostasis and malignant transformation will also be described.

2- Cell origin and plasticity

The mammary gland is a modified sweat gland derived from the ectoderm. Mammary gland development begins with ectodermal cell migration induced by the mesenchyme, followed by the formation of five pairs of disk-shaped placodes (emerging epithelial formations) and invasion of the cells into the dermis (Veltmaat, Mailleux, Thiery & Bellusci, 2003). The mesenchyme is instructive and provides critical information to drive mammary differentiation. For example, mammary mesenchyme can induce embryonic epidermis from dorsal or midventral sites to form mammary buds that will undergo functional differentiation and milk synthesis (Cunha et al., 1995), whereas recombination of embryonic mammary epithelial cells with salivary mesenchyme produces epithelial salivary structures (Sakakaura, Nishizuka & Dawe, 1976).

The stroma is not a static compartment; the cellular and ECM compositions evolve over time adapting to changes in the development of the gland. Two different mesenchymal tissues are involved in mammary gland development during embryogenesis: the fibroblastic cells surrounding the epithelial rudiment (the fibroblastic mesenchyme), and the fat pad cells (the fat pad mesenchyme). These two mesenchymes have different developmental properties demonstrated through tissue recombination

studies. The fibroblastic mammary mesenchyme induces embryonic or adult mammary epithelial cells to form atypical ductal branching with hyperplasic ducts, while the fad pad induces epithelial cell elongation and branching (Sakakura, Sakagami & Nishizuka, 1982). These changes in mammary development can be explained, in part, by differences in ECM composition between the fibroblastic mesenchyme and the fat pad. For example, expression of laminin and protoheparan sulphate induced by the fat pad occur simultaneously with epithelial rudiment elongation and branching (Kimata, Sakakura, Inaguma, Kato & Nishizuka, 1985). Similar changes in ECM composition have been found in the growing ductal structure during puberty. The BM at the tip of the duct (the invasive front) is rich in hyaluronic acid, whereas the BM surrounding the duct is composed of collagen type IV, laminin, and proteoglycans (Fata, Werb & Bissell, 2003). These data suggest that the abundance and composition of the ECM can regulate epithelial cell behavior.

Remodeling of the ECM is a tightly regulated process where the action of metalloproteinases (MMPs), the principal matrix-degrading enzymes, is regulated by tissue inhibitors of metalloproteinase (TIMPs). Inappropriate expression of MMPs or TIMPs can drive aberrant mammary gland phenotypes (Fata, Werb & Bissell, 2003). For example, MMP2-null mammary glands have an excessive lateral branching with reduced ductal length, MMP3-deficient glands can elongate the ducts but with reduced secondary branching, and TIMP1-overexpressing glands demonstrate reduced ductal length (Fata, Werb & Bissell, 2003).

The epithelial cells sense modifications in ECM composition through transmembrane receptors. These receptors, which include integrins (collagen, laminin,

and fibronectin receptors), dystroglycan (laminin-1 receptor), discoidin domain receptor 1 tyrosine kinase (collagen receptor), and syndecans (co-receptors for heparan sulfate proteoglycans and fibronectin, laminin, collagen and growth factors), can modulate branching morphogenesis (Fata, Werb & Bissell, 2003). For example, gene knockout models showed that while α2 integrin is necessary for branching morphogenesis, α3, α6 or β4 subunits are dispensable (Chen, Diacovo, Grenache, Santoro & Zutter, 2002; Klinowska et al., 2001). Similarly, mice deficient in discoidin domain receptor 1 tyrosine kinase display excessive collagen deposition, delayed ductal development, and incomplete lactational differentiation (Vogel, Aszodi, Alves & Pawson, 2001).

Increased collagen deposition can also alter the biophysical properties of the ECM augmenting extracellular tension. This elevation in tension has been shown to perturb mammary epithelial cell differentiation. For example, the functional and morphological differentiation of primary mammary epithelial cells (MECs) in response to lactogenic hormones can proceed only when mixed mammary cell populations isolated from pre-lactating mice are plated on floating collagen gels with reduced tensional forces. Indeed, mechanically-loaded collagen gels fail to support acinar morphogenesis and functional differentiation (β-casein expression), because these rigid gels (similar to two-dimensional rigid plastic) drive focal adhesion assembly to promote cell spreading, increase MMP activity, and thereby interfere with endogenous BM maturation (reviewed in Paszek & Weaver, 2004). Our laboratory has been investigating how the biophysical properties of the ECM can regulate cell shape and BM-dependent MECs morphogenesis (acini formation). Using two- and three-dimensional (2D, 3D) natural and synthetic laminin-rich matrices of precisely calibrated stiffness, we have demonstrated that substrate

compliance regulates cell shape (rounding), mammary tissue morphogenesis, and endogenous BM assembly (Paszek et al., 2005) (Fig 1). Recently, matrix compliance has also been implicated in modulating functional differentiation of MECs, as determined by β-casein expression (Alcaraz et al., personal communication).

3. Functions.

During pregnancy, epithelial cells within the alveoli proliferate and differentiate in response to lactogenic hormones and growth factors, achieving full milk production capacity during lactation. The pregnancy-induced alveolar morphogenesis of the mammary gland is dependent upon ECM cues that are interpreted by the mammary epithelial cells through β1 integrin signaling. The association of β1 integrins with their heterodimeric α integrin subunit partners, anchor the cell to the BM (through laminin and collagen IV binding) and to the surrounding stroma (such as through binding to collagen I or fibronectin). In the mammary gland, both α5β1 (fibronectin receptor) and α2β1 (collagen and laminin receptor) integrin expression levels are regulated by ovarian hormones and, as such, have been implicated as key transducers of hormonal cues that drive growth and differentiation of the gland during pregnancy (Woodward, Mienaltowski, Modi, Bennett & Haslam, 2001).

Conditional deletion of β1 integrin in luminal mammary cells demonstrated an essential role for β1 integrin in alveolar development and differentiation during pregnancy and lactation (Li et al., 2005; Naylor et al., 2005). The ablation of β1 integrin

not only resulted in malformed alveoli, but also in failure of prolactin (PRL)-induced mammary epithelial cell differentiation and milk synthesis (Naylor et al., 2005).

How does β1 integrin regulate mammary epithelial cell differentiation? In response to ECM cues such as changes in matrix composition, integrins assemble into intracellular signaling complexes that are connected to the actin cytoskeleton and that activate growth and survival pathways, thereby transmitting cues from the matrix to influence cell morphology and fate. For example, cell anchorage to laminin-1 through β1 integrin permits PRL-dependent activation of Janus Kinase-2 and signal transducer and activator of transcription-5 (Stat5) signaling pathways, and the transcription of PRL- and Stat5-regulated milk proteins (Naylor et al., 2005). The small Rho GTPase Rac1 has been shown to be a critical downstream effector of β1 integrin signaling for the activation of PRL/Stat5 signaling cascade (Akhtar & Streuli 2006). However, the precise cross-talk between integrin and PRL signaling has not been fully elucidated.

4. Associated pathologies.

Modifying ECM-integrin interactions can profoundly influence expression of the malignant phenotype in culture and in vivo (Park et al., 2006). However, the molecular mechanisms whereby altered stromal-epithelial interactions regulate tumorigenesis are not well defined. The cellular component of the stroma has been implicated in promoting breast cancer development. Infiltrating leukocytes, which are recruited to the tumor as a result of tumor cell expression of chemotactic cytokines, provide cytokines, proteases and growth factors to stimulate tumor growth and promote neo-angiogenesis (Pollard, 2004).

Moreover, the overexpression of transforming growth factor-β or hepatocyte growth factor by tumor associated-fibroblasts has also been implicated in the initiation of breast cancer (Kuperwasser et al., 2004). Besides secreting growth factors, activated fibroblasts are a vast source for ECM proteins. Changes in ECM composition can induce changes in epithelial cell integrin expression. For example, altered expression of β1-, β4-, α2-, α3- and α6- integrins has been observed in mammary cancer cells (Taddei et al., 2004).

Integrin-mediated adhesion to the ECM is essential for cell growth and survival through activation of focal adhesion kinase (FAK) signaling cascades that promote cell viability (White et al., 2004). Moreover, reciprocal interactions between epidermal growth factor receptor (EGFR) and integrin signaling pathways control proliferation and survival of MECs, such that inhibiting either β4 integrin, β1 integrin or EGFR represses the malignant phenotype of tumor MECs growing in 3D BM matrix (Weaver et al., 1997). The functional integrity of β1 integrin signaling is also essential for the induction of mammary tumors, as the ablation of β1 integrin expression in tumor cells *in vivo* inhibits proliferation and expansion of the tumors cells (White et al., 2004). Recently, it was shown that β4 integrin promotes tumor progression through amplified ErbB2 signaling, and that the loss of β4 integrin signaling suppresses mammary tumor onset and invasive growth *in vivo* (Guo et al., 2006). These data demonstrate a key role for integrins in malignant progression.

The development of breast cancer is characterized by the loss of tissue organization (Fig. 2A). Although breast tumor cells originate from epithelial cells, the stroma is an active participant of the epithelial malignant transformation. In the past decade, the stroma surrounding developing lesions has increasingly been appreciated as a

critical regulator of malignant transformation and as a vital modifier of tumor behavior including metastasis and treatment responsiveness. The stromal desmoplastic response is characterized by the activation of fibroblasts, increased deposition, cross-linking and remodeling of the ECM, angiogenesis, and invasion of leukocytes. Up-regulated ECM gene expression and elevated MMP activities are not only found in tumors but can also correlate with poor patient prognosis (Jinga et al., 2006). For example, expression levels of the ECM protein lysyl oxidase (LOX), which is responsible for collagen cross-linking, is elevated in cancer patients and associated with metastasis and reduced patient survival (Erler et al., 2006). Furthermore, the increased ratios of MMP2:TIMP2 and MMP9:TIMP1 found in malignant breast tissues have been suggested to play a role in the aggressiveness of invasive breast carcinomas (Jinga et al., 2006).

Metastasis of breast cancer cells is associated with the majority of the disease fatalities, such that restricting disease progression and preventing metastasis represents the primary objective of many cancer prevention programs. In order for a tumor cell to metastasize, it must first degrade the BM and migrate into the surrounding stroma. Cleavage of laminin-5 by MMPs (2 and 14) exposes cryptic sites of the proteins that induce epithelial migration (Giannelli, Falk-Marzillier, Schiraldi, Stetler-Stevenson & Quaranta, 1997). Another consequence of MMP activity is the release of growth factors trapped in the ECM that in turn can stimulate further epithelial cell invasion. During invasion, cells extend pseudopodia at the leading edge that attach to collagen fibers in the ECM at the migration front, allowing the cells to “crawl” linearly along the fibers toward the blood vessels (Condeelis & Segall, 2003).

Cell migration is also tightly regulated by cell adhesion, cell-generated contractility and cell haptotaxis to maximize their ligand binding and even durotaxis towards a stiffer matrix to increase cell tension (Sheetz, Felsenfeld & Galbraith, 1998; Wong, Velasco, Rajagopalan & Pham, 2003). This suggests that elevated matrix deposition and tension likely couple with degradation to modulate tumor invasion and metastasis. In this respect, small Rho GTPases are functionally-linked to cell migration and MMP-mediated invasion. Rac and Rho expression and activity are elevated in tumors and RhoC is implicated in the metastatic, aggressive phenotype of inflammatory breast tumors (Fritz, Just & Kaina, 1999; Kleer et al., 2004). Consistently, inhibition of LOX involved in collagen cross-linking and fiber formation dramatically reduces invasion and metastasis in a mouse model of breast cancer (Erler et al., 2006).

Given that the ECM profoundly modulates tissue morphogenesis and that the stroma changes dramatically during breast tumorigenesis, it is logical to ask if modifications in matrix organization and stiffness could drive tumor invasion and contribute to metastasis. Consistently, we have shown that the mammary gland progressively stiffens during tumor progression and that is associated with increased collagen deposition, cross-linking and reorientation (Paszek et al., 2005). In concordance with these results, matrix stiffness, in association with growth factors, enhances ERK activation and increases cell contractility (Fig. 2B) (Paszek et al., 2005). Interestingly, force-generated activation of ERK may also influence cell proliferation, alter tissue behavior and drive anti-estrogen resistance during breast cancer treatment, through phosphorylation of ERα, recruitment of ERα co-activators or enhanced transcriptional activity, in a ligand-independent manner (Likhite, Stossi, Kim, Katzenellenbogen &

Katzenellenbogen, 2006). Indeed, tamoxifen, the anti-estrogen used in the treatment of breast cancer, has been shown to reduce breast density and therefore the risk of recurrences (Atkinson, Warren, Bingham & Day, 1999).

We showed that matrix stiffness and/or exogenous force independently induce cell-generated contractility to promote focal adhesion maturation and enhance integrin-dependent signaling thus compromising multi-cellular tissue morphogenesis and promoting a tumor-like behavior in mammary cells (Paszek et al., 2005). This suggests that matrix stiffness likely promotes breast tumorigenesis through altering integrins and their adhesion interactions. Conversely, we found that blocking integrin-dependent cell contractility reverted the malignant phenotype in culture (Paszek et al., 2005; Weaver et al., 1997). Consistent with these findings, ectopic expression of β1 integrin mutants with increased transmembrane molecular associations (V737N, G744N), elevated cellular contractility and forced focal adhesion maturation increase integrin/growth factor-dependent signaling, again to compromise multi-cellular tissue morphogenesis and promote tumorigenic behavior in culture and *in vivo* (Paszek et al., 2005).

Investigating ECM composition and stiffness as a risk factor is critical given the profound changes in the mammary stroma associated with breast cancer and the diversity of diseases associated with changes in collagen deposition, orientation and cross-linking. Indeed, inhibition of matrix modifying ECM proteins can dramatically reduce tumor progression through effects on invasion and metastasis. It is plausible that as a consequence of matrix rigidity, altered mechanotransduction constitutes a key mechanism in regulating malignant transformation of epithelial cells. Moreover, there is evidence to suggest that changes in mammary ECM modify treatment responsiveness to anti-

estrogens promoting the progression of breast carcinoma and thereby decreasing patient survival. Understanding the molecular mechanisms behind this process could lead to the design of a unique, targeted strategy to diagnose and treat this disease.

5. Acknowledgments.

We apologize to the many authors whose work is not cited due to space limitations. This work was supported by NIH grants CA078731 to V.M.W, R01 GM072002-04 to M.D., and DOD grants DAMD1701-1-0368, 1703-1-0496, and W81XWH-05-1-330 to V.M.W.

6. References.

Akhtar, N. & Streuli, C.H. (2006). Rac1 links integrin-mediated adhesion to the control of lactational differentiation in mammary epithelia. *Journal of Cell Biology, 173,* 781-793.

Atkinson, C., Warren, R., Bingham, S.A. & Day, N.E. (1999). Mammographic patterns as a predictive biomarker of breast cancer risk: effect of tamoxifen. *Cancer Epidemiology Biomarkers & Prevention, 8,* 863-866.

Chen, J., Diacovo, T.G., Grenache, D.G., Santoro, S.A. & Zutter, M.M. (2002). The alpha(2) integrin subunit-deficient mouse: a multifaceted phenotype including defects of branching morphogenesis and hemostasis. *American Journal of Pathology, 161,* 337-344.

Condeelis, J. & Segall, J.E. (2003). Intravital imaging of cell movement in tumours. *Nature Reviews Cancer, 3,* 921-930.

Cunha, G.R., Young, P., Christov, K., Guzman, R., Nandi, S., Talamantes, F., et al. (1995). Mammary phenotypic expression induced in epidermal cells by embryonic mammary mesenchyme. *Acta Anatomica (Basel), 152,* 195-204

Erler, J.T., Bennewith, K.L., Nicolau, M., Dornhöfer, N., Kong, C., Le, Q.T., et al. (2006). Lysyl oxidase is essential for hypoxia-induced metastasis. *Nature, 440,* 1222-1226.

Fata, J.E., Werb, Z. & Bissell, M.J. (2004). Regulation of mammary gland branching morphogenesis by the extracellular matrix and its remodeling enzymes. *Breast Cancer Research, 6,* 1-11.

Fritz, G., Just, I. & Kaina, B. (1999). Rho GTPases are over-expressed in human tumors. *International Journal of Cancer, 81,* 682–687.

Giannelli, G., Falk-Marzillier, J., Schiraldi, O., Stetler-Stevenson, W.G. & Quaranta, V. (1997). Induction of cell migration by matrix metalloprotease-2 cleavage of laminin-5. *Science, 277,* 225-228.

Guo, W., Pylayeva, Y., Pepe, A., Yoshioka, T., Muller, W.J., Inghirami, G., et al. (2006). Beta 4 integrin amplifies ErbB2 signaling to promote mammary tumorigenesis. *Cell, 126,* 489-502.

Jinga, D.C., Blidaru, A., Condrea, I., Ardeleanu, C., Dragomir, C., Szegli, G., et al. (2006). MMP-9 and MMP-2 gelatinases and TIMP-1 and TIMP-2 inhibitors in breast cancer: correlations with prognostic factors. *Journal of Cellular and Molecular Medicine, 10,* 499-510.

Kimata, K., Sakakura, T., Inaguma, Y., Kato, M. & Nishizuka, Y. (1985). Participation of two different mesenchymes in the developing mouse mammary gland: synthesis of basement membrane components by fat pad precursor cells. *Journal of Embryology and Experimental Morphology, 89,* 243-257.

Kleer, C.G., Zhang, Y., Pan, Q., Gallagher, G., Wu, M., Wu, Z.F., et al. (2004). WISP3 and RhoC guanosine triphosphatase cooperate in the development of inflammatory breast cancer. *Breast Cancer Research, 6,* R110-115.

Klinowska, T.C., Alexander, C.M., Georges-Labouesse, E., Van der Neut, R., Kreidberg, J.A., Jones, C.J., et al. (2001). Epithelial development and differentiation in the mammary gland is not dependent on alpha 3 or alpha 6 integrin subunits. *Developmental Biology, 233,* 449-467.

Kuperwasser, C., Chavarria, T., Wu, M., Magrane, G., Gray, J.W., Carey, L., et al. (2004). Reconstruction of functionally normal and malignant human breast tissues in mice. *Proceedings of the National Academy of Science, U.S.A., 101,* 4966-4971.

Likhite, V.S., Stossi, F., Kim, K., Katzenellenbogen, B.S. & Katzenellenbogen, J.A. (2006). Kinase-specific phosphorylation of the estrogen receptor changes receptor interactions with ligand, deoxyribonucleic acid, and coregulators associated with alterations in estrogen and tamoxifen activity. *Molecular Endocrinology, 20,* 3120-3132.

Naylor, M.J., Li, N., Cheung, J., Lowe, E.T., Lambert, E., Marlow, R., et al. (2005). Ablation of beta1 integrin in mammary epithelium reveals a key role for integrin in glandular morphogenesis and differentiation. *Journal of Cell Biology, 171,* 717-728.

Park, C.C., Zhang, H., Pallavicini, M., Gray, J. W., Baehner, F., Park, C.J, et al. (2006) Beta1 integrin inhibitory antibody induces apoptosis of breast cancer cells, inhibits

growth, and distinguishes malignant from normal phenotype in three dimensional cultures and in vivo. *Cancer Research, 66*, 1526-1535.

Paszek, M.J. & Weaver, V.M. (2004). The tension mounts: mechanics meets morphogenesis and malignancy. *Journal of Mammary Gland Biology & Neoplasia, 9*, 325-342.

Paszek, M.J., Zahir, N., Johnson, K.R., Lakins, J.N., Rozenberg, G.I., Gefen, A., et al. (2005). Tensional homeostasis and the malignant phenotype. *Cancer Cell, 8*, 241-254.

Pollard J.W. (2004). Tumour-educated macrophages promote tumour progression and metastasis. *Nature Reviews Cancer, 4*, 71-78.

Sakakura, T., Nishizuka, Y. & Dawe C.J. (1976). Mesenchyme-dependent morphogenesis and epithelium-specific cytodifferentiation in mouse mammary gland. *Science, 194*, 1439-1441.

Sakakura, T., Sakagami, Y. & Nishizuka, Y. (1982). Dual origin of mesenchymal tissues participating in mouse mammary gland embryogenesis. *Developmental Biology, 91*, 202-207.

Sheetz, M.P., Felsenfeld, D.P. & Galbraith, C.G. (1998). Cell migration: regulation of force on extracellular-matrix-integrin complexes. *Trends in Cell Biology, 8*, 51-54.

Taddei, I., Faraldo, M.M., Teulière, J., Deugnier, M.A., Thiery, J.P. & Glukhova, M.A. (2004). Integrins in mammary gland development and differentiation of mammary epithelium. *Journal of the Mammary Gland Biology and Neoplasia, 8*, 383-394.

Veltmaat, J.M., Mailleux, A.A., Thiery, J.P. & Bellusci, S. (2003). Mouse embryonic mammogenesis as a model for the molecular regulation of pattern formation. *Differentiation, 71*, 1-17.

Vogel, W.F., Aszódi, A., Alves, F. & Pawson, T. (2001). Discoidin domain receptor 1 tyrosine kinase has an essential role in mammary gland development. *Molecular Cell Biology, 21*, 2906-2917.

Weaver, V.M., Petersen, O.W., Wang, F., Larabell, C.A., Briand, P., Damsky, C., et al. (1997). Reversion of the malignant phenotype of human breast cells in three- dimensional culture and in vivo by integrin blocking antibodies. *Journal of Cell Biology*, *137*, 231-245.

White, D.E., Kurpios, N.A., Zuo, D., Hassell, J.A., Blaess, S., Mueller, U., et al. (2004). Targeted disruption of beta1-integrin in a transgenic mouse model of human breast cancer reveals an essential role in mammary tumor induction. *Cancer Cell, 6,* 159-170.

Wong, J.Y., Velasco, A., Rajagopalan, A. & Pham Q. (2003). Directed Movement of Vascular Smooth Muscle Cells on Gradient-Compliant Hydrogels. *Langmuir*, *19*, 1908-1913.

Woodward, T.L., Mienaltowski, A.S., Modi, R.R., Bennett, J. M. & Haslam, S.Z. (2001). Fibronectin and the alpha(5)beta(1) integrin are under developmental and ovarian steroid regulation in the normal mouse mammary gland. *Endocrinology*, *142*, 3214-3222.

Figure Legends

Figure 1. Mammary epithelial growth and morphogenesis is regulated by matrix stiffness. **A)** 3D cultures of normal mammary epithelial cells within collagen gels of different concentration. Stiffening the ECM through an incremental increase in collagen concentration (soft gels: 1mg/ml Collagen I, 140Pa; stiff gels 3.6mg/ml Collagen I, 1200Pa) results in the progressive perturbation of morphogenesis, and the increased growth and modulated survival of MECs. Altered mammary acini morphology is illustrated by the destabilization of cell-cell adherens junctions and disruption of basal tissue polarity indicated by the gradual loss of cell-cell localized β-catenin (green) and disorganized β4 integrin (red) visualized through immunofluorescence and confocal imaging. On the right side of the panel is an illustration of a mammary ductal structure (luminal and myoepithelial cells surrounded by BM), and depicting MEC morphogenesis in soft and stiff gels. Scale bars represent 25μm. **B)** Confocal immunofluorescence images of MEC colonies on soft and stiff gels (140 versus >5000 Pa) stained for β-catenin (red) and E-cadherin (green), and counterstained with DAPI (blue) after triton X-100 extraction. β-catenin could be extracted from the sites of cell-cell interaction in MEC colonies formed on a stiff but not on a soft gel, indicating that adherens junctions are less stable in MEC structures formed on stiff gels. White arrows indicate diffuse staining patterns of β-catenin and E-cadherin. Modified from Paszek et al., 2005.

Figure 2. Malignant transformation of mammary epithelial cells is regulated by matrix stiffness. Breast transformation ensues through progressive acquisition of genetic alterations in the luminal epithelial cells residing within the mammary ducts. The tissue

stroma responds to these epithelial alterations by initiating a desmoplastic response that is characterized by activation and transdifferentiation of fibroblasts, infiltration of immune cells, increased secretion of growth factors and cytokines, and elevated matrix synthesis and remodeling that manifests as matrix stiffening. **A)** Cartoon depicting the stages of breast tumorigenesis, (from left to right; normal ducts, ductal carcinoma *in situ* and invasive phenotype) highlighting key desmoplastic changes within the tissue stroma. **B)** Force-dependent focal adhesion maturation mediated by elevated tumor matrix stiffness. Integrins are bidirectional mechano sensors that integrate biochemical and biophysical cues from the matrix and the actin cytoskeleton and transduce cell-generated force to the surrounding microenvironment. Activated integrins bind to ECM proteins via cooperative interactions between their alpha and beta extracellular domains and form nascent highly dynamic adhesion signaling complexes. In response to external mechanical force or elevated cell-generated contractility integrin clustering is enhanced and the recruitment of multiple integrin adhesion plaque proteins including talin and vinculin is favored. These, in turn, associate with the actin cytoskeleton and multiple signaling proteins including focal adhesion kinase (FAK), Src family kinases, and integrin-linked kinase, to promote cell growth, survival, migration and differentiation. Matrix stiffening, which reflects elevated matrix deposition, linearization and cross-linking, can cooperate with oncogenic signaling to enhance cell-generated contractility to foster integrin associations and focal adhesion maturation. Maturation of focal adhesions promotes cell generated forces by enhancing Rho GTPase and ERK-mediated acto-myosin contractility - which feed forward to further promote integrin clustering and focal adhesion assembly and transmit acto-myosin- generated cellular forces to the ECM, as outlined in Paszek et al., 2005.

Inset: Representative traction maps showing the typical force distribution in fibroblasts on soft (450 Pa) and on stiff fibronectin gels (5600 Pa). These maps allow the measurement of the forces generated by the cell, which are dependent on the stiffness of the substrate. Modified from Paszek et al., 2005.

Figure 1

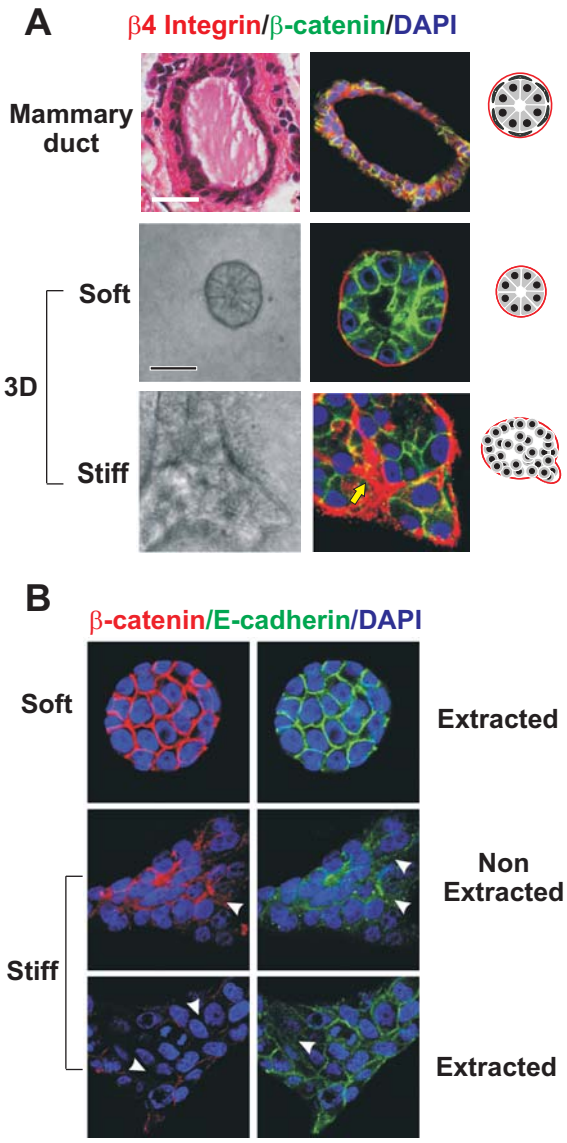
A
β4 Integrin/β-catenin/DAPI
Mammary duct
3D
Soft
Stiff
B
β-catenin/E-cadherin/DAPI
Soft
Stiff
Extracted
Non Extracted
Extracted

Figure 2

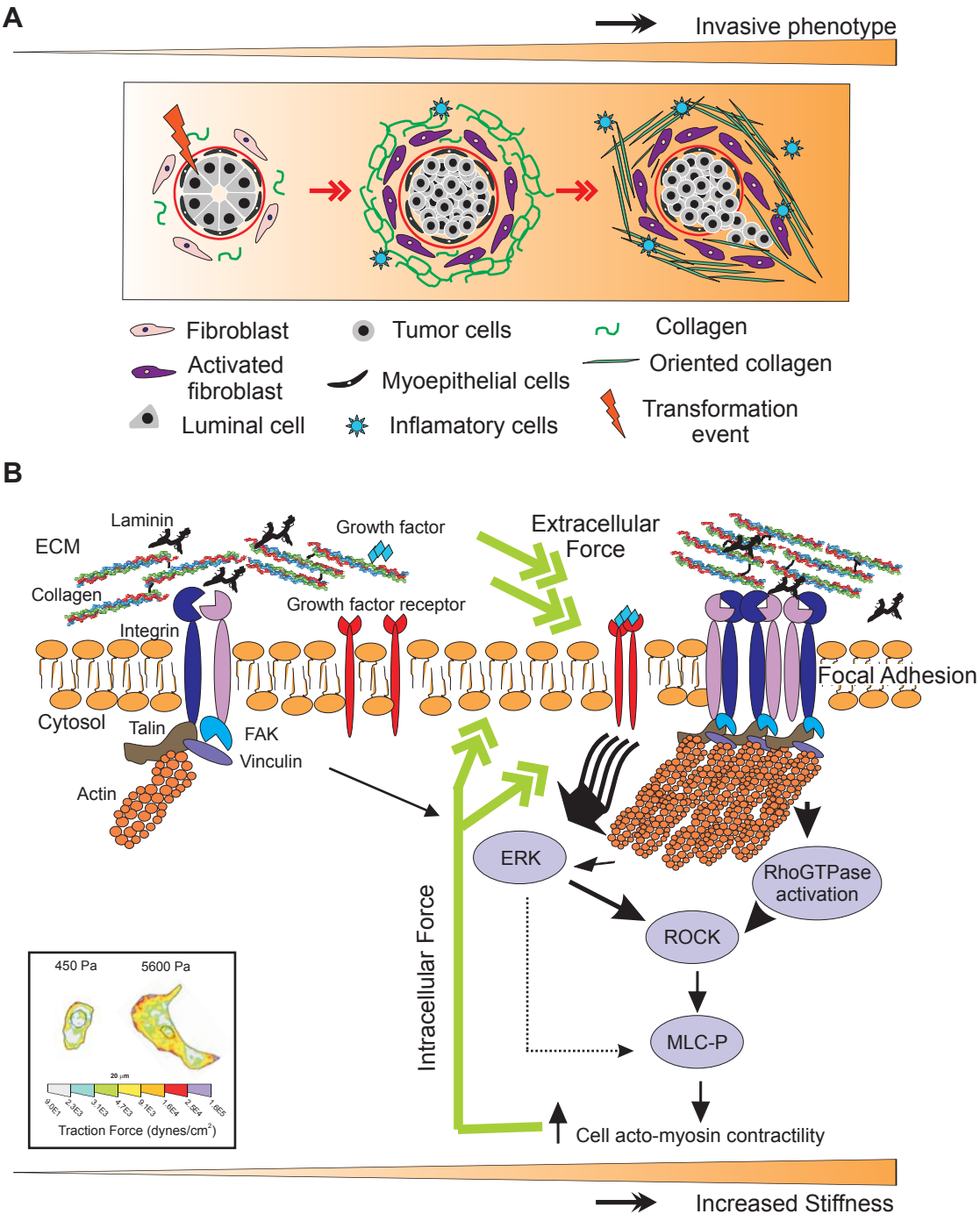
A
Invasive phenotype
Fibroblast
Activated fibroblast
Luminal cell
Tumor cells
Myoepithelial cells
Inflamatory cells
Collagen
Oriented collagen
Transformation event
B
Laminin
ECM
Collagen
Growth factor
Growth factor receptor
Extracellular Force
Integrin
Cytosol
Talin
FAK
Vinculin
Actin
Focal Adhesion
ERK
RhoGTPase activation
ROCK
MLC-P
Intracellular Force
Cell acto-myosin contractility
450 Pa
5600 Pa
Traction Force (dynes/cm²)
Increased Stiffness

Modeling Morphogenesis and Oncogenesis In Three Dimensional Breast Epithelial Cultures

Christy Hebner[1], Valerie M. Weaver[1], and Jayanta Debnath[2,] *

1) Department of Surgery and Center for Bioengineering and Tissue Regeneration, University of California San Francisco, San Francisco, California
2) Department of Pathology, University of California San Francisco, San Francisco, California

*Corresponding author.

Address correspondence to:

Jayanta Debnath, M.D.
UCSF Department of Pathology
513 Parnassus Avenue, HSW 514
San Francisco, California 94143
Phone: 415-476-1780
FAX: 415-514-3165

Emails: jayanta.debnath@ucsf.edu; HebnerC@surgery.ucsf.edu; WeaverV@surgery.ucsf.edu

Key words: three dimensional culture, ECM, lumen formation, apicobasal polarity, force

TABLE OF CONTENTS.

ABSTRACT.

Three-dimensional (3D) epithelial culture systems recreate the cardinal features of glandular epithelium *in vivo* and represent a valuable tool to model breast cancer initiation and progression in a structurally appropriate context. 3D models have emerged as a powerful method to interrogate the biological activities of cancer genes and oncogenic pathways, and recent studies have poignantly illustrated their utility in dissecting the emerging role of tensional force in regulating epithelial tissue homeostasis. In this chapter, we will overview how 3D models are being used to investigate fundamental cellular and biophysical mechanisms associated with breast cancer progression that have not been readily amenable to traditional genetic or biochemical analysis.

SUMMARY POINTS.

- Epithelial cells grown in 3D recreate several cardinal features of glandular epithelium *in vivo*, including the formation of cyst-like “acini” with a hollow lumen, the apicobasal polarization of cells surrounding this luminal space, and the tight regulation of cell growth and proliferation. Cancer genes produce diverse morphogenetic phenotypes in 3D cultures that resemble important histopathological features observed in carcinomas *in vivo*.

- Cells occupying the hollow lumen of acini normally undergo apoptosis due to the lack of extracellular matrix attachment (*anoikis*). However, numerous oncogenes and pathways aberrantly promote cell survival in the luminal space of 3D structures; the resultant phenotypes recapitulate the luminal filling observed in premalignant breast lesions.

- Apicobasal polarity is a fundamental characteristic of glandular epithelium *in vivo* and *in vitro*. Recent studies using 3D culture systems are beginning to delineate how cell polarity regulates normal gland architecture and how the disruption of this polarity may contribute to carcinoma formation.

- Studies of epithelial tumor cells in 3D culture demonstrate that modulating cell adhesion and growth factor receptor pathways can repress the phenotypic expression of their transformed state, even in the context of multiple oncogenic mutations.

- Breast cancers are characterized by a dramatic increase in tissue stiffness due in part to bulk tumor growth, altered vasculature, and the expansion of a rigid (desmoplastic)

stroma. Recent studies reveal that increasing matrix stiffness disrupts normal 3D morphogenesis and promotes several architectural features associated with malignancy.

FUTURE DIRECTIONS.

- Immortalized human MEC lines commonly utilized for 3D culture assays express markers of both luminal and myoepithelial cell lineages. The hybrid nature of such lines limit 3D culture models in terms of their ability to simulate events in breast carcinoma progression *in vivo*. Improving cell culture conditions to propagate primary human mammary cells is critical to develop faithful 3D models for studying breast cancer initiation and progression.

- A large fraction of human breast cancers are hormonally regulated; indeed, estrogen receptor (ER) and progesterone receptor (PR) status are a major prognostic determinant in breast tumors. However, due to the lack of availability of human MECs (both primary cells and cell lines) responsive to these principal mammary hormones, the impact of hormone receptor activation on 3D breast morphogenesis remains completely unknown. 3D culture systems incorporating the intricate hormonal signaling unique to the mammary gland should be developed.

- The studies discussed here utilize monotypic culture systems, in which epithelial cells are grown in isolation within a 3D scaffold. Since both normal epithelial tissues and tumors represent a community of heterotypic cell types, the use of such monotypic 3D cultures has inherent limitations. Hence, both current and future research efforts demand heterotypic culture systems that recreate the histological complexity of epithelial tissue *in vivo*.

KEY TERMS.

Acini: Although anatomically imprecise, a widely used operational term for epithelial cyst-like spheroids grown in three-dimensional culture.

Apoptosis: Programmed cell death marked by caspase activation, nuclear fragmentation, and subsequent phagocytic elimination of cellular remnants.

Autophagy: Tightly regulated lysosomal process where a cell self-digests cytoplasmic contents; proposed to mediate nonapoptotic (type 2) programmed cell death.

Apicobasal polarity: Asymmetric organization of epithelial cells within glands where the apical pole borders the lumen, while the basal surface adheres to ECM.

Extracellular matrix: Non-cellular tissue components produced by cells, such as collagen and basement membrane proteins.

Focal adhesions: Dynamic complexes of signaling, adaptor, and structural proteins that transmit ECM/integrin-based biochemical and mechanical signals to the cytoskeleton.

Reconstituted basement membrane: Preparations of basement membrane derived ECM proteins, most notably laminin, which can drive 3D epithelial acini morphogenesis.

ACRONYMS.

ADH: Atypical ductal hyperplasia

DCIS: Ductal carcinoma in situ.

ECM: Extracellular matrix

EGFR/ErbB: Members of the epidermal growth factor receptor tyrosine kinase family

EHS: Engelbreth-Holm-Swarm tumor derived basement membrane matrix.

MEC: Mammary epithelial cell.

rBM: Reconstituted basement membrane.

3D: Three dimensional.

TEB: Terminal endbud.

TLDU: Terminal ductal lobular unit.

INTRODUCTION.

Breast carcinoma is the most common female cancer in the Western world (1). For the practicing pathologist, epithelial cancers arising in the breast are remarkable both for their clinical significance as well as their diverse histopathological architecture. Breast carcinomas also represent a growing diagnostic challenge for pathologists because pre-invasive lesions, such as atypical ductal hyperplasias (ADH) and ductal carcinomas in situ (DCIS), are being diagnosed with increasing frequency (2) (3). The ability to effectively diagnose these early lesions, where the tumor does not invade the basement membrane or myoepithelial layer, and confidently predict future outcome for these patients, has assumed great significance in breast cancer diagnosis and treatment (4).

For decades, pathologists have recognized that certain histological patterns harbor valuable prognostic information. For example, in the breast, tubular carcinomas, mucinous (colloid) carcinomas, and invasive lobular carcinomas are associated with better clinical outcome compared to the most commonly diagnosed pattern, invasive ductal carcinoma (5, 6). More recently, clear relationships between a specific genomic abnormality and histological phenotype have been defined. For example, the comedo-subtype of DCIS possesses amplifications in the *HER2/NEU* oncogene, which encodes for the epidermal growth factor (EGF) family receptor tyrosine kinase, ErbB2 (7) Second, basal-like breast cancers, an aggressive subtype of invasive ductal carcinoma remarkable for significant aneuploidy and the lack of hormone receptor expression, are strongly associated with mutations in the tumor suppressor BRCA1 or abnormalities in X chromosome inactivation (8). Third, invasive lobular carcinoma is commonly associated with genomic losses in *CDH1*, which encodes for E-cadherin, an important epithelial cell-cell adhesion molecule(9). Moreover, high throughput experimental approaches have provided a large quantity of information about epithelial cancers and raised new questions on

how cancer genes and pathways influence both clinical prognosis and histological architecture (10-12). Despite these advances, much remains to be learned about the precise molecular and biophysical mechanisms that elicit the actual phenotypic changes observed under the microscope. A better understanding of the mechanisms and pathways involved in the disruption of normal tissue architecture will undoubtedly provide biological insight into breast carcinoma progression and aid in the discovery of new diagnostic markers and therapeutic strategies.

Over the past decade, three dimensional (3D) organotypic culture systems have been increasingly utilized as powerful cell-based models to investigate the functions of cancer genes and pathways in a biologically relevant context and high throughput manner (13, 14). These culture systems have provided unique insights into how basic cell biological and biophysical processes impact on higher order tissue architecture. In recent years, 3D models have significantly enhanced our understanding of carcinoma biology in the following four areas: 1) the formation and maintenance of a hollow glandular lumen and its disruption by cancer genes; 2) the regulation of apicobasal polarity in normal and cancerous epithelium; 3) the discovery that cell-cell and cell-matrix adhesion pathways can dominantly interfere with the phenotypic expression of the tumorigenic state; and 4) the emerging importance for tensional force in driving 3D tissue architecture and homeostasis. In this chapter, we exclusively focus on these four major areas of discovery and their potential implications for breast cancer pathogenesis. Importantly, we do not encyclopedically review findings in several important research areas, such as branching morphogenesis, invasion, epithelial-mesenchymal transition (EMT), and the role of the stroma in tumorigenesis, because these topics have all been covered in recent reviews (13, 14). Finally, although most of the experiments discussed here employ normal or cancerous breast epithelial cells, we also delineate salient experiments utilizing non-breast 3D culture systems, most notably, cysts derived from Madin Darby Canine Kidney cells (MDCKs), because

they provide valuable insight into the basic processes driving normal glandular architecture and its disruption in carcinomas.

MAMMARY GLAND MORPHOGENESIS IN VIVO.

Cells in the human body organize into dynamic tissue complexes, orchestrated by numerous factors including cell-cell and cell-extracellular matrix (ECM) interactions, soluble ligands, and physical force. In epithelial tissues, these elements create an intricate architecture notable for tightly controlled cell growth, proliferation, differentiation, polarity and survival. This phenotypic control is mediated not only by intracellular signaling pathways, but also by signals from the surrounding microenvironment. For instance, in the developing mouse, death signals initiated by the endoderm induce cells in the ectoderm to undergo apoptosis (15). In the developing kidney, tubule formation is mediated by soluble factors including hepatocyte growth factor and TGF-α as well as by chemical and physical cues initiated by the adjacent mesenchyme (16, 17). Furthermore, intracellular signaling pathways and physical signals initiating from force and adhesion are elaborately linked; disruption of these interrelationships plays a major role in epithelial carcinogenesis(18). Indeed, this is beautifully illustrated in the human breast.

Mammary Gland Development.

The breast is one of the few organs that develops and matures after birth, making it an ideal organ for studying tissue development. The mammary gland forms via branching morphogenesis in which a two-dimensional layer forms a fluid-filled lumen via budding through a three-dimensional mesenchymal mass (19). The mature breast is a complex organ consisting of a central lumen encapsulated by luminal epithelial cells, and further delimited by myoepithelial cells and the extracellular matrix (ECM). Hence, an unique microenvironment

influences mammary tissue homeostasis through hormones, soluble factors, stroma, and physical stress and strain (20).

The mammary gland is composed of an extensive network of branched ductal structures with epithelial cell-lined hollow luminal spaces (19, 21). Two bi-lateral ridges of epidermal tissue known as “milk lines” form during the first trimester (22). Pairs of disk-shaped mammary placodes that mark the site of each nipple separate along these lines and form a bulb-shaped bud by proliferating into the adjacent mesenchyme. This structure forms the primary rudimentary mammary gland known as an “anlage”. Upon penetration of the mesenchyme, the epithelial bud branches into the mammary fat pad and forms several ductal trees. However, upon cessation of hormonal influences in the newborn, the mammary gland enters a quiescent state until puberty.

Upon reaching puberty, hormone-dependent development of the breast initiates with expansion beginning at the ends of the ducts known as terminal end buds (TEB) (23) (Fig. 1). Two different cell types are contained within the TEB—cap cells and body cells. The cap cells are ceded as a single layer at the edge of the TEB in contact with the basal lamina whereas the majority of the TEB is composed of body cells structured in multicellular layers. The TEB undergoes ductal arborization via sprouting through the mammary fat pad. Although the resting gland is relatively static, during pregnancy, the breast undergoes dynamic changes in which lobules form on the end of the branched structures and secrete milk during lactation. With pregnancy, differentiation of the ducts occurs resulting in formation of luminal structures required for lactation. Lumen formation is intrinsic to milk production and transport and is controlled by cell death as body cells bordering the TEB exhibit high rates of apoptosis (24). Interestingly, in premalignant breast cancer lesions, either complete or partial filling of the lumen is observed suggesting that normal apoptotic pathways may be altered in the early phases of mammary carcinogenesis.

MODELING GLANDULAR EPITHELIUM USING 3D CULTURES.

Cell culture systems are well suited for dissecting the biochemical and cell signaling pathways necessary for studying oncogenic transformation. Although significant information has been gleaned from studies of two-dimensional (2D) monolayer cells, these systems do not lend themselves to the three-dimensional (3D) architecture characteristic of epithelial cells *in vivo*. To address the limitations imposed by monolayer cell culture, 3D methods have been developed to model the *in vivo* environment of epithelial cells. In contrast to mouse models or human tissue studies, 3D systems can be exploited to rapidly identify genes and deconstruct signaling pathways that regulate mammary morphogenesis and epithelial cancer development. In this review, we will focus on the use of 3D models as a means to uncover the basic cellular mechanisms that contribute to normal breast morphogenesis and malignancy.

The terminal ductal lobular unit (TDLU), which is composed of mammary epithelial cells (MEC), is the smallest functional unit of the breast (25). When MECs are placed in traditional two-dimensional cultures, they grow as monolayers and fail to differentiate, even in the presence of pro-lactogenic hormones (26). However, upon culture within basement membrane proteins, these cells organize into spherical “acini” in which the lumen becomes hollow and milk is secreted. A breakdown in this formation is seen in the early stages of breast cancer where loss of polarized organization, increased cellular proliferation, and filling of the luminal space is observed (1, 14). Therefore, understanding the basic mechanisms that regulate acini formation and luminal clearance provides key insights into the early events in carcinoma formation.

Utilizing 3D culture conditions, epithelial cells initially proliferate to eventually form growth-arrested spherical acini characterized by polarized cells surrounding a hollow lumen (12, 27, 28). Two different methods are typically used to induce acini formation (Fig. 2A). The first involves completely embedding epithelial cells within a gelled extracellular matrix, which is

grown in the presence of culture media containing growth factors and hormones (28). The second method utilizes a thin gel bed (approximately 1mm thick) of ECM molecules upon which epithelial cells are seeded as single cells and overlaid with culture media containing diluted ECM (12). Both of these methods are highly advantageous compared to traditional 2D cultures because cells proliferate and develop into polarized growth arrested structures that resemble normal glands *in vivo* (Fig. 2B).

Matrices for 3D Culture.

A salient feature of 3D organotypic methods is the utilization of an ECM to provide the necessary structural and biochemical cues for proper glandular differentiation and homeostasis. A wide variety of materials have been utilized, each with their own pros and cons (Table 1). Reconstituted basement membranes (rBM) from Engelbreth-Holm-Swarm (EHS) mouse sarcomas have been routinely employed to study mammary morphogenesis as well as for the study of cellular transformation and carcinogenesis (12, 28). EHS is composed primarily of the basement membrane components laminin-1, collagen 4, and entactin (29). Recent studies corroborate that the exogenously provided laminin in the EHS-derived matrix drives the morphogenetic process when mammary epithelial cells are cultured three-dimensionally (30). Various nontransformed mammary epithelial cell lines can be induced to undergo acinar morphogenesis, including S1 cells (from the HMT-3522 progression series), and MCF-10A cells, which are human in origin, as well as mouse mammary epithelial cell lines, such as Scp2 and Eph4 (28, 31-35). In addition, primary mouse and human mammary epithelial cells also form polarized structures with a hollow lumen when cultured three-dimensionally (30, 36).

However, because EHS is isolated from a mouse tumor xenograft, it has a complex and ill-defined composition, which is subject to inherent lot-to-lot variability. In contrast, employing

an ECM scaffold in which the stoichiometry of critical components can be easily manipulated and controlled provides certain experimental advantages. Accordingly, collagen I has been utilized as a 3D matrix. Certain epithelial cells, most notably Madin-Darby Canine Kidney (MDCK) epithelial cells, develop into polarized cysts with a hollow lumen when embedded within matrices comprised of collagen I (37). Collagen I is biologically better defined than EHS and can be easily manipulated through changes in concentration, orientation, and biochemical modification (30, 38-41). Unfortunately, numerous epithelial cell types fail to form polarized acini when cultured in collagen I gels, whereas they do in laminin-rich rBM. Growing evidence indicates that the mechanical properties of the 3D matrix are also critical for the development of polarized, differentiated acinar structures. This was originally revealed in a series of studies involving normal breast epithelium grown on top of floating or attached collagen gels; mammary architecture, metabolic function and differentiation could only be maintained in the malleable, floating collagen gel (42, 43). Nonetheless, the range in elastic modulus achieved through the use of collagen I remains limited due to biochemical constraints. This becomes especially problematic with the increasing prominence of studies deciphering the effects of mechanotransduction in tissues. Finally, like rBM, collagen I is a biologically derived material and thus can present with experimental variability between preparations. Thus, newer techniques incorporating synthetic materials are now being utilized in 3D organotypic culture systems.

One system currently in use involves the deployment of polyacrylamide gels functionally cross-linked to ECM components upon which cells can be seeded (44). Polyacrylamide is a non-reactive material that can be easily manipulated through altering the concentrations of acrylamide and bis-acrylamide crosslinker, thereby allowing for precisely controlled biochemical and mechanical properties. However, because acrylamide is cytotoxic in monomeric form, cells cannot be directly embedded in this material for 3D studies. To preclude this limitation, cells

seeded upon polyacrylamide gels are overlaid with a blanket of rBM, resulting in a pseudo-3D system (Fig. 2A) (45). As this system is neither 2D nor 3D, cell behavior can be different than that observed in more traditional 3D culture systems, which can cause difficulty in interpreting results. As an alternative, conjugated self-assembling peptide polymer gels and protein-conjugated methylcellulose and peptide-immobilized PEG gels which are biocompatible for 3D and *in vivo* studies are now available for study, yet await rigorous experimental validation (46, 47).

Overall, a variety of matrix substrates and scaffolds can be utilized for 3D organotypic culture systems. As a result, interpretations of data from such experiments need to be weighed against limitations of the particular system in use. In the following sections, we highlight some of the applications of these techniques and resulting recent findings regarding mammary development and carcinogenesis.

APOPTOSIS AND LUMEN FORMATION.

The 3D culture of mammary epithelial cell lines has been commonly used as an *in vitro* model of epithelial development. When cultured in reconstituted basement membrane, mammary epithelial cells form growth-arrested acini in an ordered sequence of events (Fig. 3). In the early stages of culture, cells form clusters surrounded by the extracellular matrix. As cultures progress, two distinct cell populations emerge within each acinus—polarized cells around the outer layer in contact with the ECM that secrete basement membrane proteins, and non-polarized cells comprising the inner region. With further culturing, these inner cells undergo cell death and clearance leading to lumen formation.

Luminal Apoptosis.

Lumen formation appears to be due in part to apoptosis. Inhibition of apoptosis with caspase inhibitors in 3D cultures of primary mouse mammary epithelial cells results in delayed lumen formation (36). This is consistent with *in vivo* data in which mice overexpressing the anti-apoptotic protein Bcl-2 in a mammary-specific fashion exhibit a delay in mammary lumen development (24). Furthermore, data utilizing the cultured non-malignant mammary cell line MCF-10A has shown similar effects. MCF-10A cells undergo polarized formation of acini and lumen formation in 3D culture (Fig 3). In experiments in which Bcl-2 or Bcl-xL were overexpressed, luminal clearance was delayed in acini, again implicating apoptosis in lumen development (48).

Epithelial cells critically depend on integrin-mediated cell adhesion to ECM for proper growth and survival; *anoikis*, a form of apoptosis that epithelial cells undergo upon detachment from ECM, may contribute to lumen formation (49-51). Protection from *anoikis* may constitute a fundamental mechanism for tumor cell survival *in vivo* and might be responsible for luminal filling in glandular structures *in vitro* and *in vivo* (52, 53). As centrally located cells do not contact ECM, these cells may undergo death through *anoikis*. Consistent with this hypothesis, both MCF-10A *anoikis* and 3D lumen formation coincide with increased levels of the BH3 only pro-apoptotic protein Bim; RNAi mediated Bim depletion prevents both MCF-10A *anoikis* as well as luminal apoptosis in 3D culture (53) (54). Moreover, disrupting Bim in the mouse mammary gland prevents apoptosis and luminal clearance in TEBs during puberty (55). Overall, these studies highlight Bim as an important regulator of apoptosis resulting from the matrix detachment of cells occupying the 3D lumen.

In addition to cell-matrix interactions, cell-cell interactions may also regulate cell death ensuing in lumen formation as well. The molecule CEACAM1 (carcinoembryonic antigen-

related cell adhesion molecule 1) is a cell-cell adhesion molecule that has been identified as a regulator of lumen development. In MCF-10A cells, inhibition of CEACAM1 function results in the inhibition of lumen formation (56). Conversely, expression of CEACAM1 in MCF-7 cells, a mammary carcinoma cell line that does not normally express CEACAM1 or form a lumen in 3D culture, results in luminal development showing that extracellular cues contribute to lumen formation as well (57).

Luminal Filling By Cancer Genes.

Though apoptosis plays an important role in the formation of the mammary lumen, inhibition of apoptotic pathways delay, but do not completely inhibit, luminal clearing. The tight control of proliferation also plays a role because overexpression of cyclin D1 or inhibition of the retinoblastoma proteins (Rb) through expression of the HPVE7 results in a similar delay in lumen clearance (48). However, as is true of apoptosis inhibition, lumen formation is postponed, not ablated, with enhanced cellular proliferation. Thus, it appears to be a combination of both apoptotic inhibition and enhanced proliferation as activation of ErbB2, the gene product of *HER2/NEU*, which can induce both proliferation and inhibit apoptosis, results in luminal filling (34, 48). Notably, in some early human breast precancerous lesions, such as atypical ductal hyperplasias, a hollow architecture is maintained in the context of hyperproliferation, whereas advanced lesions like DCIS exhibit varying degrees of luminal filling, Hence, one may speculate that in early breast lesions, architectural changes induced by proliferative signals are limited due to compensatory increases in apoptosis. In contrast, more advanced phenotypes may express anti-apoptotic signals that allow survival of these excess proliferating cells.

ErbB2 is a receptor tyrosine kinase from a group of four (ErbB1-4) that bind growth factors from the EGF family. Binding of the ErbB receptors to EGF ligands can occur via homo-

or heterodimerization thereby leading to a complex array of signaling (58-60). ErbB2 is often overexpressed or amplified in breast tumors and correlates with a poor clinical prognosis (61, 62). Activation of the ErbB2 during MCF-10A morphogenesis elicits a complex multiacinar phenotype. Similar hyperplastic lesions, notable for the presence of multiacinar clusters, have been observed *in vivo* in tumors upon transgenic expression of activated *Neu* (NeuT) in the mouse mammary gland, as well as when primary tumor cells isolated from these mice are cultured on EHS (63-65). These altered structures exhibit the cardinal features of early stage cancers, including high levels of proliferation, filling of the lumen, and the disruption of cell polarity. However, activation of ErbB2 in MCF-10A cells not cause anchorage independent growth or an invasive phenotype in 3D culture. These results suggest that ErbB2 can play a role in the initial stages of transformation, but alone is not sufficient for progression to invasive breast cancer (34).

Hence, other factors may synergize with ErbB2 to promote invasion and metastasis. Recent work utilizing a mutant of β4 integrin in which the signaling capacity, but not the ability for adhesion, was ablated demonstrates that β4 integrin can amplify the signaling capability of ErbB2 and may thereby contribute to mammary tumor progression. β4 integrin can form a complex with ErbB2, thus enabling it to activate c-Jun and STAT3 and induce two hallmarks of oncogenesis, proliferation and loss of cell adhesion. This study suggests that β4 integrin can function as both an essential component of ErbB2-induced oncogenesis and as a potential therapeutic target (66).

Following the groundbreaking studies of ErbB2 in 3D culture, the activation of numerous other growth factor receptors and oncogenes have subsequently been interrogated in the MCF-10A acini model; some examples include Colony Stimulating Factor 1 Receptor (CSF1-R) (67), Insulin Growth Factor Receptor (IGFR) (68), Akt/PKB (69), and

phosphotidylinositol 3-kinase (PI3K) (70). As predicted, activation of these pathways elicit varying degrees of luminal filling, which result from increased proliferation combined with protection from apoptosis in the 3D lumen. Nonetheless, each of these molecules mediates additional distinctive biological activities in 3D culture, which ultimately influences the morphogenetic phenotype in unexpected ways. These phenotypes, along with the corresponding *in vivo* histological correlates, have already been the subject of a recent review (14).

Autophagy.

Though much work has been done analyzing the effects of the classical pathways of cell death in lumen formation, recent work suggests that another process, autophagy, may play a role in lumen clearance. Autophagy is an evolutionarily conserved lysosomal degradation process where a cell degrades its own cytoplasmic contents (i.e. "eats itself"). In eukaryotic cells, autophagy is a key mechanism for long-lived protein degradation and organelle turnover, and serves as a critical prosurvival mechanism during nutrient deprivation or stress (71, 72). It has been proposed that when excessive autophagy occurs within a cell, a distinct form of programmed cell death ensues (termed type 2 death) (73). Remarkably, in experiments investigating the ultrastructure of cells during post-lactational involution of the mouse mammary gland, autophagic vacuoles were seen in early stages of involution (74). Similarly, 3D culture studies suggest the involvement of autophagy in lumen formation (48). Furthermore, TRAIL (tumor necrosis factor related apoptosis inducing ligand) may be involved in this process as treatment with exogenous TRAIL induces autophagy in MCF-10A cells and expression of a dominant negative TRAIL receptor cooperates with Bcl-2 overexpression to increase luminal filling (75). Although these results implicate the potential for TRAIL-induced autophagy during luminal clearance, they are nonetheless correlative and largely ignore a salient feature MCF-10A

acinar morphogenesis -- that the outer cells of developing acini exhibit direct ECM contact on their basal surface, whereas the central cells do not (48). Thus, one can alternatively predict that autophagy is actually induced during *anoikis* as a protective mechanism to mitigate the stresses of ECM detachment. Loss-of-function studies of autophagy genes (called *ATG*s) are required to precisely validate the role of autophagy in cell survival versus type 2 death during 3D lumen formation (73).

MAMMARY EPITHELIAL POLARITY.

In addition to luminal filling, mammary carcinoma can also be characterized by a loss in epithelial polarity. Glandular epithelial tissues consist of cells exhibiting a characteristic polarity in which the apical poles face inward toward the central lumen, the lateral face mediates cell-cell contacts, and the basal face contacts the ECM (Fig 4). This polarity is often disrupted in early carcinomas, which is generally considered a poor prognostic sign. 3D culture models are beginning to address if intrinsic polarity regulators directly regulate cancer-promoting functions. The best-characterized 3D model to study epithelial polarization utilizes Madin-Darby canine kidney (MDCK) cells grown in a collagen I matrix. MDCK cells undergo cystogenesis in 3D culture characterized by polarized cells surrounding a cleared central lumen; moreover, the cells comprising these cysts form tight junctions, making this model advantageous for the study of mechanisms governing epithelial polarity.

Cell intrinsic regulators of polarity.

Invertebrate models have provided a wealth of genetic information about the regulation of polarity in epithelial tissues (76, 77). Cell polarity is believed to be controlled by the interplay of three major complexes broadly defined as the Par complex, the Scribble complex, and the Crumbs complex (78, 79). The concurrent activities of these three complexes combine to

formulate apical and basal polarity in epithelial cells (80-82). Nonetheless, much remains to be learned about these fundamental regulators during cancer initiation and progression.

Recent studies of MDCK cyst formation have poignantly illustrated that specific proteins in these polarity regulator complexes are critical for the development of polarity and lumen formation. The mammalian orthologues of three genes involved in epithelial polarity in Drosophila —CRB3, PALS1, and PATJ—exist in a macromolecular complex that localizes to the tight junction in MDCK cells (83, 84). The ablation of PALS1 by RNA interference elicits a concomitant loss of PATJ in MDCK cells, and completely disrupts apicobasal polarity when these cells are grown in 3D culture. The resulting structures do not form a central lumen; instead, they contain multiple small and incomplete lumens, or completely lack a lumen altogether. In addition, well-established markers of apical polarity in MDCK cells, such as GP135, are completely mislocalized in these structures (85). Notably, the formation of multiple small lumens in these MDCK structures highly resembles the cribriform patterns observed in breast DCIS and in certain prostate hyperplasias (14).

Two recent key reports have focused specifically on the convergence of signaling pathways upon the apical protein complex Par-3/Par6/atypical PKC (aPKC) resulting in the establishment of epithelial polarity. The first analyzes a molecular mechanism connecting phosphatase and tensin homolog on chromosome 10 (PTEN) signaling to formation of the apical surface and lumen. siRNA-mediated PTEN depletion in MDCK cells grown in rBM results in the formation of multiple small lumens upon cytogenesis versus the single central lumen seen in controls, suggesting that PTEN signaling regulates epithelial polarity and central lumen formation (86). Furthermore, markers segregating with the PTEN phospholipid product PI(4,5)P2, which is normally confined to the apical border and PI(3,4,5)P3, its basolateral precursor, show altered localization. Furthermore, addition of exogenous PI(4,5)P2 basolaterally

to cysts resulted relocation of the apical marker gp135 and tight junction component zona occludins 1 (ZO-1) to basolateral membranes, thus highlighting a role for this PTEN-regulated lipid product in establishing polarity. Moreover, exogenously applied PI(4,5)P2 to the basolateral membrane of MDCK cysts also targets activated Cdc42 to the basolateral membrane. Finally, both PTEN and Cdc42 regulate the apical location of Par6/aPKC, because depletion of either molecule results in the aberrant intracellular localization of aPKC. Importantly, aPKC inhibition disrupts central lumen formation in cysts. Overall, these results elegantly delineate interconnections between PTEN, Par6/aPKC, Cdc42, and the establishment of epithelial polarity and central lumen formation.

A second report establishes a link between Par6/aPKC and the effects of the oncogene ErbB2 on polarity (87). In this report, ErbB2 activation disrupts apicobasal polarity as characterized by changes in ZO-1 and gp135 localization in 2D cultures of MDCK cells. This coincides with loss of Par6 localization at the apical-lateral border. Interestingly, activation of ErbB2 leads to a decrease in the association of Par3 with Par6 and aPKC, as seen in contact naïve cells, thereby suggesting that ErbB2 inhibits appropriate cell-cell junction assembly through inhibition of Par3/Par6/aPKC complex formation. Furthermore, ErbB2 directly associates with Par6 and aPKC suggesting that the formation of this trimeric complex inhibits Par3 association. In addition, this interaction requires ErbB2 dimerization, thereby suggesting a mechanism by which ErbB2 leads to a break down in cell-cell contacts in *HER2/NEU* positive cancers. Similar results are observed in ErbB2-expressing MCF-10A cells. Also, in 3D MCF-10A culture, multiacinar structures are observed in cells expressing wild-type Par6, but not in cells expressing an aPKC binding-deficient mutant of Par6, suggesting that the ErbB2-Par6-aPKC complex is responsible for the multiacinar phenotype induced by ErbB2. Interestingly, cellular proliferation is similar in wild type and mutant Par6 cells, demonstrating that the

signaling pathways through which ErbB2 induces proliferation are completely distinct from those altering cell polarity.

ECM and Polarity.

In addition to the cell intrinsic regulators and pathways, the ECM itself plays a critical instructive role in the generation of apicobasal polarity. Classical 3D studies investigating polarity reversal in MDCK cysts and thyroid follicles point to the importance of ECM as a polarity cue (37, 88). When grown in liquid suspension culture, these cells form structures in which the free apical surface points away from the central axis of the sphere and toward the surrounding culture medium on the outside; these structures still generate a basal surface but it is in the interior of the structure, created by depositing basement membrane into an internal cavity. When the inverted MDCK cysts are embedded in collagen I, thus providing a strong ECM cue on the outside of these structures, extensive cellular remodeling occurs, resulting in cysts with a central hollow lumen(37). The plasticity of cyst organization in response to varying external cues indicates that epithelial cells possess hard-wired mechanisms for generating polarity within the context of a 3D tissue structure and furthermore, that ECM plays a fundamental instructive role in directing these mechanisms.

Interestingly, intracellular signaling pathways have been demonstrated to regulate the polarity of a glandular structure by actively modifying the surrounding basement membrane. In MDCK cysts, the orientation of apical poles requires the small GTPase Rac1, which mediates the proper assembly of laminin at the cyst-ECM interface. Expression of a dominant negative Rac1 (N17Rac) in MDCK cysts inverts the apical pole toward the cyst periphery; remarkably, this polarity reversion is only observed in 3D, but not 2D cultures. By providing an exogenous source of laminin to the cyst periphery, one can rescue the phenotypic effects of Rac inhibition on

MDCK cyst formation (89). Once again, these results poignantly illustrate how cell intrinsic pathways can influence tissue morphogenesis.

Overall, several questions on the relationship between ECM and the generation of apicobasal polarity remain unanswered, all of which are fundamental for understanding the role of polarity in early carcinoma pathogenesis. First, what are the signaling pathways downstream of ECM, tensional force, and adhesion (integrin) receptors that are responsible for generating the proper apicobasal axis in normally formed glands? Second, what is the crosstalk between cell matrix adhesion pathways and the intrinsic polarity regulating complexes? Finally, do specific components exist in any of the aforementioned pathways that can be used as a biomarker for early detection or targeted for therapeutic intervention in premalignant breast lesions? 3D culture models will prove useful for answering these important questions.

HMT-3522 SERIES--A REVERSIBLE MODEL OF TUMOR PROGRESSION

Early studies revealed that human breast tumor cell lines do not form acini when grown in 3D culture; rather, they develop into nonpolarized clusters with limited differentiation (28). These landmark experiments demonstrated the stark behavioral contrast between normal and tumor cells in 3D culture, even though very subtle phenotypic differences were evident when the same cells were grown as 2D monolayers. They also broached a fundamental biological and clinically relevant question regarding cancerous epithelium—could the disorganized, nonpolarized phenotype of tumorigenic cells be reorganized into a well-ordered normal architecture? Subsequently, numerous studies in the HMT-3522 model of human breast cancer progression have demonstrated that modulating aberrantly expressed cell adhesion proteins in tumor cells can dominantly interfere with the phenotypic expression of the transformed state, even in the context of multiple oncogenic mutations (90).

Phenotypic Reversion in 3D Culture.

The HMT-3522 progression series is a model of human breast cancer that progressively spans the continuum of morphological phenotype from normal cells to tumorigenesis (Fig. 5). In the series, a non-malignant S1 cell population forms growth arrested normal acinar structures in 3D, pre-malignant S2 cells form non-invasive proliferating non-polarized colonies, and malignant T4-2 cells exhibit a highly disorganized rapidly proliferating invasive structure in culture (31, 91, 92) (A. Rizki and V.M. Weaver, unpublished results).

In investigating the differences in these cell lines at the molecular level, T4-2 cells were found to display dramatically higher levels of β1 integrin and epidermal growth factor receptor (EGFR) as compared to non-malignant S1 cells. The T4-2 phenotype could be reversed by blocking β1 integrin signaling via a function-blocking antibody leading to the formation of growth-arrested acini similar to those observed in S1 cells (31). The HMT-3522 series also highlighted the intricate connection between β1 integrin and the EGFR signaling pathway because the mechanism leading to T4-2 phenotypic reversion is functionally linked to downregulation of both β1 integrin and the EGFR and their associated signaling networks (93). Conversely, neutralizing EGFR signaling results in normalized levels of β1 integrin signaling. Provocatively, these observed effects on tumor behavior completely depend on a 3D context because such reciprocal crosstalk between β1 integrin and EGFR is not observed in 2D monolayer cultures. Overall, these studies highlight the interplay of cell adhesion and growth factor receptor signaling pathways essential for maintaining the complex phenotypes during breast cancer progression.

The HMT-3522 series has also facilitated the identification of novel molecules with potential tumor suppressor function. T4-2 cells possess reduced levels of α-dystroglycan (α-DG), a basement membrane receptor. Upon restoration of dystroglycan in T4-2 cells, polarized

structures that are growth arrested form in 3D cultures; these cells also exhibit reduced tumorigenicity when engrafted into nude mice (94). Finally, analysis of multiple carcinoma cell lines indicate that higher levels of α-DG correlated with the increased ability of these cells to form polarized structures in 3D culture, and examination of human breast and prostate cancers have revealed losses in DG expression (94, 95). Although the exact role of dystroglycan in breast cancer remains unclear, these initial results obtained from 3D culture assays strongly intimate that it functions as a tumor suppressor and serves as a critical mediator of polarization effects induced by basement membrane (96)

Studies in other models have further substantiated the importance of cell adhesion proteins in modulating the tumor phenotype. α2 integrin is expressed in normal differentiated mammary epithelial cells and frequently lost in undifferentiated carcinomas. Re-expression of α2 in the Mm5MT mouse adenocarcinoma cell line causes a dramatic reversion from disorganized clusters of spindle-shaped cells to organized gland-like structures in 3D culture (97). In addition, re-expression of the cell adhesion molecule CEACAM1 in the MCF-7 human breast cancer cell line and the restoration of gap junctions in MDA-435 breast tumor cells have both been shown to promote the formation of organized spheroid structures (57, 98).

Polarity and Cell Survival.

The importance of polarity in tumor cell survival has also been demonstrated through 3D culture studies of the HMT-3522 progression series and MCF-10A cells. The formation of polarized 3D structures confers protection from apoptosis to a variety of chemotherapeutic insults in both normal and malignant mammary epithelial cells from the HMT-3522 progression series and MCF-10A cells (99) (J. Friedland and V. Weaver, submitted). In contrast, nonpolarized cells are uniformly sensitive to apoptosis (99). Accordingly, disrupting the activation of the laminin

receptor, $\alpha_6\beta_4$ integrin, perturbs hemidesmosome organization, disrupts polarity and promotes apoptosis(99). Interestingly, resistance to apoptosis can be acquired in nonpolar cells by the autocrine secretion of laminin 5, which results in the ligation of α6β4 integrin, as well as the activation of Rac and NFκB, a known positive modulator of cell survival (100). The excess secretion of laminin 5 in a non-polarized manner upon hyperactivation of growth factor receptors, such as ErbB2, has also been observed during MCF-10A morphogenesis, and may contribute to the ability of cells to survive in the lumen (34). Overall, these results indicate that the prosurvival effects associated with the polarized state in 3D culture can be co-opted by the activation of specific survival signals provided by non-polarized laminin 5 secretion.

Predicting Patient Outcome Using 3D Models.

More recently, a microarray analysis was conducted in S1 cells to search for transcripts that changed upon transition to an organized, growth-arrested state in 3D culture. These expression profiles were compared against a breast cancer-specific gene expression signature derived from patients of known outcomes to identify potential prognostic markers (101). In comparing transcripts that were downregulated in growth-arrested acini to previously published human breast cancer microarray data, a group of nineteen genes were selected to test as markers for cancer prognosis. Of these nineteen genes, fourteen significantly correlated with disease free survival. In addition, using a second less-restrictive strategy, 287 genes that were downregulated with the formation of growth-arrested 3D acini were tested for their ability to predict cancer prognosis and showed significant correlation with poor prognosis patient outcomes. This study thus represents an innovative method to identify genome-wide prognostic markers in breast cancer (101).

FORCE AS A REGULATOR OF ADHESION FORMATION AND SIGNALING.

In addition to intracellular signaling pathways mediating effects on tissue morphogenesis, the impact of force upon cells is quickly emerging as a mediator of cell growth, differentiation, and 3D tissue architecture. Within a given tissue, individual cells are subject to dynamic macro-forces mediated by the tissue as a whole, as well as microphysical forces resulting from local cell-cell and cell-ECM adhesion (See Sidebar). These forces dictate tissue architecture, and have been demonstrated to be critical for normal embryogenesis. Venous embryo explants require mechanical stress and strain for normal development and tissue differentiation (102). In Drosophila, formation of the dorsal-ventral axis in the fly embryo via the Armadillo-Twist signaling pathway requires cell compression that occurs through normal movement during morphogenesis; remarkably, this compression can be simulated by externally applying force with a micropipette (103). In addition, cells transduce force onto their surrounding milieu that is required for development. For example, *Xenopus* gastrulation requires the specific patterning of the small GTP binding proteins Rho and Rac, main mediators of cell adhesion and contractility, for orientation of the trunk and head mesoderm (104, 105).

Focal Adhesions and Force.

A variety of different types of distinct adhesions form between cells and the ECM, each with their own size, shape, and molecular composition (106, 107). These include focal adhesions, focal complexes, fibrillar adhesions, and three-dimensional matrix adhesions; the best characterized of these is the focal adhesion (FA) (108-110). Focal adhesions are relatively stable complexes that form through the coordinated interactions of various signaling, adaptor, and structural molecules, thereby linking the ECM and integrin receptors to the cytoskeleton (111). Binding of the ECM by adherent cells occurs via integrins, making them a central component of

microenvironmental sensing. Interestingly, force appears to play a role in the development of FAs as maturation of this complex has been shown to require mechanical tension (112, 113). Within minutes of placement of cells upon an ECM-coated surface, cells form focal complexes, small precursor adhesions to the larger FAs (114). By utilizing flexible substrates that deform upon cellular contraction, investigators have found that FA assembly and individual FA size positively correlate with the local distribution of force at adhesions (113, 115, 116). Similarly, in experiments where external forces are applied directly to adhesions, the strength of the FA increases with the amount of force applied (117-119). These results suggest that external stress and strain promote the formation and strength of adhesion complexes.

Many signaling proteins are located at cell-ECM contacts including focal adhesion kinase (FAK) and Src family kinases (120-122). As these proteins function in growth factor-mediated signaling cascades, their presence strongly suggests that signaling through adhesions coordinates integrin and growth factor signaling; moreover, they may translate ECM-associated mechanical stimuli to elicit changes in cellular morphology and function (123). FAK is an essential regulator of mechanotransduction; increased mechanical stress at FAs through increased intracellular tension or externally applied forces results in signaling changes at FAs through FAK activation of downstream signaling effectors (124, 125) (Fig 6). When mechanical stretch is applied to cells, FAK is activated, resulting both in increased magnitude and duration of activation of the mitogen-activated protein kinase ERK, and increased cellular proliferation (126, 127). FAK activation is required for ERK activation and subsequent progression of cells through G1 (128) (Fig 6). Interestingly, use of a kinase-dead mutant of FAK results in abrogation of ERK activation and leads to a block in mechanically-induced cellular proliferation (129, 130). Conversely, expression of a constitutively activated FAK leads to cellular transformation and adherence-independent growth (131). Taken together, these results suggest that FAK serves as a

major mediator of mechanotransduction and acts to translate extracellular forces sensed by integrins into proliferative cellular cues.

Force and Mammary Tissue Homeostasis.

During mammary morphogenesis, physical force, including clefting force and surface tension resulting from the interplay between the epithelial and mesenchymal tissues, has tremendous impact on the shaping of the ductal branches (132). In similarly branched tissues, such as the lung and kidney, the activity of the small protein GTPase Rho, a major signaling molecule in intracellular tension generation, plays a regulatory role in branching morphogenesis (133, 134) intimating a similar role for Rho in the developing mammary gland. Indeed, rigid 3D collagen gels influence branching behavior of malignantly transformed mammary epithelial cells in culture by regulating RhoA GTPase activity (135). Furthermore, the mechanical properties of the basement membrane are crucial for normal 3D mammary differentiation *in vitro*, because expression of milk proteins, such as β casein expression, only occurs on a highly compliant basement membrane or on floating collagen gels (26, 42). Conversely, the morphogenesis and functional differentiation of mammary epithelial acini cannot occur when MECs are placed on rigid collagen gels because collagen I does not facilitate proper cell rounding, and thus, hinders the assembly of an endogenous basement membrane at the basal cell surface. Therefore, the mechanical environment in which MECs exist can dictate their behavior.

Breast malignancy is characterized by a dramatic increase in mammary gland tension due to increased compression force and tensile stress resulting from altered vasculature and tumor growth as well as stiffening of the ECM due to fibrosis (18, 136). Such increased rigidity has been postulated to both impede treatment effectiveness and to enhance metastasis (137, 138). Because force is required for focal adhesion maturation and FAK-induced signaling, one can

hypothesized that increased tensional force in the mammary gland contributes to tumorigenesis via activation of integrin-linked proliferative signaling pathways in individual mammary epithelial cells. Moreover, since cells grown as 3D cultures behave differently with regard to cell morphology, integrin signaling, and actin cytoskeletal structures (108, 139), it is important to analyze the contribution of force to mammary malignancy within a 3D context.

Recently, matrix stiffness was linked to malignancy in the context of 3D architecture (Fig 7) (45). Using 3D tissue culture methods utilizing basement membrane/collagen I gels of increasing stiffness, MCF-10A cells and S1 cells from the HMT-3522 series were grown and allowed to form acini. Interestingly, acinar morphology was increasingly perturbed with increases in matrix stiffness resulting in non-spherical structures devoid of a central lumen and increased cell spreading, suggesting that the architectural tension surrounding MECs can alter normal 3D morphogenesis (Fig. 3). Furthermore, increased FAK activation was observed in cells grown in a stiff environment, implying that integrin adhesions may be altered in cells grown on a stiff matrix and that maturation of focal complexes into focal adhesions may take place more readily in a stiff environment. Interestingly, expression of mutant integrin subunits that promote integrin self-association and clustering led to a stiff-matrix cell phenotype with altered acini formation and increased cell spreading in a soft matrix environment. In addition, repressing ERK activity elicited phenotypic reversion in these cells implicating ERK signaling as a critical mediator of integrin-associated sensing of ECM compliance. Finally, matrix rigidity increased Rho activity and a constitutively active Rho mutant increased the number and size of FAs as well as promoted cell spreading in a soft environment (45). Overall, these 3D studies broached the concept that changes in mechanical properties may regulate cell behavior relevant for malignant transformation.

CONCLUSION:

The studies overviewed here illustrate the power of 3D epithelial culture models as a tractable *in vitro* approach to model the early events in breast carcinoma formation. In recent years, these models have greatly illuminated our understanding of the fundamental biological processes that direct the histological abnormalities observed microscopically during the earliest stages of breast cancer. They also have provided an unique platform to discover previously unappreciated mechanical influences on glandular epithelial architecture and homeostasis. Nevertheless, current 3D culture models do have inherent limitations in modeling *in vivo* tissue behavior. The further improvement of 3D culture systems, particularly the development of innovative heterotypic co-culture strategies and tunable biomaterial scaffolds, will be invaluable in modeling cancer progression and testing novel therapeutic strategies in a biologically relevant context.

SIDEBAR

What is Force?

Cells within tissues are exposed to a variety of mechanical stresses differing in magnitude and duration. These stresses are defined as force per unit area in N/m^2 with N=Newtons and m=meters and can be macro-forces, occurring at the level of the tissue, or micro-forces, due to the interaction of the cell with other cells or with the ECM. The intrinsic resistance of a given tissue to a stress is measured by the elastic modulus of that tissue, *E*, which is defined in Pascals (Pa) and can be obtained by applying a force to a section of tissue and measuring the relative change in length or strain. Generally, cells sense mechanical stress either as a parallel applied force, also known as shear stress, or as a perpendicularly applied force that includes both compressive stresses and tensile stresses.

ACKNOWLEDGEMENTS.

V.M.W. is supported by the NIH (RO1CA078731), and the DOD (DAMD1701-1-0368, 1703-1-0496, and W81XWH-05-1-330). J.D. is supported by the NIH (K08CA098419), a Culpeper Medical Scholarship (Partnership for Cures), an HHMI Early Career Award and the UCSF Sandler Program In Basic Sciences.

LITERATURE CITED.

1. Harris J, Lippman M, Morrow M, Osborne C. 1999. Diseases of the Breast. Philadelphia, PA: Lippincott Williams and Wilkens
2. Ernster VL, Barclay J, Kerlikowske K, Grady D, Henderson C. 1996. Incidence of and treatment for ductal carcinoma in situ of the breast. *Jama* 275: 913-8
3. Page DL, Dupont WD, Rogers LW, Rados MS. 1985. Atypical hyperplastic lesions of the female breast. A long-term follow-up study. *Cancer* 55: 2698-708
4. Burstein HJ, Polyak K, Wong JS, Lester SC, Kaelin CM. 2004. Ductal carcinoma in situ of the breast. *N Engl J Med* 350: 1430-41
5. Toikkanen S, Pylkkanen L, Joensuu H. 1997. Invasive lobular carcinoma of the breast has better short- and long-term survival than invasive ductal carcinoma. *Br J Cancer* 76: 1234-40
6. Simpson JF, Page DL. 2001. Pathology of preinvasive and excellent prognosis breast cancer. *Curr Opin Oncol* 13: 426-30
7. van de Vijver MJ, Peterse JL, Mooi WJ, Wisman P, Lomans J, et al. 1988. Neu-protein overexpression in breast cancer. Association with comedo-type ductal carcinoma in situ and limited prognostic value in stage II breast cancer. *N Engl J Med* 319: 1239-45
8. Ganesan S, Richardson AL, Wang ZC, Iglehart JD, Miron A, et al. 2005. Abnormalities of the inactive X chromosome are a common feature of BRCA1 mutant and sporadic basal-like breast cancer. *Cold Spring Harb Symp Quant Biol* 70: 93-7
9. Berx G, Cleton-Jansen AM, Strumane K, de Leeuw WJ, Nollet F, et al. 1996. E-cadherin is inactivated in a majority of invasive human lobular breast cancers by truncation mutations throughout its extracellular domain. *Oncogene* 13: 1919-25
10. Perou CM, Sorlie T, Eisen MB, van de Rijn M, Jeffrey SS, et al. 2000. Molecular portraits of human breast tumours. *Nature* 406: 747-52
11. Ramaswamy S, Tamayo P, Rifkin R, Mukherjee S, Yeang CH, et al. 2001. Multiclass cancer diagnosis using tumor gene expression signatures. *Proc Natl Acad Sci U S A* 98: 15149-54
12. Debnath J, Muthuswamy SK, Brugge JS. 2003. Morphogenesis and oncogenesis of MCF-10A mammary epithelial acini grown in three-dimensional basement membrane cultures. *Methods* 30: 256-68
13. Schmeichel KL, Bissell MJ. 2003. Modeling tissue-specific signaling and organ function in three dimensions. *J Cell Sci* 116: 2377-88
14. Debnath J, Brugge JS. 2005. Modelling glandular epithelial cancers in three-dimensional cultures. *Nat Rev Cancer* 5: 675-88

15. Coucouvanis E, Martin GR. 1995. Signals for death and survival: a two-step mechanism for cavitation in the vertebrate embryo. *Cell* 83: 279-87.
16. Dressler GR. 2006. The Cellular Basis of Kidney Development
doi:10.1146/annurev.cellbio.22.010305.104340. *Annual Review of Cell and Developmental Biology* 22: 509-29
17. Barros E, Santos O, Matsumoto K, Nakamura T, Nigam S. 1995. Differential Tubulogenic and Branching Morphogenetic Activities of Growth Factors: Implications for Epithelial Tissue Development
10.1073/pnas.92.10.4412. *PNAS* 92: 4412-6
18. Paszek M, Weaver V. 2004. The tension mounts: mechanics meets morphogenesis and malignancy. *J Mammary Gland Biol Neoplasia* 9: 325-242
19. Sternlicht MD. 2006. Key stages in mammary gland development: the cues that regulate ductal branching morphogenesis. *Breast Cancer Res* 8: 201
20. Fata J, Werb Z, Bissell M. 2004. Regulation of mammary gland branching morphogenesis by the extracellular matrix and its remodeling enzymes. In *Breast Cancer Res*, pp. 1 - 11
21. Sternlicht MD, Kouros-Mehr H, Lu P, Werb Z. 2006. Hormonal and local control of mammary branching morphogenesis
doi:10.1111/j.1432-0436.2006.00105.x. In *Differentiation*, pp. 365-81
22. Howard BA, Gusterson BA. 2000. Human breast development. *J Mammary Gland Biol Neoplasia* 5: 119-37
23. Hennighausen L, Robinson GW. 2005. Information networks in the mammary gland. *Nat Rev Mol Cell Biol* 6: 715-25
24. Humphreys R, Krajewska M, Krnacik S, Jaeger R, Weiher H, Krajewski S. 1996. Apoptosis in the terminal endbud of the murine mammary gland: a mechanism of ductal morphogenesis. *Development* 122: 4013-22
25. Bissell MJ, Barcellos-Hoff MH. 1987. The influence of extracellular matrix on gene expression: is structure the message? *J Cell Sci Suppl* 8: 327-43
26. Barcellos-Hoff M, Aggeler J, Ram T, Bissell M. 1989. Functional differentiation and alveolar morphogenesis of primary mammary cultures on reconstituted basement membrane. In *Development*, pp. 223-35
27. Streuli CH, Bissell MJ. 1990. Expression of extracellular matrix components is regulated by substratum. *J Cell Biol* 110: 1405-15
28. Petersen OW, Ronnov-Jessen L, Howlett AR, Bissell MJ. 1992. Interaction with basement membrane serves to rapidly distinguish growth and differentiation pattern of normal and malignant human breast epithelial cells [published erratum appears in Proc Natl Acad Sci U S A 1993 Mar 15;90(6):2556]. *Proc Natl Acad Sci U S A* 89: 9064-8
29. Grant DS, Kleinman HK, Leblond CP, Inoue S, Chung AE, Martin GR. 1985. The basement-membrane-like matrix of the mouse EHS tumor: II. Immunohistochemical quantitation of six of its components. *Am J Anat* 174: 387-98
30. Gudjonsson T, Ronnov-Jessen L, Villadsen R, Rank F, Bissell MJ, Petersen OW. 2002. Normal and tumor-derived myoepithelial cells differ in their ability to interact with luminal breast epithelial cells for polarity and basement membrane deposition. *J Cell Sci* 115: 39-50
31. Weaver VM, Petersen OW, Wang F, Larabell CA, Briand P, et al. 1997. Reversion of the malignant phenotype of human breast cells in three- dimensional culture and in vivo by integrin blocking antibodies. *J Cell Biol* 137: 231-45

32. Niemann C, Brinkmann V, Spitzer E, Hartmann G, Sachs M, et al. 1998. Reconstitution of mammary gland development in vitro: requirement of c-met and c-erbB2 signaling for branching and alveolar morphogenesis. *J Cell Biol* 143: 533-45
33. Roskelley CD, Desprez PY, Bissell MJ. 1994. Extracellular matrix-dependent tissue-specific gene expression in mammary epithelial cells requires both physical and biochemical signal transduction. *Proc Natl Acad Sci U S A* 91: 12378-82
34. Muthuswamy SK, Li D, Lelievre S, Bissell MJ, Brugge JS. 2001. ErbB2, but not ErbB1, reinitiates proliferation and induces luminal repopulation in epithelial acini. *Nat Cell Biol* 3: 785-92
35. Dimri G, Band H, Band V. 2005. Mammary epithelial cell transformation: insights from cell culture and mouse models. *Breast Cancer Research* 7: 171 - 9
36. Blatchford DR, Quarrie LH, Tonner E, McCarthy C, Flint DJ, Wilde CJ. 1999. Influence of microenvironment on mammary epithelial cell survival in primary culture. *J Cell Physiol* 181: 304-11
37. Wang AZ, Ojakian GK, Nelson WJ. 1990. Steps in the morphogenesis of a polarized epithelium. II. Disassembly and assembly of plasma membrane domains during reversal of epithelial cell polarity in multicellular epithelial (MDCK) cysts. *J Cell Sci* 95 (Pt 1): 153-65
38. Roeder BA, Kokini K, Sturgis JE, Robinson JP, Voytik-Harbin SL. 2002. Tensile mechanical properties of three-dimensional type I collagen extracellular matrices with varied microstructure. *J Biomech Eng* 124: 214-22
39. Christner PJ, Gentiletti J, Peters J, Ball ST, Yamauchi M, et al. 2006. Collagen dysregulation in the dermis of the Sagg/+ mouse: a loose skin model. *J Invest Dermatol* 126: 595-602
40. Girton TS, Oegema TR, Tranquillo RT. 1999. Exploiting glycation to stiffen and strengthen tissue equivalents for tissue engineering. *J Biomed Mater Res* 46: 87-92
41. Martin RB, Lau ST, Mathews PV, Gibson VA, Stover SM. 1996. Collagen fiber organization is related to mechanical properties and remodeling in equine bone. A comparison of two methods. *J Biomech* 29: 1515-21
42. Emerman J, Pitelka D. 1977. Maintenance and induction of morphological differentiation in dissociated mammary epithelium on floating collagen membranes. *In Vitro* 13: 316-28
43. Emerman JT, Bartley JC, Bissell MJ. 1980. Interrelationship of glycogen metabolism and lactose synthesis in mammary epithelial cells of mice. *Biochem J* 192: 695-702
44. Pelham RJ, Jr., Wang Y. 1997. Cell locomotion and focal adhesions are regulated by substrate flexibility. *Proc Natl Acad Sci U S A* 94: 13661-5
45. Paszek MJ, Zahir N, Johnson KR, Lakins JN, Rozenberg GI, et al. 2005. Tensional homeostasis and the malignant phenotype. *Cancer Cell* 8: 241-54
46. Raeber GP, Lutolf MP, Hubbell JA. 2005. Molecularly Engineered PEG Hydrogels: A Novel Model System for Proteolytically Mediated Cell Migration
10.1529/biophysj.104.050682. *Biophys. J.* 89: 1374-88
47. Vinatier C, Magne D, Weiss P, Trojani C, Rochet N, et al. 2005. A silanized hydroxypropyl methylcellulose hydrogel for the three-dimensional culture of chondrocytes. *Biomaterials* 26: 6643-51
48. Debnath J, Mills K, Collins N, Reginato M, Muthuswamy S, Brugge J. 2002. The role of apoptosis in creating and maintaining luminal space within normal and oncogene-expressing mammary acini. *Cell* 111: 29-40
49. Meredith JE, Jr., Fazeli B, Schwartz MA. 1993. The extracellular matrix as a cell survival factor. *Mol Biol Cell* 4: 953-61

50. Frisch SM, Francis H. 1994. Disruption of epithelial cell-matrix interactions induces apoptosis. *J Cell Biol* 124: 619-26
51. Boudreau N, Sympson CJ, Werb Z, Bissell MJ. 1995. Suppression of ICE and apoptosis in mammary epithelial cells by extracellular matrix. *Science* 267: 891-3
52. Gilmore AP. 2005. Anoikis. *Cell Death Differ* 12 Suppl 2: 1473-7
53. Reginato M, Mills K, Becker E, Lynch D, Bonni A, et al. 2005. Bim regulation of lumen formation in cultured mammary epithelial acini is targeted by oncogenes. *Mol Cell Bio* 25: 491-4601
54. Reginato MJ, Mills KR, Paulus JK, Lynch DK, Sgroi DC, et al. 2003. Integrins and EGFR coordinately regulate the pro-apoptotic protein Bim to prevent anoikis. *Nat Cell Biol* 5: 733-40
55. Mailleux AA, Overholtzer M, Schmelzle T, Bouillet P, Strasser A, Brugge JS. 2007. BIM regulates apoptosis during mammary ductal morphogenesis, and its absence reveals alternative cell death mechanisms. *Dev Cell* 12: 221-34
56. Huang J, hardy J, Sun Y, Shively J. 1999. Essential role of biliary glycoprotein (CD66a) in morphogenesis of the human mammary epithelial cell lilne MCF10F. *J Cell Sci* 112: 4193-205
57. Kirshner J, Chen C, Liu P, Huang J, Shively J. 2003. CEACAM1-4S, a cell-cell adhesion molecule, mediates apoptosis and reverts mammary carcinoma cells to a normal morphogenic phenotype in a 3D culture. *Proc Natl Acad Sci*
58. Alroy I, Yarden Y. 1997. The ErbB signaling network in embryogenesis and oncogenesis: signal diversification through combinatorial lignad-receptor interactions. *FEBS Lett* 410: 83-6
59. Riese D, Stern D. 1998. Specificity within the EGF family/ErbB receptor family signaling network. *BioEssays* 20: 41-8
60. Olayioye M, Neve R, Lane H, Hynes N. 2000. The ErbB singaling network: receptor heterodimerization in development and cancer. *EMBO J* 19: 3159-67
61. Hynes N, Stern D. 1994. The biology of erbB-2/neu/HER-2 and its role in cancer. *Biochim Biophys Acta* 1198: 165-84
62. Harari D, Yarden Y. 2000. Molecular mechanisms underlying ErbB2/HER2 action in breast cancer. *Oncogene* 19: 6102-14
63. Moody SE, Sarkisian CJ, Hahn KT, Gunther EJ, Pickup S, et al. 2002. Conditional activation of Neu in the mammary epithelium of transgenic mice results in reversible pulmonary metastasis. *Cancer Cell* 2: 451-61
64. Muraoka RS, Koh Y, Roebuck LR, Sanders ME, Brantley-Sieders D, et al. 2003. Increased malignancy of Neu-induced mammary tumors overexpressing active transforming growth factor beta1. *Mol Cell Biol* 23: 8691-703
65. Wulf G, Garg P, Liou YC, Iglehart D, Lu KP. 2004. Modeling breast cancer in vivo and ex vivo reveals an essential role of Pin1 in tumorigenesis. *Embo J* 23: 3397-407
66. Wenjun G, Pylayeva Y, Pepe A, Yoshioka T, Muller W, et al. 2006. Beta four integrin amplifies ErbB2 signaling to promote mammary tumorigenesis. *Cell* 126: 489-502
67. Wrobel CN, Debnath J, Lin E, Beausoleil S, Roussel MF, Brugge JS. 2004. Autocrine CSF-1R activation promotes Src-dependent disruption of mammary epithelial architecture. *J Cell Biol* 165: 263-73
68. Irie HY, Pearline RV, Grueneberg D, Hsia M, Ravichandran P, et al. 2005. Distinct roles of Akt1 and Akt2 in regulating cell migration and epithelial-mesenchymal transition. *J Cell Biol* 171: 1023-34

69. Debnath J, Walker SJ, Brugge JS. 2003. Akt activation disrupts mammary acinar architecture and enhances proliferation in an mTOR-dependent manner. *J Cell Biol* 163: 315-26
70. Isakoff SJ, Engelman JA, Irie HY, Luo J, Brachmann SM, et al. 2005. Breast cancer-associated PIK3CA mutations are oncogenic in mammary epithelial cells. *Cancer Res* 65: 10992-1000
71. Klionsky DJ, Emr SD. 2000. Autophagy as a regulated pathway of cellular degradation. *Science* 290: 1717-21
72. Levine B, Klionsky DJ. 2004. Development by self-digestion: molecular mechanisms and biological functions of autophagy. *Dev Cell* 6: 463-77
73. Debnath J, Baehrecke EH, Kroemer G. 2005. Does autophagy contribute to cell death? *Autophagy* 1: 66-74
74. Helminen H, Ericsson J. 1968. Studies on mammary gland involution II. Ultrastructural evidence for auto- and heterophagocytosis. *J Ultrastruct Res* 25: 214-27
75. Mills K, Reginato M, Debnath J, Queenan B, Brugge J. 2004. Tumor necrosis factor-related apoptosis-inducing ligand (TRAIL) is required for induction of autophagy during lumen formation in vitro. *Proc Natl Acad Sci U S A* 101: 3438-43
76. Humbert P, Russell S, Richardson H. 2003. Dlg, Scribble and Lgl in cell polarity, cell proliferation and cancer. *Bioessays* 25: 542-53
77. Knust E, Bossinger O. 2002. Composition and formation of intercellular junctions in epithelial cells. *Science* 298: 1955-9
78. Nelson WJ. 2003. Adaptation of core mechanisms to generate cell polarity. *Nature* 422: 766-74
79. Bilder D. 2004. Epithelial polarity and proliferation control: links from the Drosophila neoplastic tumor suppressors. *Genes Dev* 18: 1909-25
80. Medina E, Lemmers C, Lane-Guermonprez L, Le Bivic A. 2002. Role of the Crumbs complex in the regulation of junction formation in Drosophila and mammalian epithelial cells. *Biol Cell* 94: 305-13
81. Suzuki A, Ohno S. 2006. The PAR-aPKC system: lessons in polarity
10.1242/jcs.02898. *J Cell Sci* 119: 979-87
82. Humbert PO, Dow LE, Russell SM. 2006. The Scribble and Par complexes in polarity and migration: friends or foes? *Trends Cell Biol* 16: 622-30
83. Roh MH, Makarova O, Liu CJ, Shin K, Lee S, et al. 2002. The Maguk protein, Pals1, functions as an adapter, linking mammalian homologues of Crumbs and Discs Lost. *J Cell Biol* 157: 161-72
84. Makarova O, Roh MH, Liu CJ, Laurinec S, Margolis B. 2003. Mammalian Crumbs3 is a small transmembrane protein linked to protein associated with Lin-7 (Pals1). *Gene* 302: 21-9
85. Straight SW, Shin K, Fogg VC, Fan S, Liu CJ, et al. 2004. Loss of PALS1 expression leads to tight junction and polarity defects. *Mol Biol Cell* 15: 1981-90
86. Martin-Belmonte F, Gassama A, Datta A, Yu W, Rescher U, et al. 2007. PTEN-mediated apical segregation of phosphoinositides controls epithelial morphogenesis through Cdc42. *Cell* 128: 383-97
87. Aranda V, Haire T, Nolan ME, Calarco JP, Rosenberg AZ, et al. 2006. Par6-aPKC uncouples ErbB2 induced disruption of polarized epithelial organization from proliferation control. *Nat Cell Biol* 8: 1235-45

88. Chambard M, Verrier B, Gabrion J, Mauchamp J. 1984. Polarity reversal of inside-out thyroid follicles cultured within collagen gel: reexpression of specific functions. *Biol Cell* 51: 315-25
89. O'Brien LE, Jou TS, Pollack AL, Zhang Q, Hansen SH, et al. 2001. Rac1 orientates epithelial apical polarity through effects on basolateral laminin assembly. *Nat Cell Biol* 3: 831-8
90. Kenny PA, Bissell MJ. 2003. Tumor reversion: correction of malignant behavior by microenvironmental cues. *Int J Cancer* 107: 688-95
91. Briand P, Petersen OW, Van Deurs B. 1987. A new diploid nontumorigenic human breast epithelial cell line isolated and propagated in chemically defined medium. *In Vitro Cell Dev Biol* 23: 181-8
92. Nielsen KV, Madsen MW, Briand P. 1994. In vitro karyotype evolution and cytogenetic instability in the non-tumorigenic human breast epithelial cell line HMT-3522. *Cancer Genet Cytogenet* 78: 189-99
93. Wang F, Weaver VM, Petersen OW, Larabell CA, Dedhar S, et al. 1998. Reciprocal interactions between beta1-integrin and epidermal growth factor receptor in three-dimensional basement membrane breast cultures: a different perspective in epithelial biology. *Proc Natl Acad Sci U S A* 95: 14821-6
94. Muschler J, Levy D, Boudreau R, Henry M, Campbell K, Bissell MJ. 2002. A role for dystroglycan in epithelial polarization: loss of function in breast tumor cells. *Cancer Res* 62: 7102-9
95. Henry MD, Cohen MB, Campbell KP. 2001. Reduced expression of dystroglycan in breast and prostate cancer. *Hum Pathol* 32: 791-5
96. Weir ML, Muschler J. 2003. Dystroglycan: emerging roles in mammary gland function. *J Mammary Gland Biol Neoplasia* 8: 409-19
97. Zutter MM, Santoro SA, Staatz WD, Tsung YL. 1995. Re-expression of the alpha 2 beta 1 integrin abrogates the malignant phenotype of breast carcinoma cells. *Proc Natl Acad Sci U S A* 92: 7411-5
98. Hirschi KK, Xu CE, Tsukamoto T, Sager R. 1996. Gap junction genes Cx26 and Cx43 individually suppress the cancer phenotype of human mammary carcinoma cells and restore differentiation potential. *Cell Growth Differ* 7: 861-70
99. Weaver V, Lelievre S, Lakins J, Chrenek M, Jones J, et al. 2002. beta4 integrin-dependent formation of polarized three-dimensional architecture confers resistance to apoptosis in normal and malignant mammary epithelium. *Cancer Cell* 2: 205
100. Zahir N, Lakins JN, Russell A, Ming W, Chatterjee C, et al. 2003. Autocrine laminin-5 ligates alpha6beta4 integrin and activates RAC and NFkappaB to mediate anchorage-independent survival of mammary tumors. *J Cell Biol* 163: 1397-407
101. Fournier MV, Martin KJ, Kenny PA, Xhaja K, Bosch I, et al. 2006. Gene expression signature in organized and growth-arrested mammary acini predicts good outcome in breast cancer. *Cancer Res* 66: 7095-102
102. Beloussov L, Lakirev A, Naumidi I. 1988. The role of external tensions in differentiation of Xenopus laevis embryonic tissues. *Cell Differ Dev* 25: 165-76
103. Farge E. 2003. Mechanical induction of Twist in the Drosophila foregut/stomodeal primordium. *Curr Biol* 13: 1365-77
104. Tahinchi E, Symes K. 2003. Distinct functions of Rho and Rac are required for convergent extension during Xenopus gastrulation. *Dev Biol* 259: 318-35

105. Ren R, Nagel M, Tahinci E, Winklbauer R, Symes K. 2006. Migrating anterior mesoderm cells and intercalating trunk mesoderm cells have distinct responses to Rho and Rac during Xenopus gastrulation. *Dev Dyn* 235: 1090-9
106. Zamir E, Geiger B. 2001. Molecular complexity and dynamics of cell-matrix adhesions. *J Cell Sci* 114: 3583-90
107. Zimerman B, Volberg T, Geiger B. 2004. Early molecular events in the assembly of the focal adhesion-stress fiber complex during fibroblast spreading. *Cell Motil Cytoskeleton* 58: 143-59
108. Cukierman E, Pankov R, Stevens D, Yakamada K. 2001. Taking cell-matrix adhesions to the third dimension. *Science* 294: 1708-12
109. Burridge K, Fath K, Kelly T, Nuckolls G, Turner C. 1988. Focal adhesions: transmembrane junctions between the extracellular matrix and the cytoskeleton. *Annu Rev Cell Biol* 4: 487-525
110. Zamir E, Katz M, Posen Y, Erez N, Yamada K, et al. 2000. Dynamics and segregation of cell-matrix adhesions in cultured fibroblasts. *Nat Cell Biol* 2: 191-6
111. Webb D, Parsons J, Horwitz A. 2002. Adhesion assembly, disassembly and turnover in migrating cells-over and over and over again. *Nat Cell Biol* 4: E97-E100
112. Ridley A, Hall A. 1992. The small GTP-binding protein rho regulates the assembly of focal adhesions and actin stress fibers in response to growth factors. *Cell* 70: 389-99
113. Balaban N, Schwarz U, Reveline D, Goichberg P, Tzur G, et al. 2001. Force and focal adhesion assembly: a close relationship studied using elastic microopatterned substrates. *Nat Cell Biol* 3: 466-72
114. Nobes C, Hall A. 1995. Rho, rac, and cdc42 GTPases regulate the assembly of multimolecular focal complexes associated with actin stress fibers, lamellipodia, and filopodia. *Cell* 81: 53-62
115. Beningo K, Wang Y. 2002. Flexible substrata for the detection of cellular traction forces. *Trends Cell Biol* 12: 79-84
116. Tan J, Tien J, Pirone D, Gray D, Bhadriraju K, Chen CS. 2003. Cells lying on a bed of microneedles: an approach to isolate mechanical force. *Proc Natl Acad Sci U S A* 100: 1484-9
117. Riveline D, Zamir E, Balaban N, Schwarz U, Ishizaki T, et al. 2001. Focal contacts as mechanosensors: externally applied local mechanical force induces growth of focal contacts by an mDia1-dependent and ROCK-independent mechanism. *J Cell Biol* 153: 1175-86
118. Galbraith C, Yamada K, Sheetz M. 2002. The relationship between force and focal complex development. *J Cell Biol* 159: 695-705
119. Choquet D, Felsenfeld D, Sheetz M. 1997. Extracellular matrix rigidity causes strengthening of integrin-cytoskeleton linkages. *Cell* 88: 39-48
120. Wang H, Dembo M, Hanks S, Wang Y. 2001. Focal adhesion kinase is involved in mechanosensing during fibroblast migration. *Proc. Natl. Acad. Sci. U.S.A.* 20
121. Volberg T, Romer L, Zamir E, Geiger B. 2001. pp60 (c-src) and related tyrosine kinases: a role in the assembly and reorganization of matrix adhesions. *J Cell Sci* 114: 2279-89
122. Felsenfeld D, Schwartzberg P, Venegas A, Tse R, Sheetz M. 1999. Selective regulation of integrin-cytoskeleton interactions by the tyrosind kinase Src. *Nat Cell Biol* 1: 200-6
123. Lee J, Juliano R. 2004. Mitogenic signal transduction by integrin- and growth factor receptor-mediated pathways. *Mol Cells* 17: 188-202
124. Sawada Y, Sheetz M. 2002. Force transduction by Triton cytoskeletons. *J.Cell Biol* 156: 609-15

125. Leopoldt D, Yee HJ, Roszengurt E. 2001. Calculin-A induces focal adhesion assembly and tyrosine phosphorylation of p125 Fak, p130 Cas, and paxillin in Swiss 3T3 cells. *J Cell Physiol* 188: 106-19
126. Torsoni A, Constancio S, Nadruz WJ, Hanks S, Franchini K. 2003. Focal adhesion kinase is activated and mediates the early hypertrophic response to stretch in cardiac myocytes. *Circ Res* 93: 140-7
127. Numaguchi K, Eguchi S, Yamakawa T, Motley E, Inagami T. 1999. Mechanotransduction of rat aortic vascular smooth muscle cells requires RhoA and intact actin filaments. *Circ Res* 85: 5-11
128. Renshaw M, Price L, Schwartz M. 1999. Focal adhesion kinase mediates the integrin signaling requirement for gowth factor activation of MAP kinase. *J Cell Biol* 147: 611-8
129. Li S, Kim M, Hu Y, Jalali S, Schlaepfer D, et al. 1997. Fluid shear stress activation of focal adhesion kinase. Linking to mitogen-activated protein kinases. *J Biol Chem* 272: 30455-62
130. Li W, Duzgun A, Sumpio B, Basson M. 2001. Integrin and FAK-mediated MAPK activation is required for cyclic strain mitogenic effects in Caco-2 cells. *Am J Physiol Gastrointes Liver Physiol* 280: G75-87
131. Frisch S, Vuori K, Ruoslahti E, Chan-Hui P. 1996. Control of adhesion-dependent cell survival by focal adhesion kinase. *J Cell Biol* 134: 793-9
132. Fleury V, Watanabe T. 2002. Morphogenesis of fingers and branched organs: How collagen and fibroblasts break the symmetry of growing biological tissue. *C R Biol* 325: 571-83
133. Miao H, Nickel C, Cantley L, Bruggeman L, Bennardo L, Wang B. 2003. EphA kinase activation regulates HGF-induced epithelial branching morphogenesis. *J Cell Biol* 162: 1281-92
134. Moore K, Huang S, Kong Y, Sunday M, Ingber D. 2002. Control of embryonic lung branching morphogenesis by the Rho activator, cytotoxic necrotizing factor1. *J Surg Res* 104: 95-100
135. Wozniak M, Desai R, Solski P, Der C, Keely P. 2003. ROCK-generated contractility regulates breast epithelial cell differentiation in response to the physical properties of a three-dimensional collagen matrix. *J Cell Biol* 163: 583-95
136. Padera T, Stoll B, Tooredman J, Capen D, di Tomaso E, Jain R. 2004. Pathology: cancer cells compress intratumour vessels. *Nature* 427: 695
137. Netti P, Berk D, Swartz M, Grodzinsky A, Jain R. 2000. Rold of extracellular matrix assembly in interstitial transport in solid tumors. *Cancer Res* 60: 2497-503
138. Akiri G, Sabo E, Dafni H, Vadasz Z, Kartvelishvily Y, et al. 2003. Lysyl oxidase-related protein-1 promotes tumor fibrosis and tumor progression in vivo. *Cancer Res* 63: 1657-66
139. Beningo K, Dembo M, Wang Y. 2004. Responses of fibroblasts to anchorage of dorsal extracellular matrix receptors. *Proc Natl Acad Sci U S A* 101: 18024-9

BRIEF PAPER ANNOTATIONS.

28. Petersen, O. W. et. al. 1992. Interaction with basement membrane serves to rapidly distinguish growth and differentiation pattern of normal and malignant human breast epithelial cells. *Proc Natl Acad Sci U S A* 89, 9064-8

Demonstrates stark phenotypic contrasts between normal cells and tumor cells when they are grown in 3D but not 2D cultures.

31. Weaver, V. M. et al. 1997. Reversion of the malignant phenotype of human breast cells in three- dimensional culture and in vivo by integrin blocking antibodies. *J Cell Biol* 137, 231-45

Blocking β1 integrin signaling in a tumor cell line reverts its abnormal tumor-like morphology in 3D culture. Thus, tissue phenotype of genotypically abnormal cells can be regulated in 3D by altering specific adhesion pathways.

34. Muthuswamy, S. K. et. al. 2001. ErbB2, but not ErbB1, reinitiates proliferation and induces luminal repopulation in epithelial acini. *Nat Cell Biol* 3, 785-92

The inducible dimerization of two closely related receptor tyrosine kinases of the EGFR family--ErbB1 and ErbB2---elicits distinct and unexpected effects on 3D epithelial architecture.

45. Paszek MJ et al. 2005. Tensional homeostasis and the malignant phenotype. *Cancer Cell* 8: 241-54

Increasing matrix stiffness disrupts normal 3D morphogenesis, demonstrating that mechanotransduction may directly regulate malignant transformation.

48. Debnath, J. et al. 2002. The Role of Apoptosis in Creating and Maintaining Luminal Space within Normal and Oncogene-Expressing Mammary Acini. *Cell* 111, 29

Demonstrates that filling of the 3D lumen commonly found in early breast cancers requires increased proliferation combined with increased survival of the excess proliferating cells in the lumen.

FIGURE LEGENDS

Figure 1. Terminal end bud (TEB) morphology. Diagram depicting the TEB including the highly prevalent body cells found adjacent to the lumen as well as the surrounding single layer of cap cells. Large numbers of stromal fibroblasts are found around the collar of the duct. Dotted line represents the thinning basal lamina that occurs at the edge of the invading ducts, though no evidence exists that ductal cells cross the basement membrane. Reproduced from (19, 21).

Figure 2. 3D Culture Methods. A) Schematic of commonly used techniques. Left: Complete embedding of MECs in rBM. Center: MECs seeded upon a thin layer of solidified rBM are overlaid with a dilute solution of rBM in culture media. Right: Polyacrylamide gel of a given elastic modulus is cast upon a glass coverslip and rBM is allowed to crosslink to the polyacrylamide. MECs are seeded upon the rBM/polyacrylamide matrix and overlaid with dilute rBM in culture media. B) Phase micrographs of day 18 MCF10A acini grown in overlay culture. Equatorial confocal cross-sections of a single acinus stained with ezrin/radixin/moesin (ERM, green), human discs large (hDLG, red), and DAPI (blue).

Figure 3. Lumen Formation in MCF-10A Acini. MCF-10A cells undergo an ordered series of morphogenetic events when grown in 3D culture. In early stages, developing cell clusters exhibit apicobasal polarization; thereafter, two distinct cell populations become discernable within each acinus--a well-polarized outer layer of cells in direct contact with ECM, and an inner subset of cells that is poorly polarized, and lacking contact with the matrix. These inners cells undergo apoptosis, characterized by expression of processed caspase 3, resulting in a hollow lumen. The hollow acinar structure remains stable thereafter. Microscopic images reproduced from (48).

Figure 4. Cross-section of polarized gland architecture. Each individual epithelial cell within an intact gland has a microvilli-rich apical membrane facing the lumen, a lateral membrane contacting adjacent cells, and a basal surface contacting the basement membrane (ECM). ECM attachment is mediated through integrin receptors and cell-cell junctions consist of tight junctions, adherens junctions and desmosomes. Tight junctions demarcate the boundary between apical and basolateral surfaces.

Figure 5. HMT-3522 Progression Series. S1 cells form normal polarized acini in three-dimensional culture (left). T4 cells show a disruption in ductal morphology and uncontrolled cellular proliferation (middle). Following treatment with an antibody blocking β1 integrin function (right), T4 cells undergo a morphogenetic reversion and form normal-appearing acini similar to the phenotype observed in S1 cells. Reproduced from (31, 91, 92).

Figure 6. Force-dependent focal adhesion assembly. Application of force implemented by the presence of a stiff matrix results in activation specific phosphorylation of FAK at tyrosine 397 and tethering of the mature adhesion complex to the cytoskeleton. Integrin clustering and subsequent focal adhesion maturation is accompanied by subsequent growth factor-induced activation of ERK signaling and potential activation of cell growth. Reproduced from (45).

Figure 7. Altered 3D growth and morphogenesis of MECs with increased matrix rigidity. (Top) Phase contrast images and images of H&E stained tissue comparing the morphogenesis of a mammary gland duct in a normal compliant environment (167 Pa) to MECs grown in rBM/collagen I gels of increasing stiffness (170-1200 Pa). (Bottom) Confocal microscopic cross-sections of a normal mammary duct versus MEC colonies cultured in increasingly stiff

environments. Staining: β-catenin (green), α6 or β4 integrin (red), and nuclei (blue). Reproduced from (45).

Table 1. Advantages and disadvantages of various matrices for 3D culture studies

Component	Advantages	Disadvantages
Reconstituted Basement Membrane	Successfully applied to many 3D systems	Pooly defined content; lot-to-lot variability
Fibrin	Successfully applied to many 3D systems	Easily proteolyzed by cellular proteases
Collagen I	More biologically defined; easy to manipulate	Lot-to-lot variability; limited range of elastic moduli
Polyacrylamide Gels	Easy to manipulate; non-reactive; large range of elastic moduli	Acrylamide toxicity; not a true 3D system

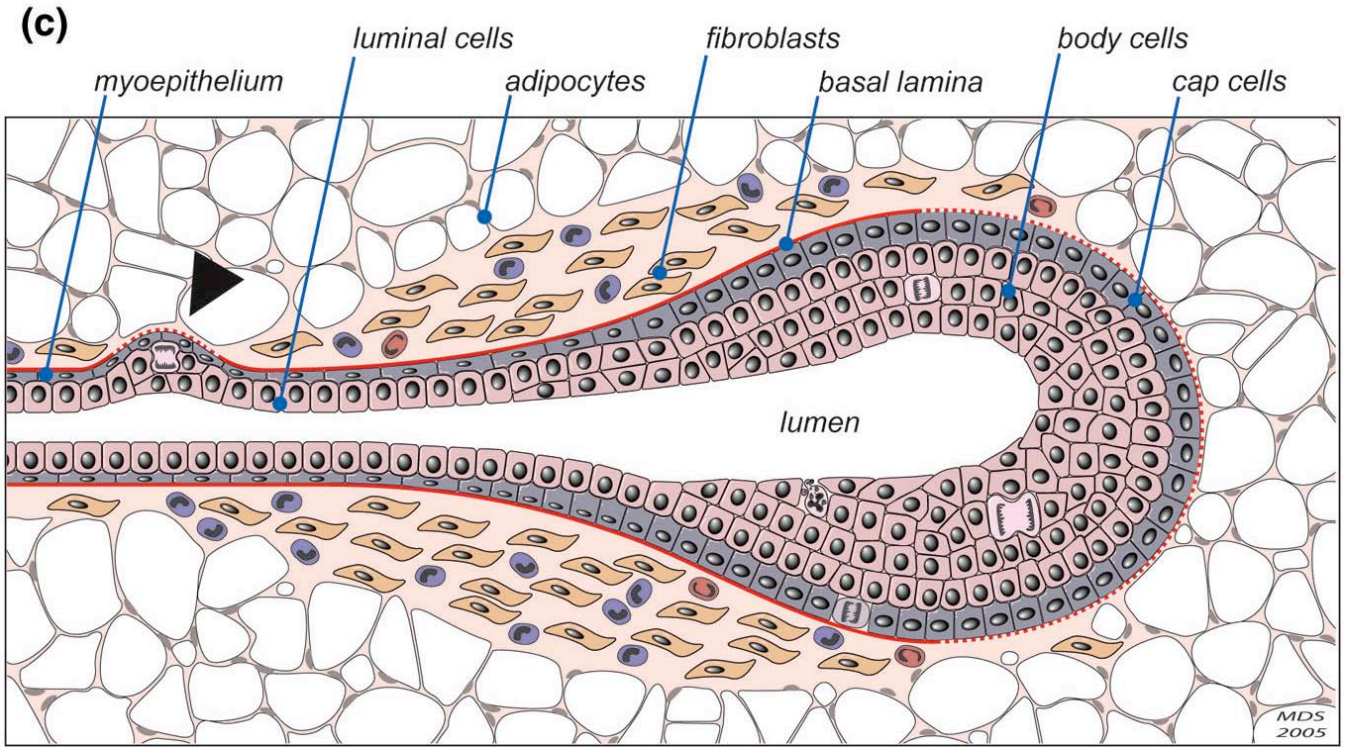
(c)
myoepithelium
luminal cells
adipocytes
fibroblasts
basal lamina
body cells
cap cells
lumen
MDS
2005

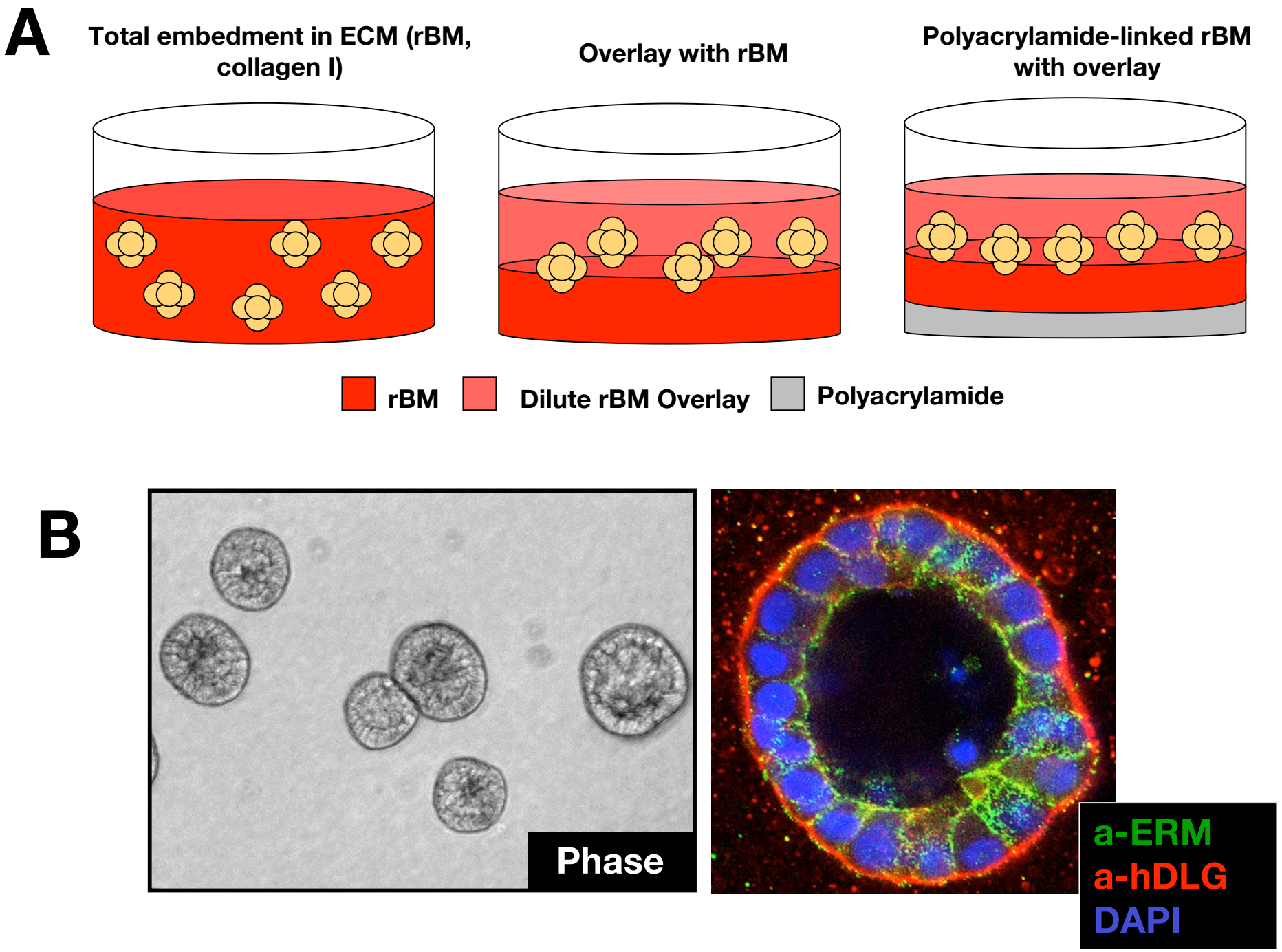
A
Total embedment in ECM (rBM, collagen I)
Overlay with rBM
Polyacrylamide-linked rBM with overlay
rBM
Dilute rBM Overlay
Polyacrylamide
B
Phase
a-ERM
a-hDLG
DAPI

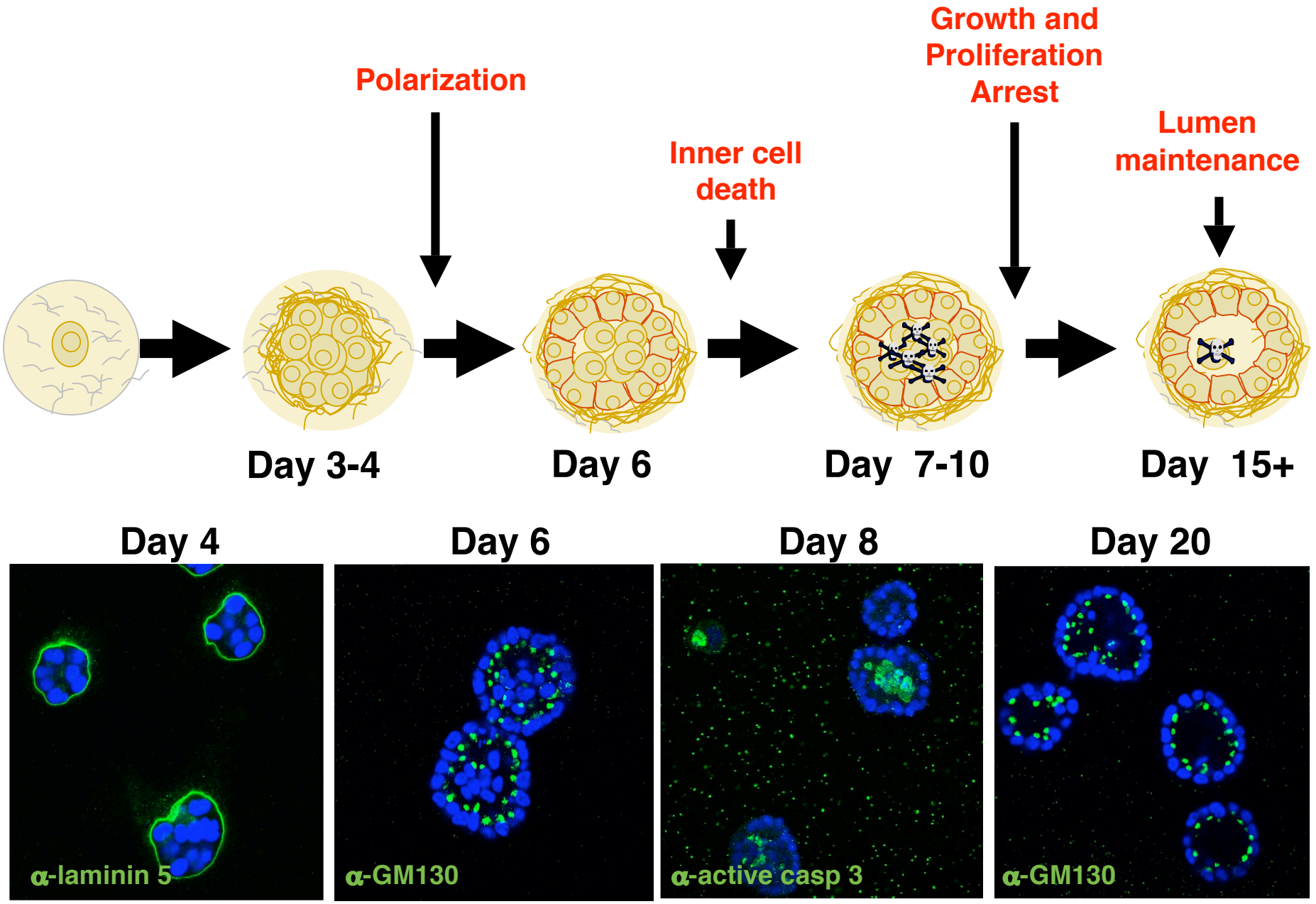
Polarization
Inner cell death
Growth and Proliferation Arrest
Lumen maintenance
Day 3-4
Day 6
Day 7-10
Day 15+
Day 4
Day 6
Day 8
Day 20
α-laminin 5
α-GM130
α-active casp 3
α-GM130

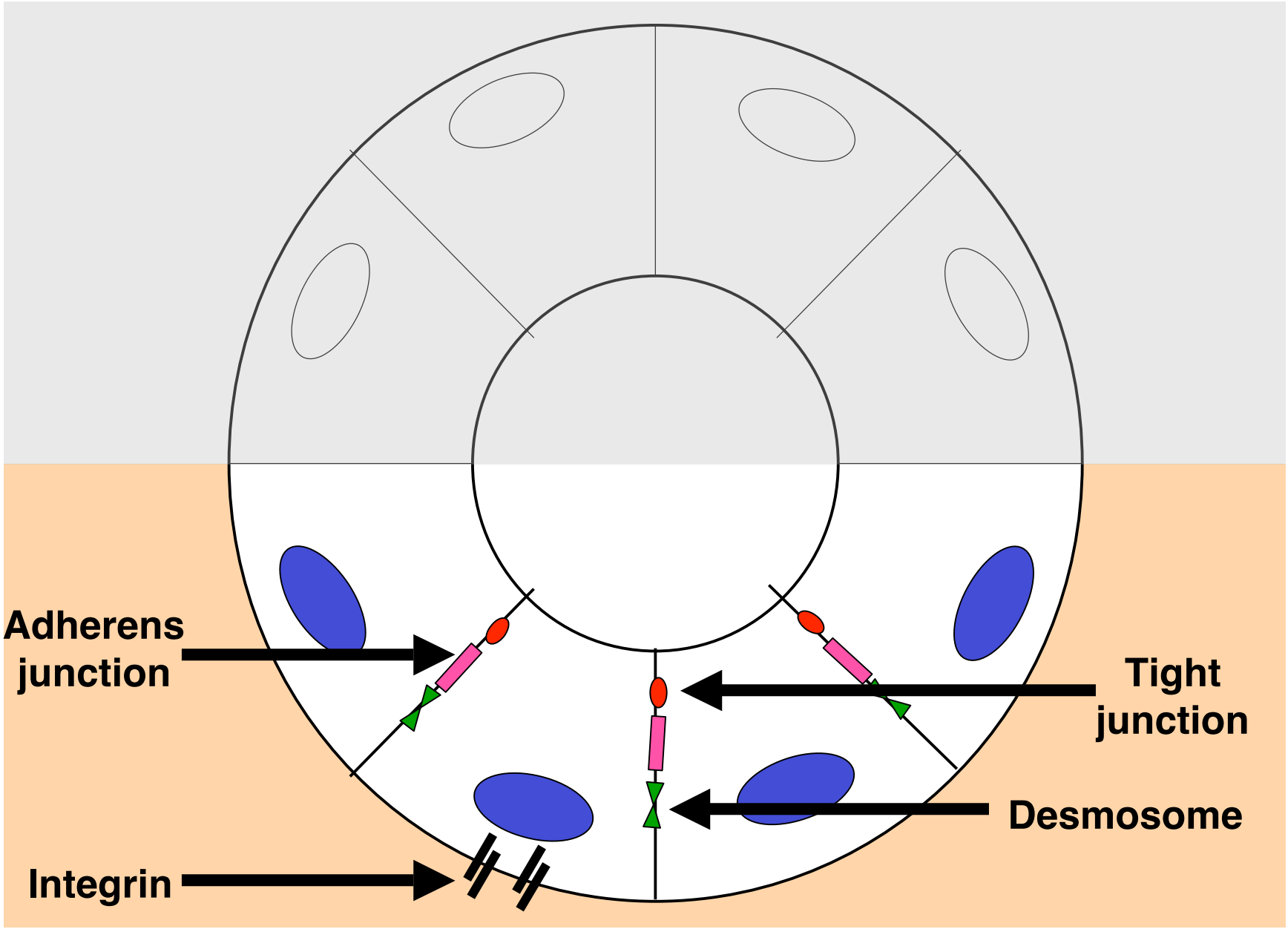
Adherens junction
Tight junction
Desmosome
Integrin

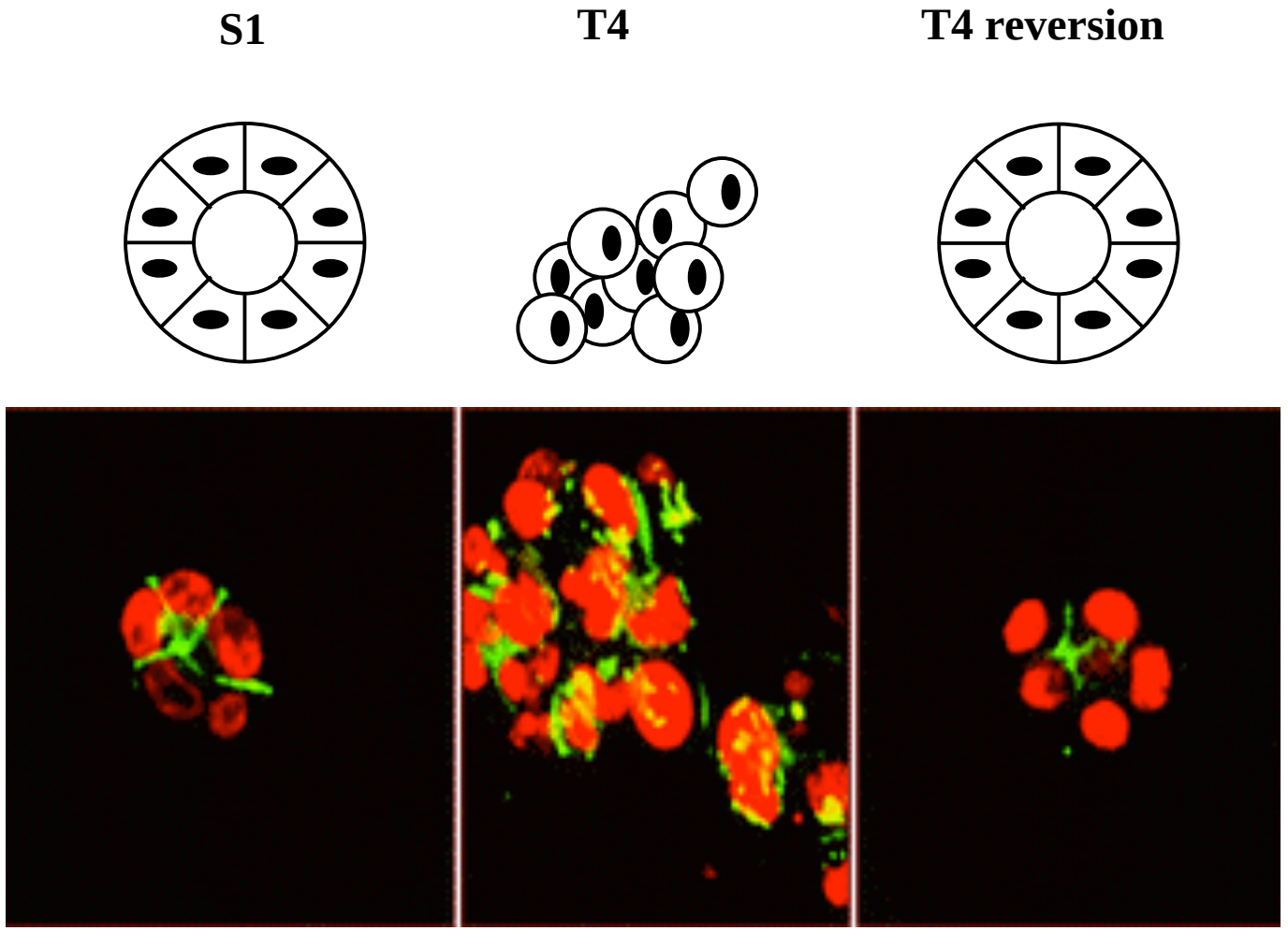
S1
T4
T4 reversion

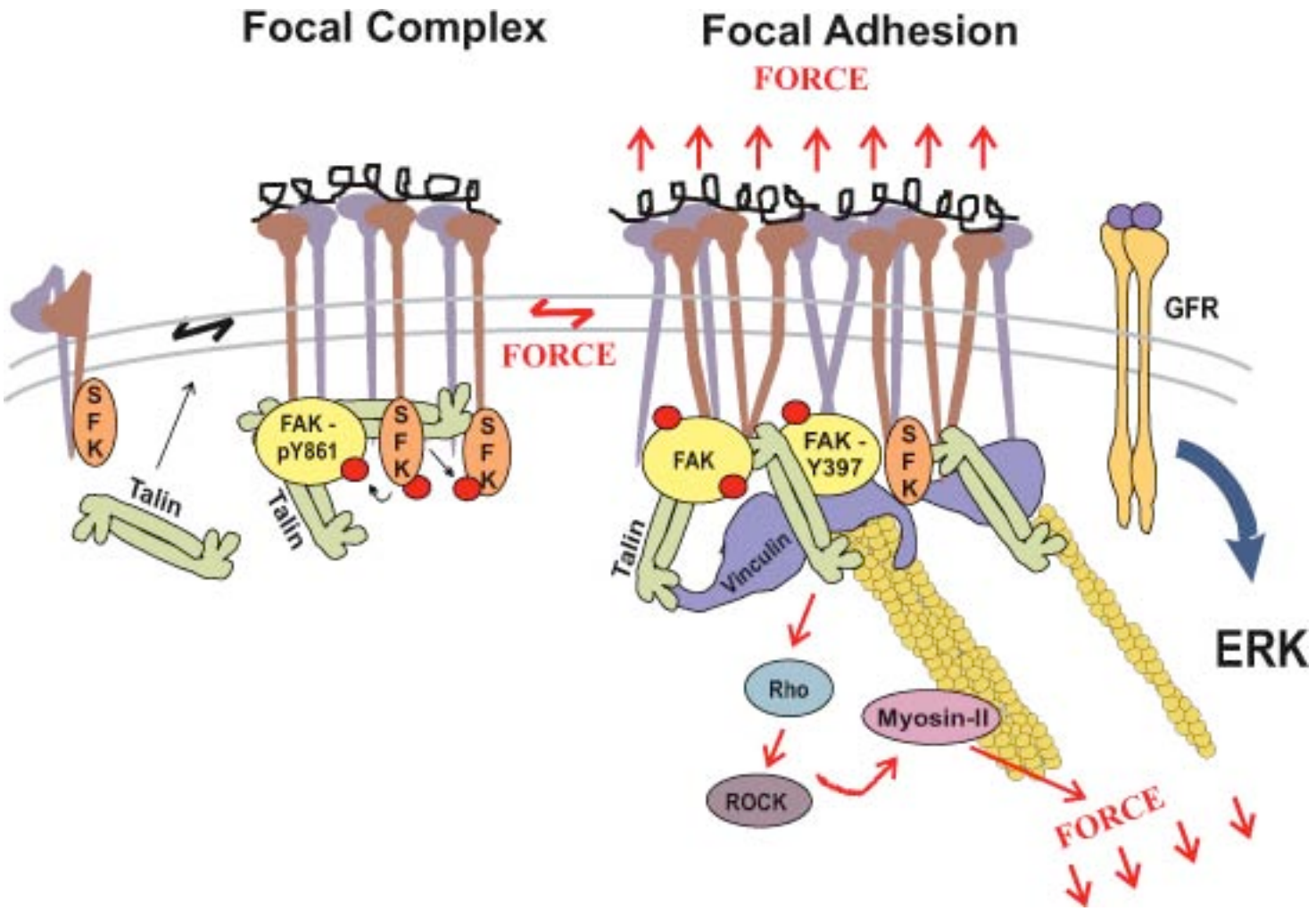
Focal Complex
Focal Adhesion
FORCE
FORCE
GFR
SFK
FAK - pY861
SFK
SFK
Talin
Talin
FAK
FAK - Y397
SFK
Talin
Vinculin
ERK
Rho
Myosin-II
ROCK
FORCE

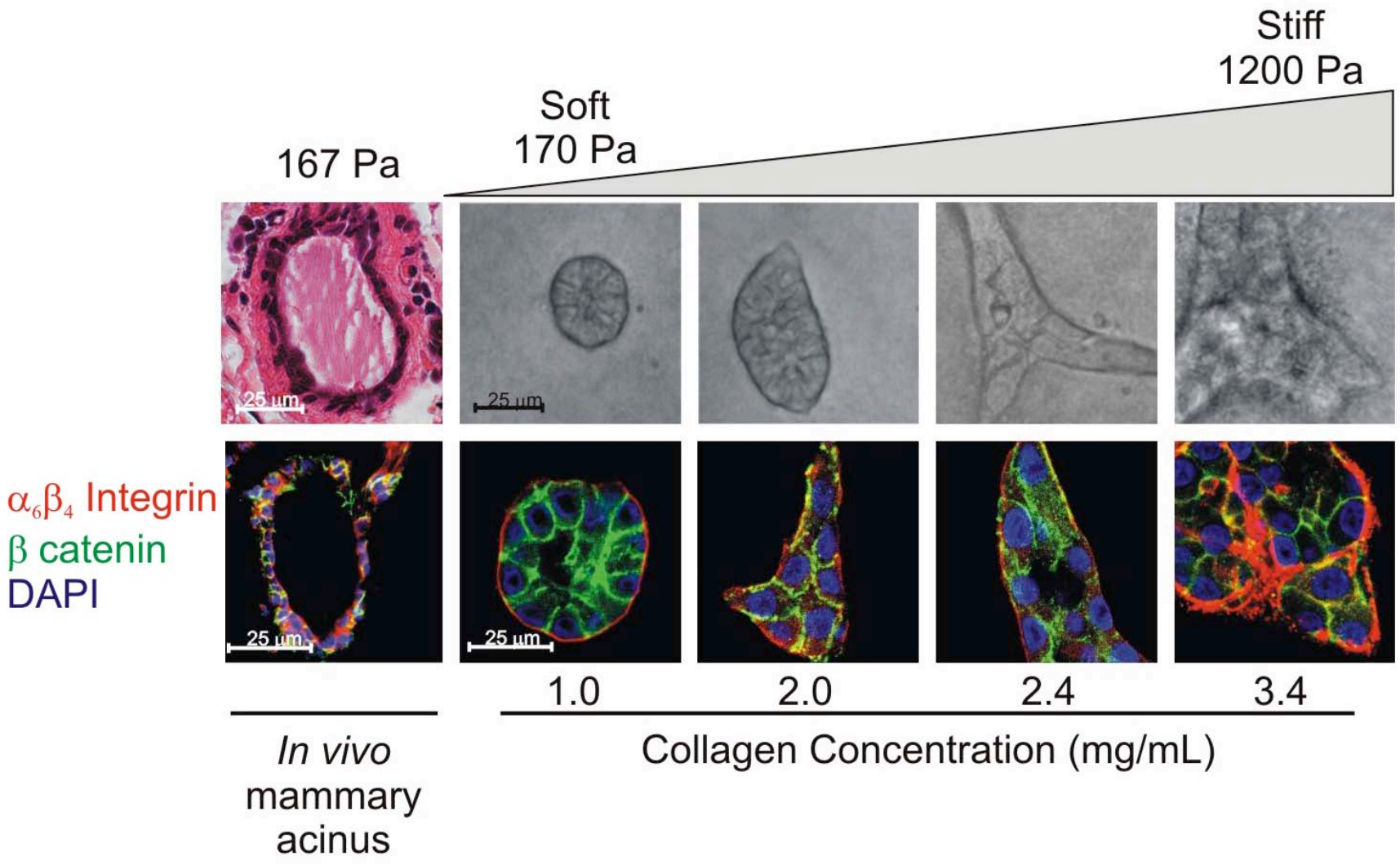
Stiff
1200 Pa
Soft
170 Pa
167 Pa
25 μm
25 μm
$\alpha_6\beta_4$ Integrin
β catenin
DAPI
25 μm
25 μm
1.0
2.0
2.4
3.4
In vivo mammary acinus
Collagen Concentration (mg/mL)